SLOVAK GEOLOGICAL MAGAZINE

VOLUME 7 NO 3 ISSN 1335-096X

Geological Survey of Slovak Republic, Bratislava
Dionýz Štúr Publishers

3/2001

ISSN 1335-096X

SLOVAK GEOLOGICAL MAGAZINE

Periodical journal of Geological Survey of Slovak Republic is a quarterly presenting the results of investigation and researches in a wide range of topics:

- **regional geology and geological maps**
- **lithology and stratigraphy**
- **petrology and mineralogy**
- **paleontology**
- **geochemistry and isotope geology**
- **geophysics and deep structure**
- **geology of deposits and metallogeny**
- **tectonics and structural geology**
- **hydrogeology and geothermal energy**
- **environmental geochemistry**
- **engineering geology and geotechnology**
- **geological factors of the environment**
- **petroarcheology**

The journal is focused on problems of the Alpine-Carpathian region.

Managing Editor: G. Šipošová

Language review and translation: M. Ondrášik and J. Janočko

Technical Editor: G. Šipošová

Address of the publishers: Geological Survey of Slovak Republic, Mlynská dolina 1, 817 04 Bratislava, Slovakia

Printed at: Gupress Bratislava

Annual subscrip lude the postage

© Geological Survey of Slovak Repub 817 04 Bratislava, SLOVAKIA

SLOVAK GEOLOGICAL MAGAZINE

VOLUME 7 NO 3

ISSN 1335-096X

Geological Survey of Slovak Republic, Bratislava
Dionýz Štúr Publishers

3/2001

The present number of the Slovak Geologic Magazine is devoted to the workshop of the GAGE Group held in Spišská Stará Ves in September 24 - 30, 2000. The main aim of the GAGE Group (Geospatial analysis of glaciated environments), which is a subcommission of INQUA, is recognition and unravelling of history of glaciated areas on the Earth. The organization of worskshop was linked to the project „GIS database on Carpathian Mts. glaciation" and the main objective of the workshop was to present history of the glaciation in the Tatry Mts., its spatial distribution, chronostratigraphy as well as its geological and geomorphological record in the area. During 3-day excursion key localities in the Tatry Mts., showing glacial and periglacial sediments and landforms, were attended. Geologists from 6 countries presented new knowledge on geospatial analysis of glaciated environments from different parts of the world. New knowledge and methods applied for research of continental and mountain glaciations were discussed. The talks and informal discussions in beautiful environment of the Tatry Mts. were surely a great asset to all participants of the workshop.

Originally, we only planned to publish papers from the workshop in the present volume. However, the editors used the chance to present some new results from the area of Slovak Qauternary geology. The presented papers show that the Quaternary geology in Slovakia plays an important role in a wide range of environmental scientific disciplines.

Juraj Janočko
Jozef Vozár

Slovak Geol. Mag., 7, 3 (2001),221 – 230

Fluvial and alluvial fandeposits in the Hornád and Torysa river valleys; relationship and evolution

JURAJ JANOČKO

Geological Survey of Slovak Republic, P.O. Box 13, 040 11 Košice

Abstract: Well developed fluvial terrace and alluvial fan systems in the Torysa and Hornád river valleys in the Košice Depression provide oportunity to analyze mutual relationship between these systems. The Torysa river formed five terrace steps which may be well correlated with toe parts of alluvial fans deposited by lateral tributaries. Alluvial fans have telescopic structure in the Torysa river valley suggesting tectonically stable source area. The Hornád river has similarly to the Torysa river five terrace steps. However, the structure of alluvial fans, deposited by the Hornád tributaries, is different. It shows gradual uplift of the source area resulting in shift of depocentrum closer to the mountain margin. Correlation of fluvial and alluvial fan deposits suggested time lag of alluvial fan sedimentation and deposition to the end of the accumulation cycle. Correlation of terrace steps between the Torysa and Hornár river valleys suggests prevailingly climatic driven erosion-accumulation cyclicity.

Key words: Quaternary, fluvial deposits, alluvial fan deposits, climate, tectonics, erosion-accumulation cycle, Hornád and Torysa rivers, Košice Depression

Introduction

Alluvial fan deposits and deposits of axial river system show distinct relationship described in many works (e.g. Schumm, 1973, Flint, 1995). The most common situation described in ancient deposits is interfingering of fluvial and alluvial deposits caused by fluctuation of deposition intensity in individual depositional systems. In the Pleistocene periglacial areas additional driving mechanisms play important role in depositions of alluvial fan and fluvial systems - high-frequency fluctuation of climate and glacial isostasy. This complicates relationship between marginal alluvial fan and axial river systems.

The main objectives of the paper are the geomorphological and geological analyses of the Torysa and Hornád terrace and alluvial fan systems in the Neogene Košice Depression and the establishment of their mutual relationship. A model of their development is given at the end of the paper.

Geological setting

The Hornád river and its left-side tributary the Torysa river are two main flows draining Košice Depression situated in the Eastern Slovakia (Fig. 1). During their Pleistocene evolution, they formed several terrace steps consisting of erosional plinths overlain by sediment bodies. Fluvial terrace steps are closely related to alluvial fans developed at the margin of the basin where high-energy relief of surrounding mountains passes into slightly undulated low relief of basin.

The Košice Depression is a part of the East Slovakian Neogene Basin bounded to the west and north by the pre-Tertiary units of the Inner Carpathians, the Central Carpathian Paleogene Basin and by flysch deposits of the Outer Carpathians (Fig. 1). The Neogene basin fill consists of marine and terrestrial mud, mudstone, sand, sandstone, gravel and conglomerate. The western part of the basin, isolated from the basin eastern area by a chain of volcanic Slanské vrchy Mountains, forms a partial Košice Depression. Two N-S extending positive morphostructures, laterally restricted by N-S faults, governed the development of three main N-S directed fluvial valleys in this region during the Quaternary period (Figs. 1 and 2).

The Hornád river and its left side tributary the Torysa river, representing axial river system in two N-S valleys, are medium-sinuosity meandering rivers with prevailing gravely and sandy load. The Torysa river flows 100 km before confluences with Hornád river, a 150 km long tributary of the Tisza river. Geologically and tectonically different areas crossed by both rivers govern extension and characters of fluvial deposits as well as morphological development of river valleys. Relatively narrow valleys with several terrace steps of the Hornád river are developed in areas consisting by crystalline and Mesozoic rocks. Broad alluvial plains with terrace flight are developed in areas composed of the Tertiary (Paleogene and Neogene) rocks.

In Košice Depression both rivers formed several terrace steps during their Pleistocene evolution. High energy relief of mountains surrounding Hornád and Torysa valleys governed development of steep-gradient perpendicular tributaries to axial rivers depositing system of alluvial fans during the Pleistocene and Holocene. Alluvial fans, hugging volcanic Slanské vrchy Mts. in the Torysa river valley, consists exclusively of monomictic

Slovak Geol. Mag., 7, 3 (2001),221 – 230

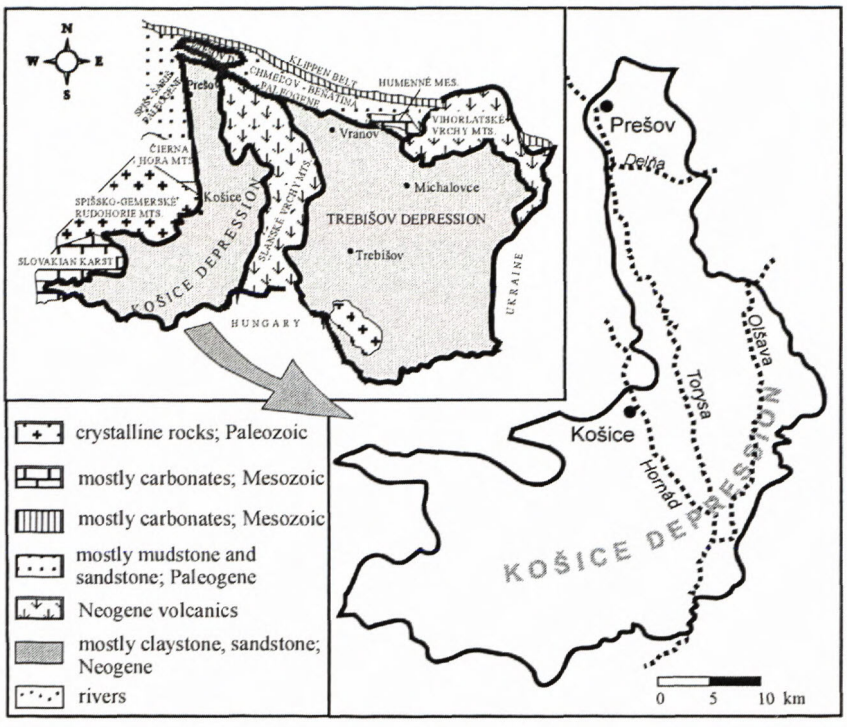

Fig. 1 Location of the Košice Depression. The Košice and Trebišov Depressions separated by the Slanské vrchy Mts. comprise the East-Slovakian Neogene Basin.

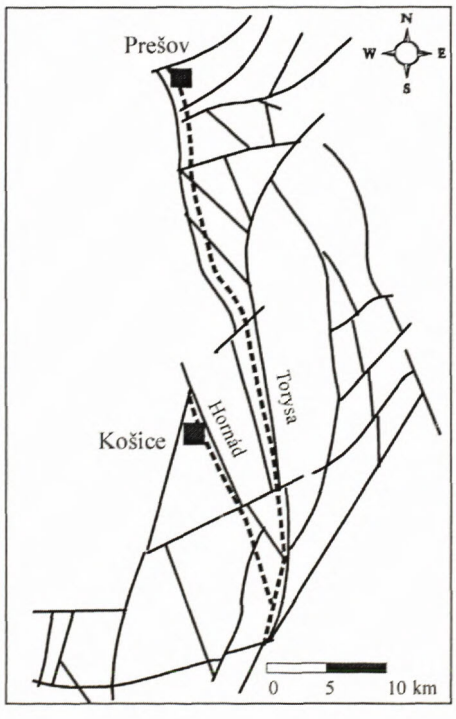

Fig. 2 Structural scheme showing neotectonically active faults in the Košice Depression. Note the N-S trending faults restricting valleys of the Hornád and Torysa rivers. Transverse faults determined origin of small depressions and elevations resulting in change of thickness of Quaternary sediments. Dashed lines represent Hornád and Torysa streams.

volcanic, mainly andesitic rocks. The difference in petrographic composition between sediments of alluvial fans and sediments of axial river system (Torysa) gave an opportunity to study lateral relationship between fluvial and alluvial fan systems.

Several authors have studied different river reaches, mainly from a geomorphological point of view (Kvitkovič & Plančár 1975, Pristaš 1979, Harčár 1972, Janočko 1989, 1990, Petro et al. 1988 1990, Spišák et al. 1990), but the lack of reliable dating analysis hampers the correlation between them. The present study is focused on the river reaches in the Neogene Košice Depression where they have built a system of terraces. The confluence of the river valleys in the southern part of the Košice Basin, facilitates correlation of both river terraces and alluvial fan systems and comparison of their Quaternary evolution. The relationship between fluvial sediments consisting of polymictic material and monomict rocks of alluvial fan sediments (exclusively volcanic material) is especially exemplary in the Torysa valley.

Methods

Both geomorphological and geological methods have been applied during the research. The terrace steps and alluvial fans were identified by mapping and aerial photographs. The geomorphological analysis included observation of relative altitude of the terrace base (bedrock bench) and surface above the recent flow and construction of longitudinal and perpendicular cross sections. The relative altitude of the base of alluvial fan deposits at the fan toe position, type of radial profiles of alluvial fans and their geomorhological development (telescopic, superimposed) have been studied. The geological methods comprise facies analysis of fluvial and alluvial fan deposits, analysis of grain-size and carbonate content, clasts morphology measurements and analyses of heavy minerals. More than 100 shallow mapping drillings (up to 30 m depth) have been used to study spatial distribution of deposits. Fossil soils were studied where present in order to get more precise dating of sediments. Two ^{14}C datings were performed on the Holocene, carbon rich fluvial overbank deposits.

Terrace and alluvial fan systems

Torysa river valley

Fluvial deposits

The Torysa river enters the Neogene Košice Depression by gateway at the northern part of the basin (Fig. 1). The gateway separates two main fluvial basins of the river. The fluvial sediments are more widespread to the north of the break-through, in the Paleogene basin ex-

tending from Brezovica to Veľký Šariš comparing to the Košice Depression to the south. This sediment distribution suggests prevailing deposition at the highland front in the middle river reach and more balanced equilibrium regime in the lower reach resembling small-scale example of three-fold catchment basin model (Starkel 1990). Four terrace steps except recent valley fill are preserved in the investigated area (Tab. 1). They comprise three steps of of the middle and one step of the low terraces. Terrace steps are disconnected and consist of erosional bench incised into the Miocene bedrock and fluvial accumulation (Fig. 3). The stratigraphy of terraces is not firmly established because of lack of pollen and fauna in the terrace accumulations older than the radiocarbon range. The main stratigraphic criteria were morphostratigraphy and correlation to overlying alluvial fan deposits dated on the base of fossil soils and to the terrace steps developed in the eastern, Paleogene part of the basin (Harčár 1974).

Tab. 1 Fluvial systems in Torysa and Hornád rivers with nomenclature and base and surface relative altitudes of individual terrace steps. Age of the fluvial accumulations in individual steps is also given.

Hornad river

Terrace system	Terrace step	Relative altitude		Age	
		Base	Surface		
Lower	1	-3 (-13)	5 - 8	Late	Pleisto-cene
Middle	3	7 - 10	9 - 12	Middle	
	2	17 -20	13 - 20		
	3	25	30 - 32		
Upper	1	50	52	Early	

Torysa river

Terrace system	Terrace step	Relative altitude		Age	
		Base	Surface		
Lower	1	-4 - -8	2 - 5	Late	Pleisto-cene
Middle	3	5 - 8	7 - 12	Middle	
	2	18 - 21	20 - 24		
	1	35 - 45 60	37 60.5		

The middle terrace system consists of three terrace steps occurring at relative altitudes 35 – 45 m (1st middle terrace), 18 – 23 m (2nd. middle terrace) and 5 m (3rd. middle terrace; Table 1). The correlation with overlying alluvial fan deposits, eolic deposits and fossil soils and the comparison to their analogue in the northern Paleogene basin (Harčár 1974) implies Middle Pleistocene age (Janočko 1991).

The first middle terrace step occurs at altitudes 35 – 45 m and is overlain by alluvial fan deposits covered by loess-like loams containing rubeficated fossil soil of Holsteinian age (Janočko 1990). The fluvial accumulation has a patchy distribution, its largest thickness, indicated by drillings, is 3.5 m. The sediment consists of erosive-based massive gravel with subrounded clasts of crystalline and Paleogene origin. The unsufficient exposures of the fluvial accumulation do not allow more precise interpretation of the fluvial sedimentary environment.

The second middle terrace step is the most conspicuous terrace in the studied region developed at the altitude 23 - 18 m. It consists of 2 – 6 m thick fluvial accumulation. The typical section has been exposed in the Prešov brick kiln in the relative altitude 20 m. Erosive based, positive graded massive gravel consists of subrounded and rounded crystalline (quartz, quartzite, chert), Paleogene (sandstone and mudstone) and neovolcanic clasts. A sharp boundary divided 2 m thick gravel bed from overlying massive matrix-supported gravel bed about 0.7 m thick. The subrounded and rounded, up to 3 cm large clasts are scattered in the medium to coarse-grained, extremely poorly sorted σ = 4.04) sandy matrix. The upper sedimentary boundary marks a slow transition from this facies to planar cross-stratified sand. The succession is capped by 1 – 1.5 m thick massive, sharply-based silt. The massive, upward-fining gravel is interpreted as a channel fill and the overlying facies probably show two types of overbank deposits. Matrix-supported gravel passing into planar cross-stratified sand represent overbank deposition during high-peak flood discharge with gradual waning of the flow energy indicated by the evolution of the small-scale planar cross-stratification indicating ripple migration. The overlying massive silt is interpreted as overbank deposit representing vertical flood plain accre-

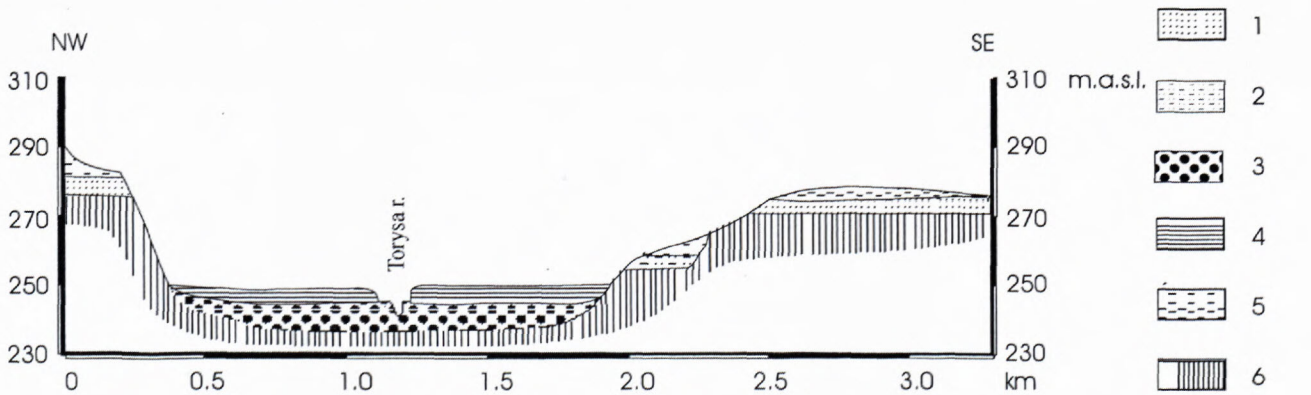

Fig. 3 Cross-section of Torysa river valley near Prešov showing first and second terrace steps of the middle terrace system.
1 – Middle Pleistocene fluvial deposits, 2, 3 – Late Pleistocene fluvial deposits, 4 – recent flood plain deposits, 5 – loess-like loams, 6 – Pre-Quaternary deposits.

tion during the low-peak floods. Although the channel facies is not sufficiently exposed to provide more detail type of sedimentary environment, the well-developed overbank deposits suggest deposition in higher sinuosity gravel bed river system. „Flashy flood" deposits suggest high fluctuation in the river discharge during the sedimentation.

Third middle terrace occurs at level 4 – 6 m above the recent floodplain. Only the gravel accumulation is preserved from the whole fluvial sequence. It consists of erosive based upward-fining massive gravel passing into moderately sorted (σ = 0,921) massive and faintly planar cross-stratified medium and fine sand. The total thickness of sediments does not exceed 3 m. The upward fining trend of gravel capped with occasionally cross-stratified sand suggests the deposition on the point bar. The channel pattern of the river was probably the same like during the deposition of older, second middle terrace deposits.

The lower terrace was formed in the coarse-grained fluvial deposits of the Late Glacial which also comprise the recent valley fill. The surface of the terrace, which is usually covered by Holocene overbank deposits, is about 2 – 5 m above the flow, the base of the terrace is about 4 – 8 m below the flow. The information about the gravely fill came only from drillings what hampered a more precise facies analysis. It shows prevailing massive, occasionally upward-fining gravel, consisting of subrounded to rounded polymictic clasts. The average thickness of gravel bed is 7 m. The gravel is overlain by 2 – 3 m thick layer of overbank silt and silty sand . Typically, two tchernozem soil horizons are developed in these sediments. The ^{14}C dating of the upper horizon yielded 5 700 years B.P. The present day river is incised into these sediments and in some sections cuts about 0.5 m of underlying gravel bed.

Alluvial fan deposits

Sharp transition between slightly undulated, low energy relief prevailing in the Torysa river valley and a high energy, sharply dissected relief of volcanic Slanské vrchy mountain neighbouring the valley from the east (Fig. 1), determined alluvial fan sedimentation recorded since the Middle Pleistocene. The almost uniform petrographic composition of alluvial fan deposits, consisting mainly of andezites, rendered a unique possibility to study their relationship to fluvial sediments of the Torysa river. The development of alluvial fans was determined by local erosive base given by the incision of axial Torysa river system. This is reflected by a very consistent morphometric characteristic of terrace steps and alluvial fan toes. Alluvial fans deposited by Delňa river, a left-side Torysa river tributary (Fig. 4) are morphologically most conspicuous. They have telescopic structure with the head of younger, lower fan segment inserted into upper fan segment (Fig. 5). The radial fan profiles reflecting erosional and tectonic changes in its source area (Bull 1963) are slightly concave (Fig. 6). This type of fan structure indicates a relatively stable position between alluvial fan and the source area (Bull 1964). The fan surface slope angle is

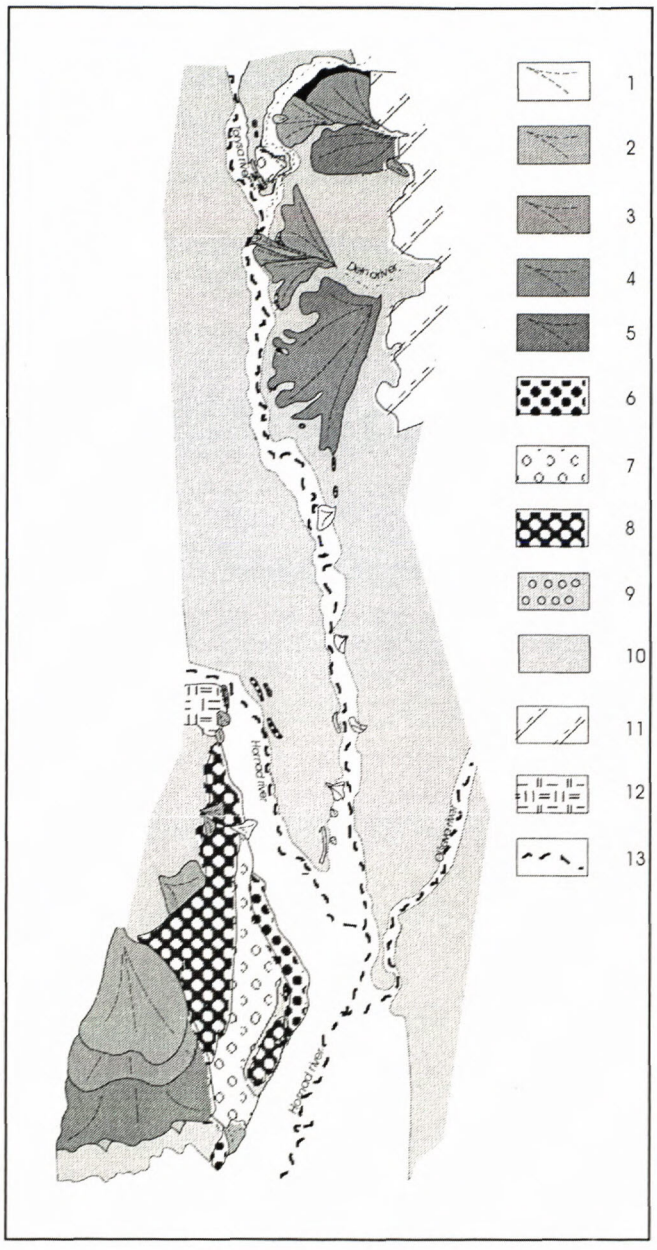

Fig. 4 Location map of the study area and the map of fluvial and alluvial fan sediments in the Košice Basin. 1–5 – alluvial fans (1 – Holocene, 2 – Late Pleistocene, 3, 4, 5 – Middle Pleistocene; 6 – 9 – fluvial sediments (6 – Late Pleistocene, 7, 8 – Middle Pleistocene, 9 – Early Pleistocene; 10 – Paleogene and Neogene sediments; 11 – Neogene volcanic rocks; 12 – Mesozoic and crystalline rocks; 13 – rivers.

small, it varies between 2 and 0.5 degrees. The ratio between the source area (21.28 km^2) to fan area (37.52 km^2) is 0.56. The fan system consists of five segments that are according to the altitude of their toe divided into middle and low alluvial fan segments.

The middle alluvial fan system comprises three fan segments (generations) which toe relative altitude 40, 20 and 6 m is consistent with the altitude of middle terrace system steps (Tab. 2). The morphometry suggests division of this fan system into first, second and third segment analogicaly to the division of middle terrace system. The

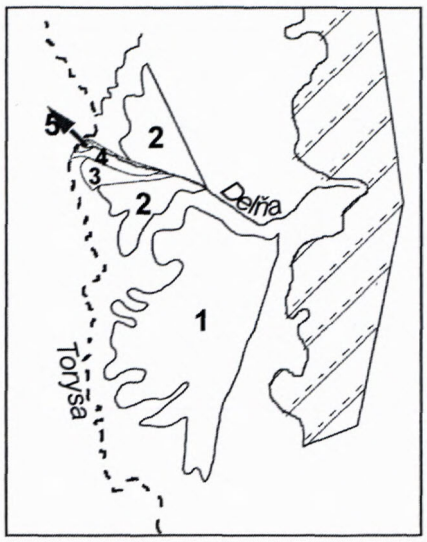

Fig. 5 Telescopic structure of alluvial fans in the Torysa river valley. The older fans are closer to the source area represented by the Slanské vrchy Mts. The oldest fan segment is labelled by number 1, the youngest one is labelled by number 5.

overlying the Torysa second middle terrace step. The low-angle cross-bedded planar beds of clast-supported gravel interlayered with massive gravelly sand are interpreted as foresets of longitudinal bars typical for braided river environment (Mial 1977). Massive, erosive-based very poorly sorted gravel fills either large channels (5 – 10 m wide, 1 m deep) or chutes. The gravelly infill occassionally contains large, up to 50 cm in diameter rip-up clay clasts of Neogene origin. Their location in the upper part of the alluvial fan sequence indicates high competence of the stream. The high energy environment is also demonstrated by massive, horizontal-bedded gravel and clast-supported gravel filling large shallow througs interpreted as flood deposits of the interchannel areas. Very scarce matrix-supported gravel with sharp or erosive base show prevailing sedimentation in the braided river system and relatively distal position on the alluvial fan.

The toe of the third middle alluvial fan segment is in the relative altitude 6 - 4 m and corresponds to the third terrace step of Torysa river. The sediments have been studied only from drillings where showed clast-supported

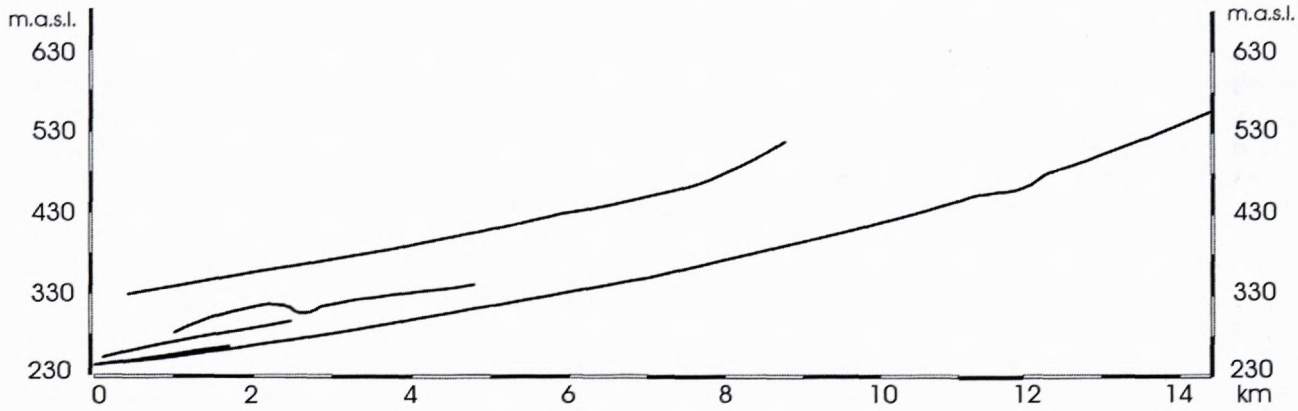

Fig. 6 Radial profile of Delna alluvial fan system.

morphometric criteria and the occurrence of Holsteinian fossil soil covering the highest fan segment demonstrate the possible correlation of middle fan system segments with middle terrace system steps.

The first middle fan segment is represented by a huge fan with the toe at the level about 40 m above the recent Tories river floodplain. Sediments of this segment superpose the first middle terrace of the Torysa river (Fig. 4). The fan is covered by thick loess-like sediments with preserved Holsteinian pseudogleyficated, illimerizated fossil soil (Janočko 1990). The fan sediments are assigned to lower part of the Middle Pleistocene. Scarce outcrops show massive clast-supported gravel with erosive and sharp base arranged into beds up to 1 m thick representing probably flood sediments deposited on the fan interdistributary area. Clasts, composed mostly of andesite, are highly weathered, easily crumbling in the hand. Occasional lateral restricted layers of massive or cross stratified coarse and medium sand originated probably during the waning of the flood.

The toe of the second middle alluvial fan segment is about 20 m above the recent Torysa flood plain and is

Tab. 2 Alluvial fan systems in the Hornád and Torysa river valleys. The table shows nomenclature of fan segments, relative altitude of fan segment toe and age of individual segments.

Torysa river

Alluvial fan system	Alluvial fan segment	Relative altitude of fan toe	Age	
Lower	2	3	Holocene	
	1	-2	Late	Pleisto-cene
Middle	3	8		
	2	22	Middle	
	1	37		

Hornad river

Alluvial fan system	Alluvial fan segment	Relative altitude of fan toe	Age	
Lower	1	60	Late	Pleisto-cene
Middle	1	40	Middle	
	2	32 - 35		

gravel with massive structure, occasionally fining-upward into granules. The bed thickness is 50 – 150 cm. They are interpreted as flood deposits in the braided river system. Both second and third fan segments are supposed to be deposited in the upper part of the middle Pleistocene.

The lower alluvial fan system is divided into first and second low alluvial fan segments. The toe of the first low alluvial fan segment has a relative altitude - 2 m and stratigraphically it is below the floodplain deposits but above the base of the fluvial fill of the valley. This segment represents part of the last sedimentation cycle from the Late Glacial.

The second lower alluvial fan segment is superimposed to Holocene Torysa flood plain deposits and represents the most recent alluvial fan deposition. Both low fan segments consist of very poorly sorted loamy, clast-supported massive gravel without distinctive bedding. This type of sediment has probably been deposited during high-magnitude floods when high amount of particles was in suspension and then abruptly settled down resembling diluted debris flows. The deposition of low alluvial fan system suppresses the Torysa river sedimentation and caused the turn of its channel westward (Fig. 4).

Hornád river system

Fluvial deposits

The Hornád river emerges from the crystalline and Mesozoic Čierna Hora geological unit to the Neogene Košice Basin at the gateway north of Košice (Fig. 1). The flat relief of the Košice basin bounded to the Bodva Horst in the south and uplifted during the Early and Middle Pleistocene (Janočko 1990), determined widespread occurrence of the Hornád river fluvial deposits. A system of five terraces except Holocene flood plain has been preserved from the Pleistocene period (Tab. 1, Fig. 7). On the base of overlying fossil soils, correlation with other fluvial and alluvial fan sediments in the Košice Basin as well as on the base of the morphostratigraphic criteria they have been grouped into the system of the upper, middle and lower terraces (Tab. 1).

The upper terrace system is preserved only in relics at the altitude 50 m above the recent flood plain. It consists of erosive-based clast-supported gravel. The gravel, consisting of resistant clasts (Permian conglomerates, cherts, quartz) shows massive structure and upward fining trend, bedding is indistinctive. It passes into 2 m thick bed of sandy silt with clasts. The shortage of good outcrops does not allow a more detail interpretation of depositional environment, but the possible interpretation of silt with gravel as overbank deposit suggests its origin in a river system with higher sinuosity.

The middle terrace system consists of three terrace steps in the relative altitudes 25, 17 – 20 and 7 – 10 m divided into first, second and third middle terrace (Table 1). The thickness of sediments in the single terrace steps is 2 – 5 m.

The first middle terrace is a most widespread terrace step in the Košice Basin (Fig. 4) having the base 25 m above the recent flow. The clast composition is similar to rocks of the upper terrace enriched in less consistent dolomites and limestones. Cross-bedded gravel overlain by cross-stratified sand suggests sedimentation on the point bar. The lateral shift of channel is well documented by the development of lateral accretion surfaces. Typical are large-scale channels reaching more than 10 m width and 60 cm height and smaller chute channels filled by poorly sorted silty and sandy gravel. The gravel is commonly overlain by silt and sandy silt with scattered small clasts interpreted as overbank deposits. The point bar structures and the development of overbank deposits indicate meandering river depositional system.

The drillings in the weakly-preserved second middle terrace accumulation shows massive, occasionally upward-fining gravel bed up to 4 m thick probably representing channel fills. Additional data are needed for more detail interpretation of sedimentary environment of this terrace step.

The sediments of the third middle terrace are exposed in numerous gravel pits in the southern part of the depression (Photo 2). They show structure typical for large channels up to 20 m long and 0,7 m high filled by massive and

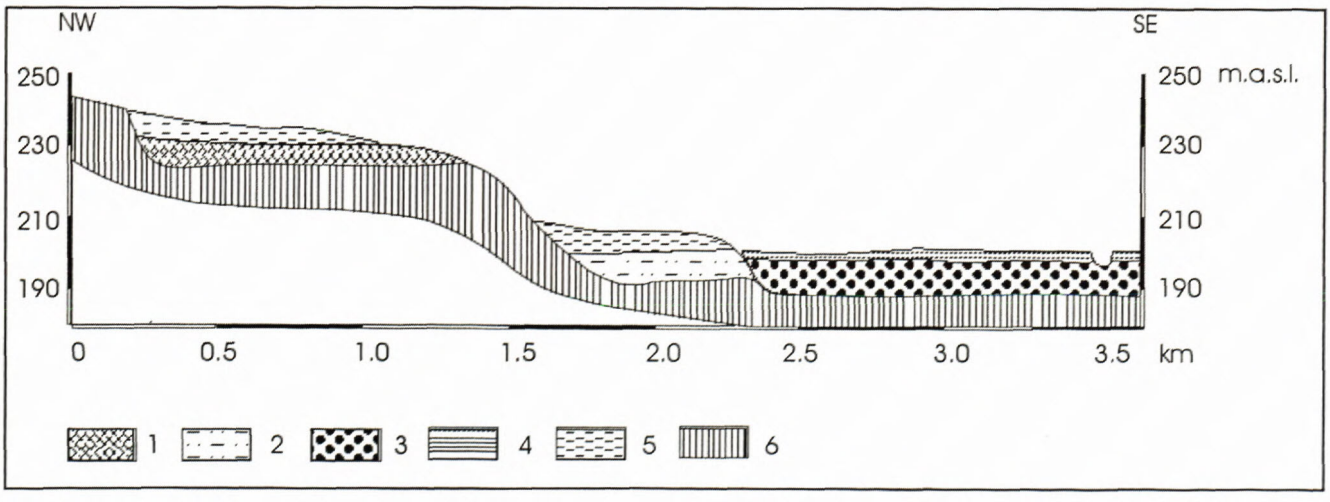

Fig. 7 Cross section of Hornád river basin showing two terrace steps from the middle terrace system. 1 – Middle Pleistocene fluvial deposits, 2, 3 – Late Pleistocene fluvial deposits, 4 – recent flood plain deposits, 5 – loess-like loams, 6 – Pre-Quaternary deposits.

Photo 1 Deposits of the lower terrace step in the Hornád valley. Typical are wide channels filled by cross-bedded sandy gravel suggesting lateral accretion process.

planar cross-bedded sandy gravel. Conspicuous lateral accretion surfaces indicate a lateral migration of channel typical for meandering rivers. The development of more channels at the same stratigraphical level points to both channel migration and switching typical for mobile channel belt built up by meandering or braided river system. Less common are smaller hollows filled by massive gravel representing probably chutes in the bars or crevasses. The absence of flood deposits indicates switching of river channels eroding the lateral flood plain deposits

The surface of *lower terrace system* is about 3 to 5 m above the recent river flow, the base is identical with the base of contemporary river valley, varying from the relative altitude -5 to -10 m. Weekly exposed sediments of this terrace step show only massive gravel with a gradual transition to well-developed silt and sand of flood plain. The good preservation of the overbank facies suggests more stable channel system with less frequent channel migration.

The Holocene fluvial sediments are represented by gravel and widespread fines of overbank deposits building up a broad, well-developed flood plain wide up to 5 km. Gravel is massive , occasionally fining upward. Flood plain facies consists of massive silt and sandy silt, usually commencing at the base with a silty clay layer thick up to 30 cm.

Alluvial fan deposits

The uplift trend of the main source area of the largest alluvial fans debauching into the Hornád valley caused different structure of the fans comparing to the fans in the Torysa river valley. The most extended is the oldest fan segment deposited during the middle Pleistocene and correlated to the first middle terrace step. Younger fan segments were deposited closer to valley mouth and overlies the older segment (Fig. 4). The material of all fan segments consists of quartz, quartzite and chert, occasionally dolomites and limestones. The difference against Hornád river fluvial clast material is the absence of violet conglomerates derived into fluvial deposits from the Permian deposits of the Čierna Hora Mts.

The oldest fan segment is composed of clast-supported horizontal bedded massive gravel with vague boundaries

Photo 2 Fluvial deposits of the 2nd terrace step of the Torysa river overlain by alluvial fan deposits. Fluvial deposits are composed of sandy conglomerate at the base passing into overlying silt representing overbank facies.

marking beds of average thickness 60 cm. This facies suggests deposition of the gravel sheets during high flood stages.

Two younger fan segments, stratigraphically correlated to the third middle terrace step and first lower terrace step (Janočko 1990) overlie the oldest fan segment. The scarce outcrops show the layer of brown silt between the oldest and younger segments and similar structures of deposits like in the oldest segment indicating prevailing sheet flood deposition in the braided ? river environment.

The relationship between fluvial and alluvial fan deposits

Different lithology of alluvial fans and fluvial terrace sediments as well as high number of mapping drillings render a good correlation between terraces and alluvial fans. Two types of alluvial fans with „telescopic„ and superimposed fan segment structures are present. The typical relationship between alluvial fans and terrace steps is recorded in Torysa river valley where during a relative stable tectonic conditions the climatic changes were the main factor governing fluvial and alluvial fan sedimentation in the Middle and Late Pleistocene and Holocene. Every segment of the alluvial fan system is superimposed to its fluvial terrace counterpart of the Torysa river (Photo 2). The preservation of this sediment succession in all stages of valley development suggests that the most active alluvial fan sedimentation took place at the end of fluvial - alluvial fan accumulation phase in the erosion - accumulation cycle of the valley development and was followed by the period of river incision. The fluvial and alluvial fan sediments were partly destroyed during the next erosive-accumulation cycle, but the erosion has never expanded laterally as far to destroy all older sediments becoming a new, lowest terrace step. Analogy to the recent relationship between fluvial and alluvial fan sedimentation and to the shift of the main river channel to the opposite side of the valley (Fig. 8) as the response to the alluvial fan invasion onto the flood plain suggest a slow migration of the river channels towards the valley side where the tributary confluences during the main period of river sedimentation, and a fast shift of the channel to the opposite side of the valley at the end of the sedimentation period.

The terrace flight with alluvial fan veneer shows a cyclicity in the sedimenta- tion of the fluvial - alluvial fan succession. Two periods of fluvial incision at the start of cold and warm periods with the prevailed sedimentation during the glacial and interglacial time are generally accepted as the explanation of the cyclic river activity in the Pleistocene (Starkel 1990, Vandenberghe 1993). The development of alluvial fan sedimentation depends on many factors among which are the most important morphology (relief), a sufficient amount of detritus in the rock drainage basin and the suitable climatic conditions (hydrological regime favouring high rainfall amount). These factors form a „geomorphological threshold" that has to be exceeded in term the alluvial fan sedimentation can start (Leeder 1982). Assuming that the main fluvial aggradation phase took place during the glacial period, the main alluvial fan deposition occurred at the end of the glacial. This indicates that the conditions favouring excess of geomorphological treshhold were present particularly at that time. An intensive frost weathering during the glacial period revealed a high amount of loose detritus. A sparse herbaceous vegetation at the end of the glacial has not been able to stabilise weathered material on the steep slopes of mountains adjacent to the low relied basin and all „prepared„ material has been redeposited during the increased rainfall governing the development of the alluvial fans at the foots of the mountains (Fig. 8). The main trend of the axial river in the main valley, suppressed by the alluvial fan to the opposite side of the valley, was incision during a time of increased runoff (Vandenberghe 1993) and therefore it has already not switched back and recovered alluvial fan sediments (Figs. 8 and 9). A new valley „storey„ has been developed after the incision representing the beginning of the new erosion - accumulation cycle.

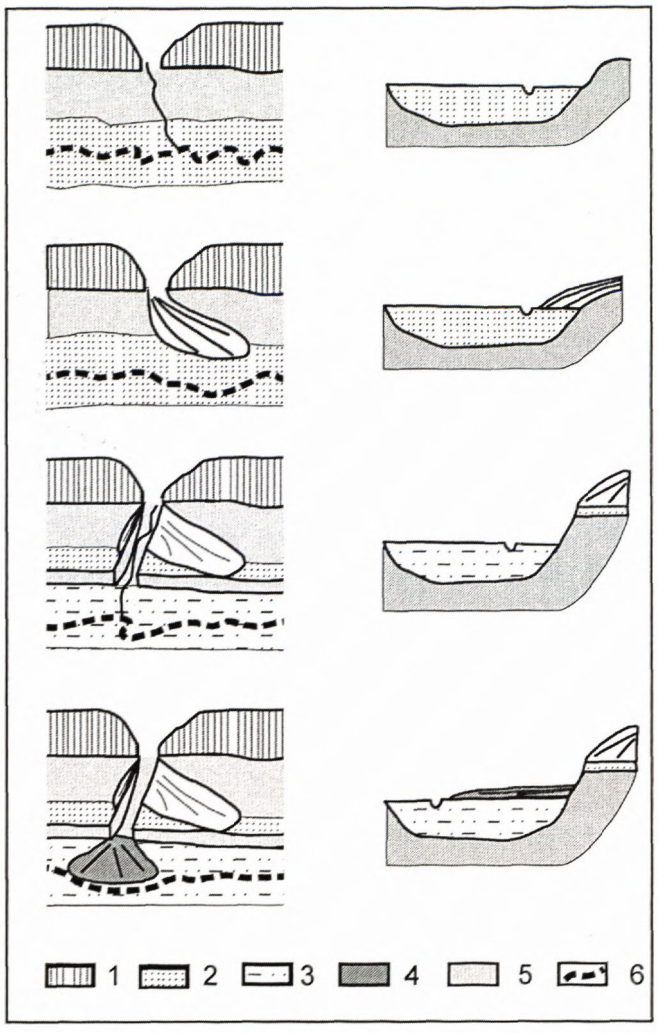

Fig. 8 Scheme of lateral shifting of axial river channel (Torys river) in interaction with deposition of alluvial fans. 1 – volcanics of the Slanské vrchy Mts., 2 – older fluvial deposits, 3 – recent fluvial deposits, 4 – recent alluvial fan, 5 – pre-Quaternary rocks, 6 – axi al river

Correlation of river terraces and alluvial fans of Torysa and Hornád river valley

The Torysa river is confluencing with the Hornád river in the southern part of Košice basin. There are four

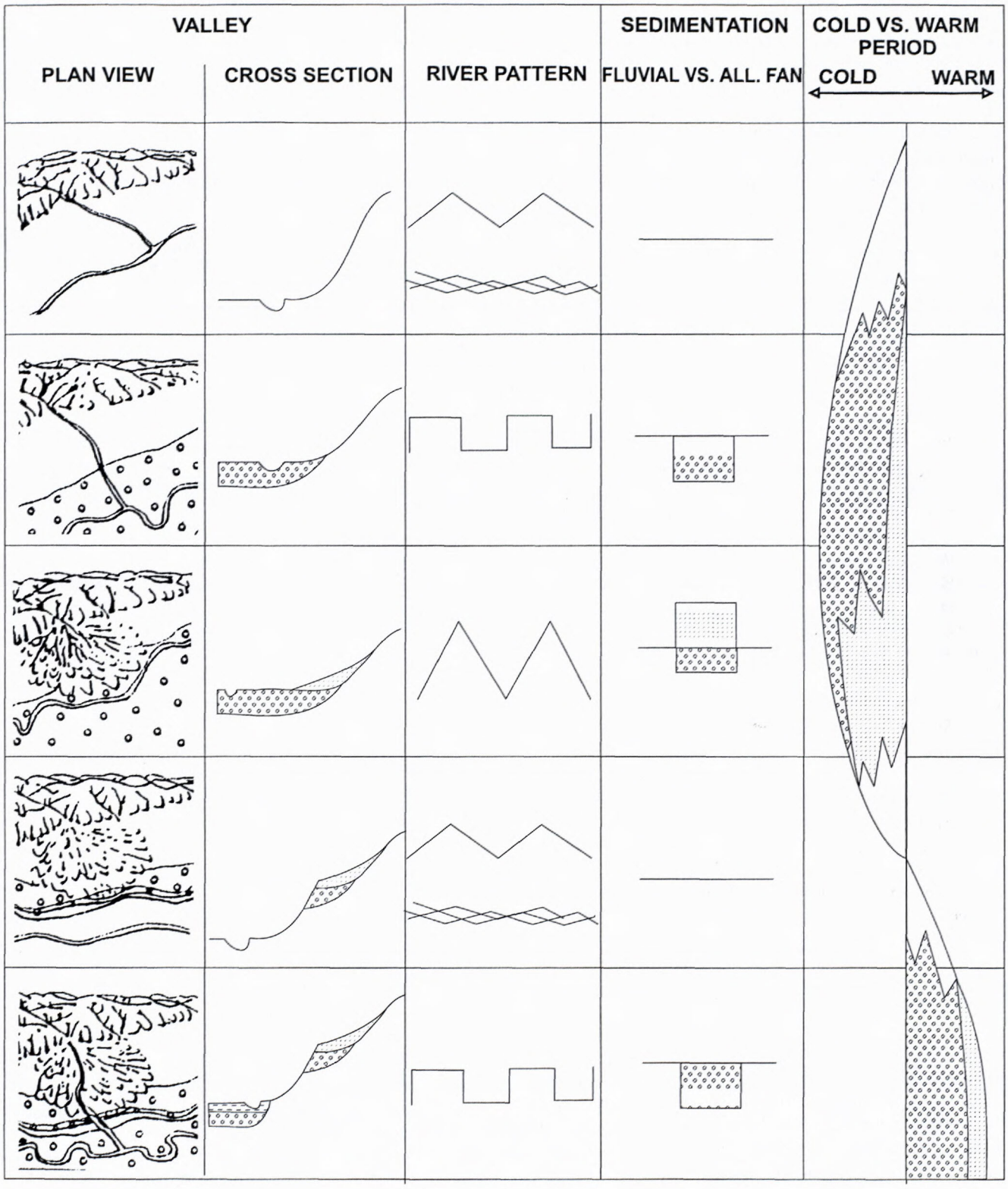

Fig. 9 Model showing succession in sedimentation of alluvial fans and fluvial sediments of axial valley rivers in the Košice Depression. Inferred river pattern and relationship to cold and warm periods is also shown.

terrace steps developed in the Torysa river and five steps in the Hornád valley. Their morphometry shows very similar evolution history of both valleys. The oldest fluvial accumulation is represented by step of the upper terrace system in the relative altitude 50 m above the recent flood plane. The Pliocene level is preserved in both valleys in about 120 m of relative altitude indicating the river incision about 70 m during the period of the lower Pleistocene. The missing sediments from this period suggest gradually increasing wide of the valleys responsible for the erosion of older fluvial deposits. Both rivers had maximum thickness of the flood plain in the lower part of

the Middle Pleistocene. The broad flood plain of the Hornád river that emerged from the gateway into a low depression relief north of the Košice (Fig. 1), resembled a large alluvial fan. At the end of the lower Middle Pleistocene glacial period (Mindelian), the fluvial sedimentation in this valley was suppressed to the east and the valley never reached the lower Middle Pleistocene expansion. Similar narrowing trend after the Early Pleistocene period is observed in the Torysa river valley and it was only interrupted in the Late Pleistocene when the increased erosion was responsible for denudation of the third middle terrace. The relative elevation of the terrace systems shows that the value of river incision between the accumulation periods has been very consistent in both valleys. A small difference between the incision values between the high and first middle terraces of rivers was caused by differentiated tectonic movements after the deposition of lower Middle Pleistocene fluvial and alluvial fan deposits (Janočko 1990). The consistent morphometry of younger terrace steps in both valleys suggests that this tectonic uplift took place in a very limited time span. A good correlation between the river systems in both valleys suggests that probably main factor causing the cyclic river incision and sedimentation was climatic change and tectonic development contributed only by a smaller extension to the valleys development. The different tectonic regime of the surrounding mountains in the Quaternary period is indicated by the different development of the alluvial fans in investigated valleys. The „telescopic„ structure of alluvial fans is typical for the Torysa river valley where the older fan segment has been entrenched in its head area and a lower segment has been developed in the lower position. The shift of the deposition loci away from the fan head and the concave surfaces of single segments suggests a relative stable fan - source area position during the development of the fan system. Different development is indicated by the alluvial fan structure in the Hornád valley. The oldest fan, related to the first middle terrace step, underlies the younger fans, which deposition locus has been shifted upstream, closer to the fan head. An active tectonic uplift of the source area during the fan development has been responsible for this type of fan structure.

Conclusion

The terraces of the Torysa river are arranged into four terrace steps and record evolution of the Torysa river valley since the Middle Pleistocene. In the Hornád valley five terrace steps record evolution of the valley since the Early Pleistocene. About 70 m deep vertical incision during the Early Pleistocene, indicated only by the difference of the Pliocene niveau and the first middle terrace, suggests widening of the valley connected to lateral erosion. This trend changed in the lower part of the Middle Pleistocene (Mindelian) when maximum width of both valleys has been reached as indicated by the most widespread fluvial and alluvial fan sediments. The vertical river incision between accumulation phases inferred from the terrace morphometry has almost been consistent in both river valleys and varies from 10 to 20 m. Well preserved overbank deposits suggest higher sinuosity river system. Superposition of alluvial fan deposits above the river terraces indicates sedimentation close to river incision phase, when there already was not enough time (and sediments) to overlie fan deposits. This suggests fan deposition at the end of the main fluvial sedimentation cycle at the glacial (stadial) termination. The different structure of fans in the Torysa and Hornád valleys resulted from tectonic activity of their source areas.

Acknowledgement

The study is a partial result of the project „Tectogenesis of sedimentary basins of the Western Carpathians" financed by the Ministry of Environment of the Slovak Republic. I am grateful for helpful reviews by Michal Kováč and Ivan Baráth.

References

Bull, W.B. 1964: Geomorphology of Segmented Alluvial Fans in Western Fresno County, California. Geological Survey Professional Paper, 352-E, 89-129.

Harčár, J. 1972: Šarišská vrchovina. Fyzicko-geografická analýza. Geografické Práce III, 1-2, 267 pp. (In Slovak, German. summ.).

Janočko, J. 1989a: Kvartérne sedimenty severnej casti Slanských vrchov. Mineralia Slovaca, 21, Košice, 141-145. (In Slovak, Engl. summ.).

Janočko, J. 1989b: Vplyv kvartérnej tektoniky na vývoj uzemia v severnej časti Košickej kotliny. Mineralia Slov., 21, Košice, 421-425. (In Slovak, Engl. summ.).

Janočko, J. 1991: K vývoju náplavových kužeľov Delne a Šebastovky v severnej časti Košickej kotliny. Mineralia Slov., 23, Košice, 61-66. (In Slovak, Engl. summ.).

Karoli, S. et al. 1987: Vysvetlivky k listu 1:25000 Košice 2. Manuscript – Geol. Survey of Slovak Republic Bratislava. (In Slovak).

Košťálik, J. 1986: Príspevok k poznaniu spraší a sprašových sedimentov v dolinách Popradu a Torysy na Východnom Slovensku. Geografický Časopis 38, 2-3, 274-285. (In Slovak, Engl. summ.).

Kvitkovič, J. & Plančár, J. 1975: Analýza morfoštruktúr z hľadiska súcasných pohybových tendencií vo vzťahu k hlbinnej geologickej stavbe Západnych Karpát. Geogr. Čas. 27, 4, 309-323, Bratislava. (In Slovak, Engl. summ.).

Leeder, M. R. 1982: Sedimentology. Process and Product. Allen & Unwin, London. 528 pp.

Michaeli, A. 1985: Príspevok k poznaniu terás Hornádu v Hornádskej kotline. Zbornik Prírodovedeckej fakulty v Prešove, roč. XXI, zv. 1, Prir. vedy, 51-75. (In Slovak).

Petro, L., Spišak, Z. & Polaščinová, E. 1984: Inžiniersko-geologická mapa, list Solivar. Manuscript, Dionýz Štúr Institute of Geology, Bratislava. (In Slovak).

Petro, L., Spišak, Z. & Polaščinova, E. 1986: Inžiniersko-geologicka mapa, list Kapušany. Manuscript – Geol. Survey of Slovak Republic Bratislava. (In Slovak).

Schumm, S.A. 1973: Geomorphic tresholds and complex response of drainage systems. In: Morisawa, M. (ed.): Fluvial geomorphology. Allen and Unwin, London, 299-310.

Siegenthaler, Ch. & Huggenberger, P. 1993: Pleistocene Rhine gravel: Deposits of a braided river system with dominant pool preservation. In: Best, J.L. & Bristow, C.S. (eds.): Braided rivers. Geological Society Special Publ. No. 75, 147-162.

Spišak, Z., Petro, L. & Polaščinova, E. 1985: Inžiniersko-geologická mapa, list Prešov. Manuscript – Geol. Survey of Slovak Republic Bratislava. (In Slovak).

Spišak, Z., Petro, L. & Polaščinová, E. 1987: Inžiniersko-geologická mapa, list Šarisské Michaľany. Manuscript – Geol. Survey of Slovak Republic Bratislava. (In Slovak).

Starkel, L. 1990: Fluvial Environment as an Expression of Geoecological Changes. Z. Geomorph.N.F., Suppl.-Bd.79, 133-152.

Vandenberghe,J. 1993: Changing fluvial processes under changing periglacial conditions. Z. Geomorph. N.F., Suppl.-Bd. 88, 17 - 28.

Vass, D. & Pristaš, J. 1979: Zhodnotenie zlomových systémov Košickej kotliny so zvláštnym zreteľom na oblasti medzi Ťahanovcami a Krásnou n.H.. Manuscript, Dionýz Štúr Institute of Geology, Bratislava. (In Slovak).

Slovak Geol. Mag., 7, 3(2001),231 – 235

Main advance directions and maximum extent of Elsterian ice sheet in the eastern part of the Šluknov Hilly Land, Northern Bohemia, Czechia

DANIEL NÝVLT

Czech Geological Survey, Department of Quaternary, Klárov 3/131, 118 21 Praha 1, Czechia, e-mail: nyvlt@cgu.cz

Abstract. During the geological mapping of Quaternary sediments in the eastern part of the Šluknov Spur nordic erratics have been recorded on places, where they were not found before. Only indicator erratics have been taken into consideration for the reconstruction of main advance directions and maximum extent of a continental ice sheet within the study area. Nordic indicators are scattered about the flat interfluves and on upper sideslopes of valleys (at altitudes 350-450 m a.s.l.) as a result of being left there as the remnants of a former basal till. That the ice sheet crossed over the flat interfluves NE of Šluknov was confirmed by records of these indicators.

Keywords: Nordic erratics, Elsterian ice sheet, Middle Pleistocene, Northern Bohemia, Czechia

Introduction

Much progress has been made in order to determinate the position of the maximum extent of the Pleistocene ice sheets in the marginal zone of central Europe, but there are still many places where the position of that line is uncertain, as in the Šluknov Hilly Land (Nývlt 1998). This is due to the removal of large volumes of glacial sediments by subsequent, mainly fluvial, erosion. The Šluknov Hilly Land lies in the westernmost part of the Sudeten Mountain System, and represents the northernmost spur of Czechia. Glacial deposits within the Šluknov Spur have not been studied in detail so far. It is believed that the ice sheet reached this area only once, and that these remained glacial sediments are of early Elsterian age (Grahmann 1933, Šibrava 1967, Eissmann 1975, 1997, Wolf and Schubert 1992, Nývlt 1998). However, the exact stratigraphic position of these sediments is due to the absence of any radiometric dating, and to the impossibility of a direct morphostratigraphical correlation with fluvial terrace system still open to debate.

In the last years new geological mapping at a scale of 1:10,000 for the Basic Geological Map of Czechia in 1:25,000 scale of the area of study has been undertaken by geologists of the Czech Geological Survey. The mapping of the whole Šluknov Spur began in 1998 and it is planned that it will be completed in 2001. The mapping of Quaternary deposits will also be focussed on the reconstruction of the maximum extent of the Elsterian ice sheet within the Šluknov Hilly Land. Final results will be presented as a GIS map, which will be one of the layers of the entire GIS system of Czechia.

The surface mapping took advantage especially of fresh-ploughed fields, mowed meadows and mole-hills. Only indicators, such as Baltic flints, Dala porphyries, Smíland granites, Áland porphyries and granitoids, have been marked on the map. These rocks place mainly relics of a basal till at positions, where the subsequent impact of fluvial erosion was insufficient to remove larger clasts. Finer matrix has usually been removed. Nevertheless tills were not widely affected in some places and will be studied in detail later.

Historical background

Hibsch (1896) described the reach of the ice sheet to Varnsdorf, to a maximum altitude of ~ 475 m a.s.l., which is considerably higher than it was believed by more recent authors. Nearly the same extent was presented by Šibrava (1967), unfortunately the Šluknov Spur was in a rather peripheral position in his work. The first detailed stratigraphy of glacial sediments within the wider area was established by Grahmann (1933). He suggested these accumulations in the lower parts (below ~ 420 m a.s.l.) of the Šluknov Spur were of Early Elsterian age. This opinion was also adopted by other authors such as by Fusán et al. (1967), Šibrava (1967), Eissmann (1975, 1997), and by Wolf and Schubert (1992). According to these authors the extent of the glaciation in the Šluknov Spur was limited to the area below ~ 420-450 m a.s.l.

The Geological Map of Czechia at a scale 1:50,000; sheet 02-22 Varnsdorf (Opletal et al. 1996) shows tills and glaciofluvial sediments in the southeastern and eastern part of the Šluknov Spur near Varnsdorf, Rumburk and Jiříkov, but the maximum extent of the ice sheet was not presented in this map. No glacial sediments are drawn in the northern part of this map in the surroundings of Šluknov, which were demonstrated by Šibrava (1967). For comparison of previous ideas on the maximum ice sheet extent see fig. 1.

Fig.1 The maximum extent of the Elsterian glaciation in the Šluknov Spur.

Results

During the mapping of Quaternary deposits at a scale of 1:10,000 on sheets Šluknov 02-221, Jiříkov 02-222 and Varnsdorf 02-224 (scale 1:25,000), new occurrences of nordic rocks have been found. The extent of glacial sediments on the sheet Varnsdorf is almost equal to that presented on the map in 1:50,000 scale (Opletal et al. 1996), the till remnants occur on sideslopes of the Mandava River in the surrounding of Varnsdorf. The results of a new mapping of Quaternary sediments by the author suggest, on the other hand, a larger glaciated region in the northern part of the spur (especially NE of Šluknov), than was indicated on the 1:50,000 map (Opletal et al. 1996), which is in good agreement with Šibrava's (1967) attempt. From the viewpoint of general geomorphology and with respect to the regional distribution of the erratics, it is possible to consider some hills (e. g. Jitrovník and Špičák) as nunataks.

Most occurrences of nordic indicators (Fig. 2) are scattered about the flat interfluves and on upper sideslopes of valleys N and E of Šluknov as a result of being left there as the remnants of a former basal till. The highest place bearing traces of nordic material is a hilltop (50°59.682' N, 14°31.833' E) near the road Šluknov-Jiříkov at an altitude of 450 m a.s.l. The occurrence of glacial deposits as high as 475 m a.s.l. (Hibsch 1896) cannot be confirmed. On the other hand, during the gas-main construction in 1998, sands and gravels with Baltic flints and nordic porphyries were exposed at the bottom of the Lesní Brook, SE of Šluknov (M. Opletal, pers. comm., April 2000). These ?glaciofluvial sediments are overlain by fluvial and colluvial deposits.

Glaciofluvial sands and gravels up to 10-15 m thick (proved by boreholes) in the northern part of the "Fukov Spur" are excavated near the Spree River. The sequence consists of two main sets of facies, the first one is horizontally more limited and is dominated by massive and trough cross-bedded sands and gravels partly of nordic origin (Fig. 3a), with the cross-bedding filling up shallow channels. In some parts the sand beds are horizontally or subhorizontally stratified. The second facies set is characterised by the sheet-like appearance of the majority of beds. Another obvious feature is absolute prevalence of well-sorted sands which is responsible for the uniform character of these mainly subhorizontal to horizontal and planar facies (Fig. 3b). Some sands are massive with no significant bedding. The sand and gravel se quence repre-

Fig. 2 Baltic flint (the orange clast top right of a lens cover) on the top of a mole-hill, lens cover ~ 60 mm (for the position of this find see Fig. 4).
Photo by D. Nývlt.

Fig. 3 Glaciofluvial sands and gravels from the "Fukov" sand pit, lens cover ~ 60 mm (for the position of sand pit see Fig. 4).
a: massive sands and gravels with rounded nordic clasts; b: sheet-like sand facies.
Photos by D. Nývlt.

Fig. 3b

sents a typical wiéde intermediate reach of a sandur, documenting the aggradation and then abandonment of channels during the glacier melting, changing with longer periods of sheetfloods with a lower drift energy of the stream.

Discussion and Conclusions

The highland relief and the marginal position of the Šluknov Hilly Land with respect to the Elsterian ice sheet enable us to study phenomena which were not pre-

Fig. 4 The main advance directions and maximum extent of Elsterian ice sheet in the eastern part of Šluknov Spur with finds of nordic indicators. Dashed line denotes uncertainty

served/are overlain by younger sediments in the lowlands of Germany and Poland; it is therefore very useful for the understanding of processes associated with the margin of continental glacier in a wider context. We can accept the outline of Šibrava (1967) as a very successful attempt to reconstruct maximum extent of the continental glacier in the northern part of the studied area, even he was focussed on the study of more eastward situated region. The other authors (Eissmann 1975, 1997, Wolf and Schubert 1992) did not reason about the ice sheet crossing over the flat interfluves N and NE of Šluknov (~ 385-400 m a.s.l.) and penetrating into the valley of Rožanský Brook and its tributaries, such as Lesní Brook (see above). This was confirmed by the author, who records the nordic indicators scattered about the interfluves and upper sideslopes of river valleys in altitudes 350-450 m a.s.l.

The distribution of nordic indicators in the eastern part of the Šluknov Spur has been used to reconstruct the main advance directions and maximum extent of Elsterian ice sheet on the map in the 1: 50.000 scale (Fig. 4). Furthermore, the position of the maximum ice sheet extent is essential for the preparation of GIS database and maps (not only for the project of the GAGE workgroup about glaciotectonic phenomena in central Europe). The study of the distribution of ice-transported indicators will follow until the next year, when the mapping of the whole Šluknov Spur should be completed.

The stratigraphic classification of these sediment remnants cannot be confirmed or challenged, therefore the Early Elsterian stratigraphic position of these accumulation proposed by Grahmann (1933) and followed by Šibrava (1967), Eissmann (1975, 1997), Wolf and Schubert (1992) and Nývlt (1998) remains still valid. However, the stratigraphic revision is required. As one possibility, the indicator statistics could be mentioned, because there is no possibility for a direct morphostratigraphic correlation with fluvial terrace system. Beside this, it exposes that a new mapping of glacial sediments in adjoining parts of Germany and a detail sedimentary research of described tills and till remnants will be very useful.

Acknowledgements

The author would like to thank Mojmír Opletal for numerous joint field investigations. In addition, I am grateful for helpful comments provided by Peter G. Hoare and Jaroslav Tyráček. This study was supported by mapping projects no. 2117 and 2138 of the Czech Geological Survey.

References

Eissmann, L., 1975: Das Quartär der Leipziger Tieflandsbucht und angrenzender Gebiete um Saale und Elbe. Schriftenreihe d. Geologischen Wissenschaften, 263 pp., Berlin.

Eissmann, L., 1997: Das quartäre Eiszeitalter in Sachsen und Nordostthüringen. Altenburger Naturwissenschaftliche Forschungen, 8, 98 pp., Altenburg.

Fusán, O., Kodym, O., Matějka, A., Urbánek, L. (eds), 1967: Geological Map of Czechoslovakia. 1 : 500,000. Central Geological Survey, Praha.

Grahmann, R., 1933: Die Geschichte des Elbetales von Leitmeritz bis zu seinem Eintritt in das norddeutsche Flachland. Mitteilungen d. Vereinigung f. Erdkunde, N. F., 132-194, Dresden.

Hibsch, J., 1896: Erläuterungen zur Geologischen Karte des Böhmischen Mittelgebirges, Blatt 1 (Tetschen). 90 pp., Wien.

Nývlt, D., 1998: Kontinentální zalednění severních Čech. Geografie - Sborník ČGS, 103, 4, 445-457, Praha. (In Czech).

Opletal, M. et al., 1996: Geologická mapa ČR 1:50.000 list 02-22 Varnsdorf. Czech Geological Survey, Praha.

Šibrava, V., 1967: Study on the Pleistocene of the glaciated and non - glaciated area of the Bohemian Massif. Sborník Geologických Věd, Antropozoikum, 4, 7-38, Praha.

Wolf, L., Schubert, G., 1992: Die spättertiären bis elstereiszeitlichen Terrassen der Elbe und ihrer Nebenflüsse und die Gliederung der Elster-Kaltzeit in Sachsen. Geoprofil, 4, 1-43, Freiberg.

Slovak Geol. Mag., 7, 3 (2001), 237 – 242

Geomorphic interpretation of landsat imagery for Western Estonia

JAMES S. ABER,[1] VOLLI KALM[2] and MIK LEWICKI[3]

[1]Earth Science Department, Emporia State University, Emporia, Kansas, 66801 USA.
[2]Institute of Geology, University of Tartu, Tartu, 51014 Estonia.
[3]Department of Geology, University of Delaware, Newark, Delaware, 19716 USA.

Abstract. The geomorphology of western Estonia is a mosaic of glacial and coastal landforms of late Pleistocene and Holocene age. We have utilized Landsat thematic mapper (TM) imagery to identify, classify, and interpret different landscape elements within this region. Image processing methods include false-color composites, normalized difference vegetation index (NDVI), tasseled-cap transformation, and isocluster unsupervised classification. The geobotanical approach was employed for interpretation of geomorphic features. The most effective false-color composite proved to be TM bands 3, 4, and 5 color coded as blue, green, and red respectively. Conspicuous geomorphic elements are peat bogs, moraines, eskers, and sand dunes. The synoptic quality of Landsat imagery allows for visual interpretation of regional landscape patterns related to ice lobes during deglaciation and to gradual emergence of coastal lands during postglacial times. Landsat imagery in combination with existing ground-based observations and maps provides for improved interpretation of regional geomorphology in western Estonia.

Key words: Estonia, glacial and coastal landforms, landsat imagery

Introduction

Estonia is situated at the eastern end of the Baltic Sea in a region that was subjected to multiple glaciations of the Fennoscandian ice sheet during the Pleistocene. Ice streams advanced from the north and northwest, repeatedly crossing the Baltic depression and ascending onto higher land to the south and east. Glacial erosion and deformation modified the Paleozoic bedrock substratum, and glacial deposition built up constructional landforms, particularly in the southern portion of Estonia. During each major glaciation, substantial crustal depression and rebound took place. Glacial lakes or interglacial seas occupied the Baltic depression and innudated the coastal lowland areas of Estonia. Following the last deglaciation, northwestern portions of Estonia have emerged, as the land raised relatively to the sea, and peat bogs have spread over sizeable portions of the country.

The goal of our research is to utilize Landsat thematic mapper (TM) imagery to identify, classify, and interpret different landscape elements within the lowland terrain of western Estonia. Both glacial and coastal geomorphic processes were important in shaping the modern landscape. The region has furthermore been subjected to a long history of human land use and modification. The land cover consists mainly of agricultural fields, forest, and peat bogs, which are the dominant features visible in Landsat TM images.

Geomorphic setting

Estonia has an area of more than 45,000 km^2, of which about one tenth is comprised of some 1500 islands and islets mainly in the west. Estonia's geomorphology acquired its present appearance under the influence of geological, glacial, biological, and anthropogenic factors, the relative importance of which has changed with time. The territory lies in a critical transition zone in the continental pattern of glacial geomorphology (Aber 1992). To the north and west, the Baltic zone of ice-sheet outflow was subjected to strong erosion during repeated Quaternary glaciations. This zone, which includes much of Finland and Sweden, is characterized by crystalline basement rocks that have been stripped of most soft sediment and soil cover. The outer geomorphic zone of glaciation to the south and east, in contrast, was a region of predominant glacial deposition and deformation of soft Paleozoic, Mesozoic, and Cenozoic sedimentary bedrock. This region is covered by a thick blanket of sediment that built up during repeated ice advances.

Estonia reflects this transition. The thickness of the Quaternary cover in the northwestern part of the territory is generally less than several meters, but in the southern part is up to 100-200 m thick (Raukas and Kajak 1997). The underlying bedrock is composed mainly of well-consolidated Ordovician and Silurian carbonate sedimentary strata in central and northern Estonia and poorly consolidated Devonian sandstone in southern Estonia. Owing to slight monoclinal dip of strata (10-15°S) and distinct lithological heterogeneity, the topography is cuesta-like, which exerted a great influence on ice movement and glacial erosion patterns.

In the territory of Estonia, glacial ice streams with different speeds and energies alternated regularly with ice-divide areas (Raukas and Karukäpp, 1993). Western Estonia, including Baltic islands, experienced strong

movement of the Riga ice lobe, which flowed toward the south-southeast (Punkari 1996). Central and southeastern Estonia, however, were interlobate regions that separated the Riga lobe from other major and minor ice lobes farther east. Many directions of ice movement resulted from expansion and contraction of these lobes and local sublobes in different phases. Estonia is, thus, situated in a position that was subjected to a complicated interplay of glacial erosion, deformation, and deposition many times during the Quaternary.

During late- and post-glacial time (last 12,500 years), a considerable area of Estonia was flooded by waters of large proglacial lakes and the Baltic Sea. Land began to emerge from the water as a result of gradual glacio-isostatic uplift. This is manifested in coastal expansion along with evidence for old strand lines inland from the present coast. Northwestern Estonia has uplifted at least 100 m relative to present sea level; whereas southern Estonia has raised up only several meters (Raukas 1997a). The result is tilting of landscape features, up to the northwest.

As glacial landforms of western Estonia emerged from the sea, they were exposed to wave erosion and beach sedimentation, which modified their exterior materials and forms. In general, glacial landforms of the western coastal region were reduced in height and smoothed during coastal emergence; whereas, beach and dune forms were built up. These various geomorphic processes have led to a complex mosaic of landforms and surficial deposits related to glaciation and coastal migration.

Image processing methods

Four Landsat thematic mapper (TM) datasets were selected from the 1980s (Table 1; Fig. 1). The datasets are nearly cloud free and represent spring and summer seasons. Landsat TM data have nominal resolution of 30 m in the

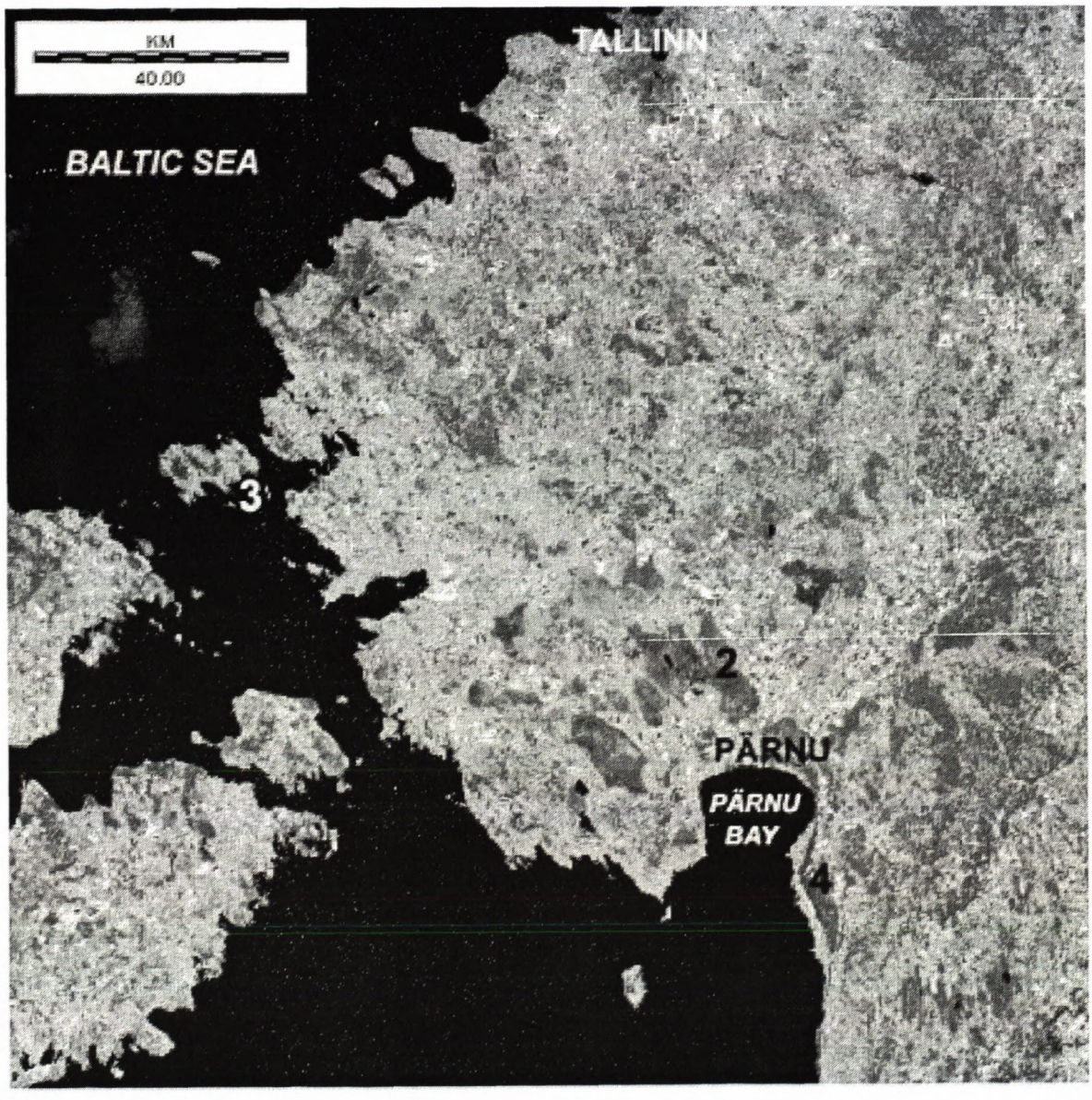

Table 1. Landsat TM datasets selected for analysis in this study. Scenes from path/row 188/19 include the mainland of western Estonia. Scenes from path/row 189/19 are centered on the Baltic islands of westernmost Estonia. All datasets contain less than 10% cloud cover. Landsat TM datasets acquired from the EROS Data Center, U.S. Geological Survey.

Scene ID number	Scene date	Path/row
LT5188019008620910	1986/07/28	188/19
LT5188019008617710	1986/06/26	188/19
LT4189019008813410	1988/05/13	189/19
LT5189019008618410	1986/07/03	189/19

visible (1, 2, 3), near-infrared (4), and mid-infrared (5, 7) bands, which were used in this investigation. The thermal-infrared (6) band was not utilized. Image processing was carried out using *Idrisi32* software following standard procedures for Landsat TM image enhancement and classification (Jensen 1996). The most useful techniques were false-color composites, normalized difference vegetation index (NDVI), tasseled-cap transformation, and isocluster unsupervised classification (Lewicki 2000). The most effective false-color composite proved to be TM bands 3, 4, and 5 color coded as blue, green, and red respectively. This composite was used as the basis for isocluster classification.

On the basis of previous experience in similar settings, the *geobotanical approach* was employed for interpretation of geomorphology (Aber and Ruszczynska-Szenajch 1997). Vegetation integrates many geomorphic variables, such as sediment and soil, land slope and aspect, and drainage. Thus, vegetation patterns, both natural and cultural, often reflect geomorphic conditions. With the geobotanical approach, vegetation, agriculture, and water bodies are primary clues for interpreting landscape elements.

In western Estonia, agricultural fields are found mainly in low-relief terrain underlain by loamy or sandy sediments. Steeper, hummocky lands are mostly forest covered. Till is the basis for spruce forest; sandy and peaty soils support pine forest. Peat bogs and mires in western Estonia are of the minerotropic type (Ilomets 1997), which developed from infilling of former lakes or marine embayments.

Various composite and classified images were examined visually and further classified to isolate selected types of vegetation, land use, and water bodies for geomorphic interpretation. The identities of Quaternary sediments and landforms were verified by reference to existing maps of Quaternary deposits (Kajak et al. 1999) and peat (Orru et al. 1993).

Geomorphic features

Peat bogs – Peat bogs are the most conspicuous features on Landsat TM images of western Estonia (Fig. 2). Peat bogs have a low level of vegetation activity combined with high moisture content that tend to depress reflection in band 4, the near-infrared. This results in low NDVI values and a relatively dark appearance in composite images. Peat bogs are further identified by their large size and irregular, rounded shapes in the landscape.

Peat bogs are divided into two general types--fens and raised bogs--based on position of peat in the landscape and types of plant species (Orru 1997). Fens develop in lowlands with nutrient-rich soil and near-surface ground water. Fens support numerous sedges (*Carex*), reeds, horsetails, and several species of trees (*Betula, Picea, Pinus*). With growth through time, fens may evolve into raised bogs, in which elevated peat accumulation is fed solely by precipitation. Peat mosses, namely *Sphagnum*, predominate along with some horsetail and pine. Fens and raised bogs are clearly distinguished in Landsat images on the basis of differences in vegetation cover (Fig. 2).

In the Pärnu region, fens and raised bogs are situated in elongated, shallow depressions that trend toward Pärnu Bay (Fig. 2). Several of the bogs are located behind a major end moraine that marks the Pandivere stage of deglaciation (Karukäpp and Raukas 1997; Kajak et al. 1999). This leads us to suppose that bog depressions were eroded as shallow troughs by movement of the ice lobe and/or by subglacial melt-water flowing toward Pärnu Bay.

Moraines – Moraines cannot be separated from other types of landforms. Moraines can, however, be recognized as linear borders between areas of quite different land use (Fig. 2). In general, hummocky topography of moraines is characterized by spruce forest with numerous peat bogs situated on the upglacier side. The proximal ice-free vicinity is covered by intensive agricultural land use based on low-relief, sandy and loamy soils of outwash fans and plains.

Among moraines, those of the Pandivere stage of deglaciation are especially prominent in the area northeast of Pärnu (Fig. 2). A moraine of this stage is also visible northwest of Pärnu. These moraines represent the lateral margins of the Pandivere ice lobe. However, the Pandivere ice margin lacks an end moraine in the immediate vicinity of Pärnu. This is the zone toward which peat bogs converge from the north. We speculate that strong melt-water flow at the ice margin either washed away or prevented deposition of an end moraine in this zone.

Eskers and drumlins – Eskers and drumlins are relatively rare in the lowlands of western Estonia according to the map of Quaternary deposits (Kajak et al. 1999). An exception to this situation is the island of Vormsi and adjacent vicinity (Fig. 3). Two mapped eskers cross Vormsi from northwest to southeast, and a third esker has a similar orientation on the adjacent mainland. These eskers are identified on the Landsat imagery by their distinctive shapes, marked by peninsulas, as well as differentiated land-use patterns.

Nearby small islands – Harilaid, Eerikulaid, Hobulaid, Rukkirahu, and Kuivarahu – display similar shapes and positions, which we suspect may be eskers (Fig. 3). Rukkirahu and Kuivarahu could be extensions of the western esker on Vormsi; imagery indicates a shallow linear connection between these islands on the seafloor. Hobulaid might be an extension of the eastern Vormsi esker. Hari-

Slovak Geol. Mag., 7, 3 (2001), 237 – 242

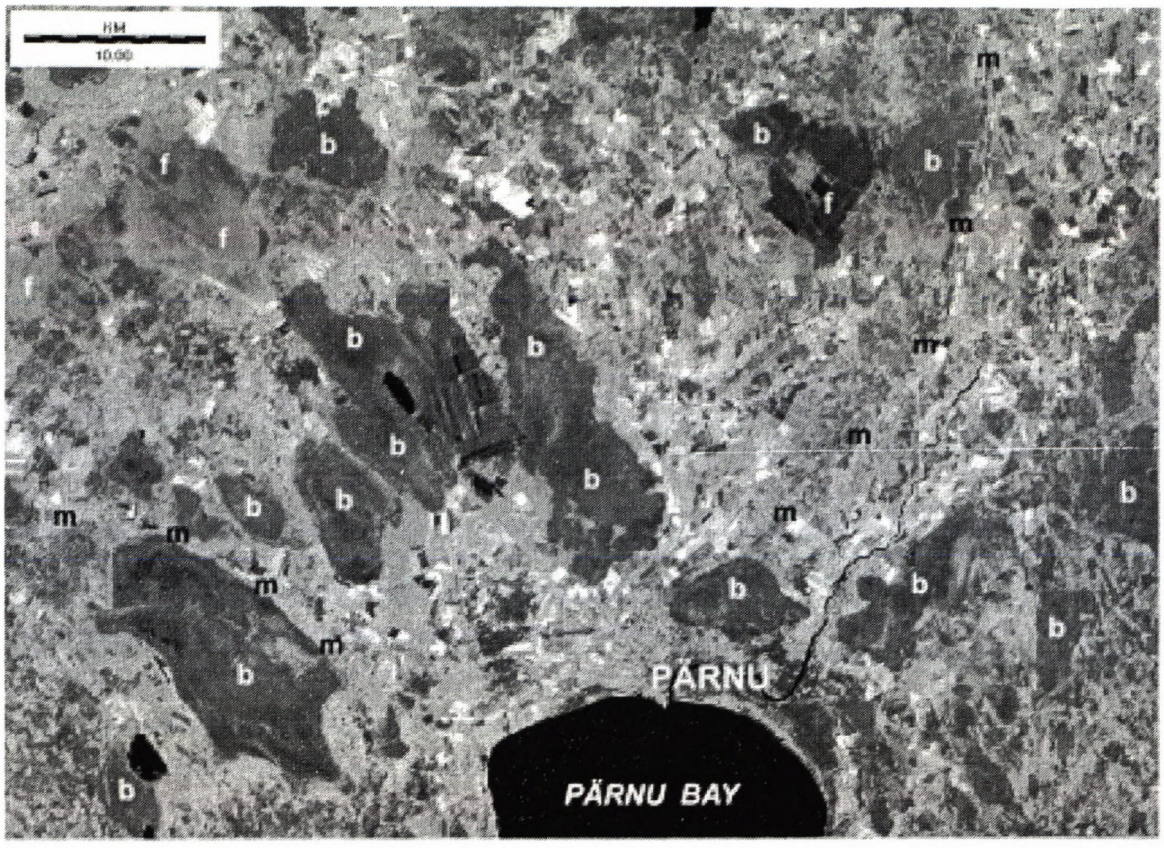

Fig. 2. Landsat TM scene of the Pärnu region, 28 July, 1986, band 4 (near-infrared). Dark gray zones depict large peat bogs: f = fen, b = raised bog. Lateral moraines of the Pandivere glacial stage are indicated by "m" northeast and northwest of Pärnu.

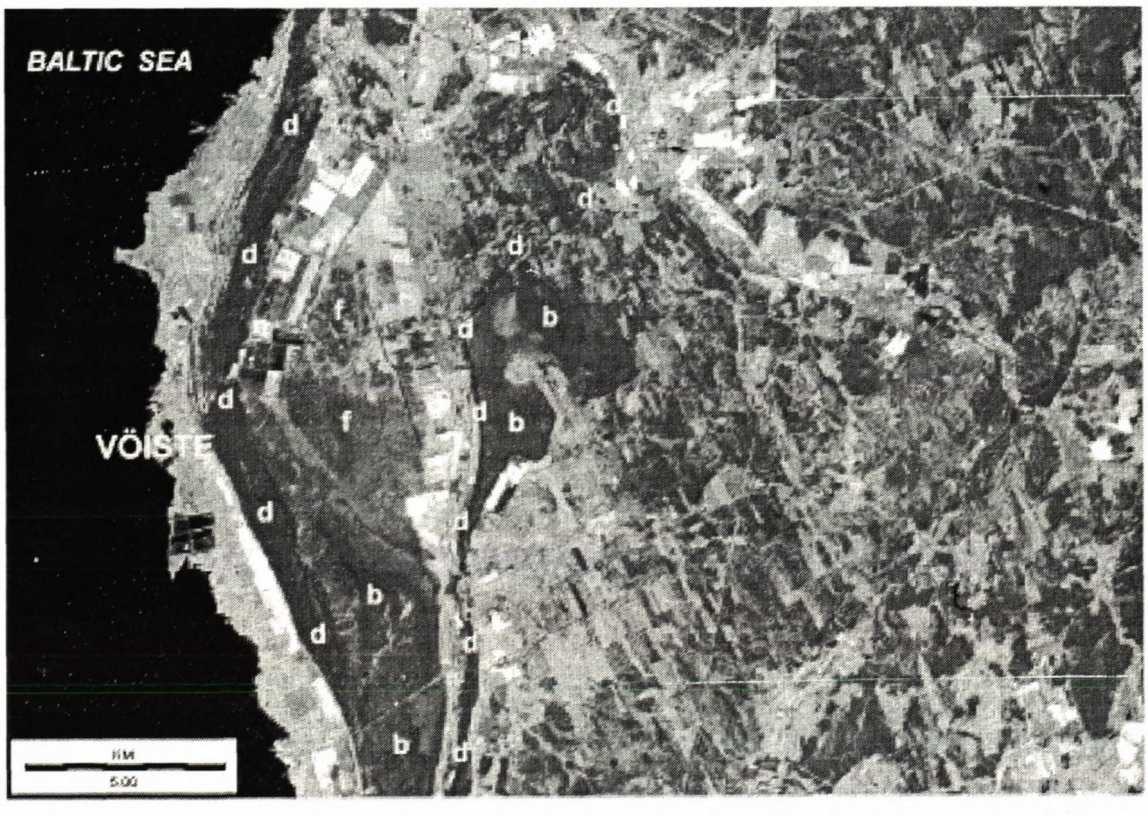

Fig. 3. Landsat TM scene of the island of Vormsi and adjacent mainland, 28 July, 1986, band 4 (near-infrared). The positions of three known eskers are indicated by "e." The eskers form distinctive peninsulas on the northern and southern coasts of the island. Suspected eskers are represented by the small islands of Harilaid, Eerikulaid, Hobulaid, Rukkirahu, and Kuivarahu.

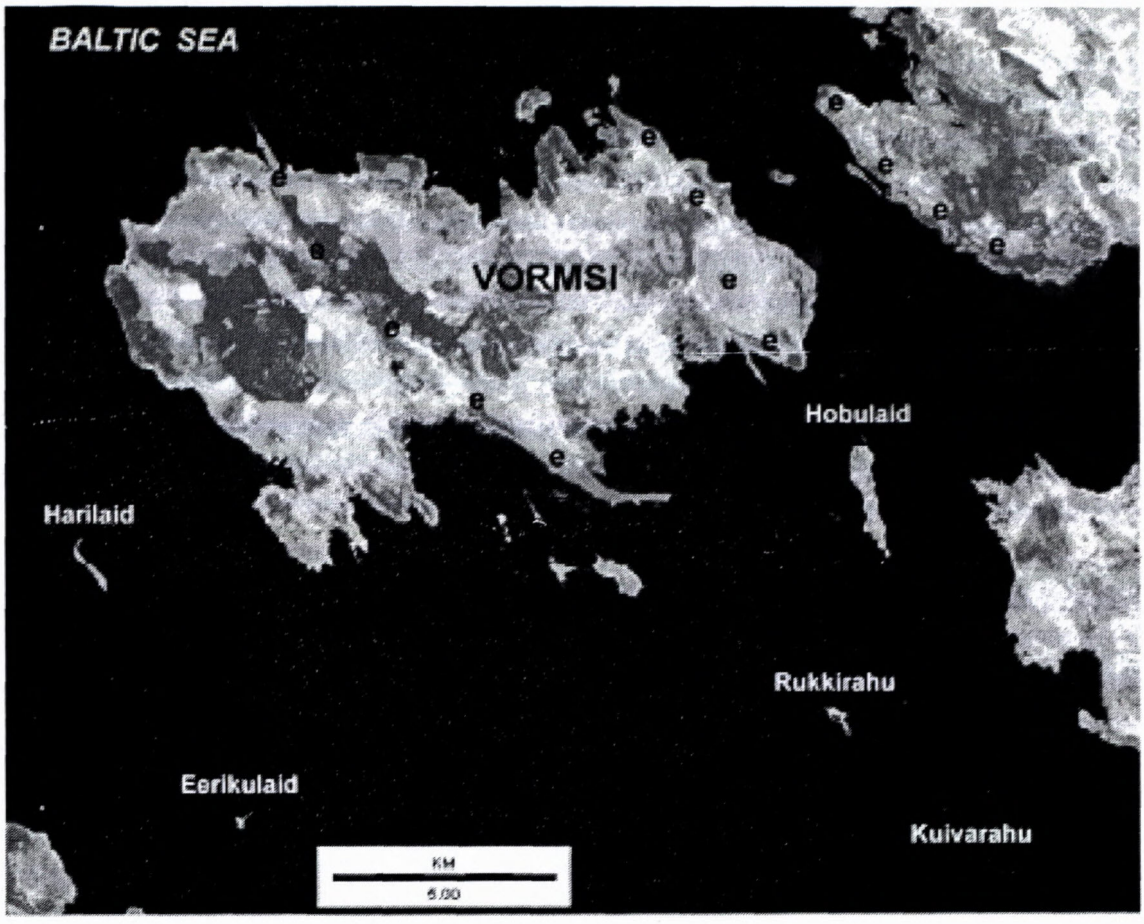

Fig. 4. Landsat TM scene of the southernmost Baltic coast of mainland Estonia, 28 July, 1986, band 4 (near-infrared). Two sets of sand dunes (d) are marked. Peat bogs are located behind each dune complex.

laid appears to be another esker west of Vormsi, and Eerikulaid may be an extension of this esker. All the known and suspected eskers follow a NW-SE trend that parallels local ice movement of the Palivere stage of deglaciation (Karukäpp and Raukas 1997). The eskers are interpreted by us as deposits of subglacial streams draining through an ice-lobe depresssion toward the Palivere glacial limit, which is situated a few km to the south of the Vormsi vicinity.

The eskers of Vormsi, nearby islands, and adjacent mainland are covered by coastal sediments of the Limnea Sea (Kajak et al. 1999), which developed about 4000 years ago (Raukas 1997a). The present land regions have emerged since the Limnea Sea regressed from the region. During the emergence, the eskers were subjected to wave erosion and beach development. Eventually the eskers of Vormsi and the mainland were uplifted above the shore zone. The uplift process continues today with the emergence of small islands west and south of Vormsi.

Sand dunes – Sand dunes form conspicuous linear or arcuate trends parallel to the coast in many parts of western Estonia (Fig. 4). Sand dunes are typically developed on top of former beach ridges. In several locations, multiple generations of dune ridges may be identified inland from the present coast. Sand dune ridges are characterized by pine forests, and peat bogs are commonly developed in former lagoons behind dune ridges.

The impressive dune ridges at Vöiste developed during transgression of the Litorina Sea, about 7000 years ago (Raukus 1997a, 1997b). The main dune complex parallels the modern coast and is about one km in width (Fig. 4). Raised bogs and fens are located behind the dune complex. Another narrow dune ridge is clearly evident inland from the main ridge. It also has a peat bog situated behind it. Only the southern portion of this second dune ridge is depicted on the map of Quaternary deposits (Kajak et al. 1999). Landsat imagery reveals that the second dune ridge extends farther to the north, where it defines a large curved embayment in the former coast.

Conclusions

Landsat TM imagery has proven effective for identifying various glacial and coastal landforms in the lowlands of western Estonia. The false-color composite based on TM bands 3, 4, and 5 was most useful for general interpretation and classification based on the geobotanical approach to recognizing landscape elements. Among the most conspicuous geomorphic features are peat bogs, moraines, eskers, and sand dunes. The synoptic quality of Landsat imagery allows for visual interpretation of regional landscape patterns related to ice lobes during deglaciation and to gradual uplift of coastal lands during

postglacial times. Landsat imagery in combination with existing ground-based observations and maps provides for improved interpretation of regional geomorphology in western Estonia.

References

Aber, J.S. 1992. Glaciotectonic structures and landforms. *Encyclopedia of Earth System Science*, vol. 2. Academic Press, San Diego. p. 361-378

Aber, J.S. and Ruszczynska-Szenajch, H. 1997. Glaciotectonic origin of Elblag Upland, northern Poland, and glacial dynamics in the southern Baltic region. *Sedimentary Geology* 111:119-134.

Ilomets, M. 1997. Genesis and development of mires. *In*, Raukas, A. and Teedumäe, A. (eds.), *Geology and mineral resources of Estonia*, Estonian Academic Publishers, Tallinn. p. 293-298.

Jensen, J.R. 1996. *Introductory digital image processing: A remote sensing perspective.* Prentice Hall Series in Geographic Information Science, 316 p.

Kajak, K., Raukas, A., Karukäpp, R., Rattas, M. and Tomberg, U. 1999. *Quaternary deposits of Estonia.* Scale 1:400,000. Geological Survey of Estonia.

Karukäpp, R. and Raukas, A. 1997. Deglaciation history. *In*, Raukas, A. and Teedumäe, A. (eds.), *Geology and mineral resources of Estonia.* Estonian Academic Publishers, Tallinn. p. 263-267.

Lewicki, M. 2000. *Landsat imagery of Estonia.* Unpub. Master's thesis, Emporia State University.

Orru, M. 1997. Mineral resources: Peat. *In*, Raukas, A. and Teedumäe, A. (eds.), *Geology and mineral resources of Estonia.* Estonian Academic Publishers, Tallinn. p. 337-346.

Orru, M., Sirokova, M., Veldre, M. et al. 1993. *Eesti sood* (Estonian peat). Scale 1:400,000. Geological Survey of Estonia.

Punkari, M. 1996. *Glacial dynamics of the northern European ice sheets.* Academic Dissertation, Faculty of Sciences (Geology), University of Helsinki, 603 p.

Raukas, A. 1997a. Evolution of the Baltic Sea. *In*, Raukas, A. and Teedumäe, A. (eds.), *Geology and mineral resources of Estonia.* Estonian Academic Publishers, Tallinn. p. 268-274.

Raukas, A. 1997b. Holocene terrestrial processes: Aeolian activity. *In*, Raukas, A. and Teedumäe, A. (eds.), *Geology and mineral resources of Estonia*, Estonian Academic Publishers. Tallinn. p. 290-293.

Raukas, A. and Kajak, K. 1997. Quaternary cover. *In*, Raukas, A. and Teedumäe, A. (eds.), *Geology and mineral resources of Estonia.* Estonian Academic Publishers, Tallinn. p. 125-136.

Raukas, A. and Karukäpp, R., 1993. Geomorphology in Estonia. *In* Walker, H.J. and Grabau, W.E. (eds.), *The Evolution of Geomorphology.* J. Wiley & Sons, New York. p. 135-142.

Slovak Geol. Mag., 7, 3(2001),243 – 246

Glaciotectonic deformation pattern in the Mummocky moraine in the distal part of Saagjärv Drumlin Field, East-central Estonia

MARIS RATTAS[1] and VOLLI KALM[2]

[1]Institute of Geology, University of Tartu, Vanemuise 46, 51014 Tartu, Estonia; Email: mrattas@ut.ee
[2]Institute of Geology, University of Tartu, Vanemuise 46, 51014 Tartu, Estonia; Email: vkalm@math.ut.ee

Abstract. In the distal part of Saadjärv Drumlin Field, east-central Estonia, an area of hummocks resting on top of drumlins occur. Determined glaciotectonic structures indicated by lithostratigraphic and superposition records suggest that deforming processes took place during at least two different glacial episodes. Deformation structures are presented in two different diamicton layers which are separated from each other by undeformed in its upper part sand and gravel sequence. The dislocation of the lower, Early Weichselian Valgjärve Till, is a result of ice push or the structure is formed by gravitational loading of a semi-liquid plastic material into the basal crevasses. The upper, Late Weichselian Võrtsjärve Till, which is capping the hummocks was definitely deposited and deformed during the final glacial advance by deforming pressure from W to E. During the ice recession the study area was not only affected by dead ice processes but the front of massive ice was probably in equilibrium state for a short time intervals and a lateral pressure resulted sediment deformations at and below the ice margin.

Keywords: diamicton, glaciotectonic deformation, hummocky moraine, drumlins, Saadjärv Drumlin Field, Estonia

Introduction

Glaciotectonic features and origin of glaciodislocations has been discussed broadly (Croot 1988, Aber *et al.* 1989, Warren & Croot 1994). The term glaciotectonic refers to structures and landforms created by glacially induced deformation of pre-existing substratum (Aber 1982) by the active or dead ice condition (Levkov 1980). Many different kinds of glaciotectonic landforms and structures, resulting from the active glacier movement, have been recognized on the territory of Estonia. Among others ridges and hills, including drumlins, built of disturbed Quaternary sediments are the most common glaciotectonic landforms in Estonia (Rattas & Kalm 1999). Only a few studies have dealt with the deformation structures in greater detail describing the role of deformations on the formation of entire landform. Previous studies (Orviku 1930, Miidel *et al.* 1969) described glaciotectonic megablocks of pre-Quaternary deposits in northern Estonia, where the Quaternary cover is very thin or even lacking.

This paper describes glaciotectonic structures in hummocks resting on the drumlins in the distal part of Saadjärv Drumlin Field, east-central Estonia (Fig. 1). Previous studies (Raukas et al. 1971) have described this group of hummocks as kames or small kame field formed in dead-ice conditions in connection with the recession of the glacier from the drumlin field area. However, determined glaciotectonic deformations of sediments in the hummocks at Inglimägi Hill point to its complicated formation process at or below active ice margin.

The Inglimägi Hill rises up to 15 m above the surrounding area, whereas the altitude of the hill top reaches 85 m a.s.l. The hill rests on the top of drumlin and consists of massive or rhythmically-bedded gravel (Gms-Gm) and fine sand (Sm) in thickness of 16-23+ m which is covered by 2-6 m thick reddish-brown massive sandy diamicton layer (Dmm) (Fig. 2). According to drilling data there is a second till horizon below of the glaciofluvial deposits at a depth of 58-65 m a.s.l. Surface of the lower, greyish-brown diamicton (Dmg) apparently denotes also the drumlin's upper surface under the Inglimägi Hill.

Earlier, in the vicinity of the study area, the glaciotectonic deformation structures were described at the site of buried Holsteinian interglacial deposits at Kõrveküla. In this section interrupted layers and dissected blocks of sapropelite were described (Liivrand & Saarse 1983, Levkov & Liivrand 1988, Liivrand 1991). It is not clear during which ice advance and from where the interglacial deposits were taken and moved into their present location. The purpose of the present investigation is to demonstrate the role of glaciotectonic processes in formation of hummocky moraine relief, to determine the direction of deforming force and reconstruct glaciotectonic history of the study area.

Deformation pattern

All the studied deformed successions were found in the Inglimägi gravel pit, in NW part of the Inglimägi Hill, and described in open sections of a nongrooved remnant in the middle part of the pit (Fig. 2). In order to reveal the types of deformations and to determine the direction of deforming force, orientation and dip of deformed beds were measured in sections Inglimägi 1 and 2. In the sec-

Slovak Geol. Mag., 7, 3(2001),243 – 246

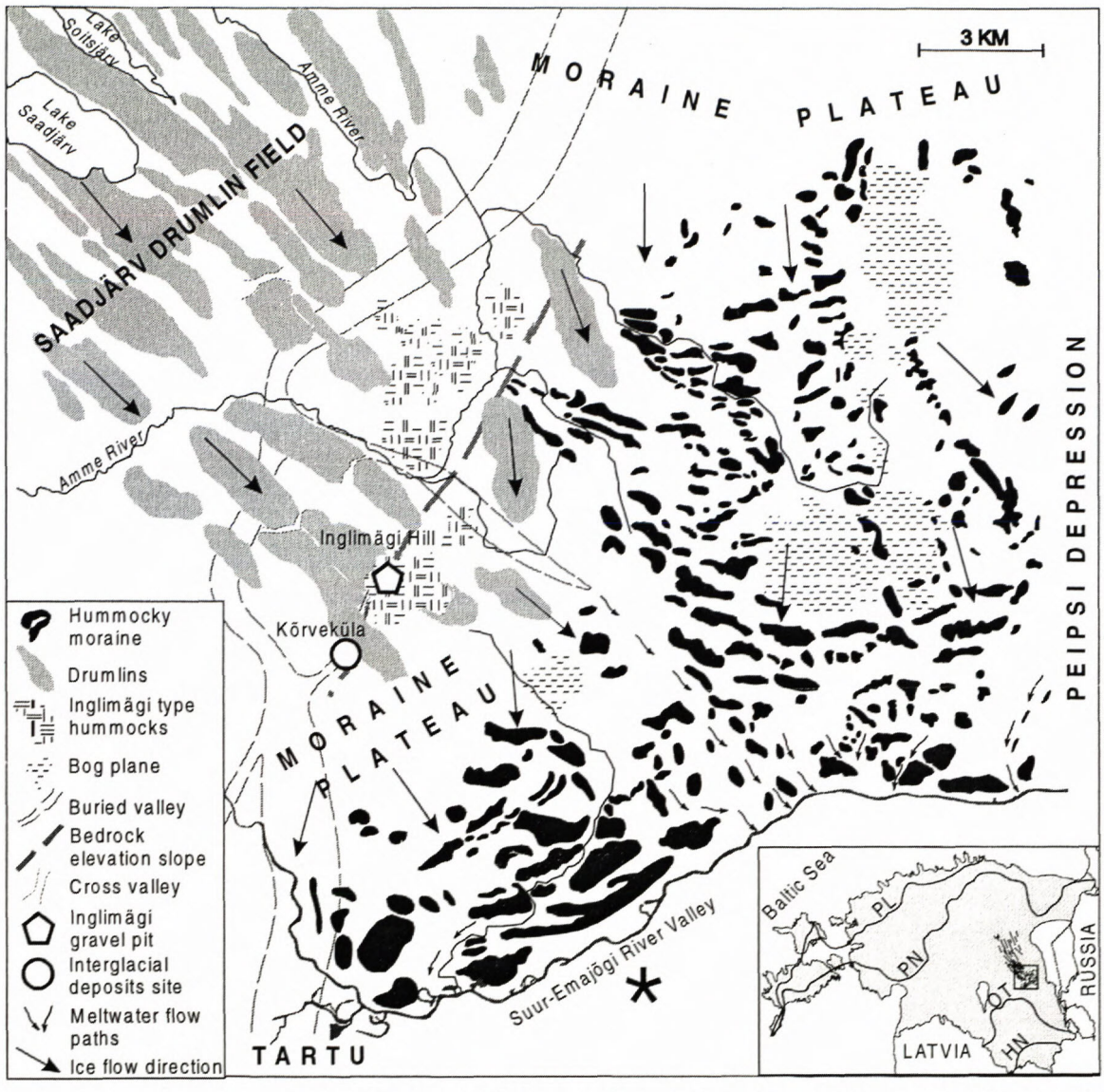

Fig. 1. A map showing the location of the Inglimägi Hill and the general morphology of the surrounding area. A scheme right blank on the map include ice margin positions during the Weichselian final deglaciation (HN-Haanja, OT-Otepää, PN-Pandivere, PL-Palivere ice marginal zones) and the location of the study area.

tion Inglimägi 3 an indistinct body of greyish-brown diamicton (Dmg) crops out. This diamicton is most probably derived from the till horizon underneath the meltwater sediment complex, which earlier was determined only in boreholes.

Section Inglimägi 1. Strongly deformed strata of the stratified diamicton (Dms) were found in NS oriented part of the open section (Fig. 2/1). Interrupted unconnected blocks of this diamicton (Dms) are incorporated into the basal layer of the overlaying massive silty-sandy matrix-supported diamicton (Dmm). Also lenses of fine sand and gravel from underlaying meltwater sequence are pushed to the surface of the stratified diamicton (Dms). Occasionally between the interrupted blocks of stratified diamicton (Dms) choatic pebbles are heaped up. The deformed part of the section is ovelain by 3-4 m thick massive, clast supported diamicton (Dmm).

Section Inglimägi 2. Glaciotectonic deformations in the basal layer of the uppermost massive diamicton (Dmm) are represented by thrust slices with dips of strata between 10-45°. Due to ice shoving of pre-existing meltwater deposits some sand and gravel lenses lie almost in vertical position (Fig. 2/2). Determined structures show that the deformations were caused by the pressure from 278° W (Fig. 2). Such structure could be interpreted as a part of fold or diapir formed during plastic deformation.

Section Inglimägi 3. An indistinct body of greyish-brown graded diamicton (Dmg) derived probably from the lower till horizon which is not cropping out in the gravel pit. The boundary between mixed unconsolidated diamicton and meltwater sand is not distinct (Fig. 2/3). According to drilling data the lower till horizon is laying at an altitude of 58-65 m a.s.l., that is about 4-5 m below the bottom of the gravel pit (Fig. 2). Most likely the body of the greyish-brown diamicton (Dmg) in the middle of rhythmically-bedded glaciofluvial sand (Sm) is a dislocation in the block or vein shape either pushed by the ice on the surface of earlier deposited sediments, or formed by

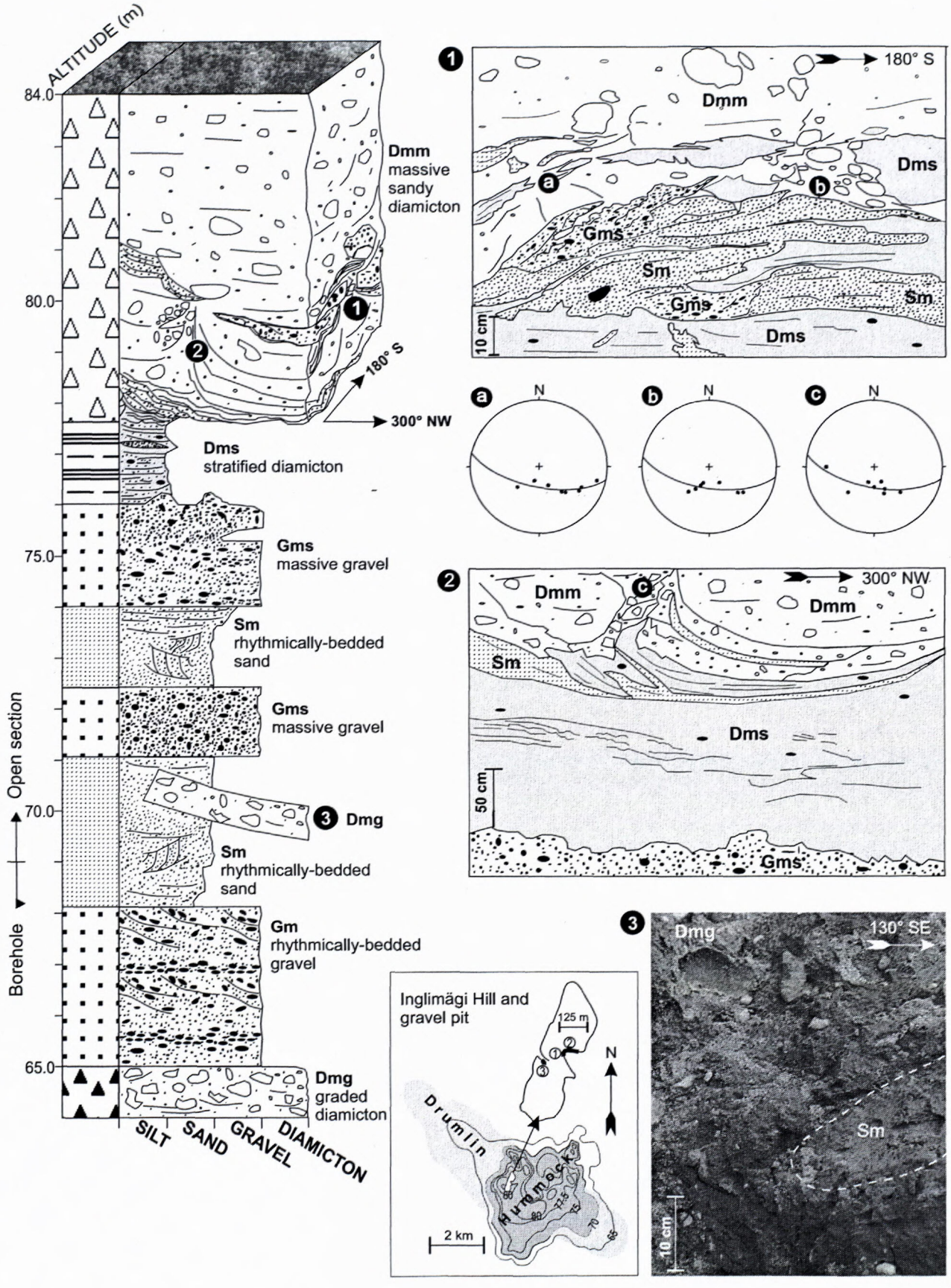

Fig. 2. General log of the hummocks at the Inglimägi Hill showing lithostratigraphy and deformed beds displayed in the Inglimägi gravel pit. Orientations of strata and shear plains are marked on the lower hemisphere of the stereographic Schmidt projection. Lithostratigraphical codes by Eyles et al. 1983.

gravitational loading of a semi-liquid plastic material into the basal crevasses of the ice.

Origin and history of deformation

Deformed suite of glacigenic deposits is located at the margin of Devonian sandstone terrain covered by till-cored hummocky moraine in south-east and drumlinized topography in north-west (Fig. 1). Deformation structures occur in two different diamicton layers which are separated from each other by undeformed meltwater sand/ gravel sequence (Fig. 2). According to the lithostratigraphic record of the area (Kajak 1965, Raukas 1978, Rattas 1997) the lower greyish-brown till horizon belongs to the Early Weichselian (Valgjärve Till) which occurs in cores of many drumlins in the Saadjärv Drumlin Field area. Controversial viewpoints were presented regarding the origin of the glaciofluvial deposits between two uppermost till horizons in drumlins' structure. In most cases they were interpreted as meltwater deposits of the Early Weichselian (Kajak 1965, Raukas 1978, Rattas 1997). However, in the southeastern part of the Saadjärv Drumlin Field they correlate with the meltwater deposits which accumulated during the Late Weichselian final deglaciation in stagnant ice phase, owing to kame and kettle topography (Raukas et al. 1971, Rõuk 1977). The uppermost reddish-brown massive till horizon has been correlated with the Late Weichselian (Võrtsjärve Till) and was deposited subglacially or by melting of dead ice rafts.

Presumably the deformations in the hummocks of Inglimägi Hill were formed at least during two different glacial episodes between of which accumulation of meltwater deposits took place. As indicated by the lithostratigraphy and the superposition records, the deforming process of Early Weichselian Valgjärve Till had to form before deposition of the glaciofluvial sequence overlaying the dislocation. The block or vein shape dislocation of the greyish-brown graded diamicton (Dmg) has inserted into the rhythmically-bedded fine grained sand (Sm) at the depth of 70 m a.s.l. Unfortunately, more detailed palaeogeographic reconstrustions are difficult, because of the lower boundary of dislocation can not be followed in the open section.

Deformations in the stratified diamicton (Dms) and uppermost massive diamicton (Dmm) were initiated by the final recession of the Late Weichselian ice sheet which receded from the area between Otepää and Pandivere stages, 12 600 and 12 250 BP, respectively. Hummocky moraine relief between the Saadjärv Drumlin Field and the Suur-Emajõgi River Valley (Rõuk 1977) refers to the contact of two different ice lobe flows - southerly direction flow along the Peipsi depression, and southeasterly direction flow over the drumlin field area, streamlining the drumlins. Adjoining of the two ice lobes caused the ice stagnantion and below the outer stagnant margins of ice lobes the hummocky moraine was produced. Deformations were caused by a small readvance of the active ice front from the west by the ice pressure to the underlaying semi-liquid glacial deposits.

Conclusions

The glaciotectonic deformation pattern in the hummocks of Inglimägi Hill has a relatively small size and the distribution of the structures suggests, that the deformations occured during two different ice advance episodes. As indicated by the lithostratigraphic record, the deforming process of the Early Weichselian Valgjärve Till had to take place before deposition of the glaciofluvial deposits overlaying the dislocation. Deformations in the Late Weichselian Võrtsjärve Till were initiated by the very last ice lobes in the area. The Saadjärv Drumlin Field area was not only affected by dead ice processes but the front of massive ice was probably for a short time intervals in equilibrium state, when a lateral pressure was causing sediment deformations at and below the ice margin.

Acknowledgements

The research was financially supported by the Estonian Science Council grants DBGGL 0754 and TBGGL 0550.

References

Aber, J.S. 1982. Model for glaciotectonism. *Bull. Geol. Soc. Denmark*, 30: 79-90.

Aber, J.S., Croot, D.G., Fenton, M.M. (Eds.) 1989. *Glaciotectonic Landforms and Structures.* Kluwer Academic Plublisher, Dordrecht, Netherlands, 200 p.

Croot, D.G. (Ed.) 1988. *Glaciotectonic Forms and Processes.* A.A. Balkema, Rotterdam, Netherlands, 212 p.

Eyles, N., Eyles, C.H., Miall, A.D. 1983. Lithofacies types and vertical profile models; an alternative approach to the description and environmental intepretation of glacial diamict and diamictite sequences. *Sedimentology*, 30: 393-410.

Kajak, K., 1965. On the geology of the Saadjärv drumlin field. In: *Lithology and stratigraphy of Quaternary deposits of Estonia,* 23-28. Tallinn (in Russian).

Levkov, E. 1980. *Glaciotectonism.* "Nauka i Technika", Minsk, Belarus, 280 p. (in Russian).

Levkov, E., Liivrand, E. 1988. On glaciotectonical dislocations of interglacial deposits in Karuküla and Kõrveküla sections (Estonia). *Proc. Acad. Sci. Est. S.S.R. Geology*, 37(4): 161-167 (in Russian).

Liivrand, E. 1991. Biostratigraphy of the Pleistocene deposits in Estonia and correlations in the Baltic region. Stockholm University (Doctoral Thesis). Department of Quaternary Research, Report 19, 114 pp.

Liivrand, E., Saarse, L. 1983. Interglacial deposits in Kõrveküla section (South-eastern Estonia) and their stratigraphic importance. *Palynologic researches in geologic studies of the Baltic Region and the Baltic Sea.* Riga, 41-50 (in Russian).

Miidel, A., Paap, Ü., Raukas, A., Rähni, E. 1969. On the origin of the Vaivara Hills (Sinimäed) in NE Estonia. *Proc. Acad. Sci. Est. S.S.R. Chemistry. Geology,* 13(4): 370-376 (in Russian).

Orviku, K. 1930. Die Glazialschollen von Kunda-Lammasmägi und Narva-Kalmistu (Eesti). *Geoloogia Instituudi Toimetised,* 23, 8 p.

Rattas, M. 1997. Moreenide litoloogia ja stratigraafia Saadjärve voorestikus (Lithology and stratigraphy of tills in Saadjärv Drumlin Field area). *MSc thesis*, Institute of Geology, University of Tartu, 73 p.

Rattas, M., Kalm, V. 1999. Classification and areal distribution of glaciotectonic features in Estonia. *Geological Quarterly*, 43: 177-182.

Raukas, A. 1978. *Pleistocene Deposits of the Estonian SSR.* Valgus Publications, Tallinn (in Russian).

Raukas, A., Rähni, E., Miidel, A. 1971. *Marginal glacial formations in North Estonia.* Valgus, Tallinn, 219 p. (in Russian).

Rõuk, M.-A. 1977. Pinnamood Vooremaa ja Emajõe vahel. *Eesti Loodus*, 3: 154-160.

Rõuk, A.-M., Raukas, A. 1989. Drumlins of Estonia. *Sedimentary Geology*, 62: 371-384.

Warren, W.P., Croot, D.G. (Eds.) 1994. Formation and Deformation of glacial deposits. A.A. Balkema, Rotterdam, Netherlands, 223 p.

Slovak Geol. Mag., 7, 3 (2001), 247 – 262

Identifying Palaeo-Ice Stream Tracks Using Remote Sensing

CHRIS R. STOKES[1] and CHRIS D. CLARK[2]

[1]Landscape and Landform Research Group, Department of Geography, University of Reading, Reading, RG6 6AB, UK.
c.r.stokes@reading.ac.uk
[2]Department of Geography and Sheffield Centre for Earth Observation Science, University of Sheffield,
Sheffield, S10 2TN, UK.

Abstract. Investigating palaeo-ice streams enhances our knowledge of Quaternary Ice Sheet dynamics and allows us to glean information about their basal processes and functioning. However, our understanding of palaeo-ice stream geomorphology is limited and they have often been postulated on a rather subjective basis, evading detailed scrutiny. In addition, many, or most palaeo-ice streams have yet to be found. To introduce more objectivity to palaeo-ice stream research, and to aid the search for new palaeo-ice stream evidence, Stokes and Clark (1999) predicted several geomorphological criteria indicative of their activity. This paper builds on that purely theoretical work by using remote sensing to identify the criteria and (i) validate the location of an already hypothesised ice stream, and (ii), find evidence for a previously undetected palaeo-ice stream

Key words: remote sensing; ice stream geomorphology

1. Introduction.

Ice streams are regions in an ice sheet which flow much faster than the surrounding ice. Most ice streams range in width from 20-30 km and reach lengths of over 300 km. Despite their large size, however, they only constitute a relatively small proportion of contemporary ice sheets, 13 % of the Antarctic coastline for example (Paterson, 1994). Their importance lies in their disproportionate ice flux and it has been estimated that they may drain as much as 90 % of the Antarctic Ice Sheet (Morgan *et al.* 1982). As such, they have a profound effect on ice sheet configuration and their activity is thought to be a key control on ice sheet stability. In recognition of this, recent research has focused on ascertaining their spatial and temporal controls, particularly in West Antarctica, an area thought to be particularly vulnerable to future climate change (Bindschadler, 1997).

Despite recent advances, ice streams still represent somewhat of an enigma. This stems from a paucity of data from the beds of contemporary ice streams, and a lack of understanding about their behaviour over longer timescales than contemporary observations permit. Both these inhibitors to ice stream research can be overcome if we investigate those ice streams which drained the now extinct ice sheets, which disappeared at the end of the last ice age. These ice sheets were also drained by ice streams and if we can find their former locations, we have an unprecedented opportunity to view their basal environment. Such research provides an enhanced understanding of the role of ice streams in Quaternary Ice Sheet dynamics. Furthermore, it may be possible to use the geomorphological products of their activity to glean information about their spatial controls and basal functioning.

Although many workers have recognised the importance of palaeo-ice stream research, they have sometimes been postulated on a rather *ad hoc* basis. A huge variety of evidence has been used to cite their former locations, but such evidence has rarely been scrutinised in detail. Put simply, their has been little theoretical work on which to base our hypotheses. This point was emphasised by Matthews (1991) who noted that the establishment of diagnostic criteria is an essential pre-requisite for finding former ice streams.

Recent work by Stokes and Clark (1999) addressed this issue by predicting several key geomorphological criteria indicative of ice streams. This theoretical work used the characteristics of contemporary ice streams as a basis for their identification in formerly glaciated areas. These criteria can be used to validate already hypothesised locations and help the search for other palaeo-ice streams yet to be identified in the geo(morpho)logical record.

Many of these diagnostic criteria are well suited to identification on satellite imagery and this paper demonstrates the suitability of this data source for palaeo-ice stream investigations. The criteria are presented and the advantages of using remote sensing to find and map them are outlined. Simple methodologies for identifying subglacial bedforms and grouping them into flow-sets are presented, and the characteristics of ice stream flow-sets are discussed. Using two case studies as examples, detection of several geomorphological criteria on satellite imagery is used to validate an already hypothesised ice stream location and identify a hitherto undetected palaeo-ice stream.

2. Geomorphological Criteria for Identifying Palaeo-Ice Streams.

Ice sheets leave behind an array of geo (morpho) logical products, from which their former activity can be inferred. These can be broadly summarised as moraines (outlining ice sheet extent and marginal positions), flow indicators (i.e. drumlins, striae and erratics) and the distribution of till (i.e. its stratigraphy and properties). For reconstructing flow patterns, the most commonly used evidence are assemblages of subglacial bedforms, such as flutings, drumlins and mega-lineations. Their distribution is a manifestation of a number of important controls, such as the underlying lithology, the basal conditions of the ice sheet and ice velocity. Because ice streams are discrete features of an ice sheet, in general we would expect them to leave behind a suite of landforms which differ in morphometry and pattern from those produced by the slower-flowing parts of the ice sheet.

In recognition of this, Stokes and Clark (1999) predicted several geomorphological criteria thought to be indicative of former ice stream activity. This purely theoretical work used the main characteristics of contemporary ice streams as a basis for their identification in formerly glaciated areas. Put simply, how would an ice stream be manifest in the geomorphological products of an ice sheet? Table 1 shows the eight criteria suggested by Stokes and Clark (1999) and how they relate to contemporary ice stream characteristics. These criteria are not definitive, but merely introduce a theoretical framework upon which palaeo-ice stream hypotheses can be better based.

Table 1. Geomorphological criteria for identifying palaeo-ice streams.

Contemporary ice stream characteristic	***Proposed geomorphological signature***
A. Characteristic shape and dimensions	**1.** Characteristic shape and dimensions **2.** Highly convergent flow patterns
B. Rapid velocity	**3.** Highly attenuated bedforms (length:width >10:1) **4.** Boothia-type erratic dispersal trains (Dyke and Morris, (1988)
C. Sharply delineated shear margin	**5.** Abrupt lateral margins **6.** Ice stream marginal moraine
D. Deformable bed conditions	**7.** Glaciotectonic and geotechnical evidence of pervasively deformed till.
E. Focused sediment delivery	**8.** Submarine till delta or sediment fan (only marine terminating ice streams)

The criteria can be grouped together to illustrate a characteristic landsystem, produced by a former ice stream. This landsystem is shown in Figure 1 where ice streams have been classified as either marine-terminating (a) or terrestrial (b). Of greater significance is the temporal context of bedform generation, see Clark (1999). Some ice streams will operate and switch off, and their geomorphology will not be significantly modified by later ice flows or deglaciation. This represents an isochronous bedform record, or 'rubber stamped' imprint, shown in (c) and (d). Alternatively, an ice stream may operate through several cycles of activation, or remain active during deglaciation. This is known as a time-transgressive record and represents a far more complex picture, i.e. a 'smudged imprint', shown in (e) and (f). A time-transgressive record of a ice stream activity may therefore leave behind several populations of bedforms, with varying degrees of cross-cutting relationships. These have been omitted from figure 1 for clarity but are shown in more detail in figure 2. Figure 2 shows how time-transgressive ice stream activity produces a confusing array of cross-cutting relationships. It is of paramount importance to acknowledge this complication, which in the past, has led to erroneous interpretations of glacial histories.

It must be remembered that these models represent the ideal geomorphological signature of an ice stream. It would not be expected to find all of the criteria produced by a single ice stream. However, it is suggested that these landsystems models (figure's 1 and 2) represent an observational template upon which palaeo-ice stream hypotheses can be better based. It is argued that the key to finding former ice streams lies in the identification of the landsystem (composing several of the criteria) rather than individual facets. To achieve this requires a synoptic view of regional scale glacial geomorphology. This is provided by satellite remote sensing.

3. Methodology: Remote Sensing of Ice Stream Geomorphology.

3.1. Advantages of Using Remote Sensing.

Traditionally, glacial geomorphology has been mapped by intensive fieldwork and/or by aerial photography. Fieldwork is often extremely time-consuming and its use is often restricted to small areas of a former ice sheet bed. This produces detailed information from discrete regions but the scale of the investigation limits its utility for an ice sheet wide reconstruction. To overcome this problem, aerial photographs have been used to map larger areas (and even whole ice sheet beds, e.g. Prest *et al.* 1968) relatively quickly, but this mapping approach is highly dependent on the solar elevation at the time of the photo-

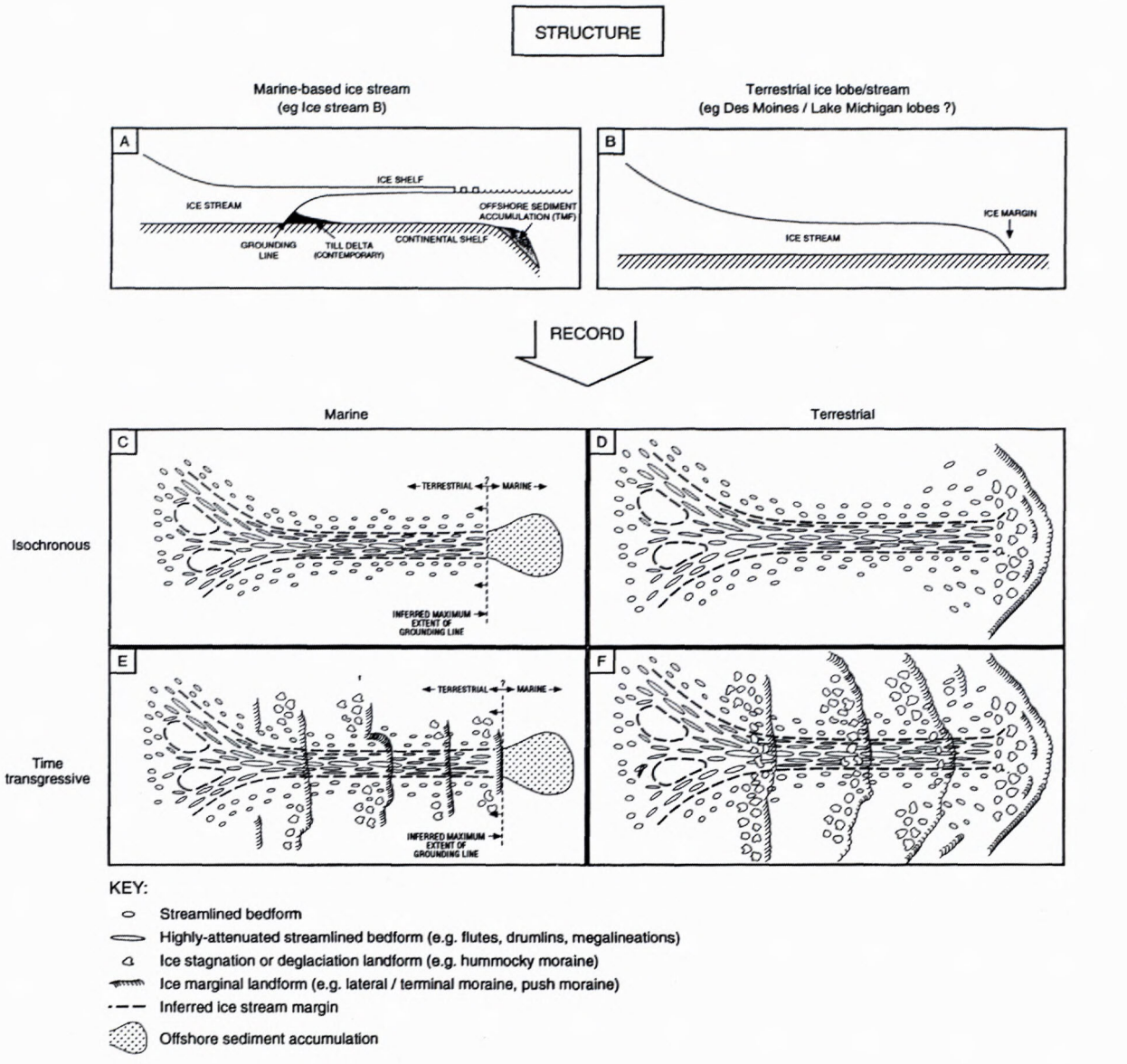

Fig.1 Conceptual landsystems of palaeo-ice stream geomorphology (from Stokes and Clark, 1999).

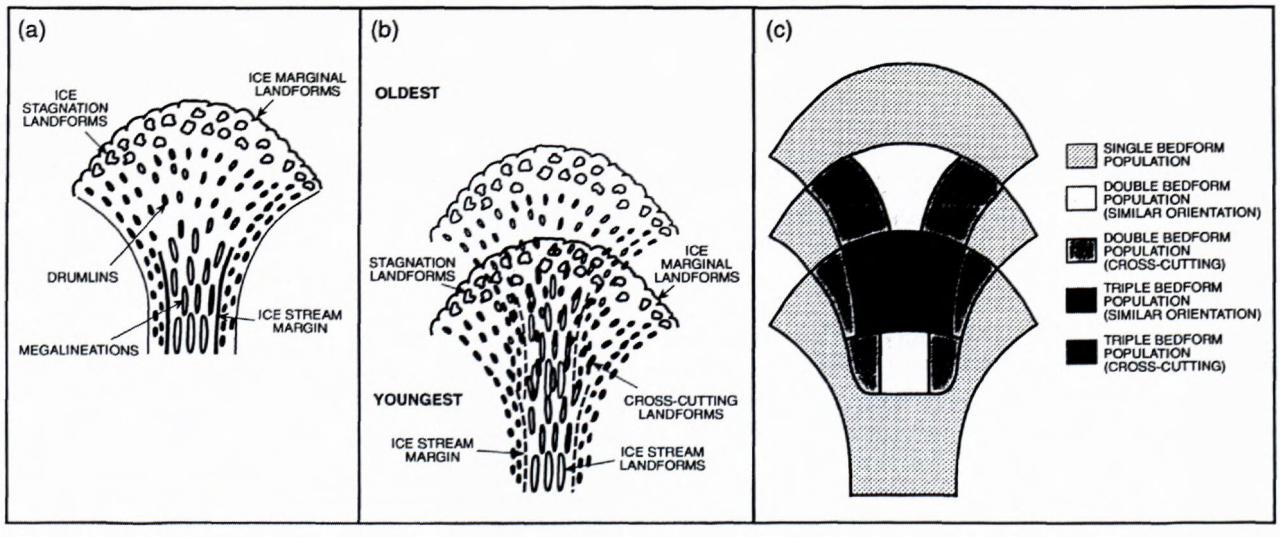

Fig. 2 Simplified bedform imprint of isochronous (a) and time-transgressive (b) ice stream activity. Note that the time-transgressive ice stream activity creates a complex assemblage of bedforms of different ages and orientations (c).

graph, the vegetation cover and the quality of the photographs (cf. Clark, 1997). Furthermore, the scale of the mapping is fixed by the resolution of the photographs, typically 1:30,000.

More recently, the use of satellite remote sensing has revolutionised the identification and mapping of glacial geomorphology and has greatly improved our knowledge of the dynamic behaviour of whole ice sheets. This is largely due to the numerous advantages it holds over fieldwork and air photograph mapping, of which Clark (1997) outlines five main benefits:

1. Satellite imagery covers large areas and this allows a single user to map geomorphology over very large regions, including whole ice sheets.
2. It is far quicker to map glacial landforms using satellite imagery than by aerial photography or fieldwork.
3. Most glacial landforms can be detected far more easily on satellite imagery than by aerial photography or fieldwork.
4. Satellite imagery allows the user to work at a range of scales.
5. The large area view of satellite imagery allows the user to discover previously unseen landforms and patterns.

For these reasons alone, satellite remote sensing is ideal for identifying palaeo-ice stream tracks. More importantly, satellite remote sensing is suited to identifying the individual geomorphological products of their activity, outlined in section 2 (table 1). The following sections briefly outline the methodology/techniques for detecting six of the geomorphological products of a palaeo-ice streams. The final two criteria in table 1 can not be identified using remote sensing. Glaciotectonic and geotechnical evidence of pervasively deformed till require identification in the field and offshore sediment accumulations can only be detected by specialised sub-marine sonar equipment.

3.2. The identification and mapping of flow-sets.

Having obtained imagery at a suitable resolution for the investigation, the flow patterns of former ice sheets can be reconstructed from an assemblage of subglacial bedforms. Most subglacial bedforms are formed parallel to ice flow (the exception being transverse ridges such as ribbed moraine) and are collectively known as 'lineations'. Using satellite imagery, these features can be mapped at a variety of scales and digitised on screen, whereby they are incorporated into a Geographic Information System (GIS).

Lineations are usually mapped by drawing a line representing the long axis of the bedform. Once identified, the length, width (and therefore elongation ratio and approximate surface area), and orientation can be measured. Overlaying a sampling grid of suitable resolution (or reconstructing a flow band) makes it possible to calculate bedform density (number of bedforms per unit area), packing (surface area of bedforms per unit area) and parallel conformity (usually calculated from the standard deviation of a sample of bedform orientations).

According to their morphometric characteristics, clusters of individual lineations can be grouped into flow-sets, which Clark (1990) defines as „integrated groups of flow lines revealing a widespread pattern of flow". The grouping of individual landforms into a flow-set is usually based on some combination of the following (cf. Clark, 1999);

a) Parallel concordance (i.e. similar orientations)
b) Close proximity to each other
c) Similar morphometry (length, width, elongation ratio)
d) Similar spacing (density)
e) Glacial plausibility

These criteria apply to any set of lineations, including a flow-set produced by an ice stream. The major challenge therefore, lies in demonstrating *why* a specific flow-set was produced by an ice stream. Here lies the importance of the diagnostic criteria outlined in section 2.

3.3. Characteristics of Ice Stream Flow-sets.

According to the criteria outlined in section 2, the flow-set needs to be large enough to have been produced by an ice stream. It would therefore be expected to be greater than 20 km wide and over 200-300 km long. However, it is acknowledged that some palaeo-ice streams may have been smaller than their present day counterparts. On the other hand, during deglaciation, ice streams may have been considerably larger than contemporary ice streams.

A flow-set produced by an ice stream would also be expected to exhibit a large degree of flow convergence in the inferred onset zone, see figure 1. The spatial extent of the transition from slow sheet flow to fast stream flow is still under debate (see Hodge and Doppelhammer, 1996), but it is suggested here, that the convergent transition zone would be expected to represent at the most one third of the ice stream length, usually less.

Most flow-sets are large and inherently convergent. Therefore, perhaps the most important criteria for identifying a palaeo-ice stream flow-set is the extremely abrupt margin to the bedform pattern. This is a unique characteristic of ice streams and it would be expected that their bedform pattern would display an abrupt margin as a result of the change in ice velocity and possibly basal thermal regime. This may be manifest as an abrupt margin with no bedforms outside it, or, a sharp zonation of landforms at the margin, as shown in figure 1. However, it must be remembered that an abrupt margin to a bedform pattern may arise from differential preservation, or abrupt changes in the underlying sedimentology. For example, Aylsworth and Shilts (1989) mapped a large area of the Keewatin Sector of the Laurentide Ice Sheet and concluded that the observed landform assemblages may be a result of the changes in underlying lithology, rather than invoking discrete ice dynamics. A major challenge therefore, lies in demonstrating why the abrupt margin is solely related to ice velocity. Questions to be answered include; what bedforms lie beyond the margin and how is their morphometry different from ice stream bedforms? Is their a change in lithology or topography which coincides with

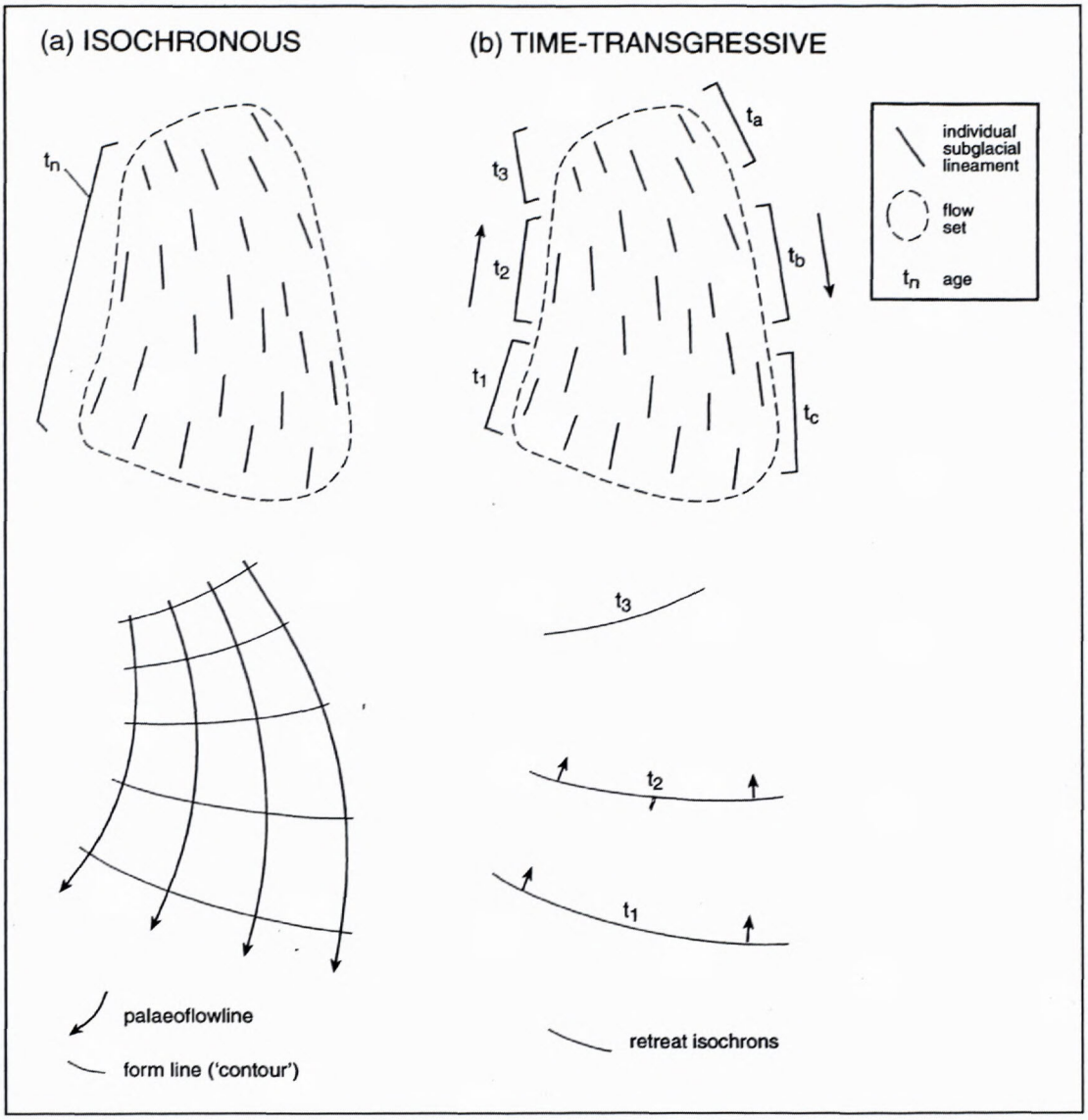

Fig. 3 Simplified diagram showing how similar bedform patterns may be produced isochronously (a) or time-transgressively (b), (modified from Clark, 1999).

the inferred ice stream margin? How has the ice stream flow-set been modified by later ice flows? Was the flow-set produced isochronously or time-transgressively?

3.4. Deciphering between isochronous and times-transgressive flow-sets.

The landsystems models in section 2 (figures 1 and 2) make a clear distinction between an isochronous record of ice stream activity and that produced time-transgressively. It is of paramount importance to make this distinction, because erroneous assumptions can lead to grave misinterpretations pertaining to the glacial dynamics. For example, a key criteria for an ice stream flow-set is a highly convergent onset zone. However, apparently convergent flow patterns can be produced isochronously or time-transgressively. This is demonstrated in figure 3 which shows how a similar flow-set can be produced by one ice flow episode, or by three separate flow events as the margin retreats.

Clark (1999) suggests several differences between an isochronous and time-transgressive bedform record. These characteristics are shown in table 2, where it can be seen that isochronous bedform patterns are generally more coherent, show a high degree of parallel conformity and display no cross-cutting relationships. This is in contrast to time-transgressive flow-sets which are generally more divergent, show abrupt discontinuities and will often exhibit cross-cutting relationships. Some of these criteria are also illustrated in the landsystems models in figure 2. In theory therefore, it should be possible to use the within flow-set variations in lineament morphometry, orientation and parallel conformity to ascertain whether the ice stream flow-set was generated incrementally (i.e. time-transgressive) or at an instant (i.e. isochronously).

If a flow-set is large enough to be considered an ice stream, and if it exhibits a convergent onset zone and abrupt lateral margins, then it may represent a good candidate for a palaeo-ice stream track. However, further

Table 2: Criteria for distinguishing between a time-transgressive and isochronous bedform record (modified from Clark, 1999).

Time-transgressive record	***Isochronous record***
Predominantly lobate or splaying flow patterns	Predominantly parallel flow patterns
Correspondence to local topography	Little or no correspondence to local topography
Likely to contain cross-cutting relationships	Unlikely to contain cross-cutting relationships
Low parallel conformity between lineations	High parallel conformity between lineations
Spatial variations in lineament morphometry abrupt	Spatial variations in lineament morphometry gradual
Probable landform association with end moraines	No landform association with moraines
Probable landform association with eskers	No landform association with eskers

evidence of ice stream activity may be found in the nature of the flow-set geomorphology. Characteristics of ice stream geomorphology are discussed below.

3.5. Characteristics of ice stream geomorphology.

It is a long held assumption in glacial geomorphology that long bedforms equal fast ice flow. Although this has never been demonstrated unequivocally, several studies report a correlation between elongated bedforms and fast ice flow (e.g. Boyce and Eyles, 1991; Clark 1994; 1997; Hart, 1999). Therefore, the rapid velocity of ice streams would produce subglacial bedforms which are highly attenuated. It could be the case that highly-attenuated bedforms may form by slow flowing ice over long time periods. However, since the discovery that the flow geometry of ice sheets are known to vary rapidly (see Boulton and Clark, 1990), it is argued that this scenario is highly unlikely.

Elongation ratio is a useful way of quantifying the degree of attenuation of subglacial bedforms (such as flutes, drumlins and mega-lineations). In theory, ice stream bedforms should exhibit high elongation ratios (>10:1), and these would be expected to be (statistically) significantly higher than neighbouring flow-sets. However, elongation ratio's within the flow-set may vary both across and within the ice stream flow-set. For example, if elongation ratio is taken as crude proxy for strain at the bed and therefore ice velocity, we would expect to find the elongation ratio's increasing from the onset zone into the main ice stream channel. Likewise, we may observe elongation ratios to decrease towards the terminus of terrestrial ice streams, where ice may be expected to slow down as it diverges (see figure 2).

In terms of the lateral variations in elongation ratio across an ice stream, we would expect little differences. This is because in contemporary ice streams fast ice flow is maintained across their whole width, a characteristic described as 'plug flow'. However, if significant drag is imparted by the margins, such as on topographic ice streams, we may expect elongation ratio to decrease slightly, reflecting the decrease in ice velocity. Examining the within stream variations in elongation ratio may provide a wealth of information pertaining to shear strain at the bed and hence ice velocity. Thus, patterns in elongation ratio can be used to support or refute the ice stream hypothesis.

The rapid velocity of an ice stream may also transport any available sediment in a distinctive pattern. Boothia-type dispersal trains form when an abrupt lateral variation in ice velocity transports distinctive sediment from a large source area, see figure 4. Such an abrupt lateral variation in velocity is a characteristic of ice streams and Boothia-type dispersal trains can be considered to be indicative of their activity. Figure 4 shows that a very similar pattern can be produced by a Dubawnt-type dispersal plume, but because the source area is localised, this implies no lateral variation in velocity. Hence, the spectral characteristics of some sat-

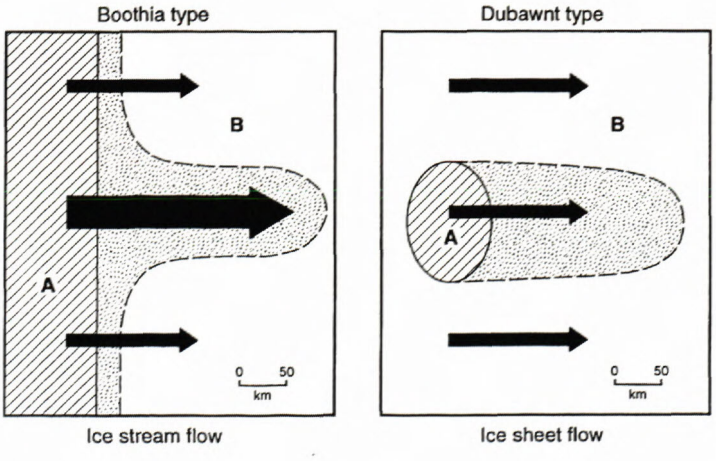

Fig. 4 Boothia-type and Dubawnt-type dispersal plumes. Only the Boothia-type dispersal plume is indicative of ice stream activity because it implies an abrupt lateral variation in ice velocity (from Dyke and Morris, 1988).

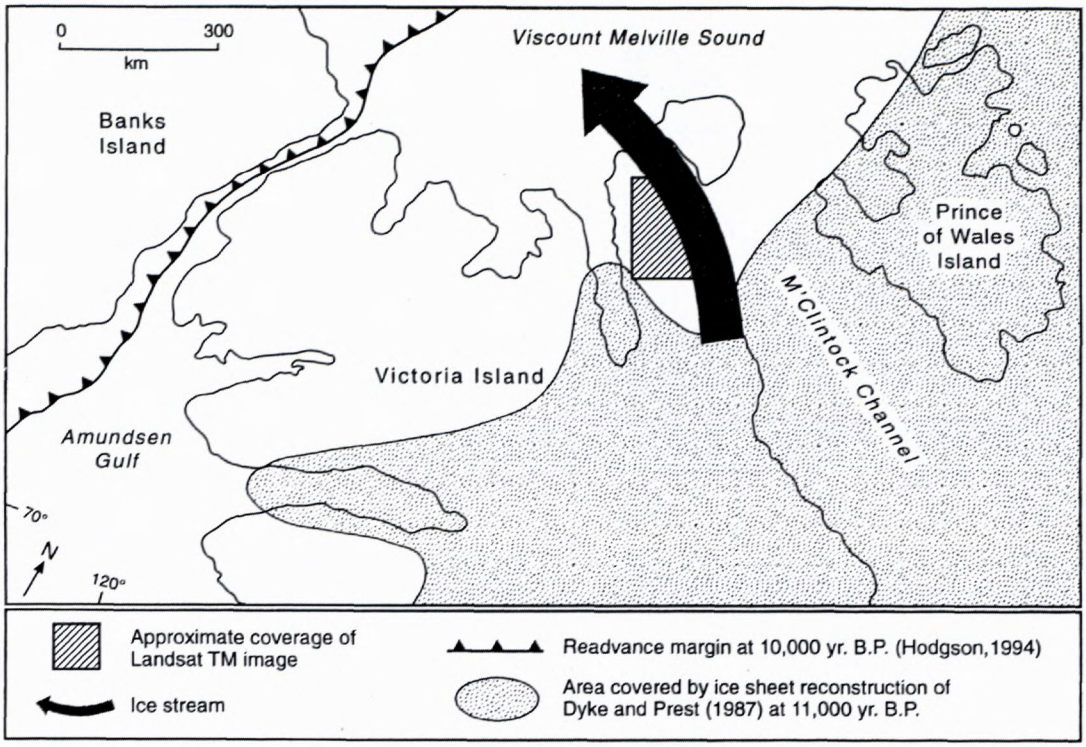

Fig. 5 Inferred location of the M'Clintock Channel Ice Stream (from Stokes, 2000).

ellite imagery (e.g. Landsat TM) can be used to identify erratic dispersal plumes and the spatial extent of the source area from which the till is transported (e.g. Dyke and Morris, 1988; Dyke *et al.*, 1992).

The marginal area of an ice stream may be characterised by unique landforms, here termed ice stream marginal moraines. Dyke and Morris (1988) were the first to identify such a feature, bordering a drumlin field on Prince of Wales Island, Arctic Canada. This feature represented a smoothly curved ridge parallel to the drumlin field. The continuity of the ridge could only be appreciated at the smaller scale on the satellite imagery and reached over 68 km in length but less than 1 km wide. Dyke and Morris (1988) suggested that it marks the boundary between fast flowing (streaming) ice and slow flowing ice and thus termed it a 'lateral shear moraine'. Hodgson (1994) also identified a similar ridge on Victoria Island (Arctic Canada) and suggested that it too marked the boundary if an ice stream. Although these features are the only documented cases of ice stream marginal moraines, further investigations using satellite imagery may reveal their occurrence to be far more widespread than these isolated cases.

3.6. Application of the Geomorphological Criteria.

The criteria outlined above and in more detail in Stokes and Clark (1999) are applicable to palaeo-ice stream research in two main ways. Firstly, the criteria can be used to provide an objective validation of already-hypothesised palaeo-ice stream locations. Once a palaeo-ice stream track has been inferred, the presence of the criteria can be used to support the hypothesis for ice stream activity. If the criteria are absent, it does not imply that ice stream activity did not take place. Some ice streams signatures may have been modified or even obscured altogether. However, explanations as to why some criteria are absent may provide fruitful answers regarding the glacial history prior to and post ice stream activity.

Secondly, the criteria can be used to search for 'new' palaeo-ice streams from previously glaciated areas. Many ice streams have yet to be identified from former ice sheets and the criteria can be used as a predictive tool to aid the search for their identification.

The following two case studies demonstrate how the criteria have been used to validate the location of an already hypothesised ice stream (the M'Clintock Channel Ice Stream) and find a new palaeo-ice stream from the Keewatin Sector of the Laurentide Ice Sheet (the Dubawnt Lake ice stream). The case studies are not intended to be exhaustive, but demonstrate the suitability of remote sensing for identifying and investigating palaeo-ice streams.

4. Application of the Criteria to Palaeo-Ice Streams Locations.

4.1. The M'Clintock Channel Ice Stream.

The M'Clintock Channel Ice Stream was first postulated by Hodgson (1994) who carried out field investigations on Storkerson Peninsula, Victoria Island in the Canadian Arctic. Figure 5 shows the location of the hypothesised ice stream as the north-western margin of the

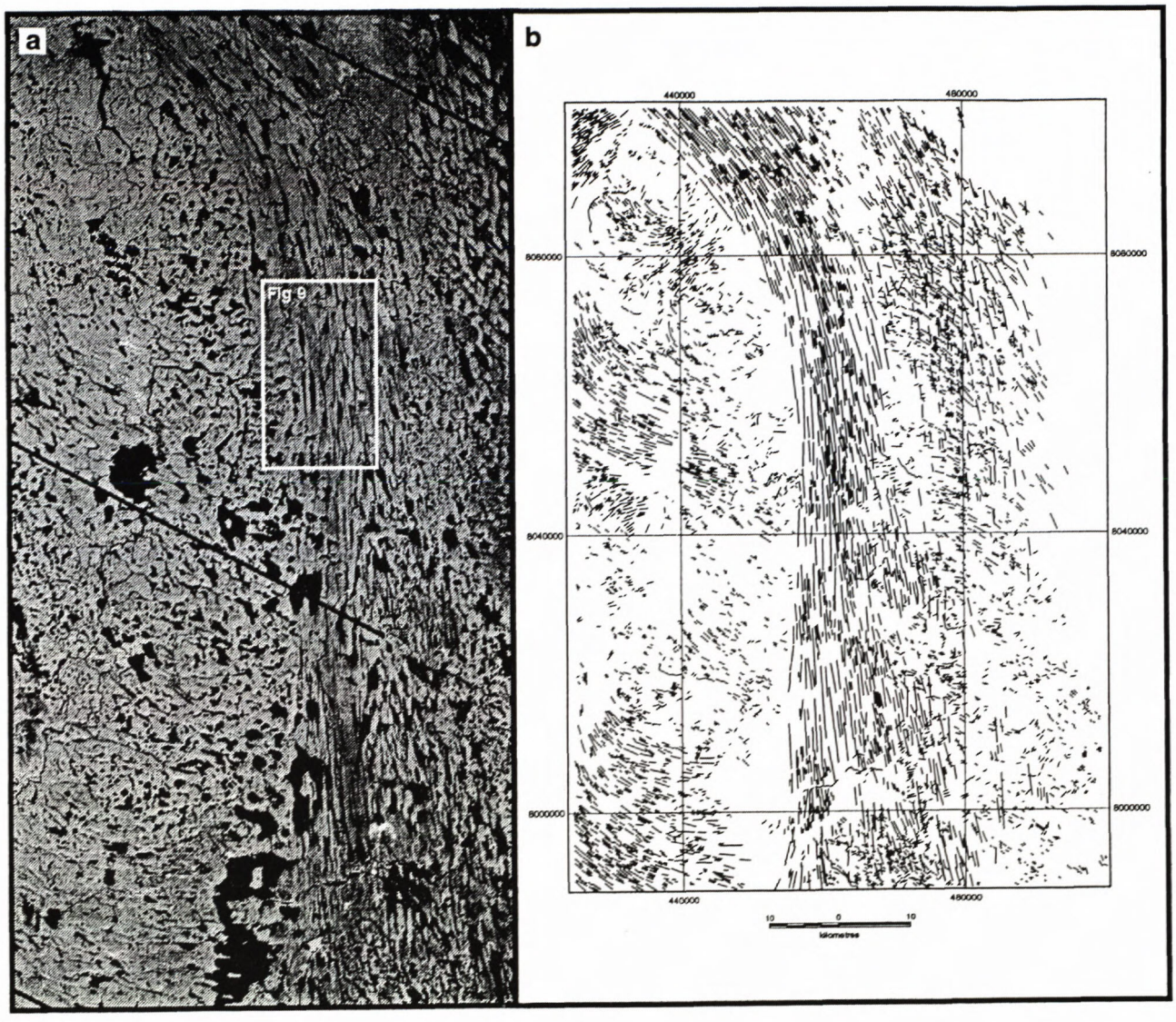

Fig. 6 Landsat TM image (band 5) of Storkerson Peninsula (a) and associated lineation map (b).

Laurentide Ice Sheet advanced between 11 and 10 ka. To assess the validity of this ice stream location and to search for the criteria outlined in section 2, a variety of imagery was obtained. A Landsat Thematic Mapper (TM) image (shown on figure 5) and four Synthetic Aperture Radar scenes were purchased covering a large part of Storkerson Peninsula and Prince of Wales Island. In addition, thirty Landsat Multi-Spectral Scanner (MSS) positives (band 4) were obtained and developed into photographs at 1:250,000. Mapping from this imagery was verified by samples of air photographs and photomaps at 10 m contour intervals.

The location of the TM image is shown in figure 5 and figure 6 shows this image (a) and all the lineations mapped from it (b). The inferred ice stream flowset runs from south to north and dominates the lineation assemblage on Storkerson Peninsula. These landforms are typically longer, closer together and show a high degree of parallel conformity. Of greatest note is the extremely abrupt western margin of the flow-set, which can be seen on the image itself (figure 6a) but is far clearer on the lineation map (figure 6b). Using the wider coverage provided by the SAR imagery and numerous MSS hard copies, this margin could be traced for several hundred kilometres upstream. Moreover, bedforms of a similar size, spacing and orientation were found further south on Victoria Island and Prince William Island and further east (across the channel) on Prince of Wales Island and Boothia Peninsula. It is suggested that these bedform patterns surrounding the M'Clintock Channel are consistent with a large ice stream which operated in the present day M'Clintock Channel but infringed on islands to the south, west and east. Figure 7 shows the reconstructed ice stream flowset which fulfils all three of the criteria for ice stream activity; it displays the characteristic shape and dimensions, exhibits a convergent onset zone in the upstream portion and displays a remarkably abrupt margin. The ice stream is thus reconstructed at around 720 km in

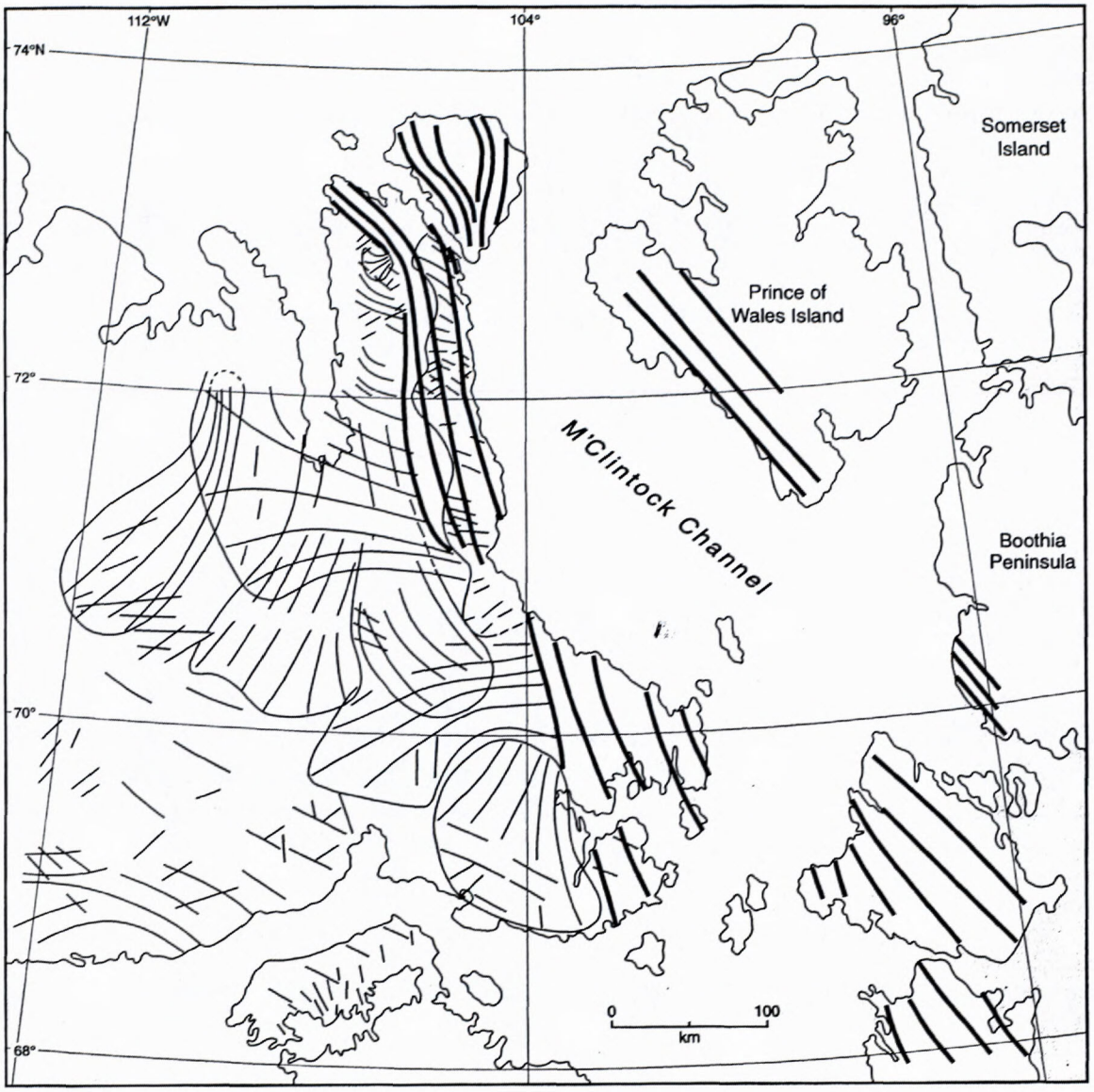

Fig. 7 Reconstructed flow-set (bold) of the M'Clintock Channel Ice Stream. Note that the ice stream is far larger than was originally inferred by Hodgson (1994) (from Clark and Stokes, in press)

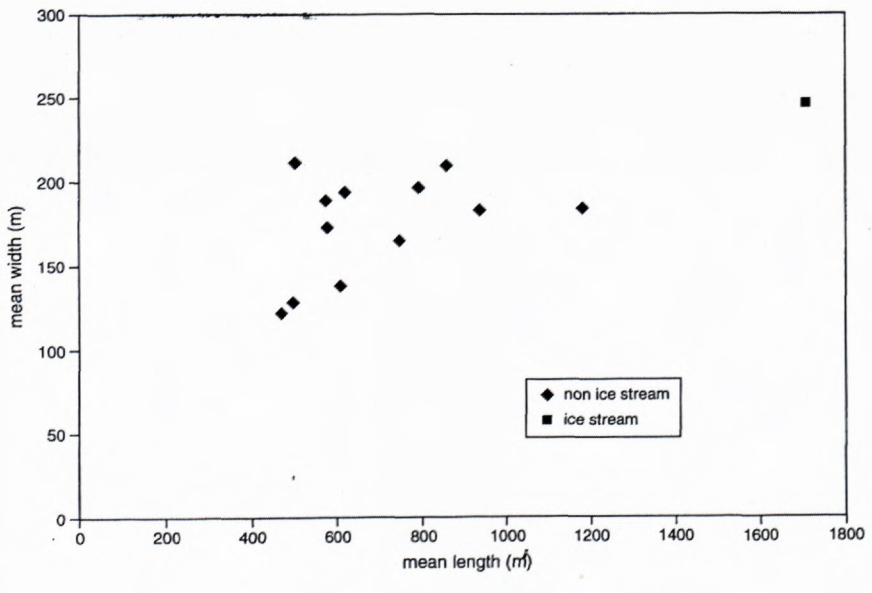

Fig. 8 Plot of mean lineament length versus mean width for each flow-set.

length which narrowed from around 330 km in the onset zone to 140 km near the terminus. This is far bigger than was first hypothesised by Hodgson (1994) (compare figure's 5 and 7) and this ice stream would have had a profound effect on the dynamics of the whole ice sheet.

The flow-set displays all of the characteristics of an isochronous bedform pattern, outlined in table 2. Compared to neighbouring flow-sets on Victoria Island, it displays a remarkably parallel pattern which lies irrespective of local topography, see figure 6b. There are no within-stream cross-cutting relationships but rather, spatial variations in lineament morphometry are gradual. It is thus inferred that the ice stream flow-set is an isochronous record which represents a snapshot view of the bed prior to shutdown.

On average, ice stream bedforms are far more elongated than neighbouring flow-sets. Figure 8 plots mean lengths against mean widths for a number of flow-sets identified on Storkerson Peninsula and it can be seen that the ice stream flow-set represents a unique population. Moreover, mean values of ice stream bedforms indicate that they are longer, wider and more elongated than any other flow-set identified. Lengths approach 8 km, with widths of up to 750 m and elongation ratios are some of the highest in the literature (approaching 30:1). The morphometry of these bedforms fulfils a fourth criteria for ice stream activity outlined in section 2. Figure 9 shows a TM image of a typical population of elongated ice stream landforms juxtaposed to the remarkably abrupt ice stream margin.

Not only is the ice stream margin abrupt, but in places it is also demarcated by ice stream marginal moraines on Storkerson Peninsula. Figure 10 shows one of these features on the TM imagery. The ice stream marginal moraines differ from the ice stream bedforms in a number of ways. Firstly, they are far longer than the largest ice stream bedforms. For example, the southern-most moraine, shown in figure 10, is over 23 km in length. In addition, the ice stream marginal moraines maintain a fairly constant width of around 500-800 m along their length. This is in contrast to the ice stream bedforms which usually taper in the downstream direction. Furthermore, unlike the ice stream bedforms which are usually straight, the ice stream marginal moraines display a degree of sinuosity. Finally, the relief of these ridges tends to be higher than the adjacent bedforms. This is shown by a transect across the ridge which indicate elevations which are typically 10 to 40 m above the surrounding terrain. The identification of these ice stream marginal moraines represents a fifth geomorphological criteria for ice stream activity.

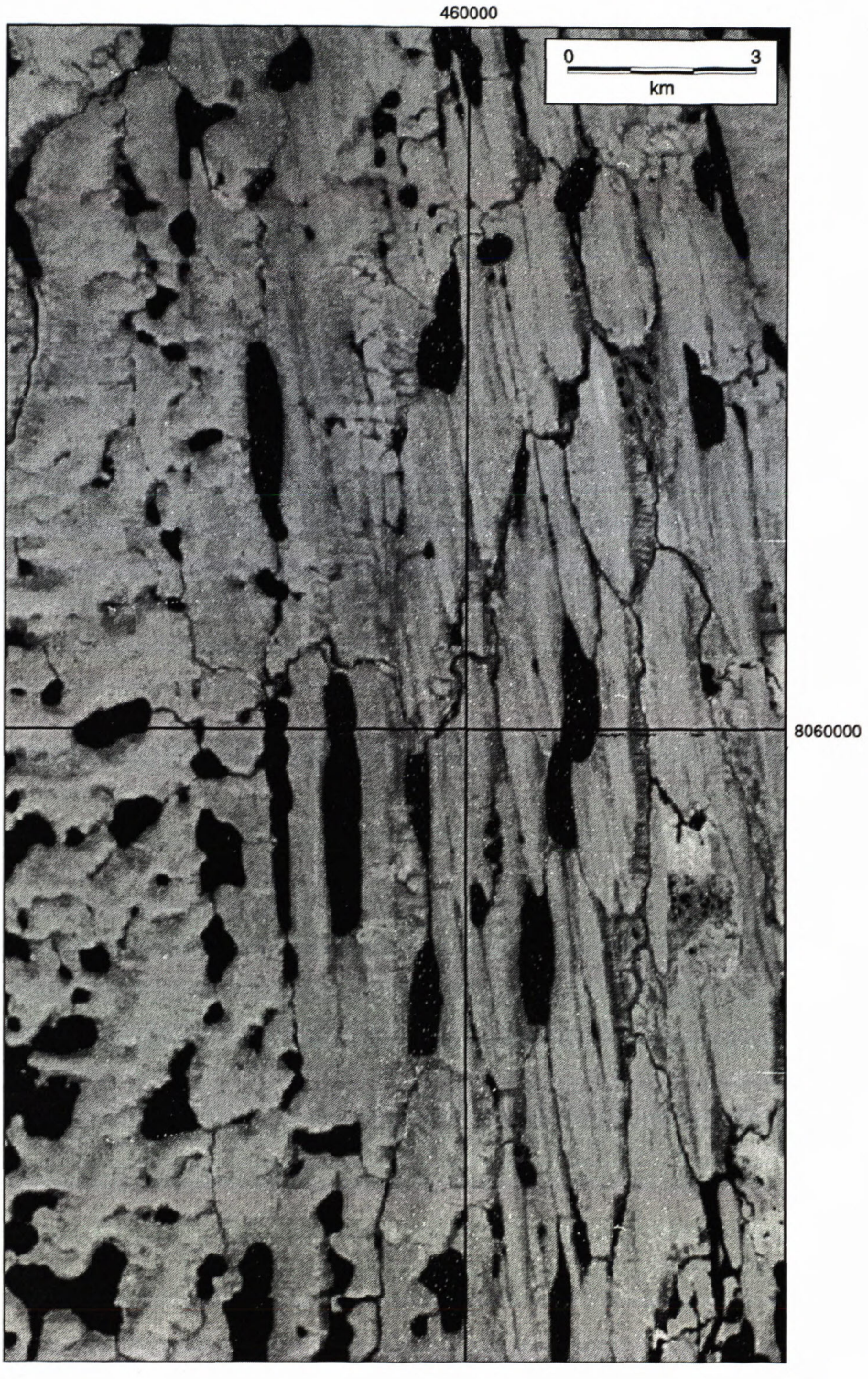

Fig. 9 Landsat TM image (band 5) of the abrupt margin of the ice stream flow-set. The location of this figure is shown on figure 6a.

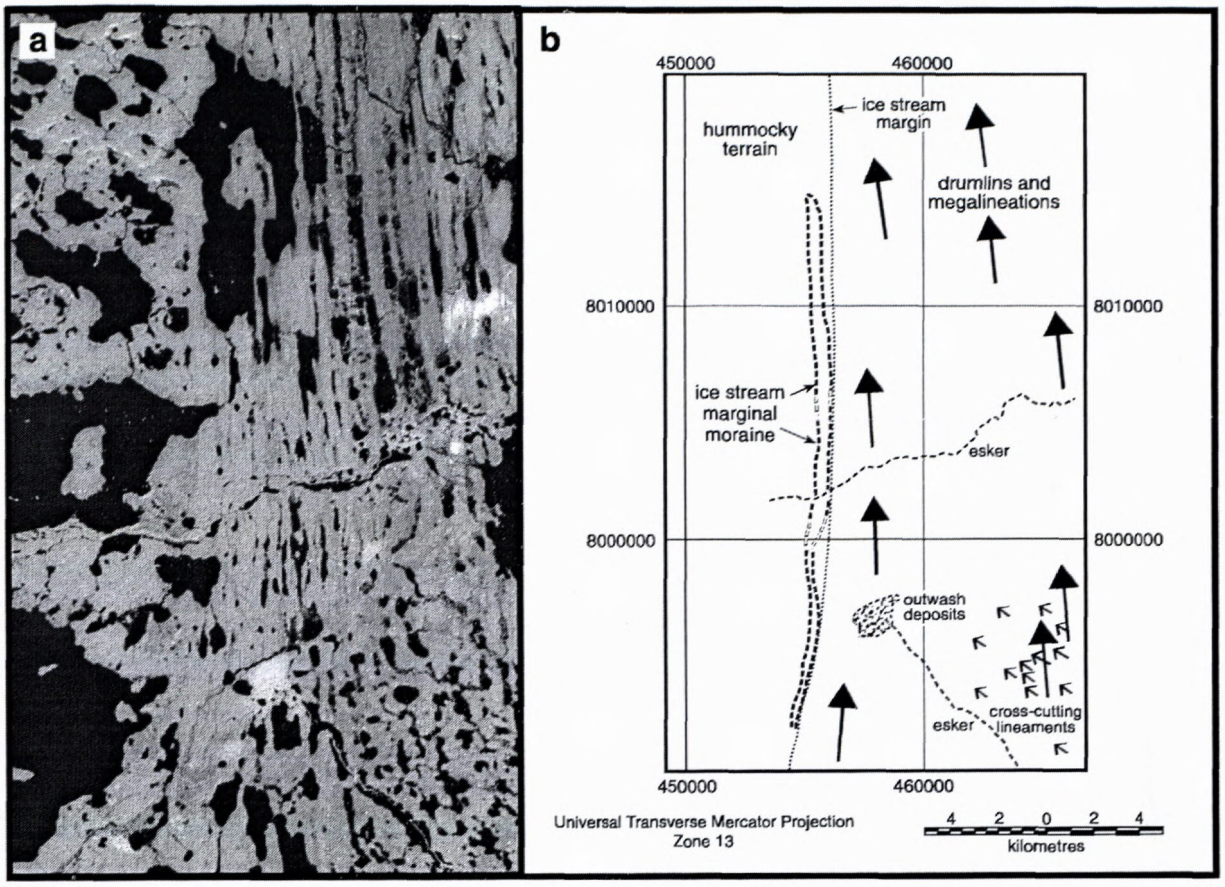

Fig. 10 Landsat TM image (band 5) of an ice stream marginal moraine on southern Storkerson Peninsula (a) and interpretation (b) (from Clark and Stokes, in press)

Of all of the criteria identifiable on satellite imagery, only the Boothia-type dispersal train is absent. The geology of the area is predominantly 'soft' carbonate sediments with only around 4% exotic lithologies incorporated from the Canadian Shield. An erratic dispersal plume was not produced because the carbonate sediments are pervasive throughout the whole region, underlying both the ice stream bed and the areas outside its margins.

Evidence of pervasively deformed till and offshore sediment accumulations may not be absent, but rather, it is suggested that they haven't been identified yet. Further investigations regarding the basal functioning of this ice stream (Clark and Stokes, in press) suggest that it may have operated by deforming the soft sediments under high pore water pressures. From his field investigations, Hodgson (1994) also commented that the ice stream „deformed and eroded a widespread cover of till". If this is the case, then a sixth criteria for ice stream activity may be identified from field evidence regarding the deformation history of the ice stream sediments. In addition, it is predicted that this deforming bed mechanism would have delivered huge amounts of sediment to the grounding line of the ice stream and that offshore sediment accumulations in Viscount Melville Sound may be present. It is noted that a distinctive sediment bulge has been identified on the continental margin at the mouth of M'Clure Strait (Zarkhidze *et al.*, 1991) and this may fulfil a possible seventh criteria for ice stream activity. Detailed examination of the architecture of this sediment fan will provide a first order test of the hypotheses regarding the ice stream flow mechanisms and sediment flux.

In summary, the M'Clintock Channel Ice Stream displays at least five (and possibly seven) out of a possible eight criteria thought to be indicative of ice stream activity. It is thus concluded that the M'Clintock Channel ice stream is one of the securest palaeo-ice stream locations ever identified. This ice stream was a considerable size and undoubtedly imparted a significant impact on the dynamics of the Laurentide Ice Sheet during deglaciation. Moreover, its bedform record is remarkably well preserved and presents an unprecedented opportunity to glean information about its basal processes and functioning. The bedform signature is described in more detail in Clark and Stokes (*in press*) where implications for ice stream operation and sediment fluxes are explored and its ice sheet wide significance is discussed.

4.2. The Dubawnt Lake Ice Stream.

Many investigations concerning the Keewatin Sector of the Laurentide Ice Sheet, west of Hudson Bay, have identified and mapped a distinct flow pattern approximately parallel to the northern shores of Dubawnt Lake and trending in a north-westerly direction (see for example,

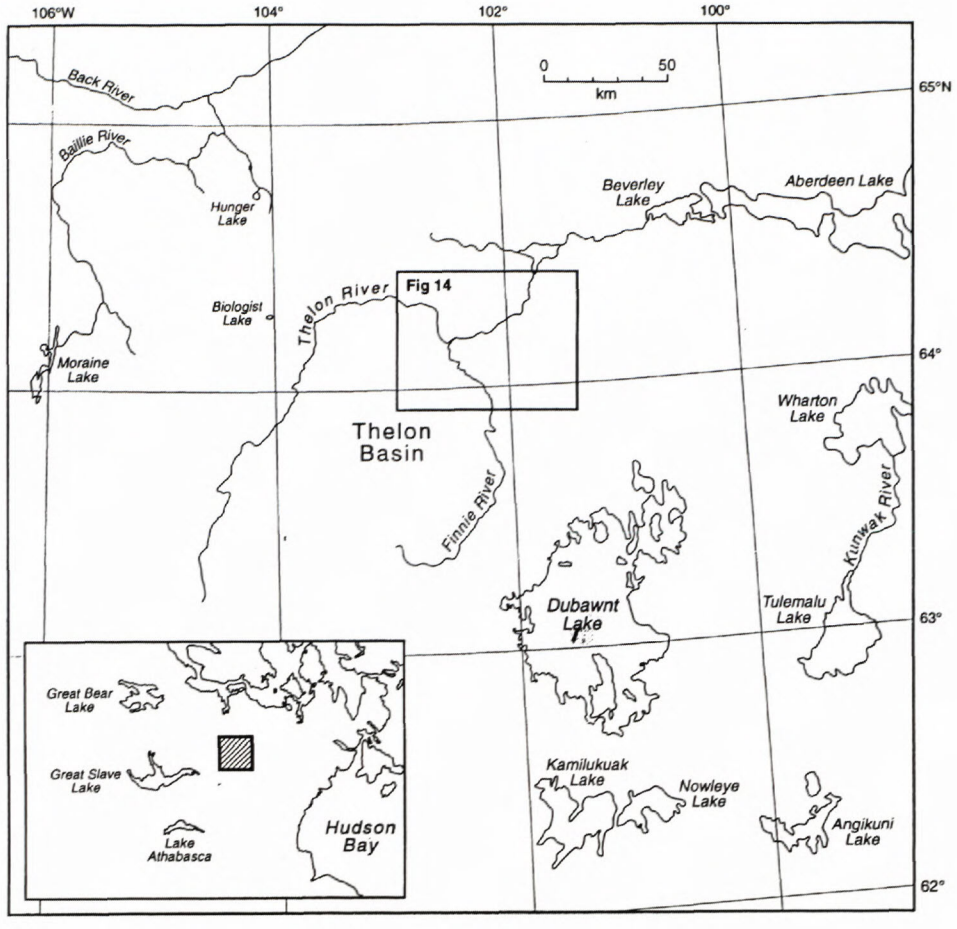

Fig. 11 Location map of the study area covered by the Keewatin sector of the Laurentide Ice Sheet.

Bird 1953; Lee, 1959; Shilts *et al.*, 1979; Aylsworth and Shilts, 1989). This highly convergent flow-set is also represented on the Glacial Map of Canada (see Prest *et al.*, 1968). Bird (1953) was the first to note the unique nature of the drumlins in the area which totally control the shape of the lakes and the pattern of stream drainage. Indeed, this spectacular fluting led Aylsworth and Shilts (1989) to speculate on the possible role of ice streaming in shaping the drumlins but they refused to postulate on the exact location of an ice stream.

To investigate this flow-set as a potential candidate for a palaeo-ice stream track, fifteen Landsat MSS positives (band 4) were obtained and developed into 1 : 250,000 hard copy photographs. This produced a complete coverage of the study area, which is shown in figure 11. Figure 12 shows the preliminary mapping of flow patterns from this area, which is totally dominated by the Dubawnt Lake flow-set, trending from the south-east to the north-west. Cross-cutting relationships with other flow-sets indicate that this flow-set is the youngest in the area. It was almost certainly fed by the Keewatin Ice Divide which migrated to its final position between 11 and 8.4 ka (Dyke and Dredge, 1989).

To investigate the Dubawnt Lake flow-set in detail and assess its validity as an ice stream track, three adjoining digital Landsat MSS images were obtained for half of the flow-set. This allowed a more refined mapping approach and the measurement of bedform characteristics. Figure 13 shows the coverage of the digital imagery and all of the lineations detected. It can be seen from Figures 12 and 13, that the ice stream flow-set is large enough to be considered an ice stream and displays a characteristically convergent onset zone. Unlike the marine-based M'Clintock Channel Ice Stream, this ice stream had no way of effectively removing ice. A result of this, was a lobate margin characterised by divergent ice flow at the terminus (see figures 12 and 13). The maximum length of the flow-set is 450 km and the width varies from 140 km at its narrowest point to over 190 km at the terminus.

It can be seen from the lineation map (figure 13) that the southern margin to the flow-set is extremely abrupt (<1 km). Outside of this margin, bedforms are scarce, but do occur further south displaying a variety of contrasting orientations, presumably from older ice flows. The abrupt ice stream margin does not coincide with a change in geology or topography. Rather, the Thelon Sedimentary basin actually traverses the margin, and it is inferred that it did not exert an influence on the width of this ice stream. Instead, it is argued that ice velocity was the only controlling factor on the position of the abrupt margin, which fulfils a third criteria for ice stream activity. The northern margin is far more difficult to define because older flow-sets have been cross-cut, with only subtle variations in orientation, see figure 12.

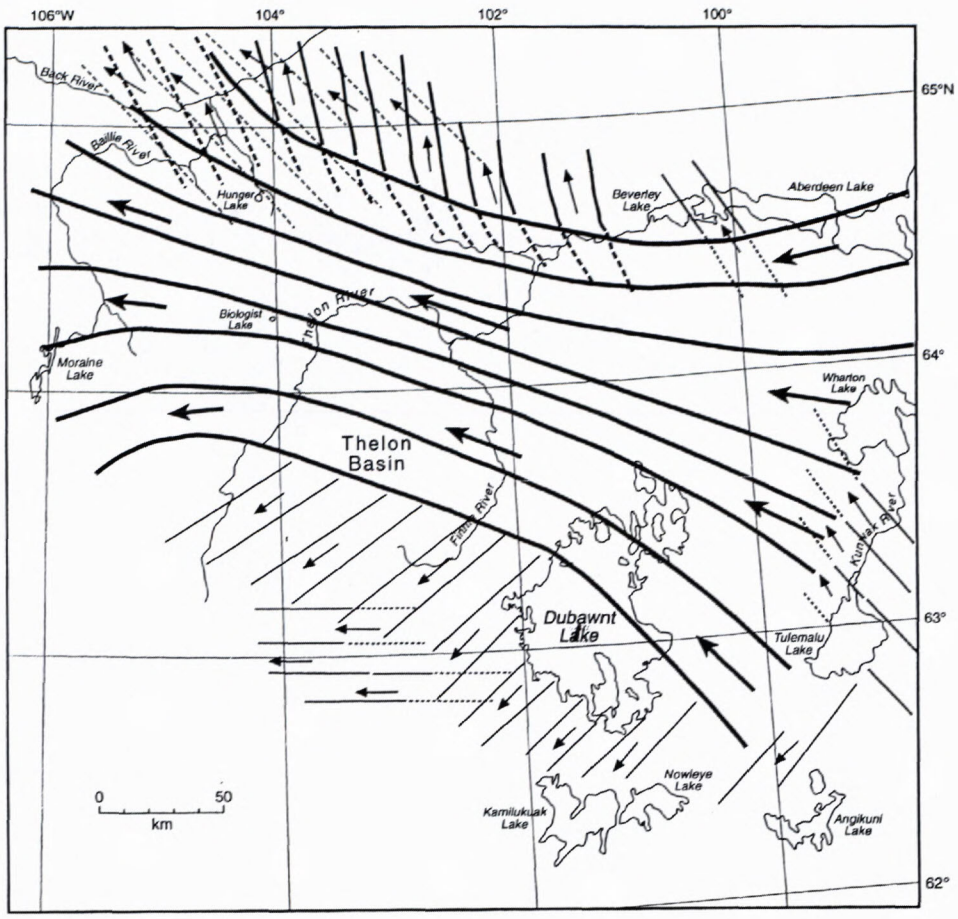

Fig. 12 Flow patterns identified on the Landsat MSS imagery. Note that the Dubawnt Lake Ice Stream (bold) dominates the regional pattern of flow.

The Dubawnt Lake flow-set meets the three criteria characteristic of an ice stream flow-set. It has the characteristic shape and dimensions, exhibits a highly convergent onset zone, and has an abrupt lateral margin.

Like the M'Clintock Channel Ice Stream imprint, it is inferred that the Dubawnt Lake ice stream record was isochronously generated. In figure 13 the lineations depict a remarkably coherent pattern, despite the convergence in the onset zone and divergence at the terminus. For the central portion of the ice stream the remarkable parallel conformity between individual lineations is so strong, that the bedform orientations only deviate by 5° along a flow-band 40 km wide and 220 km long. In addition, there are no within-stream cross-cutting relationships but rather, spatial variations in lineament morphometry are gradual. This suggests that the flow-set was generated rapidly, and was not modified during deglaciation. A result of this, is an isochronous bedform pattern which largely resembles the conceptual model outlined in figure 2.

The ice stream bedforms are exceptionally attenuated. The maximum length of the bedforms reach over 12 km in length and elongation ratios are as high as 48:1. The high parallel conformity of these drumlins and their extreme attenuation resembles a ridge/groove pattern on the satellite imagery. This is shown in figure 14 which shows lineations from a central portion of the ice stream northwest of Dubawnt Lake. These highly attenuated bedforms fulfil a fourth criteria for ice stream activity.

It is argued that these four criteria of the ice stream flow-set; characteristic shape and dimensions; highly convergent onset zone; abrupt lateral margin and highly attenuated bedforms, provide substantial evidence to invoke ice stream activity. Of the other possible criteria, there is no evidence of ice stream marginal moraines, or, Boothia-type dispersal plumes. The availability of soft sediments on the Canadian Shield is sporadic, and although major Dubawnt-type dispersal trains have been found to trend towards Hudson Bay (cf. Shilts *et al.*, 1979), Boothia-type dispersal trains are absent throughout the area. It may also be the case that ice stream marginal moraines rely on large supplies of soft sediments and the coarse grained lithology of the Dubawnt region may not be conducive to their development. Likewise, the underlying geology is unlikely to have facilitated a deforming bed mechanism for fast ice flow and pervasively deformed till is not an expected criteria.

In summary, the Dubawnt lake ice stream displays four out of a possible seven criteria for a terrestrially terminating ice stream. It has the characteristics shape and dimensions, exhibits a highly convergent onset zone and is characterised by a very abrupt lateral margin. In addition, the ice stream bedforms are some of the longest ever identified in the literature. The high parallel conformity of

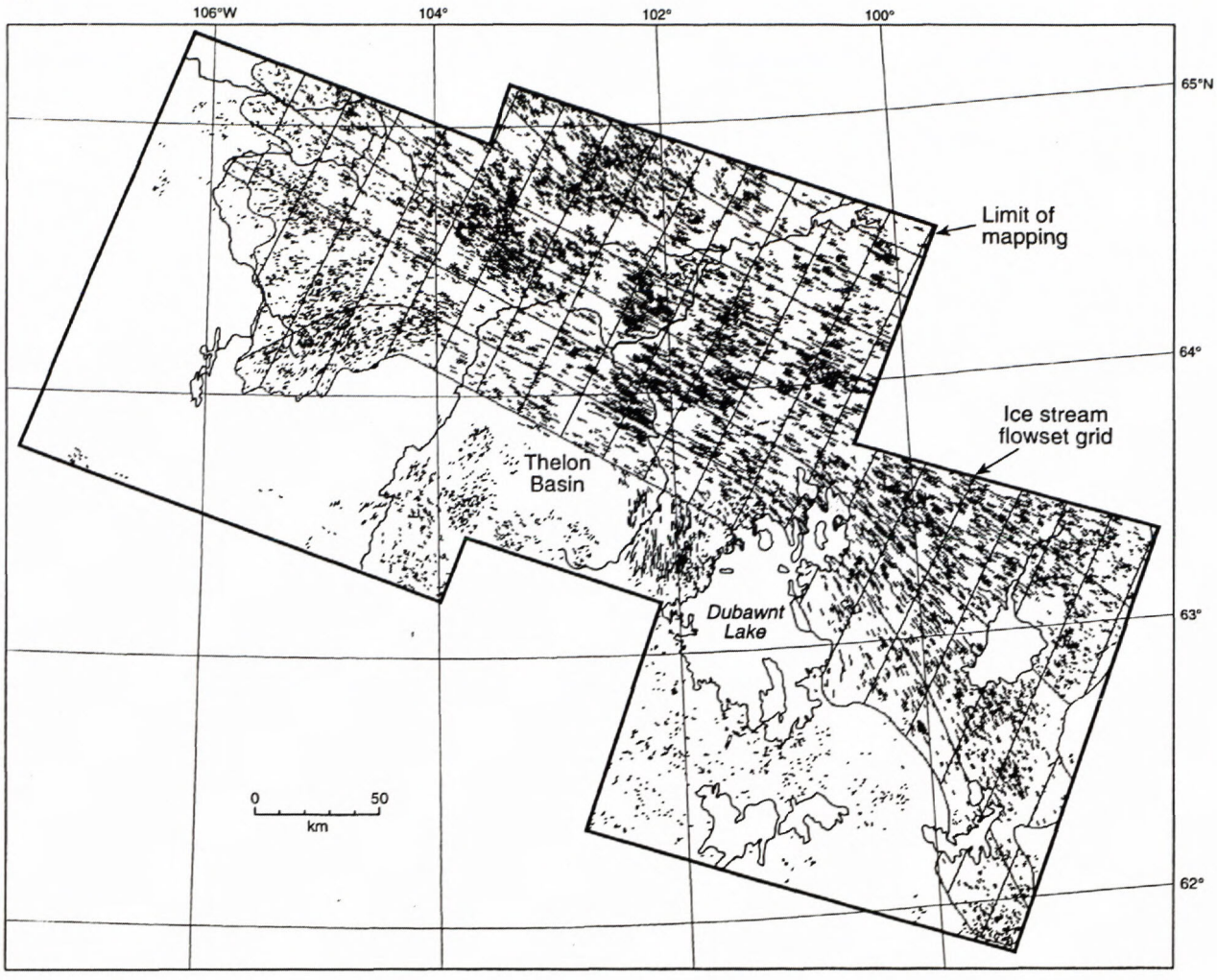

Fig. 13 Lineation map produced from three digital Landsat MSS images of the Dubawnt Lake Ice Streams.

the bedforms and the lack of cross-cutting relationships within the flow-set indicate an isochronous bedform generation. It thus represents a snapshot view of the bed, prior to ice stream shutdown. Ongoing work suggests that the well preserved bedform pattern is a useful proxy for ice velocity and may provide several insights as to the functioning of the ice stream. The ice stream probably had a significant impact on the last remnants of the Laurentide Ice Sheet west of Hudson Bay, possibly obliterating the Keewatin Ice Divide. Whether this ice stream activity was linked to that of the M'Clintock Channel Ice Stream further north and was part of a pan-ice sheet destabilisation during deglaciation is a question that deserves attention.

6. Summary and Conclusions.

Finding palaeo-ice stream locations enhances our understanding of Quaternary ice sheet dynamics and many workers have hypothesised their locations from a number of former ice sheets. Traditionally, this work has been hampered by a lack of understanding regarding the geomorphological products of ice streams, and many palaeo-ice stream hypotheses have evaded detailed scrutiny. Stokes and Clark (1999) addressed this problem by predicting diagnostic geomorphological criteria for identifying palaeo-ice streams. These criteria can be grouped into an ice stream landsystem which provides an observational template of a former ice stream signature. The identification of this landsystem requires a synoptic view of the ice sheet bed, something which is provided relatively cheaply by satellite imagery. Moreover, satellite imagery allows a single user to efficiently map geomorphology over relatively large areas very quickly. This is advantageous over field-work and aerial photograph mapping which are generally more expensive, more time-consuming and introduce a scale dependent bias.

This paper demonstrates the applicability of satellite remote sensing for identifying the diagnostic geomorphological products of palaeo-ice streams. Using the geomorphological criteria predicted by Stokes and Clark (1999) as a basis, satellite remote sensing has been used to;

- validate the location of an already hypothesised marine-based ice stream in the M'Clintock Channel, which drained the north-western margin of the Laurentide Ice Sheet between 11 and 10 ka BP.

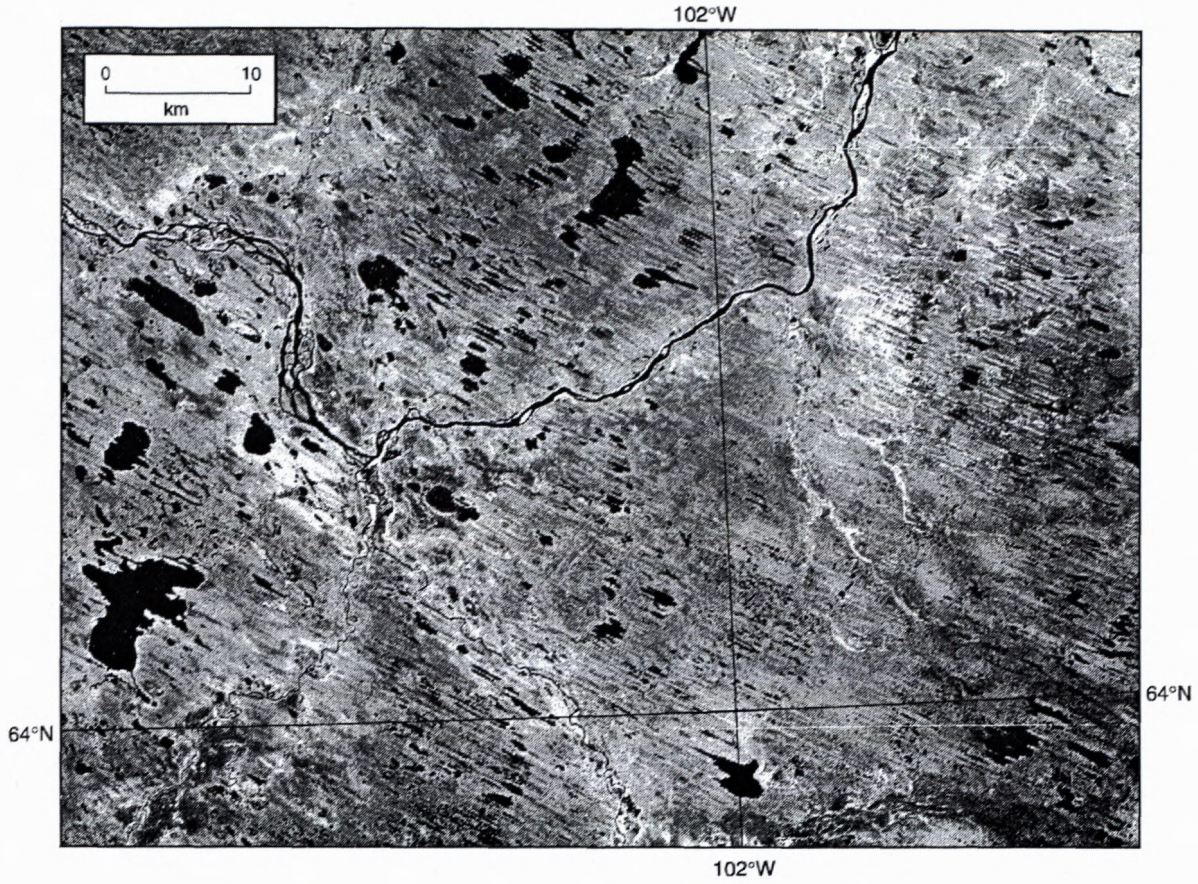

Fig. 14 Landsat MSS image of typical lineations inscribed by the Dubawnt Lake Ice Stream. The exceptional length and parallel conformity give the landscape a ridge/groove structure when viewed at this scale. The location of this figure is shown on figure 11.

- find a hitherto undetected terrestrially terminating ice stream which drained the last remnants of the Keewatin sector of the Laurentide Ice Sheet between 11 and 8.4 ka BP.

It is anticipated that this paper will go some way in helping the objective identification of ice streams from formerly glaciated areas. This will provide an enhanced understanding of Quaternary Ice Sheet dynamics which will begin to unravel the enigmatic nature of ice stream behaviour in both contemporary and Quaternary Ice Sheets.

Acknowledgements:

The authors would like to thank the staff of the Cartographic Services, Department of Geography, Sheffield University, who drew the figures for this paper. We should also like to thank the Quaternary Research Association and the British Geomorphological Research Group for their generous assistance in providing funds to CRS that helped purchase aerial photographs and satellite images.

References

Aylsworth, J.M. and Shilts, W.W. (1989) Bedforms of the Keewatin Ice Sheet, Canada. *Sedimentary Geology*, 62, 407-428.

Bindschadler, R.A. (1997) West Antarctic Ice Sheet Collapse? Science, 276 (5313), 662-663.

Bird, J.B. (1953) The glaciation of central Keewatin, Northwest Territories, Canada. *American Journal of Science*, 251, 215-230.

Boulton, G.S. and Clark, C.D. (1990a) A highly mobile Laurentide Ice Sheet revealed by satellite images of glacial lineations. *Nature*, 346, 813-817.

Boyce, J.I. and Eyles, N. (1991) Drumlins carved by deforming till streams below the Laurentide Ice Sheet. *Geology*, 19, 787-790.

Clark, C.D. (1990) *Reconstruction of the behaviour of the Laurentide Ice Sheet using satellite imagery*. unpublished Ph.D. Thesis, University of Edinburgh, UK.

Clark, C.D. (1994) Large-scale ice-moulding: A discussion of genesis and glaciofluvial significance. *Sedimentary Geology*, 91, 253-268.

Clark, C.D. (1997) Reconstructing the evolutionary dynamics of former ice sheets using multi-temporal evidence, remote sensing and GIS. *Quaternary Science Reviews*, 16, 1067-1092.

Clark, C.D. (1999) Glaciodynamic context of subglacial bedform generation and preservation. *Annals of Glaciology*, 28, 23-32.

Clark, C.D. and Stokes, C.R. (*in press*) The extent and basal characteristics of the M'Clintock Channel Ice Stream. *Quaternary International*.

Dyke, A.S. and Dredge, L.A. (1989) Quaternary geology of the northwestern Canadian Shield. In, Chapter 3 of *Quaternary Geology of Canada and Greenland*, R.J. Fulton, (Ed.); Geological Survey of Canada, Geology of Canada, No. 1 (also, Geological Society of America, The Geology of North America V. K-1.)

Dyke, A.S. and Morris, T.F. (1988) Drumlin fields, dispersal trains, and ice streams in Arctic Canada. *Canadian Geographer*, 32, 86-90.

Dyke, A.S., Morris, T.F., Green, E.C. and England, J. (1992) Quaternary Geology of Prince of Wales Island, Arctic Canada. *Geological Survey of Canada, Memoir* 433.

Hart, J.K. (1999) Identifying fast ice flow from landform assemblages in the geological record: a discussion. *Annals of Glaciology*, 28, 59-66.

Hodge, S.M. and Doppelhammer, S.K. (1996) Satellite imagery of the onset of streaming flow of Ice Streams C and D, West Antarctica. *Journal of Geophysical Research*, 101, 6669-6677.

Hodgson, D.A. (1994) Episodic ice streams and ice shelves during retreat of the northwesternmost sector of the Late Wisconsinan Laurentide Ice Sheet over the central Canadian Arctic archipelago. *Boreas*, 23, 14-28.

Lee, M.A. (1959) Surficial geology of southern District of Keewatin and the Keewatin ice divide, Northwest Territories. *Geological Survey of Canada Bulletin*, 51, 1-42.

Mathews, W.H. (1991) Ice sheets and ice streams: Thoughts on the Cordilleran Ice Sheet Symposium. *Geographie Physique et Quaternaire*, 45, 263-267.

Morgan, V.I., Jacka, T.H. and Akerman, G.J. (1982) Outlet glacier and mass-budget studies in Enderby, Kemp, and Mac. Robertson Lands, Antarctica. *Annals of Glaciology*, 3, 204-210

Paterson, W.S.B. (1994) *The Physics of Glaciers (3rd Ed)*. Pergamon.

Prest, V.K., Grant, D.R. and Rampton, V.N. (1968) Glacial map of Canada. Map 1253A, Geological Survey of Canada.

Shilts, W.W., Cunningham, C.M. and Kaszycki, C.A. (1979) Keewatin Ice Sheet - re-evaluation of the traditional concept of the Laurentide Ice Sheet. *Geology*, 7, 537-541.

Stokes, C.R. (2000) Bedform characteristics of the M'Clintock Channel Ice Stream, Victoria Island, Arctic Canada. *Quaternary Newsletter*, 91, 35-38.

Stokes, C.R. and Clark, C.D. (1999) Geomorphological criteria for identifying Pleistocene ice streams. *Annals of Glaciology*, 28, 67-75.

Zarkhidze, V.S., Fulton, R.J., Mudie, P.J., Piper, D.J.W., Musatov, E.E., Naryshkin, G.D. and Yashin, D.S. (1991). Circumpolar map of Quaternary deposits of the Arctic. Geological Survey of Canada, Map 1818A, scale 1:6 000 000.

Slovak Geol. Mag., 7, 3 (2001), 263 – 274

Mapping glacial lineaments from satellite imagery: an assessment of the problems and development of best procedure.

MIKE J. SMITH, CHRIS D. CLARK and STEVE M. WISE

Department of Geography, Sheffield University, Sheffield, S10 2TN, UK.

Abstract. Remotely sensed images are important tools in the mapping of glacial landforms and reconstruction of past glacial environments. However the quality of imagery can be highly variable, introducing random and selective bias into any landforms mapped from them. In this paper we illustrate the three main sources of bias and go onto provide a descriptive and analytical assessment of these bias. With a primary focus on visual and near infra-red sensors, we also illustrate the utility in using radar imagery, particularly as a supplemental data source. We conclude that low solar elevation is an important requirement, whilst an awareness of the selective bias introduced by solar azimuth is necessary. Landsat ETM+ imagery meets the requirements for glacial landform mapping and is our recommended data source.

Keywords: bias, mapping, satellite, imagery, glacial

Introduction

Remotely sensed images have been used for mapping glacial landforms since the widespread availability of aerial photography in the 1950's. The aerial view allows easy landform identification over large, often inaccessible, areas that would otherwise be difficult to map from field surveys. These analogue images were supplemented in the 1970's with the introduction of digital satellite imagery. The synoptic scale view (up to 180x180km per scene) and near-complete global coverage offered distinct advantages over traditional aerial photography.

Sugden (1979) first used Landsat Multi-Spectral Scanner (MSS) images to map glacial erosional landforms of the former Laurentide Ice Sheet. Since then, a variety of researchers have used images from different satellite sensors to map glacial landforms (e.g. Punkari, 1982, Boulton, 1990). Mapping has primarily been of ice-flow landforms, such as drumlins (i.e. glacial lineaments) which can then be generalised to help with the process of ice sheet reconstruction.

The use of remotely sensed imagery for glacial landform mapping is relatively new, having been developed from photointerpretive techniques applied to aerial photography and refined by different researchers over the past two decades. Clark (1997) provides a summary, from the acquisition of relevant imagery, to the production of a glacial reconstruction. During our current research into the reconstruction of the Irish ice sheet, it has become clear that the results obtained by mapping from remotely sensed imagery may vary according to the nature of the imagery used, and the skill and experience of the operator. If this method is to yield reliable results which are comparable between different areas, mapped by different researchers, then there needs to be a greater understanding of the sensitivity of the results to the exact methodology employed.

Clark's (1997) method involves two stages. The first stage is to map the individual glacial landforms from the imagery. The results from this stage will depend on the detectability of the landforms, a term which includes two elements: the degree to which the physical and spectral characteristics of the sensor allow the landforms to be distinguished from other features on the image and the success with which an observer can record these differences and thus map the landforms. The second stage involves summarising the landform information by grouping the individual landforms into sets of features which can be assumed to have been derived by a single glacial event. This is an entirely subjective process, which in many ways resembles the process by which cartographers generalise information from large scale maps to produce small scale ones. This paper is solely concerned with the first of these stages although work is also underway to provide a semi-quantitative approach to the second stage, allowing methodological checks to be implemented by the operator.

In the next section, we discuss the factors which affect the detectability of landforms on imagery. The effect of these factors has been tested in a series of experiments using multiple images of a series of test areas, and a Digital Terrain Model. The paper concludes with a discussion of the findings and some suggestions for good practice in the mapping of glacial features from remotely sensed imagery.

Landform Detectability

Central to the mapping of glacial landforms is the process of *landform detection*, which is dependent upon *landform representation* and *observer ability*. This section will discuss the factors that affect these two variables.

Landform Representation

The representation of a landform upon an image depends upon the *characteristics of the sensor*, the *characteristics of the landform*, *the illumination conditions* and sometimes the *meteorological conditions prior to and during acquisition*. The interaction of these categories combine to produce the following variables:

1) **Relative size:** the relationship of *lineament length* to *sensor spatial resolution*. The higher the spatial resolution the greater the ability to resolve shorter lineaments.

2) **Azimuth Biasing:** a bias in landform detectability arising from the difference between the *lineament orientation* and the *illumination orientation* (azimuth angle). Landforms are known to appear differently when they have different solar illumination directions. For example, a drumlin viewed side-on will look like drumlin, but when viewed head-on can look like a circular hill (Aber *et al* (1993) and Lidmar-Bergström *et al* (1991)).

3) **Landform Signal Strength:** the degree to which the landform can be distinguished from other features by tonal and textural information in the image. These variations are caused by differences between the surface cover of a lineament and its surroundings, and the relief effect arising from slopes appearing lighter or darker depending upon the height of the sun in the sky (solar elevation). High illumination angles cause lee slopes to be illuminated (so reducing textural information), whilst low illumination obscures lee slope with shadow (also reducing textural information, but highlighting the presence of the lineament). Several authors have investigated the conditions through which high contrast images depicting lineaments are obtained (e.g. Slaney, 1981). In general they conclude that a low solar elevation produces ideal imaging conditions.

Synthetic aperture radar (SAR) imagery is also used for mapping landforms but here the controls on detectability are different because of the different viewing geometry. SAR imagery is good at detecting topographic variation due to the oblique viewing angle of the sensor, as opposed to the vertical viewing angle of VIR sensors. The oblique viewing angle not only produces little variation in landform signal strength (i.e. the angle is the same for every image), but also the same azimuth biasing for every image.

The greater the difference in reflectance properties of the surface cover of the lineament when compared to surrounding terrain and the greater the *relief effect* (for VIR imagery), the greater the tonal differentiation of the lineament on the image (see Clark, 1997 and Aber *et al*, 1993 for further discussion). As lineaments are often composed of the same material as the surrounding terrain, spectral differentiation is of limited use in these situations. However Punkari (1982) and Dongelmans (1996) have successfully used spectral differentiation by taking advantage of certain regions where drumlinised terrain enhances the collection of moisture in inter-drumlin areas. This variability in surface moisture affects surface cover (i.e. inter-drumlin regions become boggy) and allows drumlin identification.

In summary, there is a minimum resolvable landform size and a range of lineament orientations that an individual sensor will be able to represent. In addition, the *definition* of these landforms is dependent upon the surface cover and the strength of the relief effect.

Observer Ability

Image interpretation is the qualitative, manual, identification of features of interest within an image and an appraisal of their significance. The ability of an observer to interpret a remotely sensed image depends on their experience in using interpretive techniques and their level of specialist knowledge pertaining to the features being mapped. Inter-operator variability is a consequence of any interpretive technique and is known to be a specific problem in geological lineament mapping (e.g. Siegal, 1977).

In summary, landform detectability is dependent upon the representation of a surface by a satellite sensor and the ability of an observer to map those landforms. This raises the following questions:

- is the available imagery representing all, or a large proportion, of the landforms present?
- is the observer able to map these landforms or are errors of omission and commission present?

The latter question has been briefly touched upon above, but is yet to receive specific examination with respect to glacial landforms. Indeed, recent research (e.g. Vencatasawmy, 1997) looked at the ability to automate the process of lineament mapping.

This research is aimed at investigating the former question by using existing imagery to model the effects of the above variables on landform representation. Operator variability in mapping is minimised through the use of one operator.

Methodology

We needed to select suitable images from a range of earth resources satellites for areas that contained enough lineaments to be statistically viable. We selected the region around Lough Gara, County Roscommon, Ireland (1539km^2), bounded by the Ox Mountains on the west and the town of Sligo to the north. There is complete coverage from the four of the five main earth resources sensors; Landsat MSS, Landsat TM, SPOT Panchromatic and ERS-1 Synthetic Aperture Radar (SAR). Unfortunately there were no suitable cloud free scenes from Landsat ETM+ available for this study area, so a second area on the Kola Peninsula (1183km^2), Russia, has been used to supplement our results.

In order to assess the accuracy with which landforms can be mapped from each type of imagery it is necessary to have some information on the landforms which are known to be present in the test area. For this purpose we used a high resolution DEM to create a morphological

map for a subset of the area (587km^2), as complete DEM coverage was not available. Hill shading is an effective way of identifying landforms on a DEM, although this suffers from the same azimuth biasing as satellite imagery. Therefore the morphological map was produced through full break-of-slope mapping using multiple illumination azimuths. The DEM was produced by the Irish Ordnance Survey from 1:40000 stereoscopic aerial photography at a spatial resolution of 50m, using a digital analytical plotter. The spatial resolution of the DEM is therefore similar to that of the imagery, but because the landform mapping is based upon stereoscopy rather than photo interpretation, and because the original photographs are at a higher resolution than the satellite imagery, the morphological map produced from the DEM will be at a higher level of accuracy than is possible using satellite imagery. A comparison of the morphological map derived from the DEM with a selection of the original stereoscopic aerial photography confirmed the accuracy of the morphological map, which was able to resolve individual drumlins, although cross-cutting patterns and smaller forms could not be distinguished.

Table 1 Satellite image meta-data used in this study (D=descending, A=Ascending).

Satellite Images	Spatial Resolution (m)	Date	Lat/Long (°)	Illumination Elevation (°)	Illumination Azimuth (°)
Lough Gara					
ERS-1 SAR	25	04/08/92	54:14N 8:53W	23.1	104D
ERS-1 SAR	25	02/03/93	54:19N 8:51W	23.1	104D
Landsat TM	30	10/12/	53:39N 7:43W	11.2	160
Landsat TM	30	06/05/89	54:51N 7:58W	48.3	147
Landsat MSS	80	06/01/83	54:51N 7:45W	10.1	157
SPOT Panchromatic	10	28/11/92	53:39N 8:20W	14.3	167
SPOT Panchromatic	10	28/11/92	54:07N 8:10W	13.9	168
Strangford Lough					
ERS-1 SAR	25	30/06/93	54:28N 6:00W	23.1	256A
Landsat TM	30	03/11/90	54:31N 4:28W	18.1	158
Kola Peninsular					
Landsat ETM+	15/30	17/07/99	66:57N 32:24E	43.8	166

Given the differences between the SAR and VIR sensors, it is not appropriate to directly compare their imagery. As a result these sensors are treated separately through a case study. Our SAR case study area (110km^2) lies west of Strangford Lough, County Down, Ireland, bordered on the south by Dundrum Bay.

Experiments

1) **Landform Signal Strength** – In order to assess the effect of varying solar elevations on landform representation, ideally we would obtain images acquired at the same time but with different solar elevations. As this was not possible, we illustrate this experiment using images with variable solar elevations.

It was also hoped to use the DEM to model the effects of landform signal strength by simulating different solar elevations through the use hill shading. However hill shading is unable to effectively model these variations and so this was not pursued.

2) **Azimuth Biasing Effect** – In order to assess the biasing effect we used an image with varying lineament orientations. A relative comparison was then performed between the image and the morphological map.

A further experiment was also performed using the DEM to investigate azimuth biasing more objectively by simulating different azimuth angles through the use of hill shading. All lineaments were mapped and then compared to the morphological map.

3) **Relative size** – In order to assess the effect of image spatial resolution on landform representation we acquired Landsat ETM+ data, which is ideally suited to this task, as the high resolution panchromatic band (15m) and lower resolution multispectral bands (30m) are acquired at the same time. We selected Band 2 to compare against the Panchromatic band, as a greyscale image was appropriate and they both record an overlapping part of the EM spectrum.

SPOT Panchromatic, Landsat TM Band 5 and Landsat MSS Band 4 were used for all lineament mapping (Table 1). The Landsat TM and MSS bands were chosen as the near-IR enhances any moisture variations (Clark, 1997), whilst tonal variations are more efficiently detected by the human eye from a greyscale image. Where appropriate all images had pre-processing techniques applied to them following the guidelines of Clark (1997). All mapping was performed by one observer.

Results

This section presents the results of interimage comparisons and our analysis of the controls on detectability. The first section provides a description both of the images and of the landforms mapped from them, whilst the second section presents summary statistics for each experiment.

Slovak Geol. Mag., 7, 3 (2001), 263 – 274

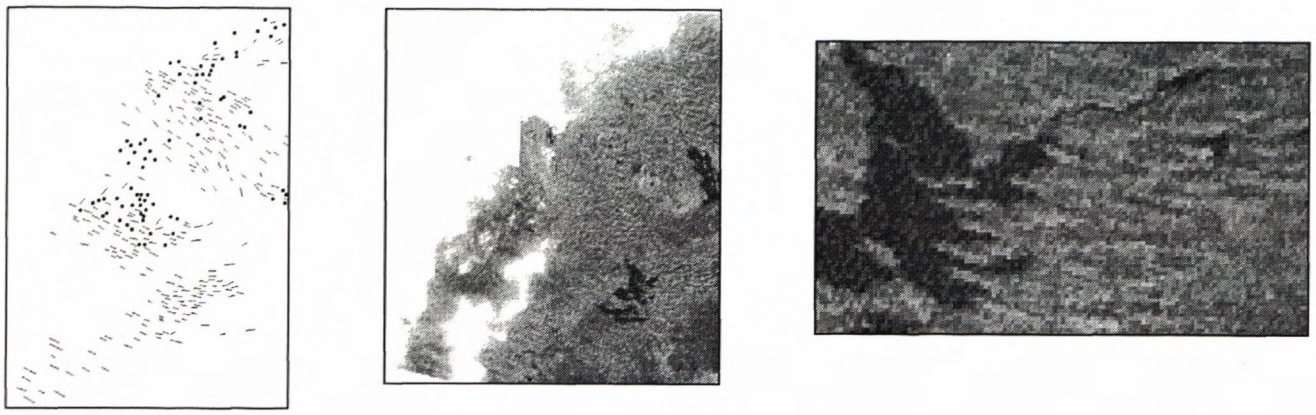

Figure 1a, b and c Landsat MSS glacial landform mapping (left), image (centre) and zoomed region (right) for Lough Gara, Ireland. The landform map shows lineaments (lines) and hillocks (points).

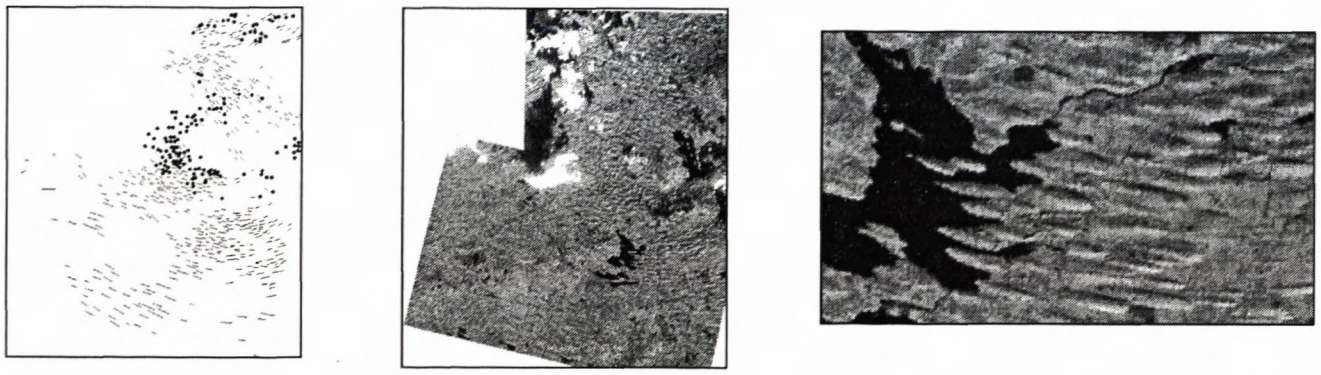

Figure 2a, b and c Landsat TM glacial landform mapping (left), image (centre) and zoomed region (right) for Lough Gara, Ireland. The landform map shows lineaments (lines) and hillocks (points).

Interimage Comparisons

Morphological Map

Figure 5 shows a map of all detectable lineaments produced from the DEM for a subset of the Lough Gara study area (approximately the southern half of the Lough Gara satellite images). There is a strong trend of lineaments oriented NW-SE, with longer lineaments in the southern area. A random spread of lineaments oriented E-W is also noticeable. There is a strong concentration of hummocky terrain in the northerly part of the map, with few hummocky forms elsewhere. The northern half of the map also contains transverse ridges, often with lineaments overlying them.

Landsat MSS Image

The low contrast and poor detectability of lineaments within the image (Figure 1b) is readily apparent. Although the southern portion of the image depicts E-W trending lineaments, curving to the NE, this is not clear and is barely detectable in many parts. The presence of hummocky terrain in the central portion is clearer, whilst the northern area depicts clearly detectable lineaments although their trend is not so obvious. The forms in the south, whilst less detectable, appear wider and longer. The overall impression is one of an ability to see lineaments, but not identify and map them precisely.

Figure 1a shows the lineaments that have been mapped from this image. There is a strong lineament orientation of NW-SE, with some lineaments in the east trending W-E and some in the north trending SW-NE. The central area has a greater abundance of hummocky terrain, with further hummocks in the northern area. In general there are far less lineaments mapped in comparison to the morphological map, however the main general trends are readily apparent, although no transverse ridges have been identified.

Landsat TM Image

The topographic shadows increase the amount of contrast present, producing a high quality image (Figure 2b) and allowing the easy recognition of landforms.

In the southern portion of the image long, broad lineaments are visible in the west (trending east-west), becoming more apparent in the east whilst curving towards the NE. The central region shows hummocky terrain, comprised of many small circular hills. In the northern part of the image there is a clear orientation NW-SE, although in the extreme NE corner lineaments are again trending E-W.

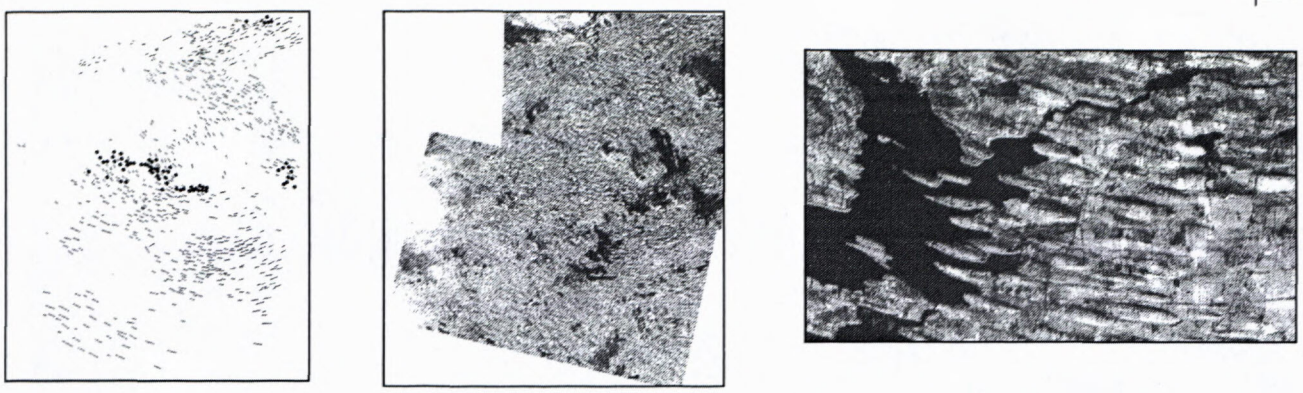

Figure 3a, b and c SPOT glacial landform mapping (left), image (centre) and zoomed region (right) for Lough Gara, Ireland. The landform map shows lineaments (lines) and hillocks (points).

In contrast to the MSS mapped data, Figure 2a shows a greater number of lineaments mapped, although still less than for the morphological map. The same general pattern is visible between all three maps. In comparison to the MSS mapped data, the eastern area shows a clear transition in lineament orientation from NW-SE to NE-SW. In addition, the northern area shows some lineaments cross-cutting one another.

SPOT Image

Simple contrast enhancements were necessary in order to make the best use of this image (Figure 3a). Initial assessment of the amount of contrast available for lineament mapping suggests a high quality image, although closer inspection reveals that the contrasts are more subdued and, although landforms are clearly visible, their representation is not as good as with the TM image. However the high spatial resolution allows detailed landform mapping, clearly showing areas of intersection between E-W and NW-SE trending lineaments in the northern region. The southern region shows longer lineaments in the W trending NW-SE, curving towards the NE-SW in the eastern area. The central region appears as a more complicated area of „hummocky" terrain, with elongate and ovoid forms present.

Like the morphological map, TM and MSS mapped data, the SPOT data again shows the same general trends (Figure 3b). There are even more lineaments mapped than in either of the previous two images (Table 2), although less than the morphological map. There are noticeably fewer hummocks than the Landsat MSS and TM images and a greater incidence of crossing lineaments in the northern portion of the image.

Landsat ETM+ Image

Panchromatic

Simple contrast enhancements were again employed to prepare the image. The high contrast within the image is mainly manifested through spectral differentiation (Figure 4a). Non-vegetated regions appear as dark areas and typically mark lineament ridges, which are often offset from elongated lakes. The high spatial resolution of the image allows clear identification of lineaments as short as 80m in length.

The mapped lineaments show a strong orientation of SW to NE, ranging up to 4km in length. The larger lineaments are clearly detectable, although they are sometimes composed of several, smaller, lineaments.

Multi-spectral (Band 2)

The multi-spectral image (Figure 4b) also allows lineament detection through spectral differentiation. The effect of decreased resolution is clearly apparent through the higher proportion of longer lineaments mapped. For example, where many individual lineaments might have been mapped on the panchromatic image, the multi-spectral image often shows a single, larger, lineament. The mapped lineaments range from 280m to 4km in length, with a strong SW to NE orientation.

Analysis of Controls on Detectability

1) Landform Signal Strength

We acquired low (11.2°) and high (48.3°) solar elevation images for our test areas, shown respectively in Figure 2b and 6a. These show the dramatic impact solar elevation has on lineament representation. The high solar elevation provides very little tonal and textural variation, whilst the lack of surface cover variation means that the lineaments are very difficult to identify.

2) Azimuth Biasing Effect

Although it is possible for the azimuth angle to vary from due east to due west, testing its effect on landform detectability is difficult as it is not possible to hold other factors, such as solar elevation, constant. As a result it is not possible to test variations in the azimuth angle using different imagery. Consequently, the effect of varying lineament orientations was used to test the azimuth biasing effect. This was achieved through the use of one image (Landsat TM) with a variety of alternately oriented lineaments. This was then compared to the morphological map derived from the DEM.

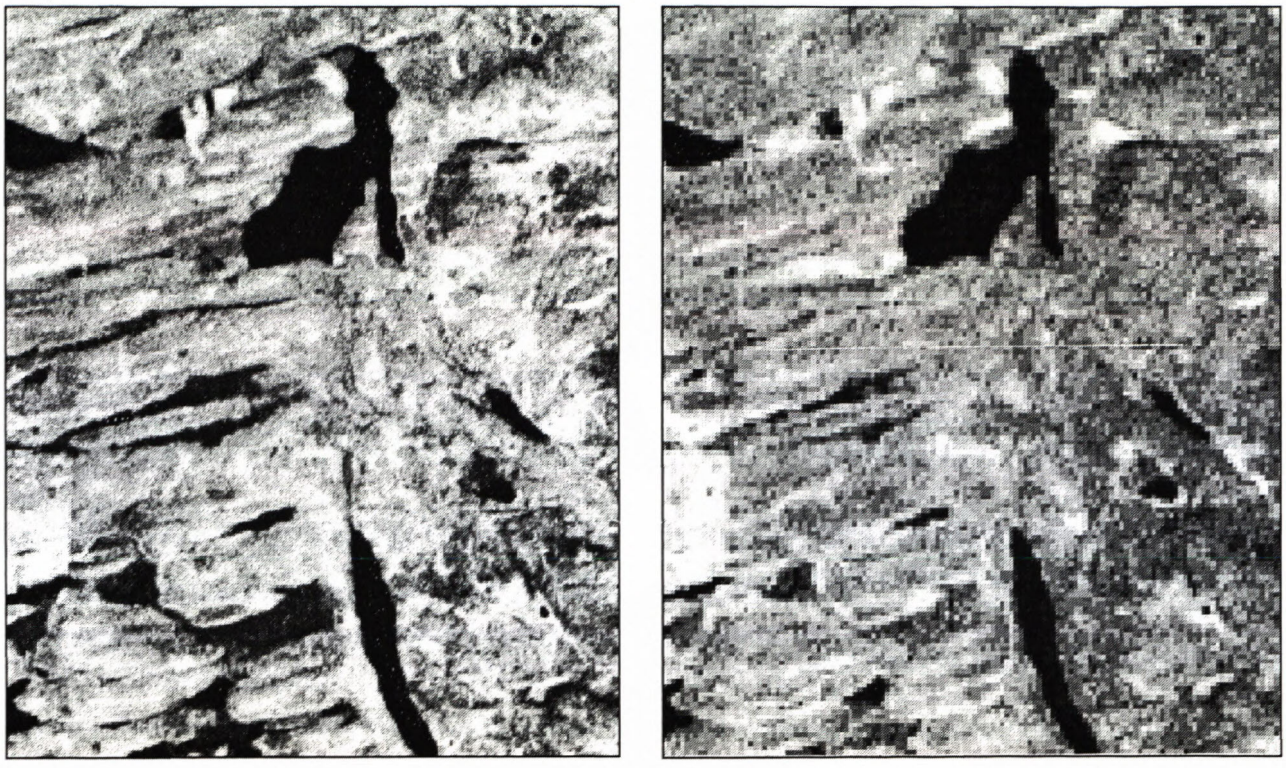

Figure 4a and b Landsat ETM+ Panchromatic (left) and Multispectral (right) images (Kola Peninsular, Russia) showing the effect of sensor spatial resolution (15m and 30m respectively) on lineament detection

Table 2 Total number of lineaments and hillocks mapped from the Landsat MSS, Landsat TM and SPOT imagery for the Lough Gara region.

Landform	*SPOT*	*Landsat MSS*	*Landsat TM*	*Landsat EMT+ Pan*	*Landsat EMT+ XS*
Lineament	576	245	394	813	473
Hillock	59	78	132	-	-

The Landsat TM image has an azimuth angle of 159.7°; so we would expect lineaments oriented in this direction to be selectively „hidden." Lineaments which have an orientation close to 160° on the morphological map (Figure 5) are often not present on the map produced from the Landsat TM image (Figure 2a). There is also a clear difference in the descriptive statistics for the two sets of lineaments (Figure 7, Table 3) caused by the omission of the lineaments parallel to the azimuth direction.

Table 3 Descriptive statistics of lineament orientation for the DEM and Landsat TM data. The higher maximum and mean for the DEM data support the selective „hiding" of lineaments oriented parallel to the illumination azimuth.

Lineament Orientation	***DEM***	***Landsat TM***
Mean (°)	109	106
Min (°)	40	24
Max (°)	161	135
Number	377	271

In order to explore this effect more fully, the DEM of the Lough Gara region was hill shaded with illumination orientations parallel, orthogonal and intermediate to the principal lineament direction. Figures 8a and b show the DEM hill shaded using an illumination orientation parallel and orthogonal directions. The difference between the two images is striking, showing not only the complete disappearance of lineaments (not visible in *parallel* that

Figure 5 Morphological map of all resolvable lineaments produced from the DEM of Lough Gara, Ireland.

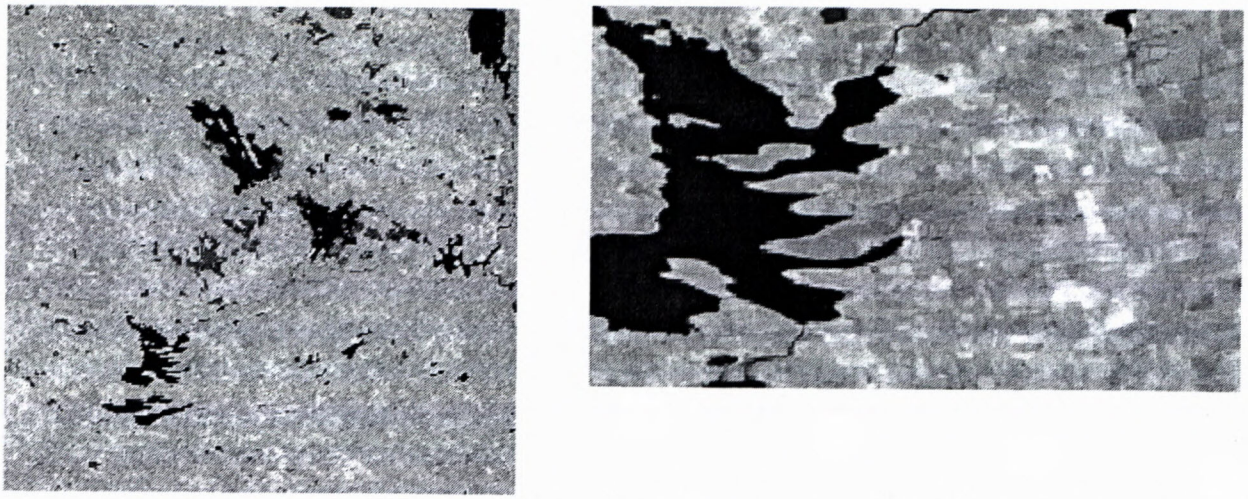

Figure 6 a and b Landsat TM image (left) of Lough Gara, Ireland, with zoomed region (right). This illustrates the low representation of lineaments as a result of the high solar elevation.

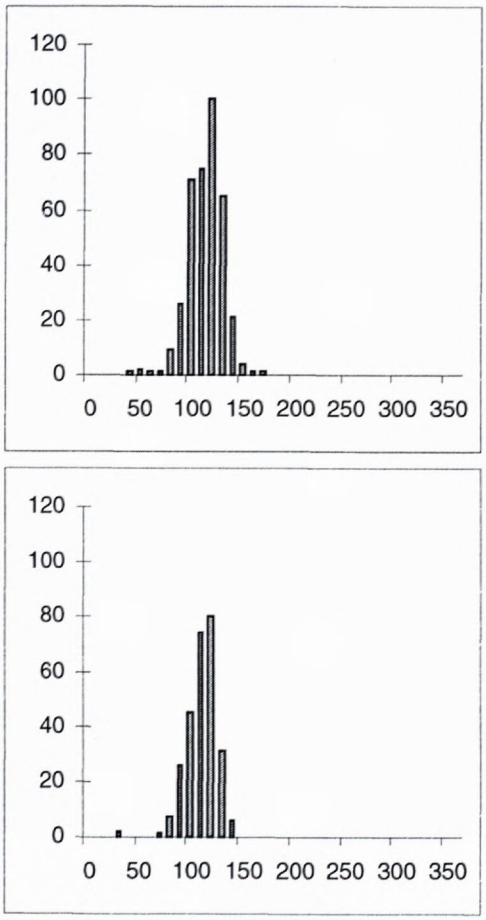

Figure 7a and b Frequency histograms of lineament orientation for the DEM (top) and Landsat TM (bottom) data. The Landsat TM shows a smaller upper tail, a result of azimuth biasing.

are visible in *orthogonal*), but also a change in the shape of other forms. This includes the appearance in *parallel* of transverse ridges, which have lineaments superimposed onto them.

The above description is supported by the statistics in Table 4. These show a dramatic reduction in the total number of lineaments mapped using a *parallel* illumination, when compared to the *orthogonal* and *intermediate* illuminations. It is also important to note that the *parallel* image identifies transverse ridges within the image and an increased number of hillocks. The transverse ridges were identified on the aerial photography, although their morphology is subdued due to their reorientation by the overlying lineaments. As a result the *parallel* image selectively enhances these, whilst the *orthogonal* image degrades them. The increase in the number of hillocks is probably due to the misrepresentation of lineaments as hillocks and consequently their misidentification.

Table 4 Total number of lineaments, hillocks and ridges mapped from the DEM for alternately hill shaded azimuth angles, illustrating the selective „hiding" of lineaments and enhancement of transverse ridges for those mapped from the parallel image.

Landform	*Orthogonal*	*Parallel*	*Intermediate*	*Complete*
Lineament	371	176	330	443
Hillock	101	120	75	109
Transverse Ridge	0	20	0	25

3) Relative Size

Intuitively we would expect that, as resolution increases, smaller lineaments become detectable and so more lineaments are mapped. As a result the value of the distribution peak of the frequency histogram for lineament length will decrease, gradually shifting in the direction of the origin.

Using the Landsat ETM+ Panchromatic (15m) image of the Kola Peninsula, 813 lineaments were mapped, compared to 473 lineaments for the multi-spectral (30m) image. This significant increase (170%) in lineaments can be attributed solely to the resolution of the sensor, as all other variables are fully controlled (e.g. solar elevation, azimuth angle). Table 5 presents descriptive statistics for these data.

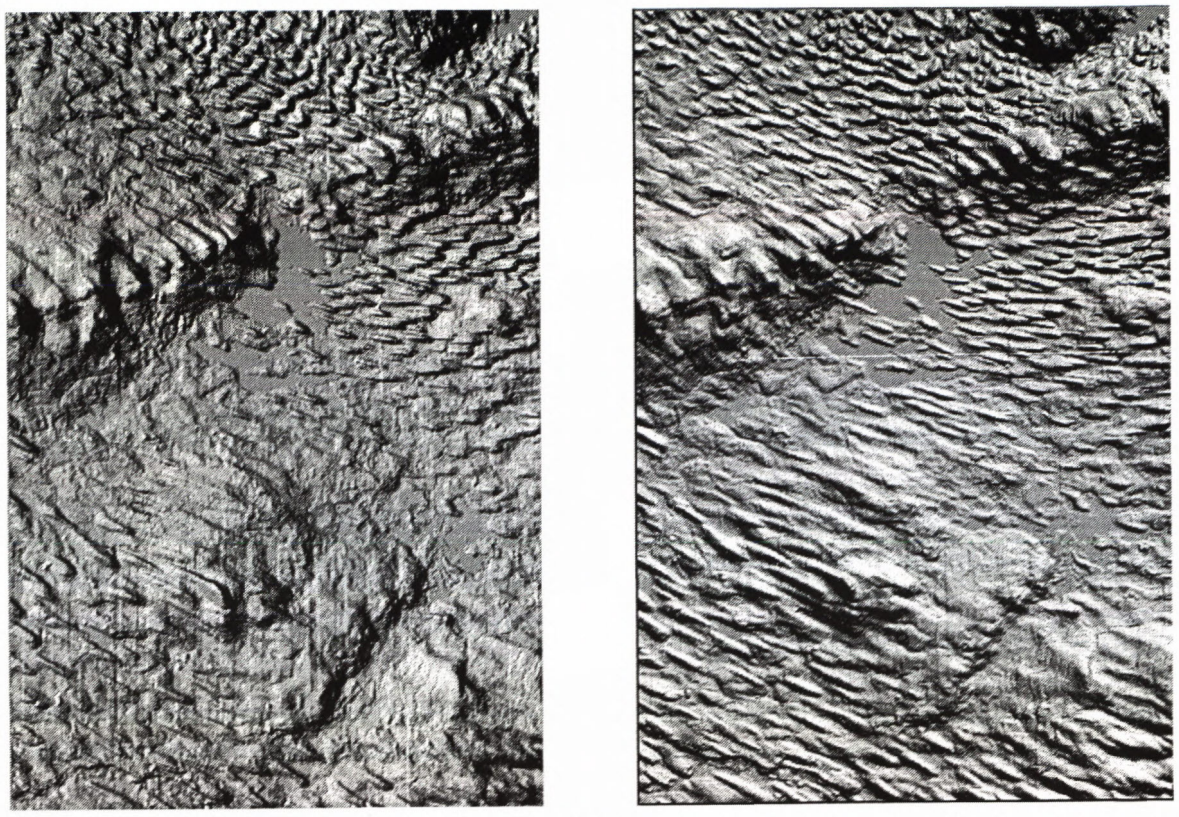

Figure 8a and b Hillshaded DEM of Lough Gara, Ireland, using an illumination azimuth parallel (left) and orthogonal (right) to the principal lineament orientation. Not the dramatic changes in lineament morphology, particularly above the centre of the image.

This shows that in addition to more lineaments being mapped, the panchromatic image represents not only shorter lineaments, but a greater number of them. This has the overall effect of reducing the mean (from 892m to 647m) and consequently shifting the histogram peak towards the origin (Figure 9a and b).

Table 5 Descriptive statistics of lineament orientation for the Landsat ETM+ Panchromatic and Multispectral data. These highlight the greater number of smaller lineaments mapped on the panchromatic image.

Lineament Orientation	*Panchromatic*	*Multispectral*
Mean (°)	647	892
Min (°)	81	282
Max (°)	3951	4040
Number	811	472

SAR Case Study

Although both Landsat TM and ERS-1 SAR have very similar spatial resolutions (and consequently relative size), it is not possible to control for the differences in landform signal strength or azimuth biasing. As a result this case study is designed to highlight the benefits in using SAR imagery to detect topographic landforms, as well as the differences with VIR imagery. In addition the active sensor operates in the microwave part of the EM spectrum which means that imagery can be obtained day or night, regardless of meteorological conditions.

Our case study was located in the Strangford Lough region of eastern Ireland where we acquired a descending ERS-1 SAR image and a cloud free, winter, Landsat TM image. The images were geocorrected and then any detectable lineaments mapped.

Figure 10 (a and b) depicts a selected region from the SAR and TM images respectively; the dominant lineament directions for SAR (north-south) and TM (east-west) are striking, and are further illustrated by the frequency histograms of lineament orientation (Figure 11a and b). Table 6 also supports these results showing a much higher mean lineament orientation for the ERS-1 SAR data.

Table 6 Descriptive statistics of lineament orientation for ERS-1 SAR and Landsat TM data for the Strangford Lough region, highlighting the different populations of lineaments (with different orientations) mapped.

Lineament Orientation	*SAR*	*Landsat TM*
Mean (°)	139	96
Min (°)	0	3
Max (°)	179	167
Number	289	349

These results are principally explained by the difference in azimuth angle between SAR and VIR imagery. SAR imagery is obtained by active detection using an oblique sensor orthogonal to the satellite track. As the

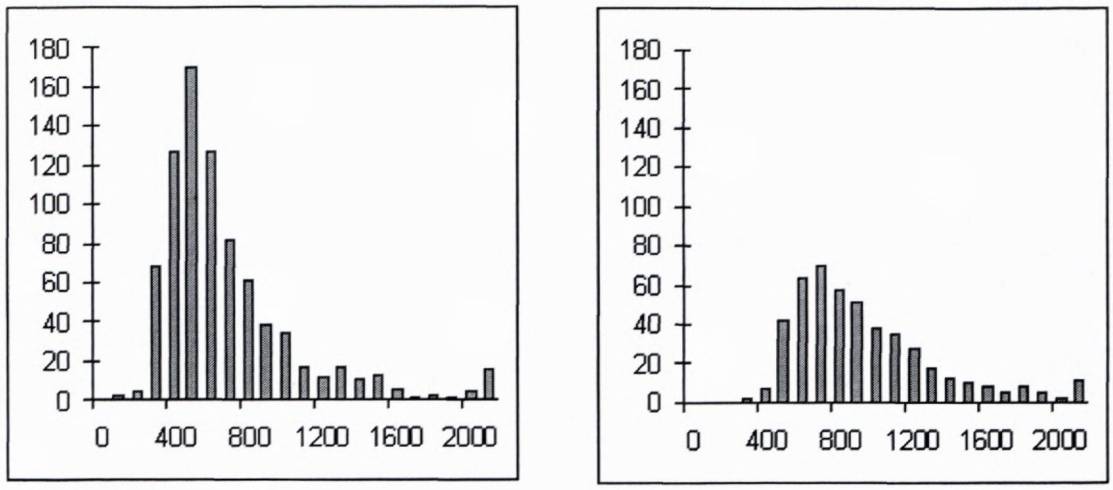

Figure 9a and b Frequency histograms of lineament length for the Landsat ETM+ Panchromatic (left) and Multispectral (right) data. These illustrate the increased number of smaller lineaments that were mapped from the panchromatic image..

satellite is polar-orbiting, this means that all images are sensed in an easterly or westerly direction depending on whether the satellite is in an ascending or descending orbit. Consequently all lineaments oriented approximately north-south are selectively enhanced, whilst those oriented approximately east-west are selectively degraded (Graham *et al* (1991).

VIR Case Study

The lineaments mapped from the Landsat MSS, Landsat TM and SPOT imagery for Lough Gara are now used to supplement the inter-image comparisons with quantitative data and so highlight the errors and bias often present within imagery acquired for landform mapping.

The solar elevation angles are so similar that we judge this to make little difference to the mapping. The effect of azimuth biasing can be significant, as illustrated by the SAR case study, although this is not the case for the Lough Gara area, because the lineaments are predominantly oriented in an east-west direction. The main difference in landform detectability between the images relates to **relative size** (i.e. resolution) where 245, 394 and 576 lineaments were mapped for Landsat MSS, Landsat TM and SPOT respectively. As resolution increases, there are more, shorter, lineaments detected. Figure 12 identifies histogram peaks at 600m, 450m and 350m respectively for Landsat MSS, Landsat TM and SPOT. This implies that the most common lineament lengths require 9, 15 and 35 pixels to identify lineaments on MSS, TM and SPOT for this region. If ~10-15 pixels are required to map a lineament, then the large number of pixels used to identify lineaments in the SPOT imagery suggests that the actual population peak has been mapped in this image, although this value will clearly vary for different regions with different lineament populations.

An important ancillary effect of being able to map smaller lineaments is the ability to be able to resolve cross-cutting patterns, which we demonstrate in the inter-image comparisons.

We also compared the coincidence of individual lineaments between images (Table 7). These show that Landsat MSS is highly coincident (~70%) with Landsat TM and SPOT, whilst Landsat TM and SPOT are poorly coincident with MSS and highly coincident with each other. These results reflect the fact that SPOT and Landsat TM have detected a greater number of lineaments which tend to be shorter, whilst MSS has detected fewer, longer, lineaments.

Table 7 Percentage coincidence of lineaments between the different satellite images and the morphological map. For example, 70% of lineaments on Landsat MSS are coincident with those on Landsat TM.

	Landsat MSS	Landsat TM	SPOT	Morphological Map Subset
Landsat MSS		50	40	19
LandsatTM	70		73	45
SPOT	78	82		49

Of further interest is the number of non-coincident lineaments. This is particularly interesting for MSS, where we expected to see high coincidence with the higher resolution imagery. Generally, this is correct, although ~30% remain non-coincident, comprising lineaments of varying orientation, length and locations. This apparent randomness in non-coincident lineaments probably relates to the mapping process. Errors in the geocorrection of the images, mapping of lineaments and visual lineament comparison can all cause errors of non-coincidence. Previous research (e.g. Siegal, 1977) suggests that inter-observation interpretation can be considerably varied, whilst geometry, mapping and comparison intra-observer variation can also occur.

In summary, for this particular case study, azimuth biasing and landform signal strength do not contribute major elements of bias. Relative size has the single largest

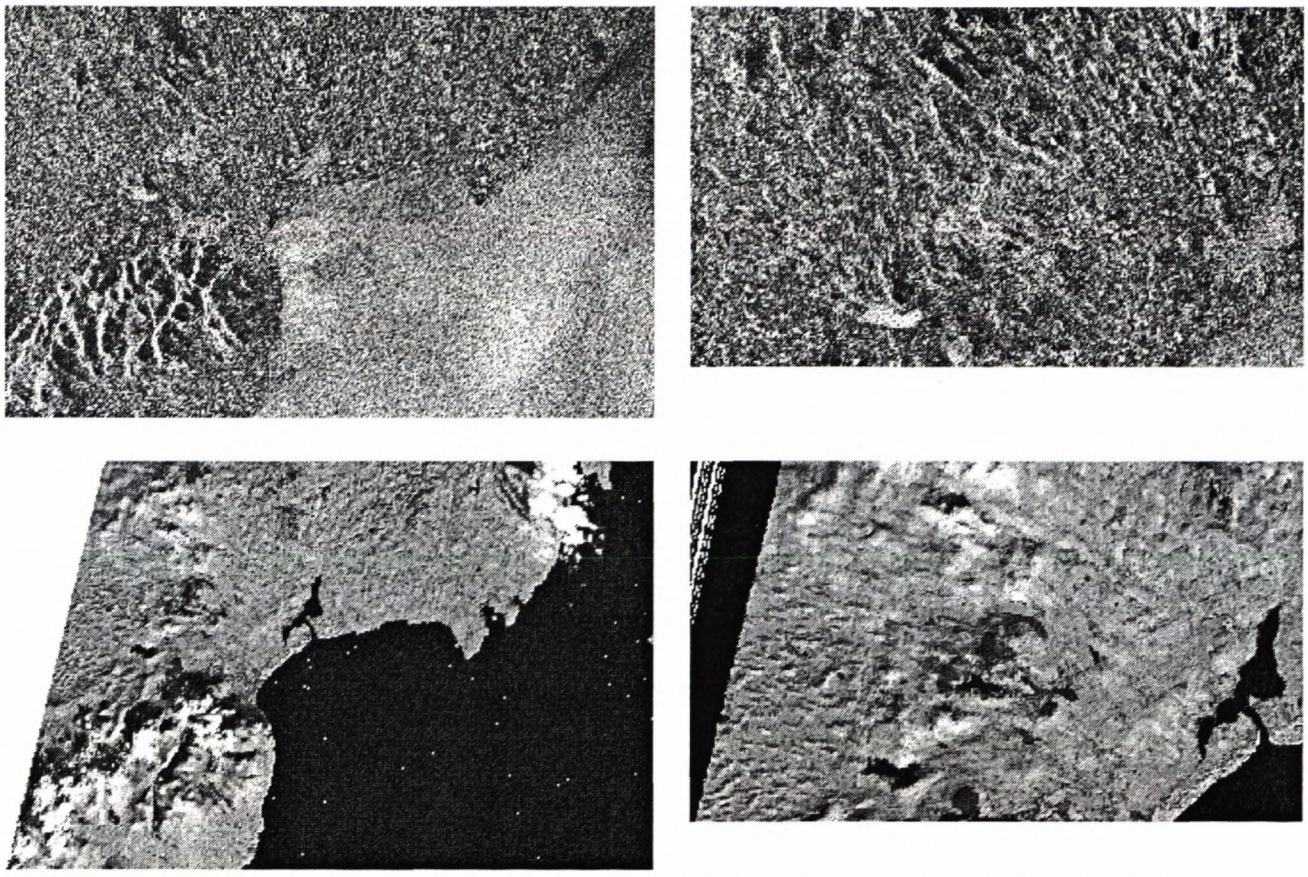

Figure 10a, b, c and d ERS-1 SAR (top left) and Landsat TM (bottom left) images (Strangford Lough, Ireland) highlighting the dramatic effect of the azimuth angle on lineament representation. Images c and d are zoomed regions. Note that the E-W trending lineaments on the Landsat TM image are not visible on the ERS-1 SAR image.

effect on mapped lineaments, whilst geocorrection, mapping and comparison errors probably account for the remaining variability.

Discussion and Recommendations

This paper has described some of benefits in using satellite imagery for glacial landform mapping. However these benefits have to weighed against weaknesses in its use. There are two main areas where error can be incorporated into a landform map (where there is a primary focus on lineament mapping). These are inherent bias within the imagery acquired and the ability of the observer to map the landforms. The latter has been touched upon by several authors whilst the former is the topic of this paper.

Image bias can occur from relative size, azimuth biasing and landform signal strength. We investigated the effect of each of these variables on lineament mapping for study areas in the Lough Gara region of western Ireland and the Kola Peninsula, Russia.

Our results suggest that low solar elevation is required (for VIR imagery) in order to selectively highlight topographic landforms (e.g. see Figures 3b and 7). From our experience we advise a solar elevation below ~20°, although <15° is desirable. Depending on latitude, solar elevations as low as 5° are possible. For Landsat ETM+, daylight imaging is not performed for solar elevations below 5°. Above 20° there is a gradual decrease in the relief effect and tonal variation to a point where lineaments are only detectable by surface cover variation. The availability of appropriate imagery from archive is variable, depending upon the latitude of the study area and the sensor desired. In mid-latitudes, winter scenes are necessary in order to acquire a low solar elevation and, coupled with the requirements for scenes to be snow and cloud free, makes suitable imagery difficult to acquire. In northerly latitudes, summer imagery is required in order acquire snow free scenes, although this is not necessarily ideal as solar elevation can be quite high (Table 1). Aber *et al* (1993) suggest that light snow cover, in association with a high relief effect, can increase detectability as tonal variation due to surface cover is effectively masked. This has to be weighed against the reduction in the relief effect with increased snow cover. Subtle topographic landforms can quickly become „hidden" making mapping of features such as cross-cutting landforms difficult.

Perhaps the single greatest bias over which the observer has little control is the azimuth biasing effect. Both the Landsat TM image for our study area and our DEM experiments suggest that large omissions can occur as a result of azimuth biasing. More particularly, the above constraints on acquisition dates for VIR imagery produce a small solar azimuth window through which images are available. As a consequence, lineaments oriented parallel to this direction are selectively diminished, such that they may change shape, appear as hillocks or completely dis-

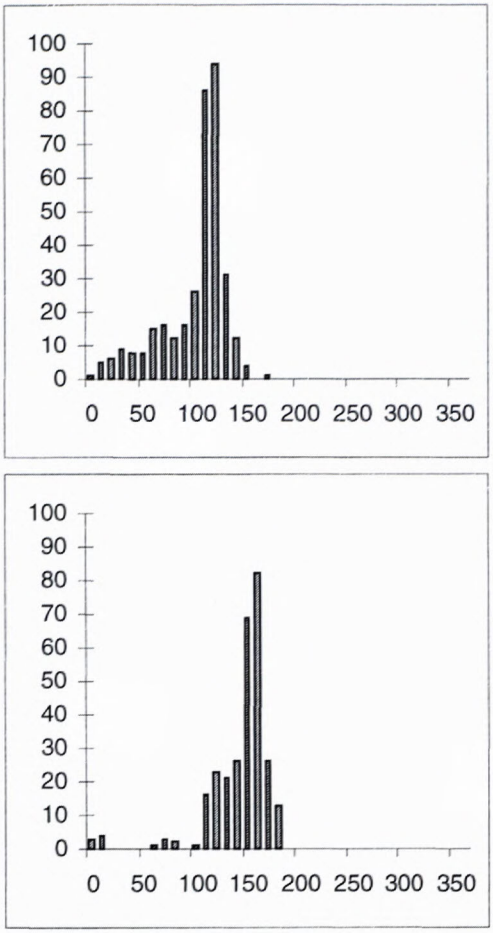

Figure 11a and b Frequency histograms of lineament orientation for Landsat TM (top) and ERS-1 SAR (bottom) data, illustrating the completely different populations of lineaments (with different orientations) mapped for exactly Strangford Lough, Ireland.

against this error. These sources include local mapping in the form of topographic maps, digital elevation models or field mapping. Where these are not available SAR imagery can be usefully used. Its alternative viewing geometry satisfactorily supplement VIR imagery, although users should not underestimate the experience required in its use (see Vencatasawmy *et al* 1998 for further discussion).

The final bias of relative size is familiar to most researchers. The higher the resolution of the satellite imagery, the greater the ability to map smaller landforms. The above results show a 170% increase in mapped lineaments by moving from 30m resolution data to 15m data. However higher precision data does not necessarily mean better quality results and it is important that researchers select imagery to match the requirements of their project. For ice sheet reconstruction, overall lineament trend is the single most important element. As a result, azimuth effects are the most serious problem since they can introduce a selective bias into the results. In contrast relative size and solar elevation are less important than azimuth bias here since the errors produced should be distributed randomly across lineaments of all orientations. From a more practical perspective, it is useful if the image coverage is as large (and cheap!) as possible. High resolution data are desirable if geomorphological or cross-cutting mapping are intended. Equally, multi-spectral data are very useful as they can be used to delimit lineaments through surface cover changes. These requirements point to Landsat ETM+ as the optimal images given the near-global coverage, large scene area (180x180km), high resolution (15m panchromatic) and multi-spectral facilities. In addition, the open access policy of NASA make the data very cheap. The disadvantage, in the short-term, is the short mission run-time which means, for mid-latitude regions, that suitable imagery may not be available.

Figure 12 Frequency histogram of lineament length for Landsat MSS, Landsat TM and SPOT for the Lough Gara region. This shows that as sensor spatial resolution increases, so the number of lineaments mapped increases, the size of lineaments decreases and the population peak shifts towards the origin.

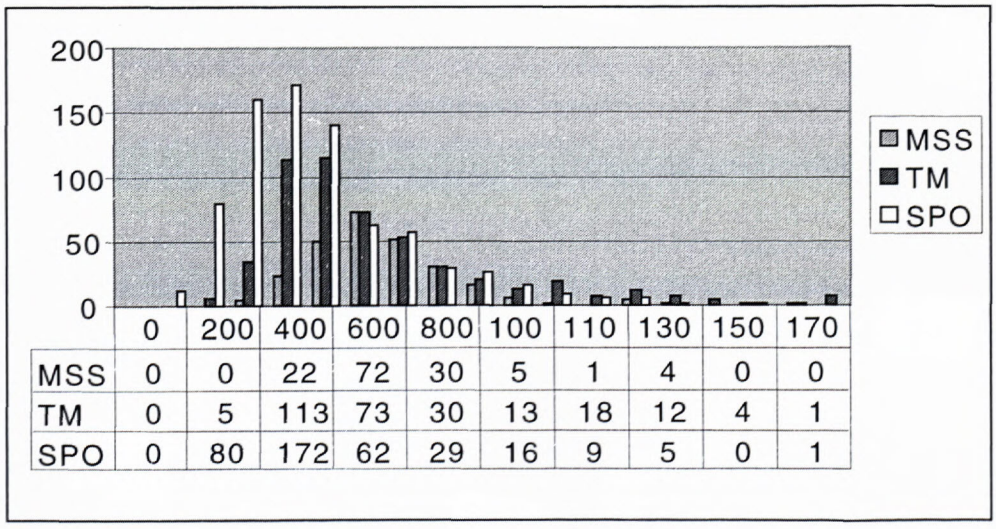

	0	200	400	600	800	100	110	130	150	170
MSS	0	0	22	72	30	5	1	4	0	0
TM	0	5	113	73	30	13	18	12	4	1
SPO	0	80	172	62	29	16	9	5	0	1

appear. It is important to be familiar with a study area in order to be aware of this problem; for some areas no action may be necessary as lineaments may not be oriented in this direction. However other areas may require the acquisition of alternative data sources in order to mitigate

If Landsat ETM+ data are not available for a particular region, then the choice of imagery becomes more difficult. SPOT are available in both high resolution panchromatic and multi-spectral formats, but the scene coverage is small (60x60km) and relatively expensive.

Landsat TM has had a longer mission time and so suitable imagery may be available that takes advantage of the larger areal coverage and multi-spectral format. Although cheaper than SPOT, Landsat TM is considerably more expensive than Landsat ETM+ and has a lower resolution (in equivalent panchromatic mode). Finally, Landsat MSS has had a very long mission time (and consequently large archive) and benefits from the areal coverage and multi-spectral format of the other Landsat missions. However it suffers from relatively poor spatial resolution.

As a result, our recommendation is to use Landsat ETM+ wherever suitable imagery is available. Otherwise, SPOT is desirable for geomorphological or cross-cutting mapping over small areas. If mapping glacial landforms over larger areas then Landsat TM is the best alternative, particularly where more detailed information on cross-cutting is required. Finally, Landsat MSS has great utility in the large archives and low cost that make it appropriate for small-scale mapping within tight budget constraints, or as a reconnaissance tool.

As a final note, users should be aware of the impending arrival of global DEM data generated by NASA from the Shuttle Radar Topography Mission (SRTM). Using SAR interferometry, a DEM covering all land masses between 60°N to 56°S will be generated at 90m and 30m spatial resolutions. The 90m data will be publicly available, whilst limited non-USA 30m data will be available to researchers upon application. This will clearly be a valuable resource for future glacial landform mapping, whilst placing new demands upon researchers in its use. There will, however, still be large previously glaciated regions that lie outside of the SRTM coverage area, making the continued use of satellite imagery necessary.

References

Aber, J. S., E. E. Spellman, et al. (1993). Landsat remote sensing of glavcial terrain. Glaciotectonics and Mapping Glacial Deposits. Proceedings of the INQUA Commission on Formation and Properties of Glacial Deposits., Canadian Plains Research Center, University of Regina.

Boulton, G. S. and Clark, C.D. (1990). „A highly mobile Laurentide Ice Sheet revealed by satellite images of glacial lineations." Nature **346**(813-817).

Clark, C. D. (1997). „Reconstructing the evolutionary dynamics of palaeo-ice sheets using multi-temporal evidence, remote sensing and GIS." Quaternary Science Reviews.

Dongelmans, P. (1996). Glacial dynamics of the Fennoscandian ice sheet: a remote sensing study. Department of Geology and Geophysics. Edinburgh, University of Edinburgh.

Graham, D. F. and D. R. Grant (1991). „A test of airborne, side-looking synthetic-aperture radar in central Newfoundland for geological reconnaissance." Canadian Journal of Earth Sciences **28**: 257-265.

Lidmar-Bergström, K., C. Elvhage, et al. (1991). „Landforms in Skane, south Sweden." Geografiska Annaler **73A**: 61-91.

Punkari, M. (1982). „Glacial geomorphology and dynamics in the eastern parts of the Baltic Shield interpreted using Landsat imagery." Photogrammetric Journal Finland **9**: 77-93.

Siegal, B. S. (1977). „Significance of operator variation and the angle of illumination in lineament analysis of synoptic images." Modern Geology **6**: 75-85.

Slaney, V. R. (1981). Landsat images of Canada - a geological appraisal, Geological Survey Canada.

Sugden, D. E. (1978). „Glacial erosion by the Laurentide Ice Sheet at its maximum." Journal of Glaciology **20**: 367-391.

Vencatasawmy, C. (1997). Statistical assessment and development of tools for mapping lineaments and landforms from synthetic aperture radar (SAR) images. Geography. Sheffield, University of Sheffield.

Vencatasawmy, C. P., C. D. Clark, et al. (1998). Landform and lineament mapping using radar remote sensing. Landform Monitoring and Analysis, Wiley.

Slovak Geol. Mag., 7, 3 (2001), 275 – 287

Villafranchian Locality Hajnáčka I: Comparison of Older Data with New Ones

MARTIN SABOL

Department of Geology and Paleontology, Faculty of Sciences, Comenius University, Mlynská dolina, 842 15 Bratislava, SLOVAKIA; sabol@fns.uniba.sk

Abstract. The Hajnáčka I site is one of the European paleontological localities dated to the Lower Villafranchian, MN 16a biozone (the Late Pliocene). From its discovery in 19th century, many scientists have dealt by the research of this site. After more than 35 years, the new systematic research started in the second half of 90s of the last century. The new research has yielded the quantity of the new material, especially paleontological one. This article gives the first results of this new research, which support the results of former researches.

Key words: Villafranchian, Late Pliocene, Hajnáčka, Slovakia

Introduction

The paleontological locality Hajnáčka I is one of the type localities of the European Neogene Mammal time scale, dated to the MN 16a zone (Lower Villafranchian, Late Pliocene) (Fejfar & Heinrich, 1987). This site is world-known by its findings of the fossil vertebrates, especially mammals, buried in the ash. Fossil skeletal remains from Hajnáčka I site are known since 1863, when first literature evidence about it was put out by Kubinyi (Fejfar, 1964). In the next years of the research, many scientists have dealt with this locality (Szabó, 1865; Paul, 1866; Krenner, 1867; Schafarzik, 1899; Kormos, 1917; Fejfar, 1961a, 1961b, 1964; Fejfar & Heinrich, 1985; Fejfar et al., 1990; Konečný et al., 1995; Lindsay et al., 1997; Lupták, 1997; Uher et al., 1999; Vass et al., 2000; Pipík, 2000; Sabol, 2000; etc.).

After more than 35 years (last time Fejfar in 1955-58), the new systematic research started in 1996. The fieldwork part of this research, which was realised by the Department of Geology and Paleontology, Faculty of Sciences, Comenius University in Bratislava and the Gemer-Malohont Museum in Rimavská Sobota in the cooperation with scientists of the other scientific institutions (State Geological Institute of Dionýz Štúr, Geological Institute of the Slovak Academy of Sciences, Slovak National Museum – Museum of the Natural History in Bratislava and the Department of Paleontology, Faculty of Sciences, Charles University in Prague), has been finished in the summer 2000. The article gives the first results of this research.

Locality

Paleontological site of Hajnáčka I is situated approximately 1 to 1.5 km SE of Hajnáčka village in the Rimavská Sobota district and 500 m N of the trigonometric point 410 m (Matrač hill) (see Fig. 1). The locality covers an area from 1,000 to 1,500 square metres (Fejfar, 1964). It consists of some deep erosive furrows (ravines) with steep walls, which are situated on the both right and left sides of way to the Békastó deck. The biggest of these erosive ravines with E-W orientation is 400 m long, to 30 m wide and its depth comes to more than 20 m in some places. On the basis of the quantity of skeleton remains, which were found here, this natural object was named as „Kostná dolina„ (Bone Valley) and proclaimed the protected natural object (see Fig. 2). The volcanic-sedimentary layers appear on the surface of these erosive furrow walls. They often contain the fossil remains of the Late Pliocene fauna and flora. From the hypsometrical point of view, the area of the paleontological site is limited by the contour lines of 233 and 287 metres above sea level.

The locality belongs to the Cerová Basalt Formation, which is mainly build up of the nepheline basanit and clastics of volcanic rocks. The radiometric age of the basalt varies since 5.03 until 1.16 Ma (Vass et al., 2000) (in older literature (Balogh et al., 1981 a Kantor & Wiegerová, 1981) the referred age is 2.7 – 1.5 Ma only). Thus, these volcanic rocks with their age correspond to the Late Pliocene to Early Pleistocene in the chronostratigraphical scale of the Paratethydian Neogene. The fossiliferous layers are situated in a maar depression of the elliptical shape (the Bone Valley maar) in the northern foothills of Matrač hill. The maar measurements are approximately 80x50 m (Bezák et al., 1992). The base of the maar filling consists of the redeposited Eggenburgian sediments of the Fiľakovo Formation (Tachty sands to sandstone) with the autochthonous tuffs, (lapilli) tuffites, fragments of basalt, and fine sands in the overlying. On the basis of the presence of the iron, some sediment is coloured to red and brown-red, and limonite crusts often envelop the sandy sediments. Also, redeposited palagonite tuffs and breccias are less frequently occurred in the maar filling. Locally, there are

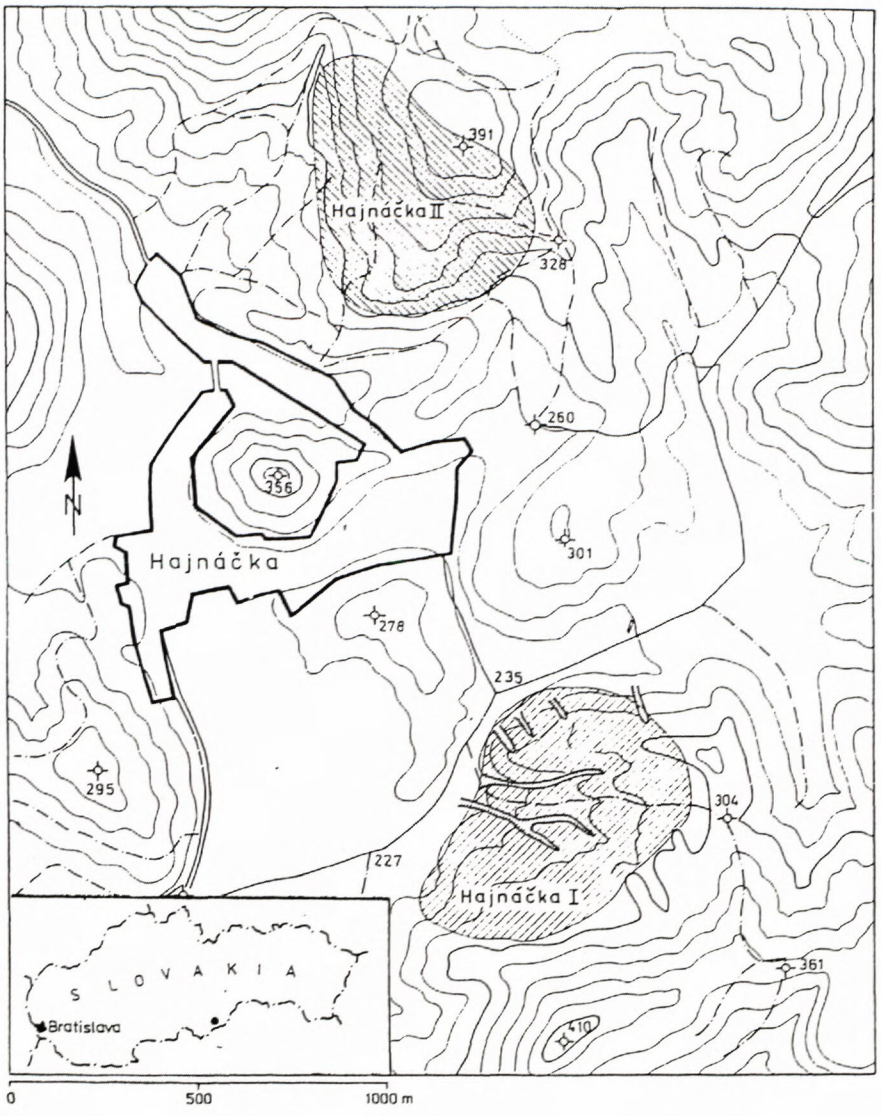

Fig. 1. Location of the paleontological site Hajnáčka I. (modified after Fejfar et al., 1990).

situated relicts of laminated bituminous beds in the upper part of this filling with the Quaternary loamy and loam-argillaceous deposits, covering the marginal parts of the Bone Valley maar. The fossil findings have been found in sediments, which were disrupted especially in the process of soil slides during the Quaternary Period. In spite of that, they are forming completely preserved stratigraphical unit, probably without hiatus.

Lithological and sedimentological description of pits, and their paleontological contents

During the new research of locality, six pits have been excavated in the upper parts of two lateral furrow outposts with SE orientation (see Fig. 2). There two vertical pits (1/96 and 2/96, which was marked as 2/97 after its broadening) and a horizontal one (3/98) have been dug in the place between probable occurring of the Fejfar´s pits 8/56 and 9/56. The pit 3/98 was situated in the area 16 square metres approximately and method of archaeological research was partly used in searching of the vertebrate remains here (see Photo 1). Other two pits were vertical. The pit 4/98 has been excavated in the place of the Fejfar´s pit 3/56, and the last one has been excavated in the place of the Fejfar´s pit 9/56 probable occurring (see Fig. 2). Besides of these pits, still one (5/98) has been dug in the place of the chance finding of more quantity of the vertebrate bones. However, this new finding place in the territory of locality will be full described in a single paper. The deposits from the Pliocene to the Holocene have been ascertained in all these pits (see Fig. 3).

The most eastern pit 1/96 (see Fig. 3) is situated in the southern wall of the upper part of the Bone Valley longest furrow outpost. The pit had average width 70 cm and it has been dug to the 6.5 metre depth. Only 10 cm thick, the Quaternary sediments are represented by the dark-brown loamy soil from the Holocene. The underlying Pliocene deposits were divided to five layers. From upper to down, they are formed by the grey to grey-brown sandy tuffites with little fragments of basalt (from 3 to 7 cm in average); light sandy tuffites; grey, grey-black to black sandy tuffites with intercalation of the rusty-brown tuffaceous sands and approximately 20 cm thick position of pyroclastic rocks in the lower part of this layer; and grey-blue to grey-black lapilli tuffs with the lenses of grey-black sandy tuffites and rusty-brown tuffaceous sands with the large basalt fragments (to 20 cm in average) and findings of fossil remains of larger vertebrates, especially mammals (*Tapirus arvernensis* CROIZET ET JOBERT, 1828; *Dicerorhinus jeanvireti* GUERIN, 1972; *Pliocrocuta perrieri* CROIZET ET JOBERT, 1828; *Proboscidea* gen. et spec. indet., cervids etc.) (see Tab. 1). Also, the postsedimentary disturbances (microtectonic ones?) have been ascertained in this layer. The lowest one consists of the more-less sterile grey to grey-blue tuff with intercalation of rusty-brown tuffaceous sands.

Besides of findings of larger vertebrates, the fossil remains of fishes, reptiles (especially turtles) and rodents have been found too on washing of these sediments, mainly of rusty-brown tuffaceous sands (see Tab. 1). The colour of fossil bones was from grey to brown, whereas the teeth was coloured to white-grey, grey until brown, but in some cases to black as well.

The pit 2/96 (see Fig. 3) is situated in the southern wall of the upper part of the Bone Valley longest furrow

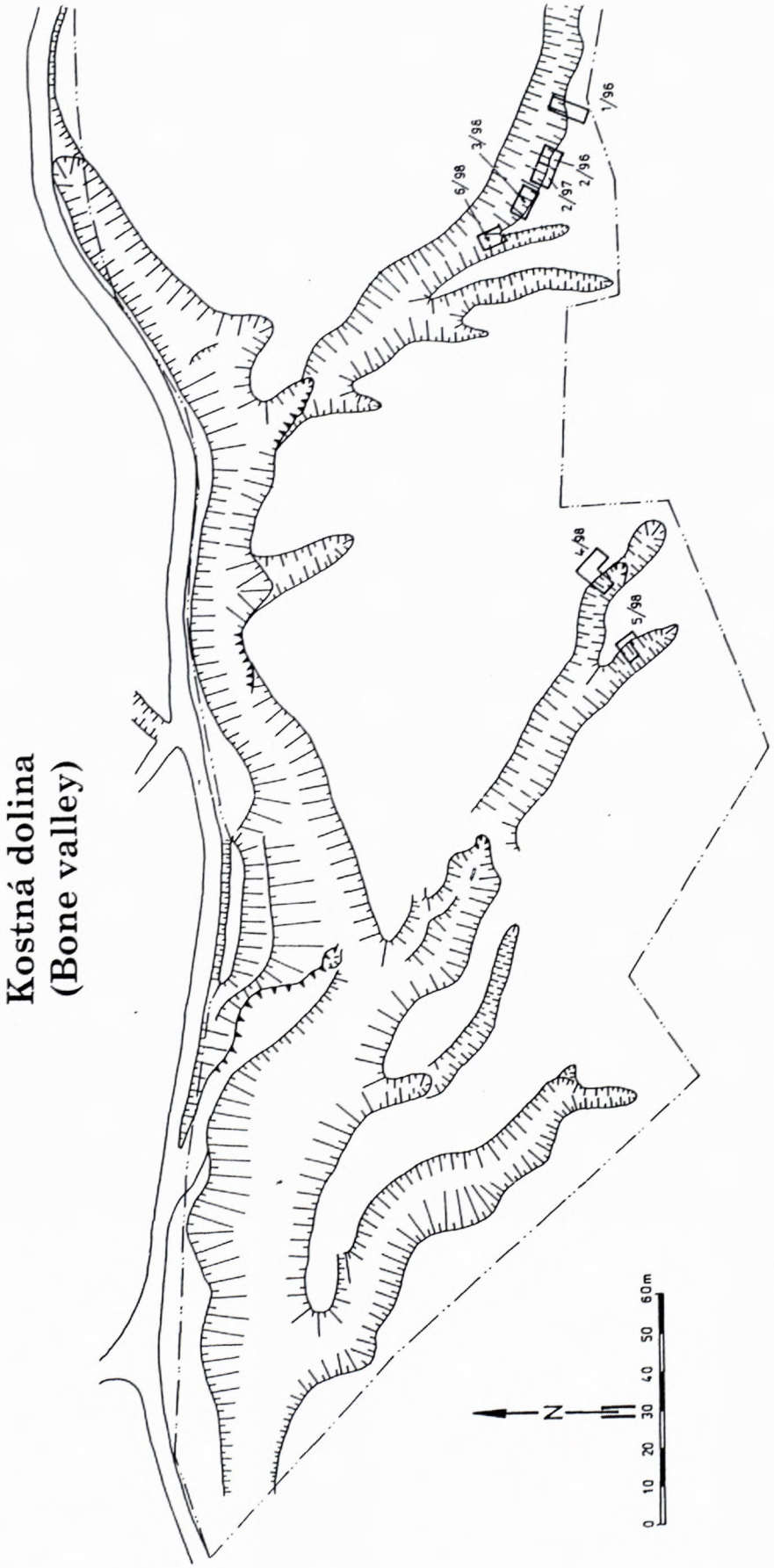

outpost too. It was orientated in a westward to north-westward direction of the pit 1/96. This pit has been dug to the almost 5 metre depth and subsequently deepened and expanded as the pit 2/97. The 5 layers have been distinguished here. The uppermost layer consists of the Holocene brown sandy loam and its thickness is 1 metre approximately. In the underlier of these Quaternary sediments, the Pliocene ones are deposited. There were ascertained grey-black to black tuffs without fragments of basalt; sandy tuffites and blue-grey to grey-black clayey tuffs with the basalt fragments (to 20 cm in average) and with the intercalation of gravel lenses of the rusty-brown tuffaceous sands, in which the fossil vertebrate remains have been found. Under this layer, that is probably equivalent of the grey lapilli tuffs with the lenses of grey-black sandy tuffites and rusty-brown tuffaceous sands in the pit 1/96, the blue-grey tuffs without fossil remains are bedded.

From the paleontological point of view, the fossil remains of fishes, frogs, turtles, snakes, insectivores, rodents, lagomorphs, proboscides, tapirs, rhinos and other mammals have been ascertained in the fossiliferous layers of this pit. Also, the teeth of little squirrel (*Sciurus* sp.) and undetermined ursid (cf. *Ursus minimus*?) have been found here. Thus, these two mammal taxa are one of new elements in the Hajnáčka biocenosis (see Tab. 1). However besides of these Pliocene vertebrates, the findings of younger Pleistocene elements have been ascertained here as well (for example *Clethrionomys*). The bones of the Pliocene vertebrates were coloured from white-grey to light-brown, brown until black. Similarly, the colour of tooth enamel was from white to grey, brown and black in solitary cases.

Fig. 2. The schematic map of the biggest furrow in Bone Valley with marked single pits, which during the new research have been excavated.

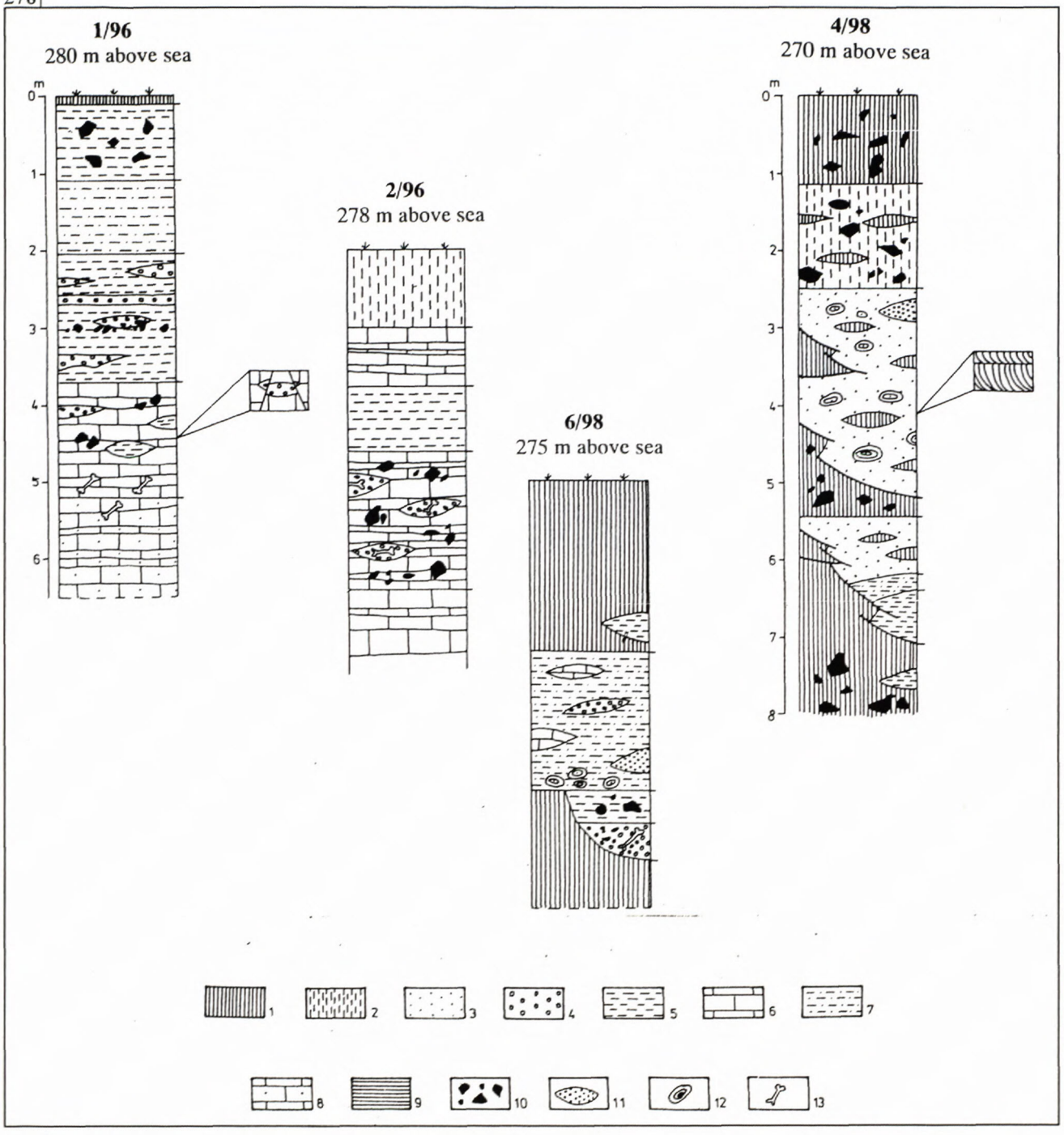

Fig. 3. The schematic sketch of the single new pits (1/96, 2/96, 4/98, 6/98) in territory of the Hajnáčka I site.
1 – Holocene dark humous loam; 2 – Quaternary light sandy loam; 3 – light unconsolidated sands to tuffaceous sands; 4 – rusty-brown tuffaceous sands often with limonite concretions; 5 – dark sandy tuffites; 6 – blue-grey to grey-black tuffs, lapilli tuffs; 7 – light sandy tuffite with intercalation of rusty-brown tuffaceous sands; 8 – tuff with intercalation of rusty-brown tuffaceous sands; 9 – fine laminated tuff; 10 – fragments of basaltic rock; 11 – lenses of volcanic material; 12 – baked sandstone; 13 – findings of vertebrates, especially mammals.

Excepting expanded pit 2/97, the horizontal pit 3/98 has been excavated in the depth of the occurrence of fossiliferous layer. The measurements of this researched area were approximately four times four metres (approx. 16 square metres). The excavations on this pit yielded numerous fossil remains of various vertebrate taxa (see Tab. 1). Besides known genera and species, some new taxa of insectivores (*Talpa* cf. *fossilis*, cf. *Deinsdorfia* sp. and *Soricidae* gen. et spec. indet.) have been ascertained too. Alike as findings of the squirrel and ursid from the former pit, these remains of shrews and mole represent new elements in the Pliocene fauna of Hajnáčka as well. Fossils, which have been found here, were coloured to same colour like findings of both pits 1/96 and 2/96-97.

The vertical pit 4/98 (see Fig. 3) has been dug to the 7.85 metre depth in the place of the Fejfar´s pit 3/56. The

Tab. 1. List of the Late Pliocene vertebrates from the Hajnáčka I site.

taxon	Fejfar et al., 1990	*Hajnáčka I (1996 – 2000)*				
		1/98	2/96-97	3/98	4/98	6/98
Osteichthyes						
Scardinus? erythrophthalmus Linné, 1758	+	+	+	+		+
Tinca furcata Agassiz, 1843	+	+	+	+		+
Esox sp.	+			+		
cf. *Parasilurus* sp.	+					
Osteichthyes gen. et spec. indet.	+	+	+	+		+
Amphibia						
Pliobatrachus sp.	+					
Bufo bufo (Linné, 1758)	+					
Rana cf. *temporaria* Linné, 1758	+					
Rana cf. *arvalis* Linné, 1758	+					
Rana cf. ex gr. *dalmatina-latastei*	+					
Anura gen. et spec. indet.	+		+	+		
Reptilia						
Chelydra aff. *decheni* H. von Meyer, 1852	+					
Emys orbicularis Linné, 1758	+					
Testudinata gen. et spec. indet.	+	+	+	+		
Serpentes gen. et spec. indet.		+	+			
Aves						
Mergus sp.	+					
Mammalia						
Desmana nehringi Kormos, 1913	+					
Talpa cf. fossilis Petényi, 1864				+		
Talpa cf. *minor* Freudenberg, 1914						+
cf. *Deinsdorfia* sp.				+		
Petenyia hungarica Kormos, 1934	+					
Blarinoides mariae Sulimski, 1959	+		+	+		
Beremendia fissidens (Petenyi, 1864)	+					
Soricidae gen. et spec. indet.				+		
Colobinae gen. et spec. indet.	+					
Lutra cf. *bravardi* Pomel, 1843	+					
Parailurus hungaricus Kormos, 1934	+					
Megantereon(?) sp.	+					
Pliocrocuta perrieri (Croizet et Jobert, 1828)	+	+				
Ursidae gen. et spec. indet.			+			
Pliopetaurista pliocaenica (Depéret, 1897)	+					
Sciurus sp.			+			
Seleviniidae(?) sp.	+					
Prospalax priscus (Nehring, 1897)	+	+		+		+
Apodemus sp.	+					
Baranomys loczyi Kormos, 1933	+					
Mimomys (Cseria) stehlini Kormos, 1931	+		+	+		+
Mimomys (Mimomys) hassiacus Heller, 1936 (=*Mimomys (M.) hajnackensis* Fejfar, 1961)	+	+	+	+		
Mimomys sp.		+	+	+		+
Arvicolinae gen. et spec. indet.			+	+		+
Germanomys sp.	+		+			+
cf. *Ungaromys* sp.						+
Castor fiber ssp.	+	+	+			
Trogontherium minus Newton, 1890	+					
Rodentia gen. et spec. indet.		+	+	+		+
Hypolagus brachygnathus Kormos, 1934	+		+			
Mammut borsoni (Hays, 1834)	+					
Annancus arvernensis (Croizet et Jobert, 1828)	+		+	+		
Proboscidea gen. et spec. indet.		+	+	+		+
Tapirus arvernensis Croizet et Jobert, 1828	+	+	+	+		+
Dicerorhinus jeanvireti Geurin, 1972	+	+	+	+		+
Rhinocerotidae gen. et spec. indet.	+	+	+	+	+	+
Sus minor (Depéret, 1890)	+					
Capreolus sp.	+					
Cervus perrieri-Arvernoceros ardei	+					
Cervus pardinensis Croizet et Jobert, 1828	+					
Croizetoceros ramosus (Croizet et Jobert, 1828)	+					
Muntjacus sp.	+	+				
Cervidae gen. et spec. indet.		+		+		
Mammalia gen. et spec. indet.		+	+	+		+
Vertebrata gen. et spec. indet.		+	+	+	+	+

Photo 1. The pit 3/98, where method of archaeological research has been used; photo J. Ferleťáková.

Photo 2. The detail view to one of fossiliferous lenses of gravel rusty-brown tuffaceous sands with the presence of the limonite concretions and small pyroclastics, pit 2/96; photo J. Ferleťáková, scale is 10 cm.

width of this pit was to 6.60 metres in the two uppermost terraces of pit and in lower ones the width was moved in the boundary from 70 to 160 cm. The uppermost layer is represented by the brown to dark-brown humous loam with basaltic pebbles. To the depth, these probably Holocene sediments grade to the yellow-brown to brown sandy loam with basalt fragments too, and with the intercalation of the overlying dark-brown loam. This light loamy layer is slightly cemented in the base. In the underlier of these sediments, the light yellow to yellow-brown unconsolidated sands to tuffaceous sands with the intercalation of dark-brown loam with the basaltic pebbles are deposited. The sands are solitarily diagonal bedded. Also, they contain baked sandstone and lenses of the tuff to tuffaceous volcanic material. The dark-brown loam with basalt fragments is situated in the depth from 5.20 to 5.45 metres. This loam grades to the more thickness in the profile left part and separates thus the overlying sands from the underlying light yellow to yellow-brown unconsolidated tuffaceous sands with intercalation of the dark-brown loam, but without the baked sandstone. Approximately 20-cm thick layer of the cemented light sandy tuffites with the rusty-brown tuffaceous sand intercalation is deposited under these light sands. In underlier of tuffaceous sands, the grey-brown sandy tuffites are situated in the profile right side, which grade toward the depth to the irregular layer of the brown to dark-brown loam with pyroclastics and with the intercalation of the grey-brown sandy tuffites. It is not out of the question that this pit has been excavated partly in the place of the secondary rede-

posited volcanic and sedimentary material, which was relocated yet during former excavations. Also, this assumption is supported by the findings of only some light brown to brown bones of rhinos and other undetermined mammals in the sand. Any micromammals have been found here.

The pit 6/98 (see Fig. 3) has been excavated in the place of the Fejfar´s pit 9/56 probable occurring. The depth of this pit was 5.5 metres approximately. More detailed determination of the single layers was limited the presence of the deposits from former field works. The uppermost layer consists of the brown loamy deposits with the occurrence of the grey-brown sandy tuffites with intercalation of the solitary grey tuffs and rusty-brown tuffaceous sands in the layer lower part. Underlying layer contains the grey-brown sandy tuffite with intercalation of the grey tuffs, rusty sands with the volcanic rock lens in the lower part, and with baked sandstone in the layer base. The brown loamy deposits form the lowest layer. There are two layers situated in its overlying in the pit right side. The upper of them is forming by the grey sandy tuffites with basaltic pebbles. Lower one consists of large lens of the rusty-brown tuffaceous sands with the volcanic rocks and with the occurrence of the vertebrate fossils. The remains of small mammals (insectivores and rodents) and large ones („mastodons", tapirs, rhinos, etc.) together with the abundant fish fossils have been found here (see Tab. 1). The insectivores are represented by one mole species only (*Talpa* cf. *minor*), but it is other new faunal element, ascertained at the locality. Also, rodent fauna from this pit probably contains new locality taxon of the subfamily *Prometheomyinae* (cf. *Ungaromys* sp.). However, the teeth of the Pleistocene voles (*Microtus* and *Clethrionomys*) have been found too. Their presence is only other evidence of the mixing older and younger sediments in the time after the extinction of Hajnáčka biocenosis, especially during the Pleistocene Period. As interesting is the colour of found fossil remains from the pit. Whereas tooth enamel is coloured from white-grey to grey, brown and black, the bones are coloured to the rusty-brown and dark brown until black. Thus, they differ from vertebrate bones of other pits.

On the basis of the existing research we are able to draw that the occurrence of the vertebrate fossil remains is especially connected with the lenses and intercalation of gravel rusty-brown tuffaceous sands, often with the presence of the limonite concretions and small pyroclastics (see Photo 2). These tuffaceous sands consist of redeposited material of the original primary maar filling, which has been deposited on the inner slopes of this maar ring (VASS et al., 2000). The bones and teeth of tapirs, rhinos, mastodons and micromammals, especially rodents (see Fig. 4) have been found the most frequently of all terrestrial vertebrates in these fossiliferous layers together with the large quantity of fish fossil remains.

Besides of vertebrate fossils, the gem varieties of corundum (sapphire) have been discovered in these lenses too. The sapphires originated in the felsitic syenite-like melt, uplifted to the surface as xenoliths or as xenocrysts by a new portion of alkali basaltic melt. However, these xenoliths (xenocrysts respectively) were not in equilibrium with this surrounding alkali basalt magma. Subsequently, the sapphires have been redeposited to the maar filling. It is not clear so far, whether these minerals come from nearby basalt lava flows or from the maar itself (Uher et al., 1999).

Discussion

More or less broken sediments, often in allochthonous attitude, have been ascertained in all studied pits. These sediments were disrupted not only during their deposition, which has realised in very short time span (Fejfar et al., 1990), but also in the period after the extinction of the Hajnáčka biocenosis. In this time, the original layers of maar sediments were destroyed by the seismic shocks connected with explosive activity, and by the processes connected with the domatic rise of the Cerová Highland (Vass et al., 2000). Also, these sediments were disturbed in the later Quaternary Period, especially during the Late Pleistocene (erosion, solifluction and repeated landslides), when they have redeposited to the bottom of the Hajnáčka depression (Fejfar, 1964). The occurrence of the Late Pleistocene loess sediments (Bezák et al., 1992) together with the Pliocene sedimentary rock is evidence of that. Apart from malacofauna these Quaternary deposits contained the fossil remains of mammoths, horses and rodents (*Microtus, Clethrionomys*) as well. The occurrence of these Pleistocene elements together with the findings of the Pliocene fauna has been early referred from this site by SZABÓ (1865) (fossil remains of bison, mammoth and horse) and Fejfar (1964) (woolly rhinos, rodents) for example. On the ground of thus destroyed suitable stratigraphical data, it is difficult exactly to reconstruct the thickness of the Pliocene sedimentary maar filling.

It was frequently in the profiles of single pits that so called „older section" (limnic sands, sandy tuffites and lapilli ash with baked limonite sandstone) (Fejfar, 1964), is situated over the younger members of deeper facies (light grey coarse deposited tuffites and tuffs). Thus, this site is differing from Hajnáčka II locality, where volcanic ash has been deposited directly on the surface above the Miocene sediments, so that so called „older section" is missing here (Fejfar, 1964). This phenomenon of the „inverted" and mixed layers, which Fejfar (1964) also described from his pits 3/56, 8/56, 9/56 and 3/57, was distinct especially in our pits 1/96 and 2/96-97. Together, the profiles of these two new pits are more or less in good agreement with profiles of Fejfar´s pit 8/56, especially in their upper and lower parts (see Fig. 5). The middle pit parts are less comparable to almost different, whereas grey-black to black tuffs (layer „2") of pit 2/96 are not correlated. It is not out of question that these dark tuffs represent isolated block of volcanic material. On the basis of this knowledge we are able to assume the lithological changes in short distances, which are the result of repeated secondary redeposition of original maar sediments.

Likewise, the sediments ascertained in the profile of pit 4/98 are relatively in good agreement with the sediments of older pit 3/56 (see. Fig. 6), but our pit was

Slovak Geol. Mag., 7, 3 (2001), 275 – 287

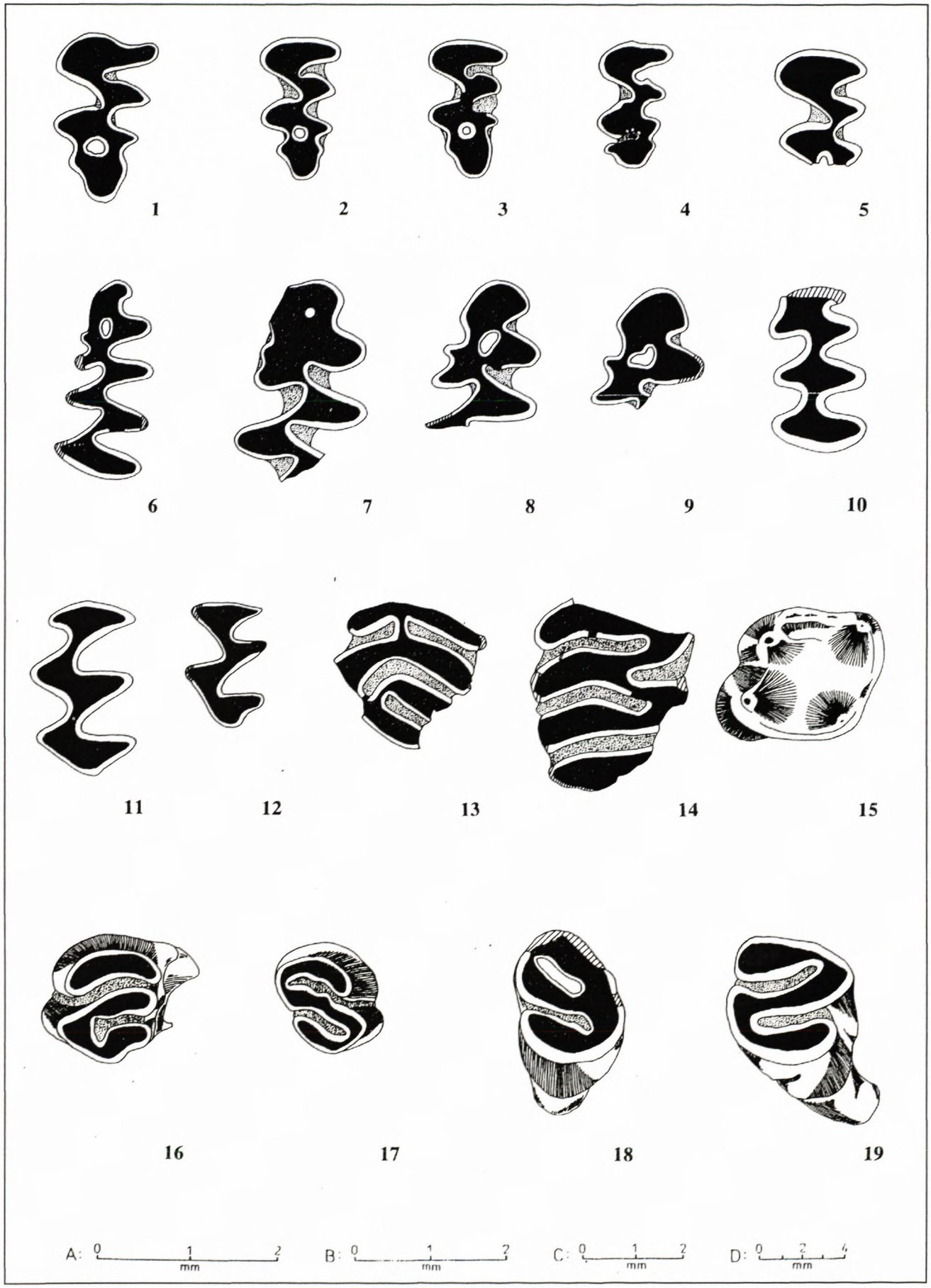

Fig. 4. New findings of rodent teeth from the Villafranchian sediments (MN 16a) of the Hajnáčka I site: deposited in the Gemer-Malohont Museum in Rimavská Sobota.

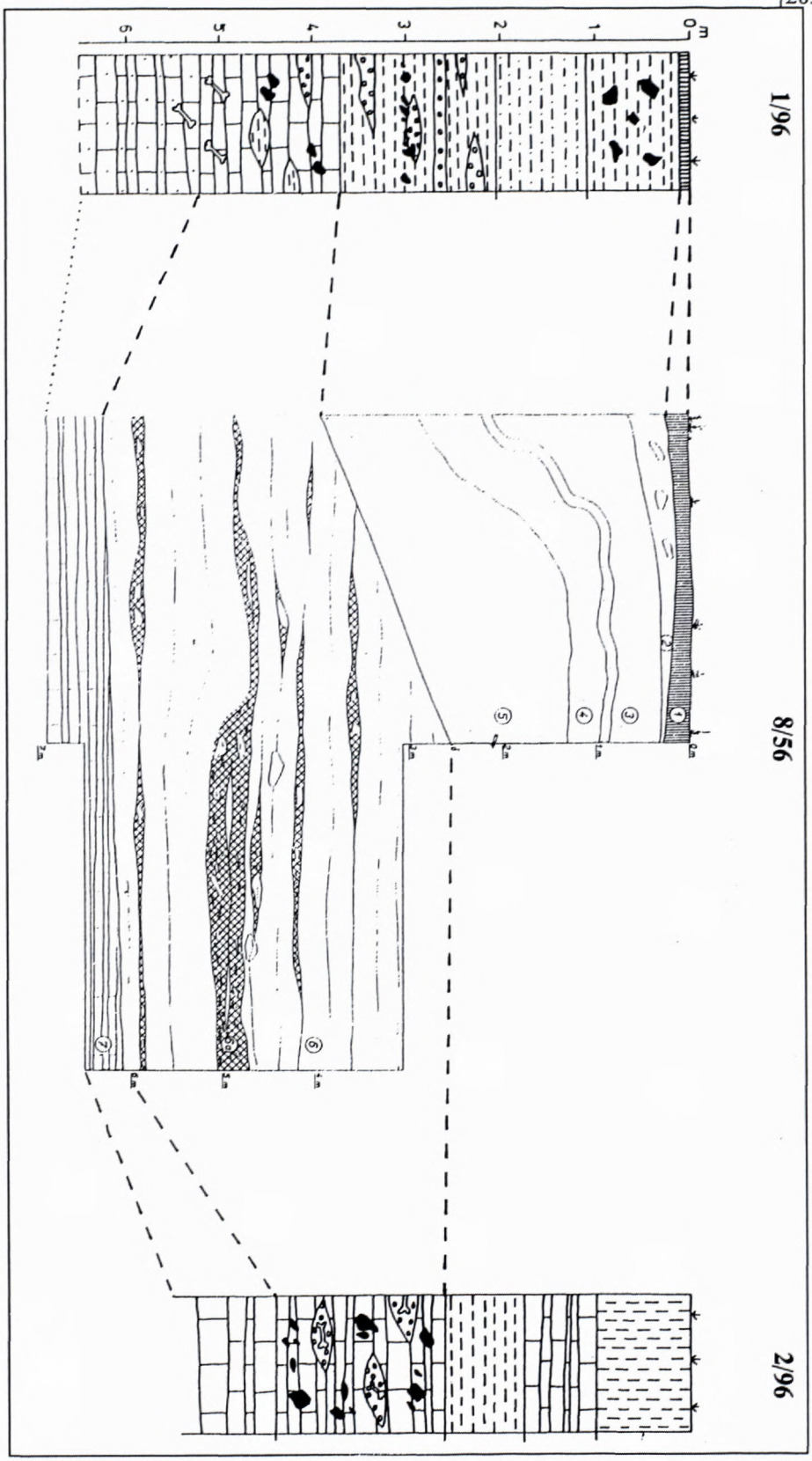

Fig. 5. The schematic comparison of the profile of pit 8/56 (Fejfar, 1964) with the profiles of new pits 1/96 and 2/96.
Notes to the pit 8/56 (Fejfar, 1964): 1 – dark brown humous loam; 2 – rusty-brown sandy loam with boulders of compact basalt; 3, 4, 5 – dark to light brown not calcareous clayey sands with sporadic skeleton finds in secondary position; 6 – light or dark rusty-brown tuffitic sands with dispersed lenses of a dark rusty-brown lapilli tuff with numerous boulders of patinated compact basalt, fragments of cemented, fine banded tuffites with numerous small phenocrysts of amphibole, and very numerous light rusty-brown skeleton finds (the lenses of tuff are marked 6a); 7 – light grey, cemented, strongly calcareous, thicker-bedded tuffites.
Notes to pits 1/96 and 2/96 see fig. 3.

Mimomys (Mimomys) hassiacus HELLER, *1936 (= Mimomys (M.) hajnackensis* FEJFAR, *1961): 5. M3 sin. (B-4140), 8. m1 dex. (inv., B-4138), 9. m1 dex. (inv., B-4139).*
cf. Ungaromys sp.: 10. m1 sin. (B-4119).
Germanomys sp.: 11. M1 dex. (inv., B-4120), 12. M2 dex. (inv., B-4017).
Castor fiber ssp.: 13. P4 sin. (B-3058), 14. M1-2 dex. (B-3106).
Sciurus sp.: 15. m2 dex. (B-4012).
*Prospalax priscus (*NEHRING, *1897): 16. M1 sin. (B-4136), 17. M2 dex. (B-4135), 18. m1 sin. (B-4112), 19. m2 dex. (B-4128).*
Scales: A – 1, 2, 7, 12, 15; B – 3, 4, 5, 6, 8, 9, 10, 11; C – 16, 17, 18, 19; D – 13, 14.

probably situated more on the left from original pit. A quantity of findings is only different between both pits. Fejfar (1964) described larger number of fossil remains from this finding place, while new research yielded hence some bones of larger mammals only.

The correlation of pit 6/98 with the pit 9/56 was limited by the presence of loamy sediments, which have been redeposited during the first phase of excavations on pits 1/96 and 2/96-97. On the basis of that, only dark grey tuffites (or tuffs resp.) with the lens(-es) of rusty-brown tuffaceous sands, and partly light grey-brown sandy tuffites with the intercalation of grey tuffs and basalt fragments have been again ascertained here (see Fig. 7). Also, the colour of found bones is in good agreement with the colour of former findings.

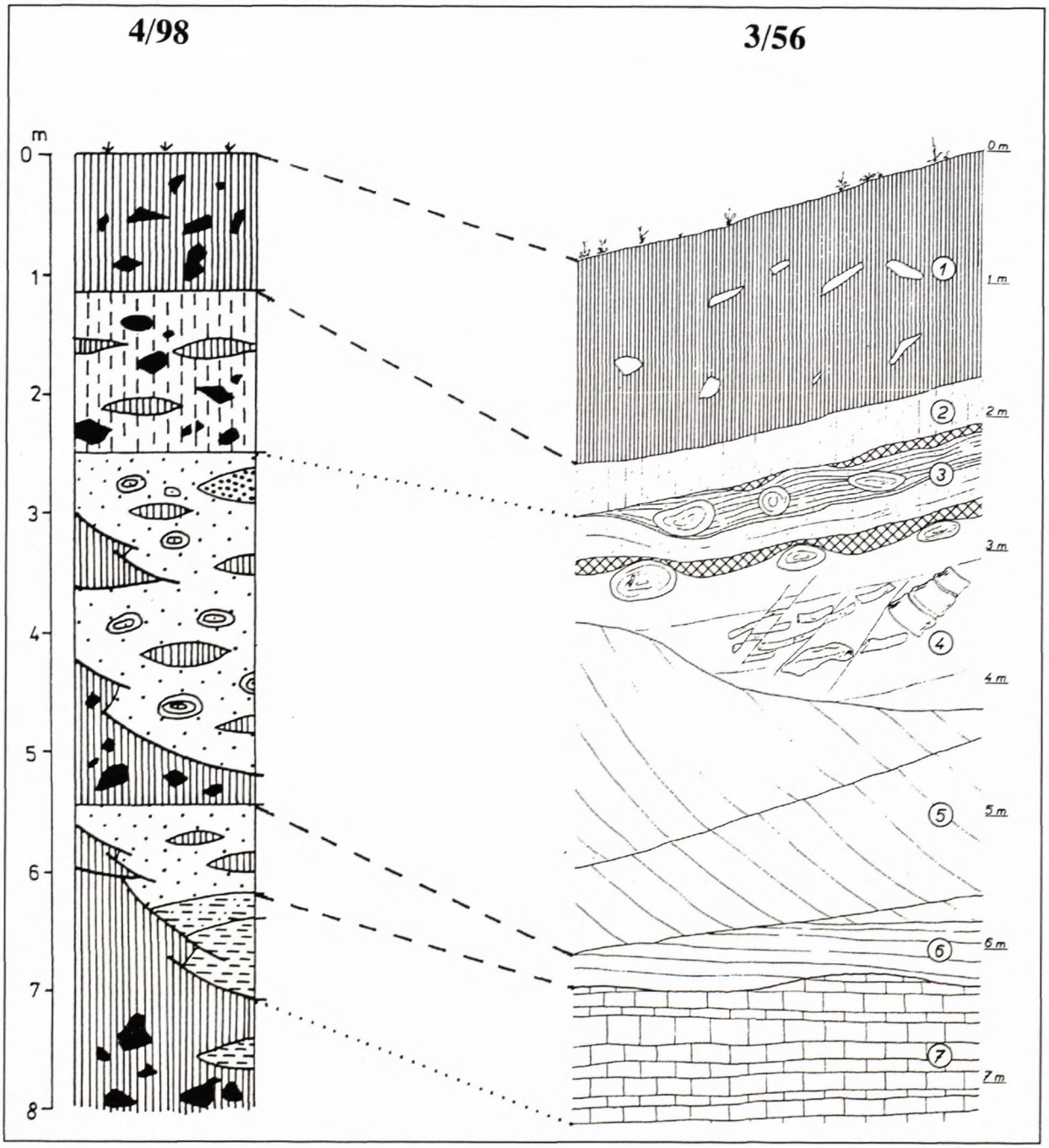

Fig. 6. The schematic comparison of the profile of pit 3/56 (Fejfar, 1964) with the profile of new pit 4/98.
Notes to the pit 3/56 (Fejfar, 1964): 1 – dark brown humous loam with basaltic pebbles; 2 – rusty-brown sandy loam with sporadic skeleton remains in secondary position; 3a – coarse greyish lapilli tuff with fragments of baked sandstones; 3b – whitish-grey approx. 10 mm thick banks of slighty cemented, strongly calcareous fine arenaceous tuffites, alternating with approx. 5 mm thick slighty calcareous grey, very fine tuffitic sands; 3c – light grey, slighty calcareous fine tuffitic sands with a distinct microtectonic; 4 – unstratified slighty calcareous light rusty-brown fine sand, on the contact with layer 3c occurs an outstretched layer of grey coarse lapilli tuffs; 5 – light greyish-brown thinly bedded tuffitic sands without finds; 6 – light grey thinly bedded tuffitic sands without finds; 7 – light grey, cemented, strongly calcareous thickly bedded tuffites. Notes to pit 4/98 see fig. 3.

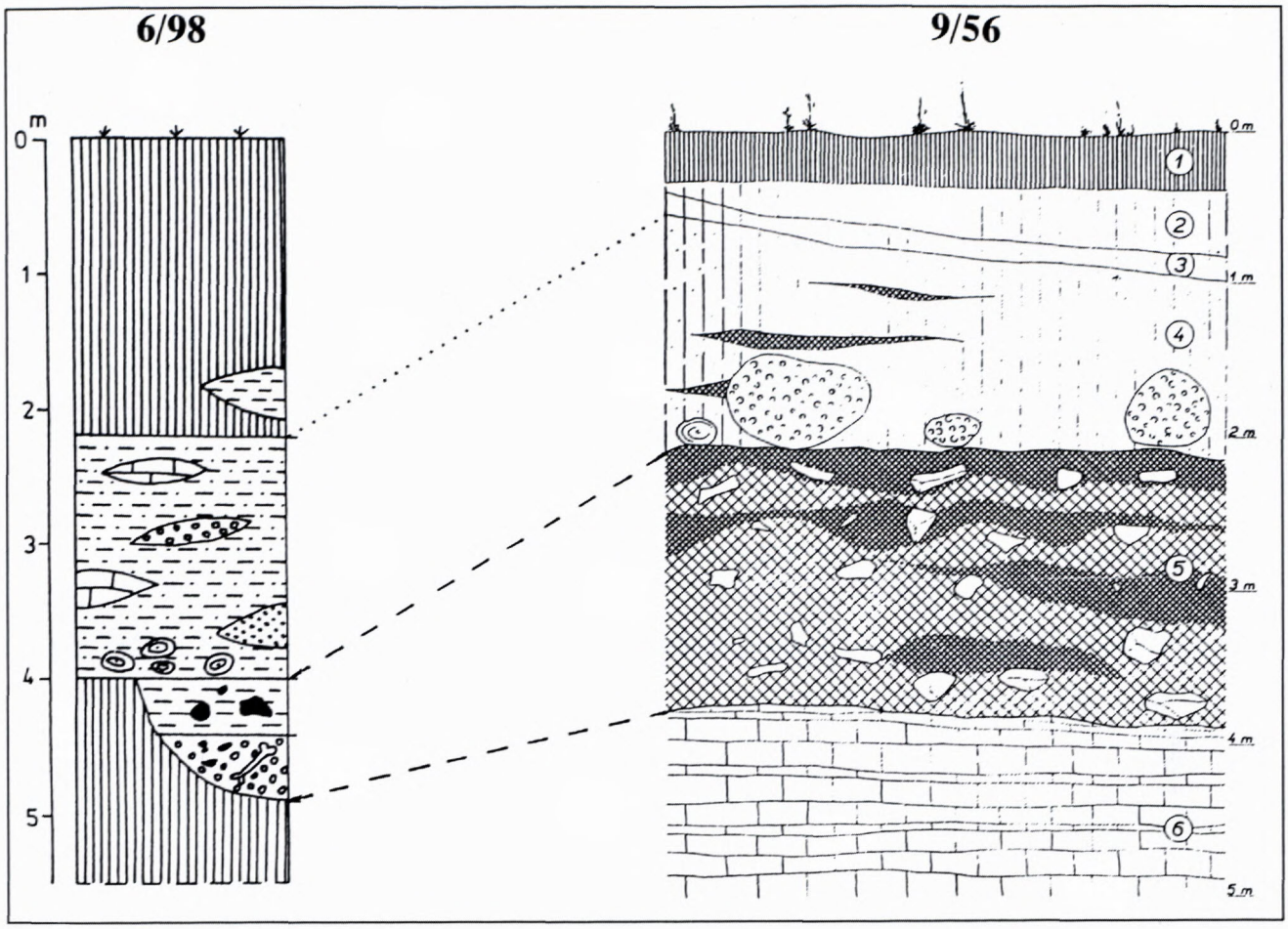

Fig. 7. The schematic comparison of the profile of pit 9/56 (Fejfar, 1964) with the profile of new pit 6/98.
Notes to the pit 9/56 (Fejfar, 1964): 1 – dark brown humous loam; 2, 3 – light brown, slighty calcareous redeposited fine sands; 4 – light greyish-brown, strongly calcareous sandy loess with intercalations of coarse greyish.black tuffs, on the basis blocks of a strongly weathered porous basalt; 5 – dark grey to grey-black lapilli tuffs with numerous blocks of patinated compact basalt with a very abundant vertebrate fauna, dispersed lenses with a finer grain-size, with a comparatively abundant mammalian microfauna, alternated with coarser layers; 6 – light grey cemented strongly calcareous tuffites. Notes to pit 6/98 see fig. 3.

After Vass et al. (2000), the layers ascertained in the pits (especially in 1/96 and 2/96-97) represent the disturbed secondary sedimentary filling, which originated in the environment of a drained lake after removal of primary one during the denudative and erosive post-volcanic period. Fejfar (1964) consider the part of these layers (lapilli tuffs with the lenses of fossiliferous rusty-brown tuffaceous sands), which have been ascertained in the pits 8/56, 9/56, 1/96, 2/96-97 and 6/98 as disrupted coastal facies of the lake sediments. The sandy material from the disintegrated underlying Eggenburgian sandstone of the Fiľakovo Formation has been also repeatedly deposited together with the tuffs and tuffites. The common occurrence of the redeposited Miocene foraminifers and shark teeth together with the Pliocene vertebrate fossils, what was referred by Kormos (1917) and Fejfar (1964) as well, is an evidence of that.

From the paleontological point of view, new research of locality yielded the enormous quantity of fossil vertebrate findings. Besides of large mammal remains, from which those of tapirs are prevailing, the fossils of small vertebrates, especially fishes and micromammals have been found too. Even thought some taxa were not again ascertained (for example *Parailurus hungaricus* KORMOS, 1934 and others), the fossil remains of seven (meanwhile) new elements of Hajnáčka biocenosis (*Talpa* cf. *fossilis* PETÉNYI, 1864; *Talpa* cf. *minor* FREUNDERBERG, 1914; cf. *Deinsdorfia* sp.; *Soricidae* gen. et spes. indet.; *Sciurus* sp.; cf. *Ungaromys* sp. and *Ursidae* gen. et spec. indet.) have been found here. Also, it is not out of question that some of these findings, especially those of shrews and squirrel, belong to the new taxa or species resp., but they are only studied now. Generally, more than 30 taxa of vertebrates have been yet recognised during research from 1996 to 2000, whereas Fejfar et al. (1990) determine 46 vertebrate taxa from Hajnáčka I site.

All these fossil remains belong to Pliocene animals, which lived in this territory during the creation of the secondary maar filling. In this time, the shallow swampy lagoons were forming on the coast of drained lake (Fejfar, 1964). The lagoons had been surrounded by the bushy humid (but after Lindsay et al. (1997) not swampy!) primeval forest with the flowing streams and backwater, in which the

Slovak Geol. Mag., 7, 3 (2001), 275 – 287

mammals as *Anancus arvernensis* (CROIZET et JOBERT, 1828); *Mammut borsoni* (HAYS, 1834); *Tapirus arvernensis* CROIZET et JOBERT, 1828; *Dicerorhinus jeanvireti* GUERIN, 1972; *Muntiacus* sp. and others dominated. The presence of the allochthonous indifferent elements, represented by the taxa *Pliocrocuta, Megantereon, Hapolagus* a *Prospalax* (FEJFAR, 1964) or *Baranomys* (FEJFAR et al., 1990) is the evidence of the presence of the steppe or open grassy land in the Hajnáčka environment too.

Generally, it can be draw that fauna and flora, which lived in the vicinity of maar during the forming of its secondary filling, constituted the uniform unit destroyed by the eruption of some near volcano (Fejfar, 1964). However, some animals were killed by the gas emanations at the lake bank still before the volcanic eruption and subsequent tephra fall. Some gnawed bones by the hyenas and their coprolites testify about it that the bodies (or remains) of dead animals were lying for some time on the coast (Fejfar, 1964). The animal carrion, which perished near lake either the suffocation by the gas emanations near drinking the water or were killed by the volcanic ash, were washed to the lake later on and deposited on its bottom near of the coast. The presence of fish bones, fragments of clam shells (probably *Anodonta* sp.) (Fejfar, 1964), and also ostracod shells (Pipík, 2000) together with the vertebrate osteological remains in the fossiliferous sediments is evidence of that. Their conservation as fossils was possible only for assumption of the quick covering their bodies (or remains) by sediments. Vass et al. (2000) suppose that skeletons of perished animals have been disintegrated by the convection in the drained lake. But some findings have been found in the autochthonous attitude too (Fejfar, 1964). On the basis of that, it is not out of the question that most vertebrate skeletons have been disintegrated together with the sediments during the later geological processes (seismic shocks, slides, solifluction and other).

From the biostratigraphical point of view, Fejfar and Heinrich (1987) have placed Hajnáčka fauna to the Late Pliocene MN 16a biozone (2.8 až 3.3 Ma). Thus, it was possible to correlate the Hajnáčka fauna with fauna from European sites Valensole (Cornillet, Grenouillet), Commenailles, Seynes, Violette, Triversa-Arondelli, San Giusto, Jucar (Carrasco, Valdeganga), Teruel (Concud, Escoriheula), Moreda, Zujar, Galera 2, and Beremend 1-3, 5 (Fejfar et al., 1999; Lindsay et al., 1997).

Conclusion

During new paleontological research of the Villafranchian locality Hajnáčka I six pits have been dug. One of them (5/98, here not described) has been dug at new place of the finding of more quantity of vertebrate fossil remains. Other five pits have been situated more or less at the place of probable occurring of older ones, which have been excavated here in the time of Fejfar´s research. Thus, it was possible to compare the results of former research with these of new one.

From the lithological and sedimentological points of view, the profiles of these five new pits are more or less in good agreement with the profiles of original pits, which were described by Fejfar (1964), and they support his results.

From the paleontological point of view, the validity of all the most important fossils have been repeatedly validated, although the fossil remains of some taxa (for example little panda and others) were not again ascertained here. On the other hand, the findings of seven new taxa of insectivores, rodents and carnivore have been found too. It is not out of question that some of them belong to new taxa or species respectively. Generally, more than 30 taxa of vertebrates have been described during new research, and the number of all known vertebrate taxa on the locality has increased meanwhile from original 46 (Fejfar et al., 1990) to 53 minimally.

However besides of fossils of the Pliocene vertebrates, the redeposited Miocene (foraminifers and shark teeth) and Pleistocene (rodents, horses and mammoths) elements have been found too. It only supports opinions about repeatedly redeposition of the underlying Eggenburgian sand and sandstone, and about the later mixture of maar sediments with the Pleistocene ones after the extinction of the Hajnáčka biocenosis.

Unlike the older research, the excavations on the pit 4/98 yielded only some fossil bones of larger mammals. In spite of it, we are able to draw that new research of the Hajnáčka I site helped to specify of our knowledge of the locality geological structure (Vass et al., 2000), and composition of this Late Pliocene biocenosis. Also, these first results support the results of former researches, but full detailed, especially paleontological results of new research will be published in short time.

Acknowledgement. The author is indebted to the Grant Agency for Science, Slovakia, for financial support (project No. 1/7304/20), and to many sponsors, especially Tauris Co. in Rimavská Sobota for financial and material support. Also he wishes to thank to Prof. Oldřich Fejfar from the Charles University in Prague for valuable advices, Mrs. Viera Matláková for her illustrations, and Mrs. Júlia Ferleťáková for photos.

References

Balogh, K., Miháliková, A., Vass, D., 1981: Radiometric dating of basalts in Southern and Central Slovakia. *Západné Karpaty*, Sér. Geol., 7, Bratislava, 113 – 126.

Bezák, V., Bodnár, J., Elečko, M., Konečný, V., Lexa, J., Molák, B., Straka, P., Stankovič, J., Stolár, M., Škvarka, L., Vass, D., Vozár, J., Vozárová, A., 1992: Notes to the Geological Map of Lučenec Basin and Cerová Highland 1 : 50 000. GÚDŠ, Bratislava, 198 (*in Slovak*).

Fejfar, O., 1961a: The Plio-Pleistocene Fauna of Vertebrates from Hajnáčka and Ivanovce (Slovakia), CSR. I. The Finding Circumstances and Stratigraphy. *N. Jb. Geol. Paläontol.*, Abh. 111, 3, Stuttgart, 257 – 273 (*in Germany*).

Fejfar, O., 1961b: The Plio-Pleistocene Fauna of Vertebrates from Hajnáčka and Ivanovce (Slovakia), CSR. II. Microtidae and Cricetidae inc. sed.. *N. Jb. Geol. Paläontol.*, Abh. 112, 1, Stuttgart, 48 – 82 (*in Germany*).

Fejfar, O., 1964: The Lower Villafranchian Vertebrates from Hajnáčka near Filákovo in Southern Slovakia. *Rozpravy Ústředního ústavu geologického*, 30, Praha, 116.

Fejfar, O., Heinrich, W. D., 1985: Importance of two sites of fossil vertebrates, Ivanovce and Hajnáčka, for mammalian palaeontology in European Pliocene and Early Pleistocene: present stage of knowledge and problems. *Věstník Ústředního ústavu geologického*, 60, 4, Praha, 213 – 224 (*in Germany*).

Fejfar, O., Heinrich, W. D., 1987: On the Biostratigraphical Division of Late Cainozoic in Europe on the Basis of Murids and Cricetids (Rodentia, Mammalia). *Čas. Mineral. Geol.*, 32, 1, Praha, 1 – 16 (*in Germany*).

Fejfar, O., Heinrich, W. D., Heintz, É., 1990: New Data on the Villafranchian of Hajnáčka near Filakovo (Slovakia, ČSSR). *Quatärpaläontologie*, 8, Berlin, 47 – 70 (*in Germany*).

Kantor, J., Wiegerová, V., 1981: Radiometric ages of some basalts of Slovakia by $^{40}Ar/^{40}K$ method. *Geologica Carpathica*, 32, 1, Bratislava, 29 – 34.

Konečný, V., Lexa, J., Balogh, K., Konečný, P., 1995: Alkali basalt volcanism in Southern Slovakia: volcanic forms and time evolution. *Acta Vulcanologica*, Vol. 7, 2, 167 – 171.

Kormos, T., 1917: The Pliocene Layers of Hajnáčka and their Fauna. *Jber. ung. geol.*, R.-Anst. 1915, Budapest, 654 – 582 (*in Germany*).

Krenner, J. S., 1867: Ancient Mammals of Hajnáčka. *Magyar Föld.*, 3, Budapest, 113 – 132 (*in Hungary*).

Lindsay, E. H., Opdyke, N. D., Fejfar, O., 1997: Correlation of selected late Cenozoic European mammal faunas with the magnetic polarity time scale. *Palaeogeography, Palaeoclimatology, Palaeoecology*, 133, Amsterdam, 205 – 226.

Lupták, P., 1997: Upper Jaw Fragment of the *Anancus arvernensis* (CROIZET & JOBERT, 1828) (Mastodontidae, Proboscidea, Mammalia) from the Villafranchian of Hajnáčka, Slovakia. *Geologica Carpathica*, 48, 5, Bratislava, 341 – 343.

Paul, C. M., 1866: The Tertiary Territory northern of the Mátra hill in Northern Hungary. *Jahrbuch geol.*, R.-Anst., 16, 4, Wien, 515 – 525 (*in Germany*).

Pipík, R., 2000: Neogene habitats and freshwater *Ostracoda* on the territory of Slovakia. *Slovak Geol. Magazine*, 6, 2-3, Bratislava, 116 – 119.

Sabol, M., 2000: Neogene carnivores of Slovakia. *Slovak Geological Magazine*, 6, 2-3, Bratislava, 124 – 126.

Schafarzik, F., 1899: Data to the geological knowledge of Bone Creek in Hajnáčka. *Földt. Közl.*, 29, Budapest, 363 – 366 (*in Hungary*).

Szabó, J., 1865: The Pogányvár hill in Gemer as a basalt crater. *Math. Term. Közl.*, 3, Budapest, 334 – 335 (*in Hungary*).

Uher, P., Sabol, M., Konečný, P., Gregáňová, M., Táborský, Z., Puškelová, Ľ., 1999: Sapphire from Hajnáčka (Cerová Highlands, southern Slovakia). *Slovak Geol. Magazine*, 5, 4, Bratislava, 273 – 280.

Vass, D., Konečný, V., Túnyi, I., Dolinský, P., Balogh, K., Hudáčková, N., Kováčová-Slamková, M., Beláček, B., 2000: Origin of the Pliocene Vertebrate Bone Accumulation at Hajnáčka, Southern Slovakia. *Geologica Carpathica*, 51, 2, Bratislava, 69 – 82.

Slovak Geol. Mag., 7, 3 (2001), 289 – 301

Bánovská kotlina Depression (northern part of the Danube Basin); Neogene stratigraphy and geological development

KLEMENT FORDINÁL[1], MICHAL ELEČKO[1], LADISLAV ŠIMON[1] and KATARÍNA HOLCOVÁ[2]

[1]Geological Survey of Slovak Republic, Mlynská dolina 1, 817 04 Bratislava, Slovakia
[2]Institute of Geology and Paleontology, Faculty of Science, Charles University, Albertov 6, 128 43 Prague 2, Czech Republic

Abstract: During the compilation of Explanatory Notes to the Geological Map of the Danube Lowland – Nitrianská pahorkatina Upland, new investigation, carried out in the Bánovská kotlina Depression, has brought new information on its Neogene sediments stratigraphy. On this basis we have redefined stratigraphic range of the Svinná Formation (Lower Badenian) and divided the so far homogeneous Ruskovce Formation into 3 lithostratigraphical units. The lower part has been assigned to the Kamenec Formation. The epiclastic volcanic sandstones and claystones, with layers of recarbonized claystones found as overlying it, have been ranged to the Handlová Formation. The presence of the mentioned formations has not been known from the Bánovská kotlina Depression till now. We have ranged the pyroclastic rocks found above the Handlová Formation to the Ruskovce Member (redefined Ruskovce Formation), which represents the peripheral member of the Vtáčnik Formation.

Key words: Danube basin, Bánovská kotlina Depression, Neogene, stratigraphy, geological development

Introduction

The Bánovská kotlina Depression (Fig.1) has been distinguished by Vass et al. (1988) as an autonomous part of the Danube Basin. From the geographical point of view it forms the northern part of the Nitrianska pahorkatina Upland.

Throughout the Neogene, the Bánovská kotlina Depression was a part of several basins. In the Lower Miocene (Eggenburgian), it was a part of the basin extending in E - W to ENE - WSW direction from the region of the present-day fore-deep through the northern area of the Vienna Basin, the Ilavská kotlina Depression as far as the Hornonitrianska kotlina and Turčianska kotlina Depressions (Gašparik, 1969; Hók et al., 1998; Kováč et al., 1989; Kováč & Baráth, 1996). In the Middle Miocene, it had a development common with the Hornonitrianska kotlina Depression and in the Upper Miocene with the Danube Basin.

With a revising study of sediments of some boreholes in the Bánovská kotlina Depression area we could obtain new data. On their basis, the stratigraphy scheme of the mentioned depression, used so far, has been changed (Tab. 1).

After thorough study of sediments from the boreholes DB-3 and DB-6 in the area of Ruskovce, it has been shown that the originally uniform Tuffitic-Detrital Formation (Brestenská et al., 1980), designated later as the Ruskovce Formation (Kováč et al., 1993b; Vass in Keith et al., 1994) has to be divided into the lower Kamenec Formation and overlying equivalents of the Handlová Formation. From the original Ruskovce Formation only its uppermost part, cropping out in the area under study, has remained. Therefore, we designate it currently as the Ruskovce Member of the Vtáčnik Formation (Šimon in Pristaš et al., 2000a).

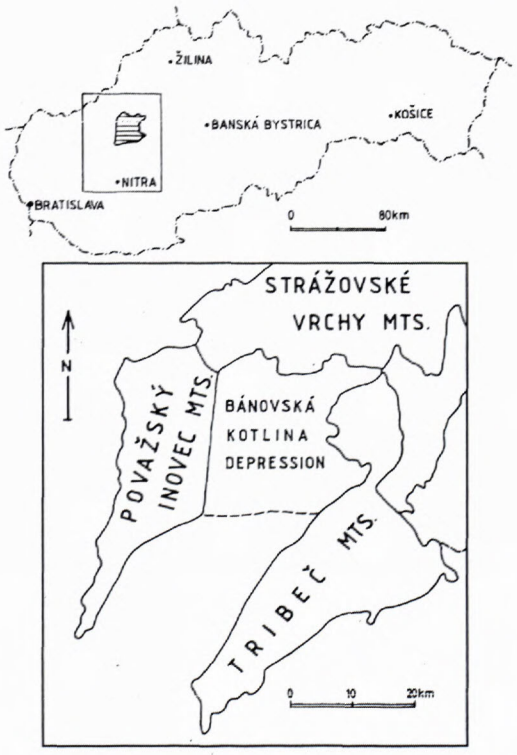

Fig. 1 Geological position of the Bánovská kotlina depression (in the sense Vass et al., 1988)

This fact has also contributed to the reconstruction of geological structure of the Badenian and Sarmatian sedi-

Period	Epoch	Stages		LITOSTRATIGRAPHY OF BÁNOVSKÁ KOTLINA DEPRESSION		
				Brestenská et al., (1980)	Vass in Keith et al., (1994)	Fordinál et al. (in this paper)
NEOGENE	PLIOCENE	Dacian		*Dacian sediments*	*Volkovce Formation*	*Volkovce Formation*
NEOGENE	NEOGENE	Pontian		*Coal formation*	*Beladice Formation*	*Beladice Formation*
NEOGENE	NEOGENE	Panonnian	upper	*Tuffo-detritic formation*	*Ruskovce Formation*	*Hlavina Member*
NEOGENE	NEOGENE	Panonnian	middle			
NEOGENE	NEOGENE	Panonnian	lower			
NEOGENE	NEOGENE	Sarmatian	upper			*Ruskovce Member*
NEOGENE	NEOGENE	Sarmatian	middle			
NEOGENE	NEOGENE	Sarmatian	lower	*Pelite formation*	*Svinná Formation*	
NEOGENE	NEOGENE	Badenian	upper			*Handlová Formation*
NEOGENE	NEOGENE	Badenian	middle			*Kamenec Formation*
NEOGENE	NEOGENE	Badenian	lower			*Svinná Formation*
NEOGENE	NEOGENE	Karpatian		*Pelitic formation*	*Bánovce Formation*	*Lakšáry Formation*
NEOGENE	NEOGENE	Otnangian		*Flyshoid formation*		*Bánovce Formation*
NEOGENE	NEOGENE	Egenburgian		*Schlier formation*	*Čausa Formation*	*Čausa Formation*
				Basal formation	*Klačno Member*	*Klačno Member*

Tab. 1 Litostratigraphic column of the Neogene fill of the Bánovská kotlina Depression (hiatus are marked with black lines)

ments in the basin's fill. The sediments of the Svinná Formation (pelitic formation) were compared by Brestenská (in Brestenská et al., 1980) with overlying clays, i. e. the Koš Formation in the Hornonitrianska kotlina Depression and ranged to the Upper Badenian. The presence of sediments of the Kamenec Formation (higher part of the Lower Badenian - Middle Badenian) and the occurrence of palynomorphs of the Lower Badenian age (Planderová, 1991) in strata overlying them have made the Upper Badenian age of the formation untenable. We have to take into consideration the Lower Badenian age of the Svinná Formation. Under these circumstances, it becomes easier to explain the presence of brackisch microfauna in the formation. We explain their presence as a consequence of sea ingressions into the limnic environment. The presence of the marine Lower Badenian is also proved from the region of the Central Slovakian neovolcanics (Gašpariková in Blaško et al., 1989) and supposed in the Hornonitrianska kotlina Depression (Elečko in Šimon et al., 1997).

Stratigraphy of Neogene sediments

Neogene sediments of the Bánovská kotlina Depression are formed by Miocene to Pliocene sediments.

The oldest Neogene sediments are of the Eggenburgian age. They are represented by the Čausa Formation. It is resting transgressively and disconformably on the pre - Neogene substratum, either on formations of the Central Carpathian Paleogene or on Alpine-folded units of the central Western Carpathians of the Mesozoic age.

Coarse-grained basal sediments are represented by the Kľačno Conglomerate. The bulk mass of the formation is formed by grey calcareous clay/claystones and silt/siltstones with sandy laminations and shaly disintegration (schlier). The schlier is resting directly on the Kľačno Conglomerate or the passage is formed by their alternation with calcareous layered sandstones.

The Čausa Formation is cropping out mainly in the northern part of the depression (Fig. 2).

The Kľačno Conglomerate represents marine littoral deposits. It is formed predominantly by conglomerates and sandstones, in which pelitic thin beds are found. The mentioned conglomerate is resting disconformably and transgressively on the considerably dissected Mesozoic substratum. These sediments are bordering the southern margin of the Strážovské vrchy Mts. between villages Trenčianske Mitice and Krásna Ves and the eastern margin of the Považský Inovec Mts. near the village Dubodiel. Most occurrences are only denudation remnants with relatively small area and thickness. The thickness of sediments verified by boreholes near Horné Motešice and Dolné Motešice attains about 40 m (Kollárik, 1962; Mikuláš, 1968).

The clastic fraction of conglomerates is almost exclusively formed by Mesozoic carbonate rocks (dolomite, limestone), subordinately by vein quartz. The size of pebbles varies from 1 to 6 cm. Larger pebbles are found rarely, they are bound to the base of beds. Besides coarse-grained conglomerates, fine-grained ones are also found, passing into coarse-grained sandstones. Lithification of conglomerate layers depends on the carbonate cement and/or on content of dolomite sand (solid and/or friable layers).

In conglomerates occurring in the villages Horné Motešice, Dolné Motešice, Kostolné Mitice and Krásna Ves, a mollusc fauna has been found. Species significant stratigraphicaly *Pecten hornensis* DEP. - ROM., *Chlamys justiniana* (FONT.), *Anomia ephippium costata* BROCC. and *Pitar schafferi* KAUTSKÝ were identified, indicating an Eggenburgian age (Ondrejičková, 1979; Váňová, 1955).

In pelitic intercalations in conglomerates, an association of foraminifers with prevalence of lagenids and agglutinates was established (Brestenská, 1977).

The Kľačno Conglomerate was formed in gravel mounds at the margin of a rocky coast. Cross bedding caused by wave activity and distinct increase in thickness of layers towards the basin, which was determined by considerable paleo-dip of the coast, has been observed (Baráth & Kováč, 1989). On the basis of mollusc fauna it may be stated that the mentioned clastic sediments were deposited into a normal marine infra-littoral environment.

Pelitic sediments of the Čausa Formation are cropping out at the northern margin of the Bánovská kotlina Depression. They are lying above the Kľačno Conglomerates or their passage is formed by alternation with calcareous bedded sandstones. The greatest verified thickness of Eggenburgian sediments is 204.4* m (the borehole DB-15, 775.0-979.4 m).

Generally there are grey, yellow-grey calcareous siltstones, claystones with sandy admixture with conchoidal and splintery fracture. To the overlying strata their sandy and calcareous character decreases.

In the borehole DB-15, in the interval 775.0-979.0 m, grey and dark-grey solid claystones with the medium grain diameter 0.0083 mm and a low sorting degree occur. The average value of the sorting coefficient SO is 3.41. The distribution character of grain size particles is

* No biostratigraphic markers of the Eggenburgian/Ottnangian boundary were found in analysed material. Therefore Brestenská mentioned Eggenburgian-Ottnangian boundary in the borehole DB-15 in her individual works variously. In the work from the year 1975a she ranged the sediments as follows: Eggenburgian (946.0-979.4 m), Eggenburgian-Ottnangian (630.6-946.0 m), Ottnangian (456.4-630.6 m) and Karpatian (2.5-456.4 m). In the Explanatory Notes to the Geological Map of the Bánovská kotlina Depression 1 : 50 000 (Brestenská et al., 1980) the sediments from the mentioned borehole were ranged to the Eggenburgian (635.0-979.4 m), Ottnangian (456.4-635.0 m) and Karpatian (2.5-456.4 m). In the article from the year 1983 she shifted the Ottnangian-Eggenburgian boundary deeper to the depth of about 913 m (recorded from the schematic profile of borehole DB-15). Ottnangian is generally correlated with regressive part of the Eggenburgian-Ottnangian cycle: representing sea level drop of cycle TB2.1 of Haq et al. 1988 (Papp et al., 1973; Cicha et al., 1998; Rögl, 1998). Based on the ecostratigraphic principle, the Eggenburgian(Ottnangian boundary can be approximately correlated with the boundary between the Čausa and Bánovce Formations (775 m of the borehole DB-15). This lithological change is connected with the basin's shallowing and decrease of its water salinity (for detailed data see below).

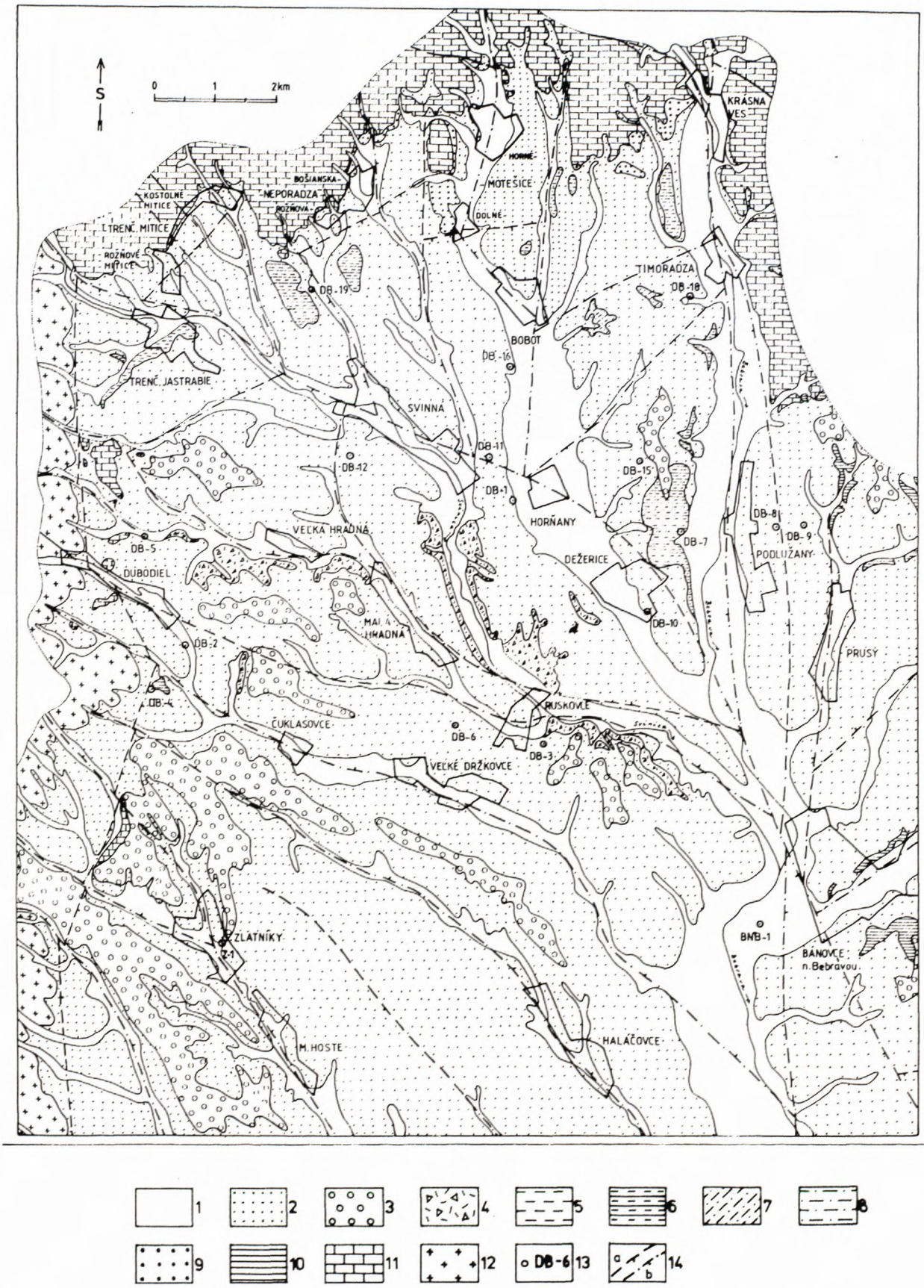

Fig. 2 Schematic geological map of the Bánovská kotlina Depression (compiled Fordinál 2001, after Pristaš et al., 2000b). QUATERNARY 1 – fluvial sediments 2 – deluvial sediments, PLIOCENE 3 – Volkovce Formation, MIOCENE 4 – Vtáčnik Formation – Ruskovce Member 5-Svinná Formation 6 – Lakšáry Formation 7 – Bánovce Formation 8 – Čausa Formation (pelitic sediments) 9 – Čausa Formation – Kľačno Member PALEOGENE 10 – Borové and Zuberec Formations, 11 – Mesozoic rocks, 12 – metamorphic and granitoid rocks, 13 – borehole, 14 – faults a, assumed b, assumed covered.

bimodal. The lower part of the mentioned sediments has the Sk values 1.88 and 1.32. The content of heavy minerals is low (mostly up to 2.34 %, exceptionally 12.73 %). High presence of authigenic minerals, like pyrite and siderite is characteristic of these sediments. In schlier layers (the interval of 775-945 m), the layers of acid (rhyodacite and rhyolite) tuffites were found (Marková, 1975).

From the clay minerals, montmorillonite predominates in the schlier lithofacies and kaolinite over montmorillonite in flysh lithofacies (Marková, l.c.).

Schlier sediments of the Čausa Formation contain a rich microfauna. Mainly on basis of the borehole DB-15 the following microfaunal associations were distinguished (Brestenská, 1975a):

1. with prevalence of lagenids and agglutinates
2. with pyritized diatoms and foraminifers
3. with radiolarians

The first association found in the borehole DB-15, in the interval of 965-979 m, is rich and diversified. It is characteristic of lagenids and agglutinates prevalence. The species *Rhizammina* aff. *algaeformis* BRADY, *Bathysiphon taurinensis* SACCO, *Spirorutilus carinatus* (ORBIGNY), *Textularia* ex gr. *gramen* ORBIGNY, *Vulvulina pennatula* (BATSCH), *Semivulvulina* ex gr. *pectinata* (REUSS), *Reticulophragmium acutidorsata* (HANTKEN), *R. rotundidorsata* (HANTKEN), *Cyclammina praecancellata* VOLOSHINOVA, *Nodosaria latejugata* GÜMBEL, *Lenticulina cultrata* (MONTFORT), *L. inornata* (ORBIGNY), *L. clericii* (FORNASINI), *L. mamilligera* (KARRER), *L. arcuatostriata* (HANTKEN), *L. meznericae* (CICHA), *Marginulina glabra* ORBIGNY, *M. hirsuta* ORBIGNY, *Marginulinopsis* aff. *fragaria* GÜMBEL, *Globulina gibba* ORBIGNY, *Sphaeroidina bulloides* ORBIGNY, *Stilostomella elegans* (ORBIGNY), *Bulimina elongata* ORBIGNY and other were found (Brestenská, 1975b). The mentioned association was also established in schlier at the locality Krásna Ves (Brestenská & Lehotayová, 1983). This assemblage is characteristic of stenohaline, lower neritic to upper bathyal foraminifers. High relative abundance of agglutinated species is well comparable with isochronous assemblages from other parts of the Central Paratethys (Bathysiphon-Cyclammina schlier in the Vienna basin (Cicha et al., 1998) and assemblages from the upper part of Szecsény schlier in the Fiľakovo/Pétervására Basin (Halásová et al., 1996). During this interval, broad communication with Vienna basin and the Fiľakovo/Pétervására basin can be expected (Halásová et al., l.c.).

The second association was found in the borehole DB-15, interval 947-964 m. On the contrary to the first association, it is less diversified and is characteristic of pyritized foraminifers and diatoms. Composition of assemblages frequently shifts. From foraminifers, *Saccamina* sp., *Cibicidoides budayi* (CICHA et ZAPLETALOVÁ), *C. ungerianus* (ORBIGNY), *Bulimina elongata* ORBIGNY, *Chilostomella ovoidea* REUSS, *Reophax sp.*, *Caucasina schischkinskaye* (SAMOILOVA), *Virgulinella pertusa* (REUSS), *Cibicides lobatulus* (WALKER et JACOB), *Cribrononion minutum* (REUSS), *Lagena vulgaris* WILLIAMSON, *Siphonina reticulata* (CZJEZEK), *Ammonia* ex gr. *beccarii* (LINNÉ) and *Protelphidium* ex. gr. *granosum* (ORBIGNY) occur most often, Brestenská (1975a; 1977). Assemblages from this interval characterise upper neritic and episodically low-oxic or euryhaline paleoenvironment. They reflect beginning of the basin's isolation.

In both intervals, calcareous nannoplankton was observed (Tab. 2). Assemblages are dominated by *Coccolithus pelagicus* (Wallich) Schiller and *Reticulofenestra pseudoumbilica* (Gartner) Gartner. Occurrence of *Helicosphaera ampliaperta* Bramlette et Wilcoxon enables to correlate these intervals with the transgressive Eggenburgian sediments from the Central Paratethys basins, including stratotype sections in the Lower Austria. *H. ampliaperta* Bramlette et Wilcoxon appears in the middle part of the NN 2 Zone (Fornaciari & Rio, 1996). Reworked Cretaceous, Eocene and Oligocene nannoliths occur mainly in the second interval (Fig. 3).

In the strata overlying both mentioned intervals (the depth 775-945 m), probably bathymetrycally deepest sediments of the schlier formation were found. They contain redeposited radiolarians and represent the third distinguished association. Calcareous nannoplankton was not observed in this interval, with the exception of very rare Eocene and Cretaceous reworked nannoliths. Sediments containing an association with radiolarians were also found in the borehole DB-8 (12-84 m). They are formed predominantly by grey non-stratified clay, with the layers of grey sandstones (Brestenská, 1977; Seneš & Brestenská, 1963). Besides boreholes, the sediments with radiolarians were also found in the outcrops between Trenčianske Mitice and Timoradza (Brestenská, 1977). To the south of Bošianska Neporadza, the vitreous tuffite was also found in these sediments (Marková, 1977).

In sediments of the Čausa Formation, the presence of calcareous nannoplankton was established also in the other sections and boreholes. Their occurrence was recorded in grey calcareous clays in borehole DB-9 (57-58 m). Species *Discoaster aulakos* GARTNER, *D. aster* BRAMLETTE et RIEDEL, *Reticulofenestra excavata* Lehotayová and *R. bisecta* (HAY, MOHLER et WADE) ROTH were determined, presence of *Discoaster druggi* BRAMLETTE et WILCOXON, indicate the NN2 Discoaster druggi Zone (Lehotayová, 1977; 1982).

Pelitic sediments from the localities Kostolné Mitice, Rožňová Neporadza, Horné Motešice, Krásna Ves and from the boreholes DB-15 (815,1-819,2 m) and DB-19 (53,6-53,8 m), with nannoflora containing the species *Coccolithus pelagicus* (WALLICH) SCHILLER, *Cruciplacolithus tenuiforatus* CLOCCHIATI et JERKOVIĆ and *H. carteri* (WALLICH) KAMPTNER was found (Lehotayová, 1976; 1977; 1982; Brestenská & Lehotayová, 1983; Žecová, 1999). *Helicosphaera ampliaperta* BRAMLETTE et WILCOXON, enable to correlate this section with the upper part of NN 2 Zone, i.e. with the Eggenburgian.

In schliers of the Čausa Formation in Rožňová Neporadza, a rich association of molluscs was found, containing the species: *Nucula nucleus* (L.), *N. compta* GOLD., *Yoldia nitida* (BROCCHII), *Anadara diluvii* (LM.), A. darwini (MAYER), *Anadara sp.*, *Glycymeris sp. Modiolus sp.*, *Musculus philippi* (WOLF), *Pinna pectinata brocchii* ORBIGNY, *Pinna* sp., *Lentipecten corneum denudatum*

Tab. 2 Quantitative representation of calcareous nannofossils in the well DB-15, Horňany (compiled Holcová 2001).

Species	Reworked	975-976 m	963.5 m	959.5 m	953.5 m	942.5 m	914.5 m	884 - 885 m	864 - 865 m	836.5 m	802.5 m	769.5 m	729.5 m	691.5 m	675 m	640.5 m	625.8 m	606.8 m	584 - 585 m	554.5 m	535.8 m	533.4 m	512.5 m	491.5 m	466.5 m	420.5 m	353.3 m	334.4 - 334.6 m	298 m	279.5	249.5 m	227.5 m	202.5 m	185.5 m	132.5 m	105.5 m	98.5 m	87.5 m
Reticulofenestra excavata LEHOTAYOVA		0.0	0	0.0	0.0																										0.0	0.0		0.0	0.8	0.0	0.0	0.0
Reticulofenestra minuta ROTH		1.4	12.9	0.0	0.0																										6.7	0.0	+	9.8	5.3	6.0	1.1	6.6
Reticulofenestra pseudoumbilica (GARTNER) GARTNER		15.3	6.5	15.4	10.1	+			+																						20.0	13.6		4.5	5.3	12.0	4.4	1.9
Reticulofenestra pseudoumbilica (GARTNER) GARTNER - small-sized		9.7	2.4	0.0	0.0																										0.0	0.0		0.0	0.0	0.0	0.0	0.0
Reticulofenestra daviesi (HAQ) HAQ	O	0.0	0.8	0.0	0.8																										0.0	0.0		0.0	0.8	2.0	0.0	0.0
Reticulofenestra bisecta (HAY, MOHLER et WADE) ROTH	O	6.9	2.4	0.0	2.3															+											6.7	0.0		0.9	1.5	2.0	3.3	1.9
Reticulofenestra bisecta (HAY, MOHLER et WADE) ROTH - small-sized	O	4.2	4.8	7.7	0.0										+																0.0	4.5		0.0	1.5	0.0	0.0	0.0
Reticulofenestra lockeri MULLER	O	0.0	0.0	0.0	0.0																										0.0	0.0		0.0	0.8	0.7	0.0	0.0
Reticulofenestra umbilica (LEVIN) MARTINI et RITZOWSKI	E	1.4	1.6	7.7	2.3	+																									0.0	0.0		0.0	0.0	0.7	0.0	0.0
Coccolithus pelagicus (WALLICH) SCHILLER		50.0	34.7	46.2	53.5		+								+													+		50.0	40.9	+	68.8	38.3	46.0	44.4	30.2
Cyclicargolithus abisectus (MULLER) BUKRY	O	4.2	0.0	0.0	0.0																										0.0	0.0		0.9	0.0	0.0	3.3	0.9
Cyclicargolithus floridanus (ROTH et HAY) BUKRY		0.0	0.0	15.4	3.1																										0.0	0.0		0.9	1.5	0.7	1.1	1.9
Cribrocentrum reticulatum (GARTNER et SMITH) PERCH-NIELSEN	E	1.4	0.0	0.0	0.0																										0.0	4.5		0.0	0.0	0.0	0.0	0.9
Cruciplacolithes sp.	E	0.0	0.0	0.0	0.8																										0.0	4.5		0.0	0.0	0.0	0.0	4.7
Transversopontis pulcher (DEFLANDRE) PERCH-NIELSEN	O	1.4	0.0	0.0	0.0																										0.0	0.0		0.0	0.0	0.0	0.0	0.9
Helicosphaera ampliaperta BRAMLETTE et WILCOXON		0.0	0.0	0.0	0.8																										0.0	0.0		8.9	15.8	2.0	10.0	0.9
Helicosphaera ampliaperta BRAMLETTE et WILCOXON - narrow central opening		1.4	0.0	0.0	0.0																										0.0	0.0		0.9	0.0	0.7	1.1	0.9
Helicosphaera carteri (WALICH) KAMPTNER		0.0	0.0	0.0	0.0																										3.3	0.0		0.0	0.0	6.7	0.0	0.9
Helicopshaera mediterranea MULLER		0.0	0.0	0.0	0.8																										0.0	0.0		0.0	0.0	0.0	0.0	0.0
Helicosphaera scissura MILLER		0.0	0.0	0.0	0.8																										0.0	0.0		0.0	0.0	0.7	0.0	0.0
Pontosphaera multipora (KAMPTNER) ROTH		1.4	0.8	0.0	0.0																										0.0	0.0		0.9	0.0	4.0	0.0	0.0
Sphenolithus heteromorphus DEFLANDRE		0.0	0.0	0.0	0.0																										0.0	0.0		0.0	0.0	0.7	0.0	0.0
Sphenolithus moniformis (BRONNIMANN et STRADNER) BRAMLETTE et WILCOXON		5.6	0.8	0.0	0.8																										3.3	4.5		0.9	0.8	2.7	0.0	0.0
Cricolithus jonesi COHEN		0.0	12.1	0.0	0.0				+																						0.0	0.0		0.9	22.6	6.7	22.2	23.6
Discoaster droogi BRAMLETTE et WILCOXON		0.0	0.0	0.0	0.0																										3.3	0.0		0.0	0.0	0.0	0.0	0.0
Discoaster deflandrei BRAMLETTE et RIEDEL	O	0.0	0.0	0.0	0.0																										0.0	0.0		0.0	0.0	2.0	0.0	0.9
Discoaster saipanensis BRAMLETTE et RIEDEL	E	0.0	0.0	0.0	0.0																										0.0	0.0		0.0	0.0	0.0	0.0	0.9
Zyghrabdulus bijugatus DEFLANDRE	O	0.0	0.0	0.0	0.0																										0.0	0.0		0.0	0.0	0.0	0.0	0.9
Braarudosphaera bigelowi (GRAN et BRAARUD) DEFLANDRE		0.0	0.0	7.7	0.0																										0.0	0.0		0.0	0.0	0.0	0.0	0.0
Thoracosphaera sp.		0.0	0.0	0.0	0.0																		+			+			+		0.0	0.0		0.0	0.0	0.7	1.1	0.0
Arkhangelskiella sp.	C	0.0	0.0	0.0	0.8																										0.0	0.0		0.0	0.0	0.0	0.0	0.0
Watzenaueria sp.	C	1.4	10.5	0.0	15.5																		+			+	+	+			6.7	13.6	+	1.8	2.3	1.3	5.6	14.2
Crethorabdulus sp.	C	0.0	0.0	0.0	0.8																										0.0	0.0		0.0	0.0	0.0	0.0	0.0
Micula sp.	C	0.0	0.8	0.0	3.9	+																	+								0.0	0.0		0.0	0.0	0.0	1.1	4.7
Chiasmolithus sp.	E	0.0	0.0	0.0	0.8																										0.0	4.5		0.0	1.5	0.0	1.1	0.0
Isthmolithus recurvus DEFLANDRE	E	0.0	0.0	0.0	0.8																										0.0	0.0		0.0	0.0	0.0	0.0	0.0
Eifelithus sp.	E	0.0	0.0	0.0	1.6																										0.0	9.1		0.0	0.0	0.0	0.0	1.9
Nannolith abundance		common	common	rare	common	very rare	very rare	absent	very rare	absent	absent	absent	absent	absent	very rare	absent	absent	absent	absent	absent	very rare	absent	very rare	absent	absent	absent	very rare	very rare	absent	very rare	rare	rare	very rare	abundant	abundant	abundant	abundant	common
Diatoms abundance		common	absent	absent	absent	absent	common	absent	rare	rare	absent	absent	absent	absent	absent	rare	rare	absent	absent	absent	absent	common	absent	absent	absent	very rare	very rare	common	very abundant	very abundant	common	rare	common	abundant	abundant	common	absent
Radiolaria																					+	common	absent	very rare	absent	absent	very rare	very rare	absent	very rare	very rare	very rare	very rare	very rare	very rare	very rare	very rare

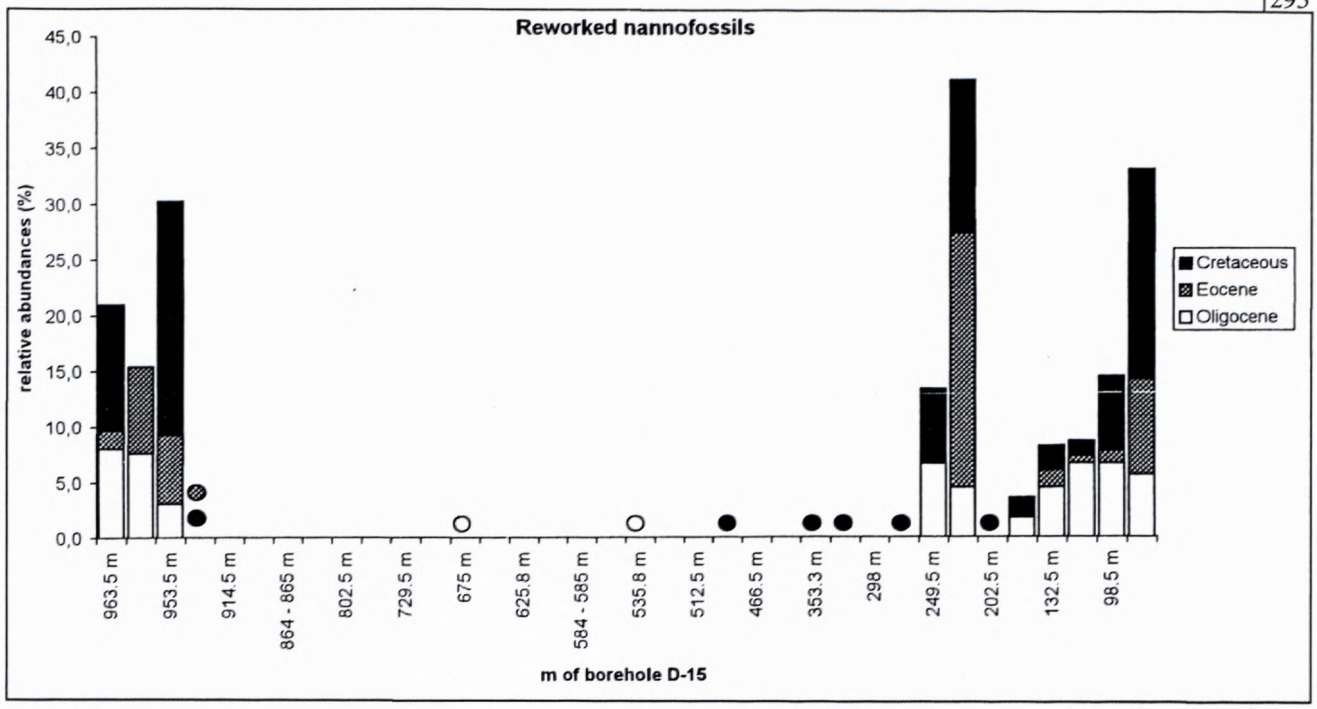

Fig. 3 Quantitative representation of reworked nannofossils in the well DB-15, Horňany (compiled Holcová 2001).

(REUSS), *Cyprina islandica rotundata* BRAUN and other (Ondrejičková, 1979).

The Bánovce Formation s. str. is formed by alternating clayey and sandy beds (flyschoid formation) with the thin layers of conglomerates. It is resting on the Čausa Formation. Based on its superposition, the Ottnangian age is interpreted for the Bánovce Formation.*

The average grain size of sandy layers is shown by a medium value 0.2 mm. The average of sorting coefficient is 2.17. Silts of the flyshoid formation have the medium grain diameter 0.019 mm, the average So value is 2.89. The particles distribution type is always bimodal and Sk negative. Clays have the least quantitative share in the Bánovce Formation. Their average Md is 0.008 mm, the average So 2.81, the distribution type is bimodal and Sk always negative (Marková, 1975).

It crops out in the northern part of territory, between the Jastrabie and Bebrava (Timoradza) faults, in area between the villages Timoradza, Horňany and Svinná. In the southern part, it is covered by sediments of the Lakšary Formation of Karpatian age. The Bánovce Formation was established in the boreholes DB-15 (456.4-635.0 m) (Brestenská et al., 1980), DB-18 (3-150 m) (Brestenská et al., 1976) and DB-19 (14.3-53.2 m). The greatest thickness of the Bánovce Formation was established in the borehole DB-15, i. e. 178.6 m.

The Bánovce Formation is very poor in organic remnants. In basal sediments of this formation, thecamoebian associations, formed by the *Silicoplacentina* occur. They were established in the borehole DB-15 (635-771 m) (Brestenská 1975a; 1977). Besides thecamoebian, a poor fauna of molluscs was found in the borehole DB-15 at depth of 577.5 m. The species *Mytilus* sp. indet, *Congeria* sp. indet., *Gyraulus trochiformis dealbatus* (BRAUN) and *Ancylus moravicus* RZEHAK were identified there (Ondrejičková, 1975). This fauna may be paralleled with the „Rzehakia Member" of southern Moravia (Ondrejičková, l.c.). Further on, fragments of small bones, fish teeth, carbonized remnants of plants and redeposited foraminifers, radiolarians and skeletal elements of siliceous sponges were found.

The Lakšáry Formation. At the base, it is formed by grey medium to coarse-grained calcareous sandstones with scattered pebbles as well as layers of conglomerates and to a less extent also claystones. The pebbles are formed by quartzite, quartz and dolomite. In the most cases they are well rounded. In claystones, laminae of diatomites (up to 1 mm) and worm tubes were found. These sediments were established in the borehole DB-15 (304.0-438.35 m) only. The sediments represent probably the transgressive littoral lithofacies resting with hidden uncorformity on Ottnangian sediments of the Bánovce Formation. The Karpatian age of this sediment is confirmed by occurrence of Karpatian diatoms. Other microfossils in this horizon are similar to microfossils in the Bánovce Formation. These sediments gradually pass into lithofa-

* The Bánovce Formation s.l. of the Ottnangian – Karpatian age has been divided by Vass (2001) in two parts. He assigned the Ottnangian sediments to the Bánovce Formation and for the sediments of the Karpatian age, he took the name from the Vienna Basin – the Lakšáry Formation. He has assumed that the originally outlined Bánovce Formation (s.l. – i.e. of the Ottnangian – Karpatian age) consists of two sedimentation sequences. The different opinion has been presented by Kováč (2000) and Kováč et al., (2001). He has announced that in the Bánovce Formation s.l., by means of sedimentology there cannot be established a transition from the transgressive system tracts to the highstand system tracts. This opinion has been based on the situation found out exclusively in the borehole DB-15. Consequently there cannot be definitely determined which of both opinions is closer to the reality. In this paper we have seized the opinion of Vass (2001).

alternating with grey calcareous claystones (flyshoid development). The occurrence of these sediments was established in the borehole DB-15 (200-304.0 m), as well as on the surface south to the village Trenčianske Mitice.

The upper part of sediments is formed by calcareous claystones (schliers). The formation's Karpatian age has been well documented in its upper part because of index Karpatian foraminifer *Uvigerina graciliformis* P. T. found there, as well as nannoliths *Sphenolithus heteromorphus* DEFLANDRE. The average grain size value of these sediments Md is 0.03 mm (0.007-0.05 mm), average So is 2.58 (1.73-4.63). The distribution character of grain size fractions is mostly bimodal, with the main maximum in grain size fraction 0.05-0.02 mm, the lognormal character of distribution with maximum in category 0.1-0.05 (Marková, 1975) is less found. In these sediments, the occurrence of volcanic glass (DB-15, 26-145,5 m) was established, indicating autochthonous or redeposited products of rhyodacite or rhyolite volcanism.

In the Lakšáry Formation, three micropaleontological types of association were distinguished from the base upwards (Brestenská, 1977):

1. very poor association with rare occurrence of fish remains and reworked foraminifers
2. association with prevalence of diatoms
3. an abundant association of planktonic foraminifers

The first association has been directly linked to Ottnangian associations. It is characteristic of basal and flyshoid sediments. Only fragments of fish bones and fish teeth together with carbonized plant remnants are found in it. Cretaceous reworked nannofossils occur in the upper part of this horizon. In the claystone layer (DB-15; 388-400 m) laminae of diatomites, 1 mm thick. The species „*Actinocyclus undatus* (CLEVE) RATRAY (predominating species), *Coscinodiscus gorbunovii* SHESH. var. *ethmodiscoides* MOISS, *C. pannonicus* f. *minima* HAJÓS, *C. variabilis* KRASSSKE, *Cyclotella meneghiniana* KÜTZ., *Melosira praeislandica* JOUSÉ, *M. praeislandica* JOUSÉ f. *curvata* JOUSÉ, *Stephanodiscus astrea* (EHR.) GRUN. var. *minutula* (KÜTZ) GRUN., *Synedra rumpens* KÜTZ. var. *fragilarioides* GRUN and Chrysostomatacea were determined there. This is a mixed association of marine planktonic and freshwater forms indicating the Karpatian age (Hajós in Brestenská et al., 1976).

The second association has been characterized by a rich occurrence of diatoms. Concerning the lithology, this is the uppermost part of flyshoid formation and the lower part of pelitic (schlier) formation of the Karpatian age.

Sediments characteristic of a rich diatom occurrence were found in the boreholes DB-15 (95-288 m), DB-16 (40-100 m), they also crop out in surroundings of the village Bobot. In the lower part of these sediments only sporadic, minute, discoid, non - pyritized diatoms and scarce foraminifers, represented mainly by the species *Ammonia* ex. gr. *beccarii* L. occur. In the borehole DB-15 (185.5 m), notable endemic foraminifer of the genus *Montspeliensina* was found. This genus appeared in the Ottnangian of Upper Austria and then in the Medokýš Member of the Novohrad Basin (Holcová, 1996). Occurrence of the genus indicates marine communication among these areas. Damaged ostracode tests of the genera *Cytheridea* and *Xestoleberis* Scarcela were also scarcely present. The middle part is similar to the lower part, only diatoms are represented in a larger amount and they are pyritized. The upper part of sediments with predominating diatoms represents a transition between the association with rich occurrence of diatoms and the association with an abundant plankton. In this part discoid pyritized diatoms also predominate, but layers with foraminifers are more frequent, richer and more diversified. From benthic foraminifers the species *Praeglobobulimina pupoides* (ORBIGNY), *Heterolepa* ex gr. *dutemplei* (ORBIGNY), *Valvulineria complanata* (ORBIGNY), *Melonis soldanii* (ORBIGNY), *Stilostomella elegans* (ORBIGNY) etc. are most often found. The plankton is represented by pteropods and by the foraminifers *Globigerina praebulloides* BLOW and *Globigerina angustiumbilicata* BOLLI (Brestenská, 1977).

Changes in calcareous nannoplankton assemblages and relative abundance of reworked nannoliths in this interval of the borehole DB-15 well correlate with a lithological change in the level 200 m (Tab. 2, Fig. 3). Rare nannofossils with high abundance of reworked species and dominance of *Coccolithus pelagicus* (WALLICH) SCHILLER and *Reticulofenestra pseudoumbilica* (GARTNER) GARTNER occur in the flyshoid sediments. In overlying schlier, abundant assemblages with common *Cricolithus ionesi* COHEN characteristic of the Karpatian assemblages also in other Central Paratethys basins, were observed. From the stratigraphical point of view, appearance of the NN 4 Zone index species *Sphenolithus heteromorphus* DEFLANDRE is important. Low abundance of reworked nannolith may reflect highstand deposits.

The third association has been characterized by rich assemblages of foraminifers with abundant plankton. Sediments, in which the mentioned association has been found, were present in the boreholes DB-7 (87-150 m), DB-10 (112-177 m), DB-15 (7-95 m), DB-16 (0-70 m), DB-17 (0-201 m) and in surface outcrops of the Karpatian deposits (Dežerice, Bobot).

From benthic forms of foraminifer assemblages, *Bathysiphon taurinensis* SACCO, *Haplophragmoides vasiceki* CICHA et ZAPLETALOVÁ, *Budashevaella wilsoni* (SMITH), *Reticulophragmium karpaticum* CICHA et ZAPLETALOVÁ, *Lenticulina depauperata* (REUSS), *L. cultrata* (MONTFORT) are found, from planktonic forms *Globigerina praebulloides* BLOW, *G. angustiumbilicata* BOLLI, *G. ciperoensis ottnangensis* RÖGL and *G. quinquelobata* NATLAND (Brestenská, 1977) occur. These assemblages indicate the lower neritic, stenohaline environment.

Besides foraminifers, molluscs also occur in sediments of the Karpatian age. In the borehole DB-15 (75.8-80.9 m) *Amusium* sp. and *Pinna* sp. have been identified and in the borehole DB-17 (41.0-154.0 m) *Venus* sp., *Aturia aturi* BASTEROT, *Clio (Balantium) bittneri* (KITTL), *C. (B.) pedemontanum* (MAYER) a *?Vaginella* sp. have been found (Ondrejičková, 1975).

In the assemblage of sporomorphs found in Karpatian sediments in the borehole DB-10 (148.0-176.0 m), the Middle Miocene plant elements have been present. There are represented by tropical plants of the genus *Lygodium*

and families Gleicheniaceae, Sapotaceae, Hystrichosphaeridae and *Deflandrea*, which indicate a marine environment, are also abundant. Forms of the genera *Engelhardtia*, *Pterocarya*, *Carya* and family Myricaceae have been also found in a large amount . The mentioned assemblages of plants indicate a warm subtropical climate (Planderová, 1965).

Generally, the pollen spectrum has been characterized by a rich occurrence of marine plankton, pollen grains of coniferous and cryptogam plants. The composition of sporomorphs indicates a warm subtropical climate and the presence of marginal swamps, in which Taxodiacea-Nyssaceae-Mastixiceae dominate (Brestenská et al., 1983; Planderová, 1984).

Besides the borehole DB-15, calcareous nannoplankton was analysed in sediments at the localities Dežerice, Rožňové Mitice and in the borehole DB-19 (13.5-13.7 m) (Lehotayová, 1976; 1977; 1982; Lehotayová in Brestenská et al., 1980; Žecová, 1999). The species *Coccolithus miopelagicus* BUKRY, *C. pelagicus* (WALLICH) SCHILLER, *Coronasphaera mediterranea* (LOHMANN) GAARDER, *Cyclococcolithus rotula* KAMPTNER, *Cyclicargolithus floridanus* (ROTH et HAY) BUKRY, *Helicosphaera carteri* (WALLICH) KAMPTNER, *H. ampliaperta* BRAMLETTE et WILCOXON, *Pontosphaera multipora* (KAMPTNER) ROTH, *Reticulofenestra bisecta* HAY-MOHLER-WADE, *R. pseudoumbilica* (GARTNER) GARTNER have been found, indicating the NN-4 Zone.

Sediments of the Lakšáry Formation were generally found in the borehole DB-7 Podlužany (8.7-150.0 m) (Brestenská, 1977; originally ranged to the Eggenburgian (Seneš & Brestenská, 1963), DB-10 Dežerice (112.5-177.0 m), DB-15 (2.5-456.3 m), DB-16 Bobot (0-100 m) (Brestenská et al., 1976), DB-17 (Zemianske Mitice (0-201 m) (Brestenská 1977) and DB-19 Rožňová Nepomoradza (2.1-14.3 m) (Žecová, 1999).

The Svinná Formation is resting disconformably on older Miocene sediments. As for its stratigraphy, it was ranged to the Upper Badenian (Brestenská et al., 1980) and Upper Badenian to Lower Sarmatian (Vass in Keith et al., 1994). Occurence of the Kamenec Formation (upper part of the Early Badenian – Middle Badenian, see later) at its roof points to the Early Badenian age of the Svinná Formation.

Sediments of the Svinná Formation deposited in a freshwater environment, but in some horizons, the foraminifers *Ammonia* ex gr. *beccarii* (L.) and ostracods of the genera *Amnicythere* and *Mediocypris* have been found. Presence of the ostracod genus *Mediocypris* indicates the Middle Miocene age of the Formation. Generally, the occurrence of the above mentioned foraminifers and ostracods poits to the short-term sea ingressions (Brestenská, 1965; 1969; Brestenská in Brestenská et al., 1980). In the Middle Miocene, the most proximate existence of a marine environment was in the Hornonitrianska kotlina Depression, namely during the Early Badenian (Gašpariková in Blaško et al., 1989). Discovery of the mentioned sea ingressions also points to the Early Badenian age of the Svinná Formation.

Finding of a microfloral assemblage in sediments of the borehole DB-6 (462 m) represents another argument for the Early Badenian age of this Formation. It was correlated with the assemblage detected in the marine Early Badenian sediments of the borehole HV-9 (450-710 m) from the Hornonitrianska kotlina Depression (Planderová, 1991).

Sediments of the Svinná Formation are formed predominantly by grey claystones. They have splintery or shaly jointing and contain carbonized remnants of plants. Within claystones, rare layers of fine grained sandstones with silt and tuffit admixtures and coal layers occur. In the basal part of the formation marly limestones have been found.

On the basis of a distinct geomagnetic anomaly, we assume an occurrence of volcanic bodies in the basal part of the Svinná Formation. Following a volcanological analogy, the mentioned complex represents extrusive dome-shaped andesite bodies.

This formation is widespread in the Bánovská kotlina Depression, south of the Jastrabie fault. The Svinná Formation crops out near Dežerice, Vlčkov, Horňany, Svinná, Veľká Hradná and in the neighbourhood of Trenčiasnske Jastrabie and Dubodiel (Fig. 2), (Brestenská et al., 1980). It was encountered in the boreholes DB-1 Svinná (10-59 m) and DB-2 Dubodiel (6-100 m).

Fossil remnants found in the Svinna Formation may be divided into two groups (Brestenská, 1977):

1. autochthonous, with ostracodes (*Candona, Darwinula, Iliocypris, Mediocypris, Amnicythere*), foraminifers (*Ammonia* ex. gr. *beccarii* (L.)), fragments of molluscs, remnants of fish (teeth, bones, otoliths), oogoniums of characeans, carbonized and pyritized plants remains (*Glyptostrobus europeus* (BRNGT) HEER).

2. allochthonous, including redeposited remnants of marine microfauna (skeletal fragments of siliceous sponges, radiolarians, foraminifers; Cretaceous to Lower Miocene).

Redeposited paleothanatocenoses of foraminifers are represented by forms of Cretaceous age (globotruncanas), which are found very rarely, further by foraminifers of Paleogene and Lower Miocene age. These paleothanatocoenoses are sorted by size (Brestenská l.c.).

On the basis of amount of individual autochthonous and allochthonous elements, the Svinná Formation was divided into three parts (Brestenská l.c.).

The lower part of the mentioned formation was encountered by the borehole DB-12 (1025-1199 m) only. Occurrence of redeposited planktonic foraminifers of the Early Miocene age is characteristic of this section. From autochthonous elements, the fragments of mollusc shells, remnants of fish and very rare ostracods have been represented.

The middle part of the Svinná Formation has been characterized by prevalence of autochthonous elements, thin-walled ostracods and oogoniums of characea. From ostracods, the genus *Amnicythere* has been found in the higher section of the middle part and in its lower part tests of the genus *Mediocypris* occur.

Slovak Geol. Mag., 7, 3 (2001), 289 – 301

The upper part has been characterized by the occurrence of mollusc fragments and concretions. Ostracodes, fish remnants as well as redeposited elements are represented rarely.

The Kamenec Formation was not known in the Bánovská kotlina Depression up to now. It has been defined in the Hornonitrianska kotlina Depression as a formation of epiclastic volcanic conglomerates and sandstones with non-volcanic material (Konečný et al., 1983) representing a succession of volcano-clastic, volcano-sedimentary and sedimentary rocks with autochthonous pyroclastics, which deposited from the Early to Middle Badenian in a fluvial, lacustrine and terrestrial environment. Its material originated from the Badenian volcanics of the Vtáčnik Mts., Kremnické vrchy Mts. and Štiavnické pohorie Mts. In the Hornonitrianska kotlina Depression, the Kamenec Formation is overlying marine sediments of the Early Badenian age (Šimon et al., 1997).

In the the Bánovská kotlina Depresion in the boreholes DB-3 (125.0-307.7 m) and DB-6 (117.6-450.0 m), the lower part of the so-called Tuffite-Detrital Formation (Brestenská et al., 1980), later the Ruskovce Formation (Kováč et. al., 1993b; Vass in Keith et al., 1994) was corelated to the Kamenec Formation (Šimon in Pristaš et al., 2000a) on the basis of the rock lithology and petrography of the pebbles. Planderová (1991) correlated a microfloral assemblage distinguished in the mentioned sediments in the borehole DB-6 (240 m) to the assemblage found out in sediments with coal of the Kamenec Formation (so-called Nováky layer) in the Hornonitrianska kotlina Depression [VTH-2 (21.0-78.5 m); VTH-3 (74.0-78.0)].

Based on the mentioned data we removed this lower part from the Ruskovce Formation s.l. assigning it to the Kamenec Formation.

The formation has high lateral variability in its lithological composition. The rocks consist predominantly of suboval and perfectly oval fragments of andesites and fragments of non-volcanic material. Matrix is sandy, tuffaceous-sandy or sandy-clayey.

Rock fragments are formed by hypersthene-amphibolic andesite, amphibole-pyroxenic andesite, hypersthene-amphibolic andesite with garnet, pyroxenic andesite, quartzite, quartz, granite gneiss and limestone. The size of fragments is from 0.5 to 5 cm and they are represented in the amount from 0 to 50 %. The colour of andesites is light-grey, dark-grey, brown or black. In fine beds of claystones and siltstones, there is a coal substance (i.e. recarbonized small woods, for instance in the borehole DB-6 at depth of 135-152 m or 287-296 m). Described part of the Formation represents a relic of the distal zone of the Štiavnica stratovolcano, which developed here also to the north-western part of the stratovolcano and this area has preserved owing to the sunken tectonic block in the Bánovská kotlina depression only.

The Handlová Formation was not known in the Bánovská kotlina Depression up to now. It was described in the Hornonitrianska kotlina Depression only (Čechovič, 1959, Konečný et al., 1983, Vass, 2001), where it is formed by clayey-sandy and tuffite sediments, which gradually transfer into dark to black claystones with coal seams. Thickness of the Formation is 50 m. It is overlying the Kamenec Formation.

Similar situation has been found out also in the Bánovská kotlina Depression, where gray epiclastic volcanic sandstones with interlayers of dark carbonized claystones and coaly clays (former a part of the Ruskovce Formation s.l.), have been identified. The microflora with sporomorphs domination of the subspecies *Polypodiaceoisporites gracillimus semiverrucatus* W. KR. have been distinguished there. Sporomorphs of the genera *Quercus, Salix, Eleagnus* etc. (Planderová, 1991) have been present in lesser amount. Planderová (l.c.) correlated the above mentioned microflora to the coal seams microflora of the Handlová Formation in the Hornonitrianska kotlina Depression. In the Bánovská kotlina Depresion these sediments reach the thickness of just 10 m.

We assigned these sediments to the Handlová Formation on the basis of their lithology, superposition (overlying the Kamenec Formation), as well as after the occurrence of similar microfloral assemblage.

The Ruskovce Member of the Vtáčnik Formation, former the Tuffite-Detrital Formation (Brestenská in Brestenská et al., 1980) and the Ruskovce Formation (Kováč et. al., 1993b; Vass in Keith et al., 1994). Sediments of the Ruskovce Formation were assigned to the Sarmatian – ?Panonian (Brestenská et al., 1980, Kováč et al., 1993b, Vass in Keith et al., 1994) according to their analogy with sediments of the Hornonitrianska kotlina and Turčianska kotlina depressions.

After petrographical study there has been found out that volcanic rocks forming the upper part of the Ruskovce Formation s.l. (look at the Kamenec Formation) belong to the Vtáčnik Formation (Šimon in Pristaš et. al., 2000a) of the Middle Sarmatian age (Ďurkovičová in Šimon et al., 1994). As for their hierarchy, we have had to redefined them as a Member i.e. the Ruskovce Member having been assigned to the Middle Sarmatian.

It is formed by redeposited pyroclastics, epiclastic volcanic claystones, sandstones and conglomerates. The conglomerates are formed by andesites of subangular, suboval, oval or perfectly oval shape. The andesites are of porous, foamy as well as compact structure. The size of fragments is 1-20 cm (mostly 1-10 cm). Concerning their petrography, they consist generally of pyroxenic andesites, in less amount amphibole-pyroxenic andesites. Sporadically also other petrographic types of andesites, typical of Central Slovakian neovolcanics, are present. The matrix is predominantly sandy-tufaceous. In the case of redeposited pyroclastics the matrix contains small shreds and fragments of yellow or light-white pumice. In sediments of the Ruskovce Member, non-volcanic material is sporadically also present.

Individual layers are formed by laterally shaped beds. Sometimes lenticular layers occur. The beds have mostly chaotic arrangement of fragments. They have either a supporting structure of fragments or a supporting structure of matrix. In the case of fine layers, the beds are massive, rarely laminated. In some beds, diagonal and cross bedding is present. Occurrence of the Ruskovce Member

was established in the boreholes DB-3 (2.0-114.8 m) and DB-6 (45-111 m).

The Ruskovce Member is a succession of volcanoclastic rocks of volcanic-sedimentary origin, evolving during development of the Vtáčnik stratovulcano. Its sediments were formed by fluvial streams, rapid downwash, lahars and mud flows, rock debris flows and avalanches. The shallow sedimentary environment was systematically controlled by fault activity enabling the deposition of the Gilbert type „fan delta" (Kováč et al., 1993b). The Ruskovce Member of the Vtáčnik Formation represents the distal part of the Vtáčnik stratovolcano, which developed in the Middle Sarmatian.

The Beladice Formation of the Upper Pannonian to Pontian age (in the sense of Fordinál et al., 2001) overlies the sediments of Paleogene age (on the Závada-Bielica elevation) and underlies sediments of the Volkovce Formation (Dacian).

Sediments of the Beladice Formation are formed by blue-green, grey and dark-grey clays with interlayers of black coal clays or thin horizons of lignite. The sediments consists also of sands and clayey gravels. The gravel is polymict and fine grained. Towards the basin's margin, number of gravel beds as well as their thickness increase. In sediments of the Beladice Formation, there have been found Ostracodes *Candona (Candona)* sp., *Candona (Fabaeformiccandona)* sp., *Ilycypris* ex gr. *gibba* (RAMDOHR), *Amnicythere* sp. and *Pseudocandona marchica* (HARTWIG). Additionally, redeposited foraminifers and radiolarians have been established (Brestenská et al., 1980).

The marginal member of the Beladice Formation is the Hlavina Member of the Late Pannonian age. It consists of freshwater limestone, which crops out in a quarry in the village Malé Kršteňany. The limestone contains gastropod fauna with the species: *Aegopinella orbicularis* (KLEIN), *Leucochroopsis kleini* (KLEIN), *Tropidomphalus* (*Mesodontopsis*) cf. *doderleini* (BRUSINA), *Aplexa* cf. *subhypnorum* GOTTSCH *Viviparus* sp. (TÖRÖKOVÁ & FORDINÁL, 1999).

The Volkovce Formation of the Pliocene age has the largest areal extension on the territory of the Bánovská kotlina Depression. Sediments of the Volkovce Formation are overlying Lower (Čausa Fm., Lakšáry Fm.), Middle (Svinná Fm., Ruskovce Fm.) and Upper Miocene (Beladice Fm.) sediments.

Occurrence of gravels and sands is characteristic of the Volkovce Formation. The gravel is mostly poorly sorted and interlayers of clayey sands or sandy clays are also present. The pebles are of various size and roundness degree. At the basin's margin even larger boulders are not rare. The pebles consist mainly of vein quartz and quartzites. Further on, granites, schists, Mesozoic limestones, dolomites, Paleogene sandstones, conglomerates and limestones with nummulites occur. According to their character and superposition, we consider the sediments for fluvial to fluviolacustrine.

Sediments of the Volkovce Formation were found in the boreholes DB-5 (1.4-3.0 m) and DB-9 (2-41 m) (Seneš & Brestenská, 1963).

Geological development

In the Early Miocene the territory of the Bánovská kotlina Depression was a part of the system of depressions, which were extending as wrench furrows at the margin of the Klippen Belt. These depression of E-W to ENE-WSW directions were extending from the northern margin of the Vienna Basin through the middle Váh valley to the Bánovská kotlina, Hornonitrianska kotlina and Turčianska kotlina depressions (Kováč et al., 1989). They originated due to the Savic orogenic movements. The depressions were parts of a dissected archipelago with clastic sedimentation (Kováč et al., 1993a).

At the beginning of the Lower Miocene, the territory of the Bánovská kotlina Depression was encroached by the Eggenburgian sea. On pre-Teriary rocks and/or Paleogene sediments revealed by erosion, coarse clastic sediments (the Kľačno Conglomerates) and later during sea deepening, also sandy and pelitic sediments (schliers) of the Čausa Formation deposited. The tuffitic horizons within these sediments indicate the coeval distant centres of acid volcanism. To the end of the Eggenburgian a shallowing of sedimentary environment and salinity decrease took place.

In the Ottnangian, communication with open sea was restricted as shown by the mollusc fauna (*Mytilus* sp. indet., *Congeria* sp. indet, *Gyraulus trochiformis dealbatus* (BRAUN), *Ancylus moravicus* RZEHAK) indicating a reduction of environment's salinity.

During the Karpatian, normal marine sedimentation was gradually renewed. In the lower part of the Karpatian, conditions of isolation still persisted (sea with reduced salinity) as indicated by the poor fauna. In the upper part, sedimentation environment deepened and the presence of rich microfaunal associations points to a connection with open sea. Also in sediments of the Karpatian age, layers of tuffites indicating coeval acid volcanism are found.

An independent development continued also in the Middle and partly in the Upper Miocene. At that time, the Závada-Bielice elevation played a significant role, separating the Danube Basin's area of the Rišňovce depression from geological development of the present-day Bánovská kotlina Depression area.

After orogenic processes in the Early Badenian, an emergence and denudation of the Lower Miocene sediments took place. This is testified by lack of the Upper Karpatian sediments (Globigerinoides sicanus Zone) (Lehotayová, 1976; 1977; Kováč et al., 1999) as well as by a large amount of the redeposited Lower Miocene foraminifers in the Lower Badenian Svinná Formation.

During the Middle Miocene, the synsedimentary Jastrabie fault predisposed an area south of the fault to sedimentation.

The Svinná Formation of the Lower Badenian age, formed by claystones and sandstones with layers of lignites, originated under limnic freshwater conditions with irregular sea ingressions from an area of the Hornonitrianska kotlina Depression and from territory of the present-day Central Slovakian neovolcanics. This environment can be most likely characterized as a semi-closed

depression with insufficient circulation of water masses and reduction conditions at the floor as indicated by the rich occurrence of organic substance, clay ironstones, pyrites as well as rarely occuring phosphates. This depression became occasionally a shallow marginal part of the sea, due to temporary marine ingressions. Marine ingressions resulted in transitory brackish conditions as shown by the occurrence of foraminifers and ostracodes. Presence of acid and intermediate elements as well as tuffite layers in the upper part of the Svinná formation point to a contemporary volcanism. This formation attains greatest thickness in the Bánovská kotlina Depression.

During subsequent parts of the Badenian, sediments of the Kamenec Formation (the Lower - Middle Badenian) were gradually evolving under freshwater conditions from the underlying formation. They are formed by epiclastic volcanic claystones, breccias, and conglomerates with non-volcanic material. In the Upper Badenian, in a swampy environment, preconditions for development of sediments containing carbonized plant remnants, an equivalent to the Handlová Formation, were created. Predisposition to coal sedimentation was presumably not so distinct as in the Hornonitrianska kotlina Depression (essentially reduced thickness, absence of coal seams). After a short period of erosion in the Middle Sarmatian, the conditions for formation of prograding alluvial fans, associating with the gravitational flows of „grain flow and debris flow" type were created. They were transported from the area of the present-day Vtáčnik Mts. into a swampy-lacustrine environment at the territory of the present-day Bánovská kotlina Depression (Ruskovce Member, Vtáčnik Formation) (Kováč et al., 1993b). The andesite material in gravitational flows testifies the products of several volcanic phases.

In the Middle Miocene, connection between sedimentation areas of the Bánovská kotlina and Hornonitrinska kotlina depressions was most likely throughout the area of the southern part of the „Chalmová Island" and through an area around the town Partizánske.

In the Upper Miocene the Závada-Bielice elevation lost its barrier function and the Bánovská kotlina Depression became a part of the Danube Basin's bay. Sediments of the Upper Miocene (upper part of the Pannonian and Pontian - the Beladice Formation) and the Pliocene (Dacian - the Volkovce Formation) are present. They originated under fluvio-limnic conditions of sedimentation (gravels, sands and variegated clays). At the Depression's margins, the layers of sandstones, fine grained conglomerates and/or breccias occur.

References

Baráth, I. & Kováč, M., 1989: Podmienky sedimentácie a zdrojové oblasti egenburských klastík v západnej časti Západných Karpát. Miscellanea micropaleontologica IV, Knihovnička Zemního plynu a nafty, sv. 9, Hodonín, 55-86 (In Slovak, English summary).

Blaško, D., Juriš, F., Tupý, P., Lafférs, F., Hruškovičová, M., Malý, S. & Klubert, J., 1989: Handlová - východ, VP - uhlie. Záverečná správa a výpočet zásob. Manuskript - Geofond Bratislava (In Slovak).

Brestenská, E., 1965: Mikropaleontologické spracovanie vrtu DB-10, 11 z Bánovskej kotliny. Manuskript - archív Štátneho geol. úst. D. Štúra Bratislava (In Slovak).

Brestenská, E., 1969: Záverečná správa o mikropaleontologickom spracovaní sedimentov vrtu DB-12 v Bánovskej kotline. Manuskript - archív Štátneho geol. úst. D. Štúra (In Slovak).

Brestenská, E., 1975a: Záverečná správa o vrte DB - 15 Horňany v Bánovskej kotline. Manuscript - archív Štátneho geol. úst. D. Štúra (In Slovak).

Brestenská, E., 1975b: Správa o mikrobiostratigrafickom hodnotení sedimentov vrtu DB-15 Horňany v Bánovskej kotline. Manuscript - archív Štátneho geol. úst. D. Štúra (In Slovak).

Brestenská, E., 1977: Mikrobiostratigrafia miocénu Bánovskej kotliny. Manuskript - archív Štátneho geol. úst. D. Štúra (In Slovak).

Brestenská, E., 1983: Litostratigraphy of the Lower Miocene of Bánovská kotlina (depression). In: Samuel, O. & Gašpariková, V. (edit.): 18th European coloquy on micropaleontology. Excursion-guide. Geol. Úst. D. Štúra, Bratislava, 101-105.

Brestenská, E., Havrila, M., Kullmanová, A., Lehotský, I., Remšík, A., Vaškovský, I., Gross, P. & Maheľ, M., 1980: Geologická mapa a vysvetlivky k regiónu Bánovskej kotliny (1 : 50 000). Manuskript - archív Štátneho geol. úst. D. Štúra (In Slovak).

Brestenská, E. & Lehotayová, R., 1983: Loc. 14 - Krásna Ves. 18th European colloquy on micropaleontology. Excursion-guide. Geol. Úst. D. Štúra, 106-108.

Brestenská, E., Lehotayová, R. & Planderová, E., 1983: Loc. 15 - Dežerice. 18th European colloquy on micropaleontoly. Excursion-guide. Geol. Úst. D. Štúra, 108-111.

Brestenská, E., Remšík, A. & Lehotayová, R., 1976: Vysvetlivky neogénu geologickej mapy 1 : 25 000 list Svinná. Manuskript - archív Štátneho geol. úst. D. Štúra (In Slovak).

Cicha, I., Rögl, F., Rupp, Ch. & Čtyroká, J., 1998: Oligocene-Miocene foraminifera of the Central Paratethys. Abh. senckenberg. naturforsch. Ges., 549, 1-325.

Čechovič, V., 1959: Geológia treťohorných vrstiev severného okraja handlovskej uhoľnej panvy. Geol. prace, Zošit 53, Bratislava, 5-58.

Fordinál, K., Nagy, A. & Vass, D., 2001: Problémy stratigrafie a litostratigrafie vrchného miocénu dunajskej panvy. Mineralia Slovaca 33, 1, 7-14. (In Slovak, English summary).

Fornaciari, E. & Rio, D., 1996: Latest Oligocene to early middle Miocene quantitative calcareous nannofossil biostratigraphy in the Mediterranean region. Micropaleontology, 42 (1), 1-36.

Gašparik, J., 1969: Paleogeografia a rozšírenie neogénu Hornonitrianskej kotliny. Zborník geologických vied, Západné Karpaty, zv. 11, Bratislava, 172-182 (In Slovak, Deutsch resume).

Halásová, E., Hudáčková, N., Holcová, K., Vass, D., Elečko, M. & Pereszlenyi, M., 1996: Sea ways connecting the Fiľakovo/Petervasara Basin with the Eggenburgian/Burdigalian open sea. Slovak Geol. Mag., 1(2), 125-136.

Haq, B.U., Hardenbol, J. & Vail, P. P., 1988: Mesozoic and Cenozoic chronostratigraphy and cycles of sea-level change. In: Wilgus, C. K. (ed.): Sea-level changes - an integral approach. SEPM Spec. publ., 42, 71-108.

Holcová, K., 1996: Monspeliensina and Spiroloxostoma, paleogeographically significant foraminiferal genera from the "Rzehakia (Oncophora) Beds" (Upper Ottnangian, Miocene) in the South Slovak Basin (Central Paratethys). Acta Mus. Nat. Pragae, Ser. B, Hist. Nat., 50 (1-4), 101-110.

Hók, J., Kováč, M., Rakús, M., Kováč, P., Nagy, A., Kováčová-Slamková, M., Sitár, V. & Šujan, M., 1998: Geologic and tectonic evolution of the Turiec depression in the Neogene. Slovak Geol. Mag. 4, 3, 165-176.

Keith, J. F., Vass, D. & Kováč, M., 1994: The Danube Lowland basin. ESRI Publication, new series, No 11A Slovakian Geology, Memorial to T. Koráb, 63-86.

Kollárik, E., 1962: Hydrogeologický posudok na vrt. studňu pre 9-14 tr. školu v Motešiciach. Manuskript - archív Štátneho geol. úst. D. Štúra (in Slovak).

Konečný, V., Lexa, J. & Planderová, E., 1983: Stratigrafické členenie neovulkanitov stredného Slovenska. Západné Karpaty, sér. geol. 9, Bratislava, 203 s. (In Slovak, English Summary).

Kováč, M., 2000: Geodynamický, paleogeografický a štruktúrny vývoj karpatsko-panónskeho regiónu v miocéne. Nový pohľad na neogénne panvy Slovenska. Veda, Bratislava, 176 s. (In Slovak).

Kováč, M. & Baráth, I., 1996: Tektonicko-sedimentárny vývoj alpsko-karpatsko-panónskej styčnej zóny počas miocénu Mineralia Slovaca., 28,1, 1-11 (In Slovak, English summary).

Kováč, M., Baráth, I., Holický, I., Marko, F. & Túnyi, I., 1989: Basin opening in the Lower Miocene strike-slip zone in the SW part of the Western Carpathians. Geol. Zbor. Geologica Carpathica, 40, 1 Bratislava, 37-62.

Kováč, M., Holcová, K. & Nagymarosy, A., 1999: Paleogeography, paleobatymetry and relative sea-level changes in the Danube Basin and adjacent areas. Geologica Carpathica (Bratislava), 50, 4, 325-338.

Kováč, M., Marko, F. & Baráth, I., 1993a: Štruktúrny a paleogeografický vývoj západného okraja centrálnych Západnych Karpát v neogéne. In: Rakús, M., Vozár, J. edit.: Geodynamický model a hlbinná stavba Západnych Karpát. Konf., Symp., Semináre, Geol. Úst. D. Štúra, Bratislava, 45-56. (In Slovak).

Kovác, M., Nagymarosy, A., Holcová, K., Hudacková, N. & Zlinská, A., 2001: Paleogeography, paleoecology and eustacy: Miocene 3 rd order cycles of relative sea-level changes in the Western carpathian - North pannonian basins. Acta Geologica Hungarica 44/1, 1-45.

Kováč, M., Nagy, A. & Baráth, I., 1993b: Ruskovské súvrstvie - sedimenty gravitačných tokov (sz. časť Bánovskej kotliny). Mineralia Slovaca, 25, 2, 117-124 (In Slovak, English summary).

Lehotayová, R., 1976: Vápnitá nanoflóra spodného miocénu niektorých lokalít z listu Svinná. In: Brestenská, E., Remšík, A. a Lehotayová, R., 1976: Vysvetlivky neogénu geologickej mapy 1 : 25 000 list Svinná. Manuskript - archív Štátneho geol. úst. D. Štúra (In Slovak).

Lehotayová, R., 1977: Vápnitá nanoflóra miocénu Bánovskej kotliny. Manuskript - archív Štátneho geol. úst. D. Štúra (In Slovak).

Lehotayová, R., 1982: Miocene nannoplankton zones in West Carpathians. Záp. Karpaty, sér. Paleont. 8, 91-110.

Marková, M., 1975: Mineralogicko-petrografické vyhodnotenie miocénneho súvrstvia vrtu DB-15 z Bánovskej kotliny. Manuskript - archív Štátneho geol. úst. D. Štúra (In Slovak).

Marková, M., 1977: Mineralogicko-petrografický výskum sedimentov vo vrte DB-17 a ich korelácia s vrtom DB-15 v Bánovskej kotline. Manuskript - archív Štátneho geol. úst. D. Štúra (In Slovak).

Mikuláš, E., 1968: Vyhodnotenie hydrogeologických prieskumných vrtov HM-1 a HM-2 na lokalite Motešice. Manuskript - archív Štátneho geol. úst. D. Štúra (In Slovak).

Ondrejičková, A., 1975: Mäkkýše z miocénnych sedimentov Bánovskej kotliny. Manuskript - archív Štátneho geol. úst. D. Štúra (In Slovak).

Ondrejičková, A., 1979: Eggenburgian Mollusc of Bánovská kotlina depression. Záp. Karpaty, sér. Paleont. 4, 81-104.

Papp, A., Rögl, F . & Seneš, J., 1973. Chronostratigraphie und Neostratotypen 3. Ottnangien. Vyd. Slov. Akad. Vied, Bratislava, 841 s.

Planderová, E., 1965: Palynologické vyhodnotenie vrtov DB-10 a DB-11. Manuskript - archív Štátneho geol. úst. D. Štúra (In Slovak).

Planderová, E., 1984: Sporomorphs and Plankton of the Karpatian from the lokality Dežerice. Záp. Karpaty, sér. Paleont. 9, 111-130.

Planderová, E., 1991: Ekostratigrafický výskum terciéru Kremnických vrchov a priľahlých oblastí. Manuskript - archív Štátneho geol. úst. D. Štúra (In Slovak).

Pristaš, J., Elečko, M., Maglay, J., Fordinál, K., Šimon, L., Gross, P., Polák, M., Havrila, M., Ivanička, J., Határ, J., Vozár, J., Tkáčová, H., Tkáč, J., Liščák, P., Jánová, V., Švasta, J., Remšík, A., Žáková, E., & Töröková, I., 2000a: Vysvetlivky ku geologickej mape Podunajskej nížiny - Nitrianskej pahorkatiny 1 : 50 000. Štátny geologický ústav Dionýza Štúra, Vyd. Dionýza Štúra, Bratislava, 250 s. (In Slovak, English summary).

Pristaš, J. (red.), Elečko, M., Maglay, J., Fordinál, K., Šimon, L., Gross, P., Polák, M., Havrila, M., Ivanička, J., Határ, J., Vozár, J., Mello, J. & Nagy, A., 2000b: Geological map of Danube lowland – Nitrianska pahorkatina upland. Štát. geol. ústav D. Štúra, Bratislava. (In Slovak, English summary).

Rögl, F., 1998: Paleogeographic considerations for Mediterranean and Paratehys seaways (Oligocene to Miocene). Ann. Naturhist. Mus. Wien, 99A, 279-310.

Seneš, J. & Brestenská, E., 1963: Základný geologický výskum Bánovskej kotliny so zvláštnym zreteľom na jej uhľonosnosť Manuskript - archív Štátneho geol. úst. D. Štúra (In Slovak).

Šimon, L:, Elečko, M., Gross, P., Kohút, M., Miko, O., Pristaš, J., Lexa, J., Mello, J., Hók, J., Macinská, M., Köhler, E., Jánová, V., Raková, J., Snopková, P:, Samuel, O., Stolár, M., Vozár, J., Kováč, P:, Vass, D., Marcin, D., Ďurkovičová, J., Sládková, M. & Wiegerová, V., 1994: Vysvetlivky ku geologickým mapám 36-133 (Handlová), 35-244 (Prievidza-4), 36-131 (Ráztočno-časť). Manuskript - archív Štát. Geol. ústavu D. Štúra, Bratislava (In Slovak)

Šimon, L., Elečko, M., Lexa, J., Kohút M., Halouzka, R., Gross, P., Pristaš, J., Konečný, V., Mello, J., Polák, M., Vozárová, A., Vozár, J., Havrila, M., Köhlerová, M., Stolár, M., Jánová, V., Marcin. D. & Szalaiová, V. 1997: Vysvetlivky ku geologickej mape Vtáčnika a Hornonitrianskej kotliny. GS SR, Bratislava, 281 s. (In Slovak, English summary).

Töröková, I. & Fordinál, K., 1999: Fresh-water limestones of the Hlavina Bed in the Rišňov furrow and Bánovce Depression. Slovak Geol. Mag., 5, 3, 213-226.

Váňová, M., 1955: Burdigalská fauna z okolia Dolných Motešíc (Gauss-Krügerov listoklad M-34-109-C-b). Manuskript - archív Štát. Geol. ústavu D. Štúra, Bratislava (In Slovak).

Vass, D., 2001: Lithostratigraphy of West Carpathian Neogene. Štát. Geol. ústavu D. Štúra, Bratislava (in press). (In Slovak, English summary).

Vass, D., Began, A., Gross, P., Kahan, Š., Krystek, I., Köhler, E., Lexa, J., Nemčok, J., Ružička, M. & Vaškovský, I., 1988: Vysvetlivky k mape Regionálne geologické členenie Západných Karpát a severných výbežkov panónskej panvy na území ČSSR 1: 500 000. Geol. ústav. D. Štúra, Bratislava, 65 p. (In Slovak, English summary).

Žecová, K., 1999: Vyhodnotenie vápnitého nanoplanktónu zo severnej časti regiónu Nitrianska pahorkatina (vrty DB-5, DB-19, lokalita Neporadza). Manuskript - archív Štát. Geol. ústavu D. Štúra, Bratislava (In Slovak).

Slovak Geol. Mag., 7, 3 (2001),303 – 308

IUGS UNESCO P 442

Plagioclase-clinopyroxene hornfels: raw material of 4 lengyel culture axes (Svodín, Slovakia)

DUŠAN HOVORKA[1], ĽUDMILA ILLÁŠOVÁ[2] and JÁN SPIŠIAK[3]

[1]Faculty of Natural Sciences, Comenius University, Mlynská dolina, 842 15 Bratislava, Slovak Republic
[2]Archaeological Institute of Slovak Academy of Sciences, Akademická 2, 949 21 Nitra, Slovak Republic
[3]Geological Institute of the Slovak Academy of Sciences, Severná 5, 974 01 Banská Bystrica, Slovakia

Abstract. Among numerous polished stone artefacts, which have been collected during systematic excavation of site Svodín in the past, we have studied 4 small non bored axes of very similar shape and identical raw material. It is represented by very fine-grained plagioclase-diopside hornfels of granoblastic fabric. We suppose central Slovakia Late Tertiary volcanic area to be provenience of raw material of the given type. Identity of raw material of all 4 axes allow us to consider their in situ production (from one block of the rock).

Key words: 4 axes, plagioclase-diopside hornfels, lengyel culture, Svodín, Slovakia

Introduction

Site Svodín (Fig. 1) systematicaly excavated in the past (1971-1983: Němejcová-Pavúková) belongs to the most extended polycultural sites of the lengyel culture in the whole central Europe. Unfortunatelly sudden death of formerly expert (Němcová-Pavúková) of this site unabled her to finish planed systematic studies of implements of the given site in the past. Mentioned author published (1995) problematic of roundels and determined four stratigraphic as well as cultural-typological horizons. In more than 150 skeletal graves rich inventory of polished implements have been gathered. Implements of chipped type have been studied and published by Kaczanowska and Kozlowski with contribution by Němejcová-Pavúková (1991). First results of laboratory studies of polished implements have been outlined by Pavúk et al. (2000). From the set of stone implements 4 small (4-6 x 3-4 x 0.8-1.3 cm) non bored flat axes constructed from hornfels have been documented (Fig. 2). One of them is insignificantly demaged on its sharp end, and the other one is represented by axe fragment. Studied axes are deposited under denomination: 1364, 1379, 1624 and 1876 in deposit of the Archaeological Institute of the Slovak Academy of Sciences in Vozokany. On one of them (1364) on surface rough brownish "skin" formed by products of weathering processes (mostly carbonates) is present (Fig. 3).

In the frame of systematical thin section studies we have identified 4 axes made of identical raw material. Consequently we have studied mentioned raw material in detail using electron microprobe for determination of composition of rock-forming minerals of the given rock. Obtained results allow authors to follow "geological history" of the given raw material type and consequently to consider provenience of its occurrences in nature.

Fig. l. Location of site Svodín

In the set of several hundreds thin section studied till now no contact thermic hornfelses have been described yet (for review see paper by Hovorka and Illášová 2000) in Slovakia.

Raw material of axes

Discussed raw material type is aphanitic, with very slightly developed flaky polished surfaces of artefacts. Flakes are represented by irregular portions of various (but generaly light) tints of ash-gray colour. Raw material on cutted surfaces bears no signs of weathered outer zones - tint of the raw material on polished surfaces and in cutted planes is identical.

Thin sections image of the rock under consideration is simple. Discussed rock is composed of two main mineral phases: plagioclases and clinopyroxenes. Both of them are very fine-grained (less than 0.1 mm). Their distribution in detail is uneven (Figs. 4, 5). In small areas of thin section one of them dominates. Limits of such irregular areas are non sharp. Fabric of the given rock is granoblastic, mostly massive, in places weakly

Slovak Geol. Mag., 7, 3 (2001), 303 – 308

Fig. 2. Morphology of implements made of plagioclase-clinopyroxene hornfels, Svodín

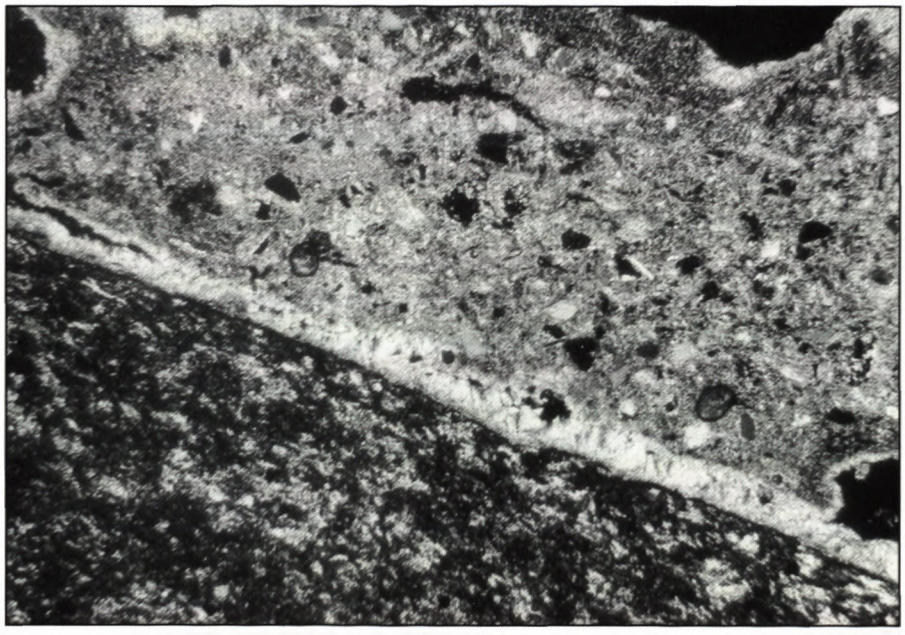

Fig. 3. Product of weathering processes (mostly carbonates: lighter portion of thin section) on axe surface (No 1346). Enlarg. 27x, // polars

expressed foliation is observable (Fig. 6). In artefact No. 1624 one vein-like (of 0.6 mm thickness: Fig. 7) arrangement of shortcolumnar clinopyroxenes is observable. Size (0.2-0.3 mm) of individual clinopyroxene crystals in this case is pronouncedly greater than matrix Cpx size. Clinopyroxene crystals within "vein" have locally radial orientation, and individual pyroxene crystals are of shortcolumnar habit. Submicroscopical isometric nonzonal and non twinned plagioclases represent disseminated crystals within clinopyroxene mass, or they are concentrated in "spots" of irregular shape and non sharp limits. Quantitative ratio of clinopyroxene vs. plagioclase in given rock is approx. 60 vs. 40 vol. per cents.

Clinopyroxenes of the rock are represented by uniform type and following IMA clinopyroxene classification (Morimoto et al. 1988) they are projected into field of diopside. In general clinopyroxene studied are of non- or very weakly zonal composition. Exception represents axe No. 1379, in which clinopyroxenes two zones are present. The lighter zone in comparison to the darker one is enriched in Fe - this is the case of shifting their projection point in direction to the hedenbergite field (Fig. 8). For all analysed clinopyroxene crystals very low or even non detected content of Ti and Na is characteristic (Tab. I).

Plagioclases have high An content and are represented by labradore to bytownite. The highest detected An content (An 85) has plagioclase from sample 1624, which has simultaneously the highest content of Mg in clinopyroxenes.

Plagioclases analysed are fresh and have homogeneous (nonzonal) composition (Tab. 2).

In the given rock type in accessory amount tiny crystals of **apatite, pyrite** and **titanite** were detected. In the case of last mentioned mineral it appears as submicro/

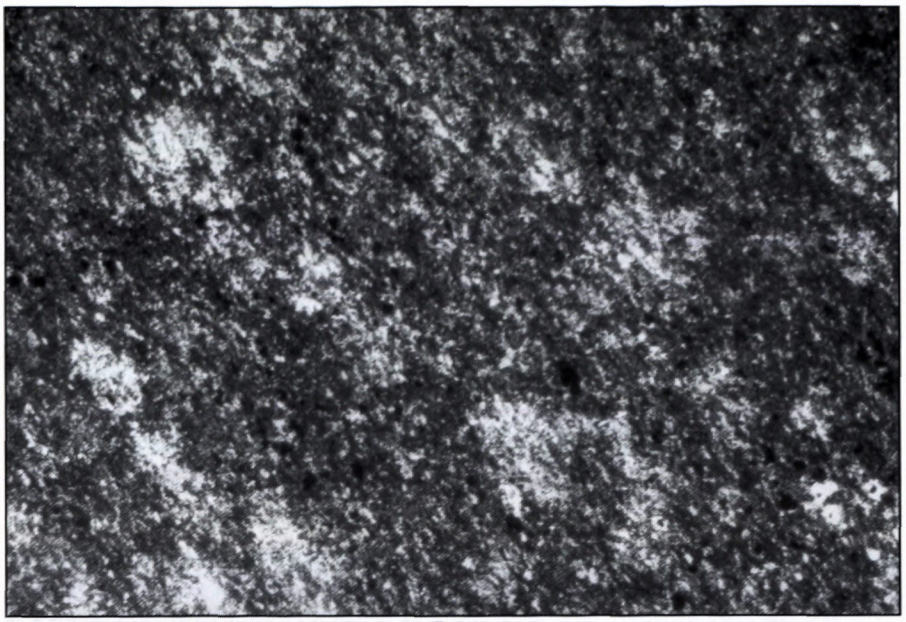

Fig. 4. Spotty pattern of the plagioclase-clinopyroxene hornfels

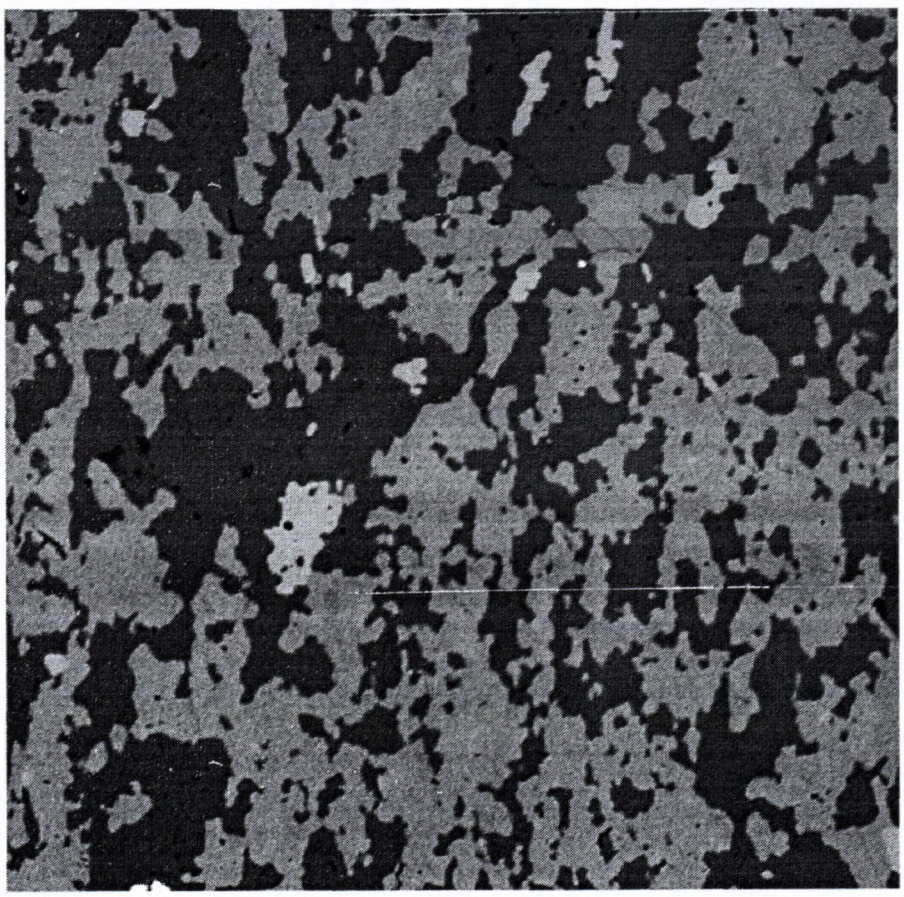

Fig. 5. Back scattered electron image of the studied rock. Axe No. 1364. Light portions = clinopyroxenes, dark portions = plagioclases.Enlarg.180 x.

scopical crystals allways in clinopyroxenes. Its origin in breakdown process of original clinopyroxene is probable.

Discusion and conclusion

Identical mineral composition of all 4 axes found within one archaeological site and one culture allows to suppose:

a) one rock block to be raw material source,

b) this rock block have been elaborated just on the axes finding site,

c) transport of mentioned block in "distance of one or several days walk" is the most probable,

d) non significant textural (pattern) differences should reflect spatial location of given partial piece in the frame of bigger block used for discrete implement construction.

Based on mineral composition of the given rock and namely on its texture (pattern) contact-thermic recrystal-

Tab. 1 Composition of clinopyroxene

Sample	1379	1379	1379	1634	1634	1634	1876	1876	1876	1364	1364	1364
N. anal.	3	4	6	8	10	11	15	16	17	21	22	23
SiO_2	51.28	50.44	52.07	51.34	51.84	52.45	52.07	52.26	52.23	51.93	51.89	51.71
TiO_2	0.00	0.00	0.00	0.25	0.00	0.00	0.00	0.00	0.00	0.00	0.00	0.00
Al_2O_3	0.84	0.42	0.48	1.71	0.32	0.67	0.46	0.49	0.51	0.49	0.71	1.25
FeO^+	14.03	17.44	13.16	12.67	11.27	12.61	12.80	11.90	12.04	13.51	14.71	13.90
MnO	0.44	0.35	0.00	0.00	0.00	0.28	0.36	0.33	0.26	0.00	0.41	0.32
MgO	9.14	7.21	9.68	9.83	11.62	10.47	9.94	11.06	10.50	9.73	8.87	9.32
CaO	24.22	23.55	24.74	24.09	24.01	24.40	24.07	24.40	24.22	24.07	24.08	24.14
Na_2O	0.00	0.00	0.00	0.12	0.00	0.10	0.00	0.00	0.00	0.00	0.00	0.00
K_2O	0.00	0.00	0.00	0.00	0.00	0.00	0.00	0.00	0.00	0.00	0.00	0.00
TOTAL	99.95	99.41	100.13	100.01	99.06	100.98	99.70	100.44	99.76	99.73	100.67	100.64
Formula based on 6 O												
Si^{IV}	1.98	1.98	1.99	1.96	1.98	1.98	2.00	1.98	1.99	1.99	1.99	1.97
Al^{IV}	0.02	0.02	0.01	0.04	0.01	0.02	0.00	0.02	0.01	0.01	0.01	0.03
Al^{VI}	0.02	0.00	0.01	0.04	0.00	0.01	0.02	0.00	0.01	0.01	0.02	0.03
Ti	0.00	0.00	0.00	0.01	0.00	0.00	0.00	0.00	0.00	0.00	0.00	0.00
Fe^{2+}	0.45	0.57	0.42	0.40	0.36	0.40	0.41	0.38	0.38	0.43	0.47	0.44
Mn	0.01	0.01	0.00	0.00	0.00	0.01	0.01	0.01	0.01	0.00	0.01	0.01
Mg	0.53	0.42	0.55	0.56	0.66	0.59	0.57	0.63	0.60	0.56	0.51	0.53
Ca	1.00	0.99	1.01	0.98	0.99	0.99	0.99	0.99	0.99	0.99	0.99	0.99
Na	0.00	0.00	0.00	0.01	0.00	0.01	0.00	0.00	0.00	0.00	0.00	0.00
K	0.00	0.00	0.00	0.00	0.00	0.00	0.00	0.00	0.00	0.00	0.00	0.00

FeO^+ = total Fe as FeO

Tab. 2 Composition of plagioclases

Sample	1379	1379	1624	1624	1876	1876	1876	1364	1364	1364
N. anal.	1	5	7	9	12	13	14	18	19	20
SiO_2	49.81	49.03	46.80	46.38	50.68	51.51	49.85	49.40	48.72	48.06
Al_2O_3	31.90	32.18	34.56	34.29	31.34	30.85	32.00	32.45	32.13	33.43
FeO	0.37	0.00	0.00	0.00	0.00	0.00	0.00	0.00	0.00	0.24
CaO	15.18	15.06	17.57	17.63	13.51	12.94	14.46	15.00	15.12	15.58
Na_2O	3.17	2.75	1.75	1.56	3.90	3.93	3.35	3.01	3.06	2.47
K_2O	0.11	0.00	0.08	0.10	0.00	0.00	0.12	0.13	0.08	0.00
TOTAL	100.54	99.02	100.76	99.96	99.43	99.23	99.78	99.99	99.11	99.78
Formula based on 8 O										
Si^{IV}	2.27	2.26	2.14	2.13	2.32	2.35	2.28	2.26	2.25	2.20
Al^{IV}	1.71	1.74	1.86	1.86	1.68	1.65	1.72	1.74	1.75	1.80
Al^{VI}	0.00	0.01	0.00	0.00	0.01	0.01	0.00	0.01	0.00	0.01
Fe^{2+}	0.01	0.00	0.00	0.00	0.00	0.00	0.00	0.00	0.00	0.01
Ca	0.74	0.74	0.86	0.87	0.66	0.63	0.71	0.73	0.75	0.77
Na	0.28	0.25	0.15	0.14	0.35	0.35	0.30	0.27	0.27	0.22
K	0.01	0.00	0.01	0.01	0.00	0.00	0.01	0.01	0.01	0.00
Or	0.60	0.00	0.50	0.60	0.00	0.00	0.70	0.80	0.50	0.00
Ab	27.30	24.80	15.20	13.70	34.30	35.50	29.30	26.50	26.70	22.30
An	72.10	75.20	84.30	85.70	65.70	64.50	70.00	72.80	72.90	77.70

FeO^+ = total Fe as FeO

lization of its protolith has been the leading process of the origin of this raw material type.

As the site Svodín is located on southwestern rim of the central Slovakia Late Tertiary volcanic province, thermic effect of volcanic/subvolcanic bodies on adjacent rock complexes is considered. In individual cases also blocks of surrounding rocks should have been incorporated into thermally not yet consolided lava flows or subvolcanic bodies and underwent thermic recrystallization under pyroxene hornfels facies pT conditions.

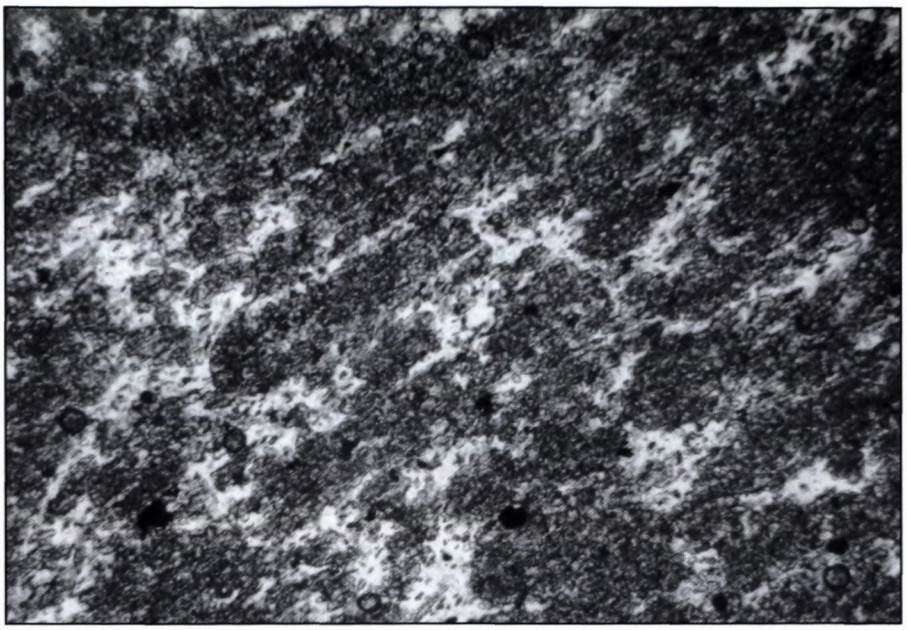

Fig. 6. Expresionless foliation of plagioclase-diopside hornfels. Enlarg. 90x, // polars

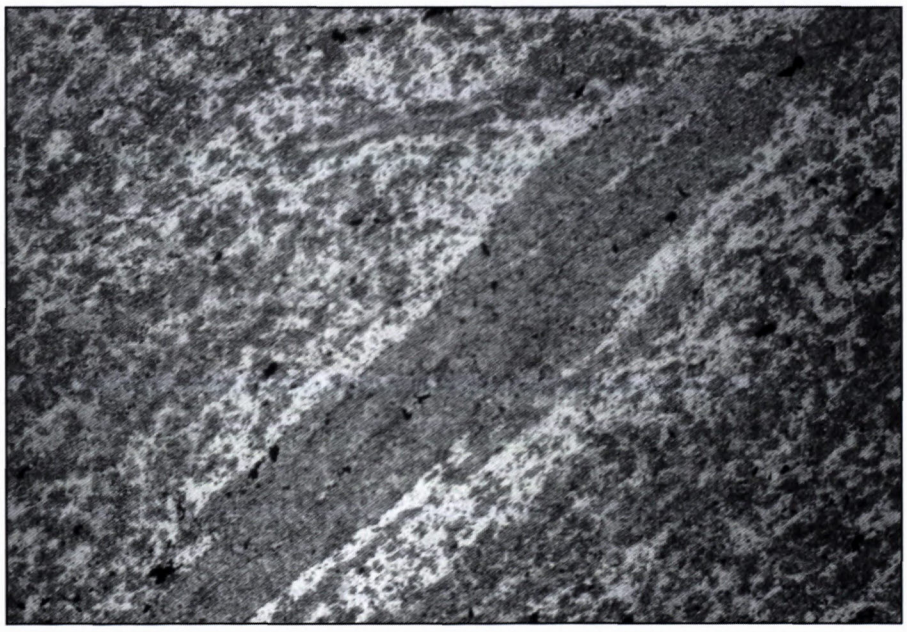

Fig. 7. Monomineralic clinopyroxene "vein" in hornfels (No. 1264) on the rim of which higher concentration of plagioclases is visible. Enlarg. 27x, // polars

Rapid diminishing of heat flow and the absence of water vapor in both media resulted in the absence of retrogressive stage mineral association in the given rock. More-or-less homogeneous grain size and homogeneous distribution of mineral phases in the rock allows to suppose fine grained premetamorphic protolith of the discussed hornfels. Based on the determined content of main oxids, namely those of SiO_2, Al_2O_3, CaO and FeO, in leading mineral phases (clinopyroxenes and plagioclases), fine grained volcaniclastics of andesito-basaltic composition should be considered as original premetamorphic rock. Due to the fact that mineral composition of the axes under study is simple (basically, only two mineral phases are represented) and they are rather evenly grained to tried to calculate their chemical composition. We did this on the basis of modal composition detected with electron microrpobe (Fig. 5) and from analyzed mineral composition. Density values for individual minerals were taken from Deeer et al. (1983) and we considered the minerals closest in composition to our minerals being compared. The most suitable samples for calculation were Nos. 1364 and 1876. The initial value and the resulting chemical composition are given in the Table 3 the supplementary information on the original rocks which the axes were made from. The calculated data result in the following conclusions:

i) the contents of all main oxids except for CaO point to the basic character of the original rocks

i) compared to common basalt types the axes under study show increased CaO contents.

The increased CaO content and consequently modal composition as well may be a reflection of two possible primary sources:

1. the original (premetamorphic) rocks of axes were basic volcaniclastic rocks with an admixture of carbonate material (increased CaO content)

Table 3. Composition of main phases of hornfels being basis for rock chemistry calculations

Minerals	Cpx	Plg	Cpx	Plg
Sample	1876	1876	1364	1364
N. anal.	17	12	10	19
SiO_2	52,23	50,68	51,84	48,72
TiO_2	0,00		0,00	
Al_2O_3	0,51	31,34	0,32	32,13
FeO^+	12,04	0,00	11,27	0,00
MnO	0,26		0,00	
MgO	10,50		11,62	
CaO	24,22	13,51	24,01	15,12
Na_2O	0,00	3,90	0,00	3,06
K_2O	0,00	0,00	0,00	0,08
TOTAL	99,76	99,43	99,06	99,11
Density	3,43	2,71	3,43	2,71
Vol.%	49,80	48,90	47,00	50,00
Weight part	170,81	132,32	161,21	135,70
Weight %	56,35	43,65	54,30	45,70

Table 4. Calculated composition of rocks

Sample	1364	1876
	Weight %	Weight %
SiO_2	50,88	51,75
TiO_2	0,00	0,00
Al_2O_3	15,00	14,02
FeO^+	6,18	6,81
MnO	0,00	0,15
MgO	6,37	5,94
CaO	20,13	19,62
Na_2O	1,41	1,71
K_2O	0,04	0,00
TOTAL	100,01	100,00

2. The original rocks of axes were basic rocks with high clinopyroxenes and basic plagioclases contents originated by fractionation and/or differentiation.

Taking into account all available information we prefer possibillty presented ad 1).

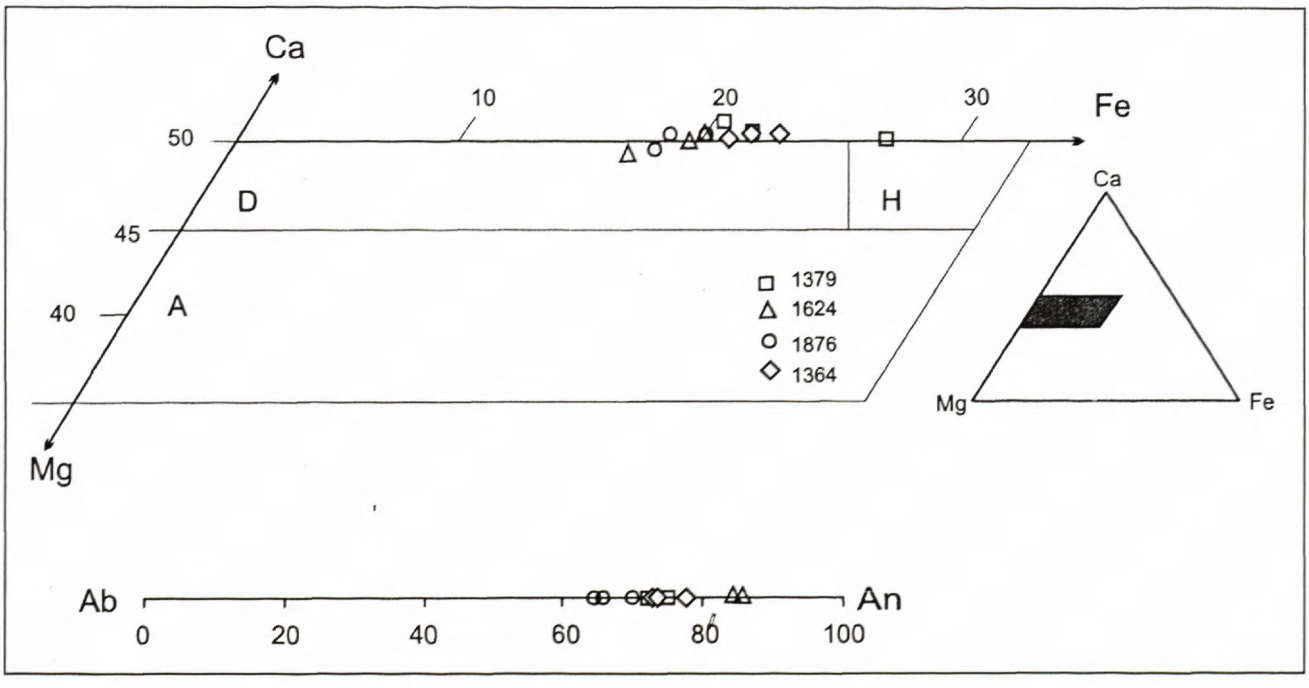

Fig. 8. Plot of analysed clinopyroxenes and plagioclases in diagram

References

Hovorka, D. and Illášová, Ľ. 2000: What do we know about abiotic raw materials used by the Neolithic/Aeneolithic populations on the territory of nowadays Slovakia? Krystalinikum, 26, 83-110, Brno.

Kaczanowska, M. und Kozlowski, J. K. 1991: Spaltindustrie der Lengyel-Kultur aus Svodin, Slowakei. Uniw. Jagielonski - Panstw. wydaw. Naukowe, 116 S., Warszawa - Kraków.

Morimoto, N., Fabries, J., Ferguson, A. K., Ginzburg, I. V., Ross, M., Seifert, F. A., Zussman, J., Aoki, K. and Gottardi, G. 1988: Nomenclature of pyroxenes. Amer. Mineralogist, 73, 1123-1133.

Němejcová-Pavúková, V. 1995: Svodín. Zwei Krerisigrabenanlagen der Lengyel-Kultur. Studia archaeologica Mediaevalia, Tomus II, 1-249, Bratislava.

Pavúk, J., Hovorka, D. and Illášová, Ľ. 2000: Svodín - raw material used by population of type locality of the lengyel culture (Aeneolithic): western Slovakia. 3rd workshop of the IGCP/UNESCO Project No. 442, 19-20, Eggenburg, Austria

Slovak Geol. Mag., 7, 3 (2001), 309 – 312

The Documentation of Geological and Archaeological Features using the Lacquer-Film Method.

IVAN DOLEŽAL

DOLMAT, Sámova 945/22, Prague 10, Czech Republic,
e-mail:dolezal@dolmat.com, http://www.dolmat.com

1. Introduction

This article brings to the general public a description of the production and presentation of lacquer-films.

1.1 A History of the Origins of Lacquer-Films

The documentation of the archaeological and geological sciences today includes not only curated or collected old sherds, bones, fossils, minerals and rocks or related photographs and drawings, but also actual archaeological sondages or geological profiles, usually open only for a short period. These, with all their textural and structural markers, are unique features, which would be better reserved for later (more detailed) study in the laboratory. For this reason, Hamburg professor of Geology and Palaeontology Prof. Dr. Ehrhard Voigt developed in 1933 a method which was able to take from the least hard minerals a section transferable from nature to the indoors. In the land of its origin, this original preparation became known as „Der Lackfilm„ (in English-language literature „the lacquer-film„). From the terminological point of view, it is unfortunate that the term does not correspond to the reality of geological (petrological, sedimentological, pedological, archaeological) features, a problem particularly acute in the Czech language where it comes partly from the translation of the German specifications.

1.2 The Presentation of Lacquer-Films

Lacquer-films were first exhibited in the former Czechoslovakia from the 1st to 30th June, 1988. The Geological-Palaeontological Institute, the Hamburg University Museum and the Department of Petrology of the Faculty of Natural Sciences of Charles University together exhibited 37 of the best films owned by Hamburg University in the Cross Hall of the Karolinum in Prague. The films put in place sunken microdepressions and micro-debris, ice wedges, texture slippages, gravitational and cryoturbational deformations, secondary seepage of inorganic soil colours, chaotic peat sediment layers and the like. The exhibition was called "Geology in Pictures: Nature and Art", and was seen by around 2000 visitors. As a result of the great interest in the lacquer-film method generated by the exhibition, from June 27th-30th 1989 the Geological-Palaeontological Institute, the University of Hamburg and the Faculty of Natural Sciences of Charles University jointly ran the first field course in lifting lacquer-films in the former Czechoslovakia. The course was preceded by a petrological seminar entitled "A Discussion on the Texture and Structure of Sedimentary Rocks", and the specialist course then took the form of three working visits to selected locations. The course was attended by 25 professionals from institutes of higher education, geological and archaeological institutes and museums.

After these two major events, which did a great deal to broaden interest in this method of documentation, there came a five year pause in the presentation and manufacture of lacquer-films. The reasons for this are that the lifting and subsequent processing of lacquer-films (the latter in particular) are neither so easy nor so unproblematic as they appear at first sight. After problems with their technical character in particular, interest in lacquer-films declined.

Not until 1993 was the work of the late 1980's followed up by the local firm Dolmat, which provides geological and ecological consultancy, and consultancy in the extraction and regeneration of natural resources. It was in the framework of such work that the company first became interested in specialist documentary methods. The result of several years of research undertaken on sedimentary rocks and loose material, and experiments with dyes, adhesives and resins, was the successful production of the first sedimentological lacquer-film.

The company has expanded its methods to the documentation not only of geological and sedimentological features, but also to the direct study of palaeontology and especially archaeology. At the end of 1994, the company lifted films as part of the excavation of a mediaeval (14th Century) hearth in Pštrossova ul.; the result was a unique archaeological film of a mediaeval stratigraphic sequence measuring 1225 x 940mm. Later, the firm concentrated mainly on lifting films of moldavite-bearing sediments, most commonly with moldavites *in situ*. These can be seen today in, for example, the Týn nad Vltavou and České Budějovice Museums, and have been prepared for exhibition in the National Museum in

Fig. 1 Brown-coal bearing sediment lacquer-film from the Jan Šverma coal mines, Czech Republic. Actual size 640 x 370 mm. Photo by Petr Korbel. Dolmar depository.

Fig. 2 Moldavite-bearing sediment lacquer-film from Vrábče u Českých Budějovic. Actual size 1100 x 900 mm. Photo by Petr Korbel. Dolmat depositury.

Prague, the Kadaň Museum, the Moravian Provincial Museum, and others. The firm returned to archaeological sites in 1997 when staff took part in the rescue excavation (by the PÚPP - Prague Institute for Monument Care) of a mediaeval cemetery in Vladislavova ul., employing the method to lift a film of a mediaeval (12th Century) grave pit. The film lifted from mediaeval layers measured 1255 x 995 mm.

Dolmat's presentation activities with lacquer-films culminated in an exhibition entitled "Geology in Pictures - Lacquer-Films" at the National Museum in Prague from August 12th to September 8th 1997, published in *Archeologické rozhledy* ("Archaeological Perspectives") 4/97. This singular event, the first exhibition of its kind in the Czech Republic, displayed a total of 20 lacquer-films that were a cross-section of the company's documentary work to date. With the exception of some particularly interesting lacquer-films of moldavite-bearing sediments with moldavites *in situ*, these were all attractive sedimentological and **palaeolontological** lacquer-films from the Czech brown-coal basin and both the aforementioned archaeological lacquer-films from sites in Prague. The exhibition lasted almost a month, and was seen by 1500 domestic and foreign visitors.

Other exhibitions undertaken by the firm include an exposition of lacquer-films at the mineral and fossil exchange in the Prague Eden on November 14th and 15th 1997, and an exhibition of lacquer-films in Klašterec nad Ohří from April 1st to June 30th 1998. The company organised an independent exhibition at the Moravian Provincial Museum in the same year. In the years that followed the company participated in numerous other events and fairs including its lacquer-film exhibition in late 1999 in the historical spa town of Karlovy Vary. Dolmat took an active part in several international conferences in 2000 including 2000 PAGES International Conference on Past Global Changes and Praga 2000 Natura Megapolis. Dolmat lacquer-films have been a topic of national newspaper articles and several radio and TV programs in recent years.

Actual size 900 x 500 m.m

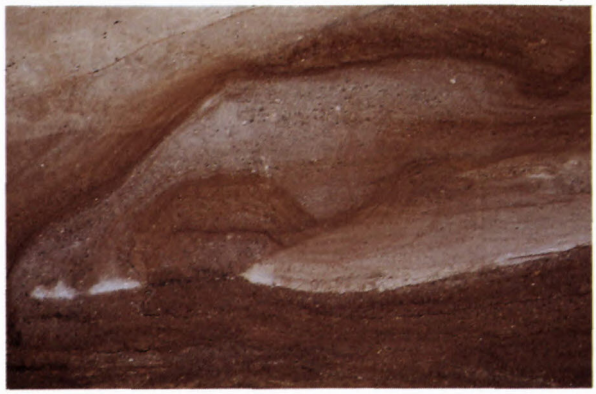

Actual size 850 x 500 mm.

Actual size 800 x 550 mm.

Actual size 800 x 550 mm.

Actual size 700 x 550 mm.

Actual size 700 x 550 mm.

Fig. 3 Laquer-films of Pliocene gravels belonging to the Vildštejn formation from the Dřenice gravel pit. Photo by Petr Korbel. Depository of Tekaz, s.r.o., Czech Republic.

2. Characteristics of pictured materials

The production method makes possible the acquisition of lacquer-films only from the least hard rocks and minerals. Therefore, the process can be elaborated not only for the homogenous sediment types of aleurites and pelites (dust, clay, loess, soil, peat) but also for heterogenous minerals such as psephites or psammites (various conglomerates, sands, gravels, or disintegrated matter). In the same way, evidence of human activity in artificial features (fills, hearths, graves, wastes, discarded materials, kilns etc.) can be lifted in cases where they are found in loose materials and/or are actual formations.

Slovak Geol. Mag., 7, 3 (2001), 309 – 312

The main requirement for the successful lifting of a lacquer-film is the low moisture content of the material, dependant on the content of clay particles and permeability (i.e. porosity). The temperature of the surrounding environment should not be less than 12 °C, and the relative humidity no more than c. 80 %. The ideal conditions for work are thus warm, dry weather; these short-term unfavourable impacts can however be eliminated by more rigorous working procedures.

3. The Methodology of Producing Lacquer-Films.

The methodology of documenting archaeological sections with the aid of lacquer-film makes possible the conservation of important profiles capturing the main stratigraphic relations of anthropogenic layers. The lacquer-film method preserves any and all natural materials exactly as they are observed in the field, i.e. saving all the main components and an admixtures of all of the material structures making up the layers and features. A section conserved with the aid of lacquer-film can be examined in a dry or in a wet state, so that even after several decades (with the help of advanced techniques) we can assess the stratigraphic relationships of individual elements. The methodology is particularly useful for archaeological rescue excavations, for the entirely unique way in which it supplements field drawn and photographed documentation, these remaining the only practicable means of documenting endangered sites.

3.1 Fieldwork

Fieldwork consists of smoothing chosen sections of bare earth with suitable tools (mattock, blade with small garden hoe, "scraper" etc.) to a plane close to the vertical (c. 80 °C). Afterwards, the profile is sprayed with a penetratitive lacquer, which impregnates and hardens without corrupting textural, mineral or colour characteristics of the profile. After the prepared area dries, the undiluted lacquer and thin fabric are stronger. If after repeated dryings the fabric is carefully removed, the lacquer retains a thin layer of the prepared situation, which holds the natural aspect of the sediments and all of their attributes. The outcome is thus a sort of "carpet" made up of one or two layers of fabric, to which are attached a strong sediment layer several millimetres to centimetres thick. The preparation thus obtained can be removed to the workshop for final processing.

3.2 Workshop Processing

The prepared sheet of several dm^2 to m^2 is removed to a workshop for its finishing touches and conservation. The lifted profile is fastened to a wooden board, dried, conditioned and impregnated. After the final steps of the conservation process and complete drying, the sheet is formed, edged and has a wooden frame fitted, with reinforced metal corner pieces and fitted picture hooks for hanging. The complete film is then ready for distribution.

4. The Distribution of Lacquer-Films

In order to meet storage and mobility needs, every picture is packed in a recyclable cardboard box, in which it can be safely transported. Every film is accompanied by handling elements (hooked nails, hooks), a professional specification and pertinent photodocumentation.

5. Conclusions

Thanks to our experience and a thorough elaboration of the method, it is possible to lift films of a wide range of sediments, even warm and dry weather not being an essential condition. It is, however, worth reflecting that when the sediment is damp, more compact, less porous and thus less permeable, the amount of work required in the field and in laboratory processing increases. The resulting lacquer-films have no exacting storage requirements, are relatively resistant to mechanical wear, are colour-fast and do not cause health problems. They can be vacuum cleaned, dusted or wiped over with a damp cloth.

In conclusion it can be said that every lacquer-film is an original, which can faithfully represent and at the same time preserve for a long period any natural situation, and along with its obvious professional qualities it is distinctly decorative.

Slovak Geol. Mag., 7, 3 (2001), 313

Palaeoglaciological investigations exploiting remote sensing, elevation models and GIS

CHRIS D. CLARK[1], ROBBIE MEEHAN[2], CLAS HATTESTRAND[3], PAUL CARLING[4], DAVE EVANS[5] and WISH MITCHELL[6]

[1]Department of Geography and Sheffield Centre for Earth Observation Science, University of Sheffeld, UK.
c.clark@sheffield.ac.uk
[2]Teagasc, Kinsealy Research Centre, Dublin, Ireland
[3]Department of Physical Geography, University of Stockholm, Sweden
[4]Department of Geography, University of Southampton, UK
[5]Department of Geography and Topographic Science, University of Glasgow, UK
[6]Department of Earth Sciences, University of Luton, UK.

Evidence-based reconstructions of the configuration and behaviour of the last great mid latitude ice sheets have been executed by either a bottom-up approach (i.e. 'cut and paste' of a multitude of field-scale observations) or top-down (ice sheet scale mapping of moraines and flow patterns, controlled by selected field observations). Wide differences in data quality and interpretation, and patchy coverage make reconstructions by the bottom-up approach difficult. For the Laurentide and Scandinavian ice sheets the top-down approach has been used to good effect yielding coherent reconstructions at the ice sheet scale. We argue that this is a good approach, and it operates at a scale appropriate for testing numerical ice sheet models and helps guide as to the most pertinent field sites for detailed investigation. However, although providing good building blocks for reconstruction it can be hard to link the landform patterns to the wealth of literature on field-scale observations including stratigraphy and dating control. Both approaches can be integrated using a GIS, and this work is now under way for the British Ice Sheet. Evidence pertaining to the Dimlington Stadial British Ice Sheet is being entered into a GIS for the purpose of making a full ice sheet reconstruction and producing a glacial map of Britain.

With regard to the mapping of large-scale glacial geomorphology, recent developments will be reviewed and illustrated via a series of case studies. The new higher resolution (15 m) afforded by Landsat-7 ETM + data will be discussed, as will the advantages of acquiring data with a low solar elevation and thin snowcover, and the use of digital elevation models. The case studies will draw on palaeoglaciological information derived by these methods for ice sheet behaviour of Ireland; Kola Peninsular, Arctic Russia; and Altai Mountains, Russia.

Instructions for authors

Slovak Geological Magazine – periodical of the Geological Survey of Slovak Republic is quarterly presenting the results of investigation and researches in wide range of topics: regional geology and geological maps, lithology and stratigraphy, petrology and mineralogy, paleontology, geochemistry and isotope geology, geophysics and deep structure, geology of deposits and metallogeny, tectonics and structural geology, hydrogeology and geothermal energy, environmental geochemistry, engineering geology and geotechnology, geological factors of the environment, petroarcheology.

The journal is focused on problems of the Alpine-Carpathian-Balkan region

General instructions

The Editorial Board of the Geological Survey of Slovak Republic – Dionýz Štúr Publishers accepts manuscripts in correct English. The papers that do not have sufficient accuracy in language level will be submitted back for language correction.

The manuscript should be addressed to the Chief Editor or the Managing Editor.

Contact address:

Geological Survey of Slovak Republic – Dionýz Štúr Publishers, Mlynská dolina 1, 817 04 Bratislava, Slovak Republic

e-mail addresses: jvozar@gssr.sk
gabina@gssr.sk
http://www:gssr.sk

The Editorial Board accepts or refuses a manuscript with regard to the reviewer's opinion. The author is informed of the refusal within 14 days from the decision of the Editorial Board. Accepted manuscript is prepared for publication in an appropriate issue of the Magazine. The author(s) and the publishers enter a contract establishing the rights and duties of both parties during editorial preparation and printing, until the time of publishing of the paper.

Text layout

The manuscript should be arranged as follows: TITLE OF THE PAPER, FULL NAME OF THE AUTHOR(S); NUMBER OF SUPPLEMENTS (in brackets below the title, e.g. 5 figs., 4 tabs.), ABSTRACT (max. 30 lines presenting principal results) – KEY WORDS – INTRODUCTION – TEXT – CONCLUSION – ACKNOWLEDGEMENTS – APPENDIX – REFERENCES – TABLE AND FIGURE CAPTIONS – TABLES – FIGURES. The editorial board recommends to show a localisation scheme at the beginning of the article.

The title should be as short as possible, but informative, compendious and concise. In a footnote on the first page, name of the author(s), as well as his (their) professional or private address.

The text of the paper should be logically divided. For the purpose of typography, the author may use a hierarchic division of chapters and sub-chapters, using numbers with their titles. The editorial board reserves the right to adjust the type according to generally accepted rules even if the author has not done this.

Names of cited authors in the text are written without first names or initials (e.g. Štúr, 1868), the names of co-authors are divided (e.g. Andrusov & Bystricky, 1973). The name(s) is followed by a comma before the publication year. If there are more authors, the first one, or the first two only are cited, adding et al. and publication year.

Mathematical and physical symbols of units, such as %, ‰, °C should be preceded by a space, e.g. 60 %, 105 °C etc. Abbreviations of the units such as second, litre etc. should be written with a gap. Only SI units are accepted. Points of the compass may be substituted by the abbreviations E, W, NW, SSE etc. Brackets (parentheses) are to be indicated as should be printed, i.e. square brackets, parentheses or compound. Dashes should be typed as double hyphens.

If a manuscript is typed, 2 copies are required, including figures. The author should mark those parts of a text that should be printed in different type with a vertical line on the left side of the manuscript. Paragraphs are marked with 1 tab space from the left margin, or by a typographic symbol. Words to be emphasized, physical symbols and Greek letters to be set in other type (e.g. *italics*) should be marked. Greek letters have to be written in the margin in full (e.g. *sigma*). Hyphens should be carefully distinguished from dashes.

Tables and figures

Tables will be accepted in a size of up to A4, numbered in the same way as in a text.

Tables should be typed on separate sheets of the same size as text, with normal type. The author is asked to mark in the text where the table should be inserted. Short explanations attached to a table should be included on the same sheet. If the text is longer, it should be typed on a separate sheet.

Figures should be presented in black-and-white, in exceptional cases also in colour which must be paid approx. 100 EUR per 1 side A 4. Figures are to be presented by the author simultaneously with the text of the paper, in two copies, or on a diskette + one hard copy. Graphs, sketches, profiles and maps must be always drawn separately. High-quality copies are accepted as well. Captions should be typed outside the figure. The graphic supplements should be numbered on the reverse side, along with the orientation of the figures. Large-size supplements are accepted only exceptionally. Photographs intended for publishing should be sharp, contrast, on shiny paper. High quality colour photographs will only be accepted depending on the judgement of the technical editors.

If a picture is delivered in a digital form, the following formats will be accepted: *.cdr, *.dxf, *.bmp, *.tiff, *.wpg, *.fga., *.jpg *.gif, *.pcx. Other formats are to be consulted with the editors.

References

Should be listed in alphabetical and chronological order **according to annotation in the text** and consist of all references cited.

Standard form is as follows: 1. Family name and initials of author(s), 2. Publication year, 3. Title of paper, 4. Editor(s), 5. Title of proceedings, 6. Publishers or Publishing house and place of publishing, 7. Unpublished report – manuscript should be denoted MS. Unpublished paper can appear as personal communications only. 8. Page range

Quotations of papers published in non-Latin alphabet or in languages other than English, French, Italian, Spain or German ought to be translated into English with an indication of the original language in parentheses, e.g.: (in Slovak).

Example:

Andrusov, D., Bystrický, J. & Fusán, O., 1973: *Outline of the Structure of the West Carpathians*. Guide-book for geol. exc. of Xth Congr. CBGA. Bratislava: Geol. Úst. D. Štúra, 44 p.

Beránek, B., Leško, B. & Mayerová, M., 1979: Interpretation of seismic measurements along the trans-Carpathian profile K III. In: Babuška, V. & Plančár, J. (Eds.): *Geodynamic investigations in Czecho-Slovakia*. Bratislava: VEDA, p. 201-205.

Lucido, O., 1993: A new theory of the Earth's continental crust: The colloidal origin. *Geol. Carpathica*, vol. 44, no. 2, p. 67-74.

Pitoňák, P. & Spišiak, J., 1989: Mineralogy, petrology and geochemistry of the main rock types of the crystalline complex of the Nízke Tatry Mts. MS – Archiv GS SR, Bratislava, 232 p. (in Slovak).

Proofs

The translator as well as the author(s) are obliged to correct the errors which are due to typing and technical arrangements. The first proofs are sent to author(s) as well as to the translator. The second proof is provided only to the editorial office. It will be sent to authors upon request.

The proofs must be marked clearly and intelligibly, to avoid further errors and doubts. Common typographic symbols are to be used, the list and meaning of which will be provided by the editorial office. Each used symbol must also appear on the margin of the text, if possible on the same line where the error occurred. The deadlines and conditions for proof-reading shall be stated in the contract.

Final remarks

These instructions are obligatory to all authors. Exceptions may be permitted by the Editorial Board or the managing editor. Manuscripts not complying with these instructions shall be returned to the authors.

1. Editorial Board reserves the right to publish preferentially invited manuscript and to assemble thematic volumes,
2. Sessions of Editorial Board – four times a year and closing dates for individual volumes will be on every 31th day of March, June, September and December.
3. To refer to one Magazine please use the following abbreviations: *Slovak Geol. Mag.*, vol. xx, no. xx. Bratislava: D. Štúr. Publ. ISSN 1335-096X.

Indexed/Abstracted in: Chemical Abstracts, Ulrich´s International Periodicals